UNIVERSITY OF BAHRAIN

College of Information Technology



The Application of Visible Light Communication (VLC): An Experimental Study

A Thesis Submitted in Partial Fulfillment of the Requirements for the Master Degree in Information Technology

Submitted by

Khalil Jasim Ebrahim Isa

University number: 19960618

Supervised by

Dr. Alauddin Yousif Mahmood Alomary

(Associate Professor)

University of Bahrain

Kingdom of Bahrain

November, 2015

DECLARATION

I declare that this work is the result of my own investigation and that it has not already been accepted in substance for any degree, nor is it currently submitted for any degree.

Signed: ---------- Date: 24/11/2015

Khalil Jasim Ebrahim Isa (Candidate)

The Thesis defense committee considers the Thesis titled:

The Applications of Visible Light Communication (VLC): An Experimental Study

Submitted by Khalil Jasim Ebrahim Isa to the College of Information Technology is satisfactory and acceptable for the Master of Science in Information Technology.

Thesis Defense Committee:

Dr. Alaudin Al-Omary
(Supervisor)

Department of Computer Engineering
University of Bahrain

Prof. Abdulnasir Yahya Hossen
(Member)

Sultan Qaboos University
Muscat, Sultanate of Oman

Dr. Riyadh Al-Hakim
(Member)

Department of Computer Engineering
University of Bahrain

Abstract

The need for wireless connection has increased due to the development in the social media, mobile application, and the limitations of the Wi-Fi in some applications such as hospitals, airplanes, hazardous environments. Therefore, researchers started investigating the use of Visible Light as a medium for communication (VLC) which is also known as Light Fidelity (Li-Fi). This thesis aims to fill the gap in the previous research by studying the effect of the weather influence such as sandstorm and dust storm on the outdoor VLC applications mainly in the Arab Gulf country which was not investigated before. In addition, the result of this thesis can be beneficial worldwide because most studies have focused on the application and improving the VLC for indoor purpose and a few studies have investigated the effect of the sun and the fog for outdoor VLC applications.

The work in this thesis is based on theoretical and simulation framework. A mathematical model has been derived for dust and sand particles and is used in the simulation. The simulation is conducted using Vehicular to road VLC (V2LC) Outdoor application and is aimed to study the effect of sandstorm and dust storm of the Gulf environment as a weather influence on the use of VLC. The main contribution of this research is to fill the gap in the literature as no research is conducted to study the sandstorm effect which is an important weather influence in the Gulf region.

The study is conducted using different sand particles size and concludes that sandstorm and dust storm affect VLC connectivity due to the density of the sand and dust particles. It is noticed that when the road visibility decreases to less than 1Km and the sandstorm particles radius is less than 36 micrometers, the density of the storm becomes high and the maximum distance that could be achievable is below 100 m. Also, the simulation shows that when the distance between the transmitter and the receiver is 2.864 for the low-density clay sandstorm, power received is -10.234 dBm and the SNR is 100 dB and BER reaches 4.6E-46. Besides, when the distance increases to 500m, the power received reaches -54.166 dBm and the SNR is recorded 25.693 dB and BER increases up to 3.8E-13. Finally, the type of the sandstorm particles has an effect on the communication as well. This is because different particles have different refractive indexes which affect the medium by the absorption or reflection of the light. The results of this study show general similarities with past research conducted to investigate the effect of fog and rain on VLC. The work of this thesis fills a gap in the current VLC research and encourages future research to develop the findings using real prototype system.

To my parents who dedicated their life to their children. To my wife who stands behind me and helps and pushes me to success, to my children.

My thesis is dedicated to them.

Acknowledgements

I would like to express my sincere appreciation to those who provided me with help and inspiration to conduct this study.

First of all, I would like to thank Allah for all the strength and patience that He had given to me to finish this project.

My deep thanks and respect for all my family for their encouragement, confidence in me and prayers. It is my parents who believe strongly that I could do a Master degree and support me in all the stages. I really appreciate the help, support, prayers, and patience of my wife because she helps me in proofreading my thesis and always pushes me to finish the work in the thesis. To my dear family, I dedicate my thesis.

I must acknowledge the contributions, help and support of my dear supervisor Dr Alauddin Alomary for his critical comments that help me to improve my work. He has been always supportive, patient, understanding, and encouraging me in all the stages of my research.

Very special thanks for all my special friends and colleagues for the great help and support especially Sumesh because he is always pushing me to finish the thesis because he wants to see how this idea can work. I have to acknowledge that the energy I had to do all this work was the energy of the great love of Allah and all my beloved people.

List of Content

Subject	Page Number
Declaration	I
Abstract	II
dedication	III
Acknowledgements	IV
List of Content	V
List of Tables	VIII
List of Figures	X
List of Appendixes	XVI
Chapter One Introduction	
1.1 Research Problem	4
1.2 Research Questions	5
1.3 The Objectives of Research	5
1.4 Significance of the Research	5
1.5 The Limitations of Research	6
1.6 Research Terminology	7
Chapter Two Literature Review	
2.1 Background and History	11
2.2 Introducing the Concept of VLC	13
2.3 Development of Modulation Techniques	17
2.4 VLC Applications	23
2.5 Improvement in Transmitters and Receivers	28
2.6 Indoor VLC Studies	33
2.7 Outdoor Studies for VLC Application	38

Subject	Page Number
2.8 Summary	39
Chapter Three Methodology	
3.1 Research Methods	43
3.2 Research Model and Tools	44
3.3 Research Approach	45
3.4 Research Procedures	46
3.4.1 Theoretical Background	46
3.4.2 The Simulation Equation	50
3.4.3 Noise Effect Calculation	51
3.4.4 VLC Modulation	52
Chapter Four Results, Discussion and Recommendations	
4.1 Simulation Scenarios	60
4.1.1 Experiment 1: Simulate Clear Weather	61
4.1.2 Experiment 2: Simulate the Effect of Clay Particles on VLC	64
4.1.3 Experiment 3: Simulate the Effect of Silt Particles on VLC	74
4.1.4 Experiment 4: Simulate the Effect of Sand Particles on VLC	83
4.1.5 Experiment 5: Simulate the Effect of Gravel Particles on VLC	93
4.2 Discussion of the Results	107
Chapter Five Conclusions, Recommendations and Future Work	

Subject	Page Number
5.1 Conclusions	115
5.2 Recommendations and Future Work	117
Bibliography	119
Appendixes	
خلاصة تطبيقات إستخدام الضوء المرئي في الإتصالات (VLC): دراسة تجريبية	

List of Tables

Table Number	Subject	Page Number
4.1	The parameters used to simulate clear atmosphere	61
4.2	The parameters used to simulate clay (Montmorillonite) particles with the visibility 5 Km	65
4.3	The parameters used to simulate clay (Montmorillonite) particles with visibility 1 Km	68
4.4	The parameters used to simulate clay (Montmorillonite) particles with visibility 0.1 Km	71
4.5	The Parameters used to simulate silt particles with visibility 5 Km	74
4.6	The Parameters used to simulate silt particles with visibility 1 Km	77
4.7	The Parameters used to simulate silt particles with visibility 0.1 Km	80
4.8	The parameters used to simulate sand particles with visibility 5 Km	84
4.9	The parameters used to simulate sand particles with visibility 1 Km	87
4.10	The parameters used to simulate sand particles with visibility 0.1 Km	90
4.11	The parameters used to simulate gravel particles with visibility 5 Km	93

Table Number	Subject	Page Number
4.12	The parameters used to simulate gravel particles with visibility 1 Km	96
4.13	The parameters used to simulate gravel particles with visibility 0.1 Km	99
4.14	Comparison of the received power for different sandstorm particles	103
4.15	Comparison of the Signal to Noise Ratio (SNR) for different sandstorm particles	104
4.16	Comparison of the Bit Error Rate (BER) for different sandstorm particles	106

List of Figures

Figure Number	Subject	Page Number
3.1	Kumar et al. V2LC proposed application	45
3.2	Sandstorm wall	47
3.3	Number of days with dust storm or sand storm when visibility 1 Km or less	48
3.4	Number of days with dust storm or sand storm when visibility between 1 Km and 3 Km	48
3.5	Number of days with dust storm or sand storm when visibility between 3 Km and 5 Km	49
4.1	The received power when the weather condition is clear atmosphere	62
4.2	The signal to noise ratio (SNR) when the weather condition is clear atmosphere	63
4.3	The bit error rate (BER) when the weather condition is clear atmosphere	63
4.4	The received power for the VLC affected by clay particles when the visibility is 5 Km	65
4.5	The signal to noise ratio (SNR) for the VLC connectivity affected by clay particles when the visibility is 5 Km	66
4.6	The bit error rate (BER) for the VLC connectivity affected by clay particles when the visibility is 5 Km	66
4.7	The received power for the VLC affected by clay particles when the visibility is 1 Km	68

Figure Number	Subject	Page Number
4.8	The signal to noise ratio (SNR) for the VLC connectivity affected by clay particles when the visibility is 1 Km	69
4.9	The bit error rate (BER) for the VLC connectivity affected by clay particles when the visibility is 1 Km	69
4.10	The received power for the VLC affected by clay particles when the visibility is 0.1 Km	71
4.11	The signal to noise ratio (SNR) for the VLC connectivity affected by clay particles when the visibility is 0.1 Km	72
4.12	The bit error rate (BER) for the VLC connectivity affected by clay particles when the visibility is 0.1 Km	72
4.13	The received power for the VLC affected by silt particles when the visibility is 5 Km	75
4.14	The signal to noise ratio (SNR) for the VLC connectivity affected by silt particles when the visibility is 5 Km	75
4.15	The bit error rate (BER) for the VLC connectivity affected by silt particles when the visibility is 5 Km	76
4.16	The received power for the VLC affected by silt particles when the visibility is 1 Km	78

Figure Number	Subject	Page Number
4.17	The signal to noise ratio (SNR) for the VLC connectivity affected by silt particles when the visibility is 1 Km	78
4.18	The bit error rate (BER) for the VLC connectivity affected by silt particles when the visibility is 1 Km	79
4.19	The received power for the VLC affected by silt particles when the visibility is 0.1 Km	81
4.20	The signal to noise ratio (SNR) for the VLC connectivity affected by silt particles when the visibility is 0.1 Km	81
4.21	The bit error rate (BER) for the VLC connectivity affected by silt particles when the visibility is 0.1 Km	82
4.22	The received power for the VLC affected by sand particles when the visibility is 5 Km	84
4.23	The signal to noise ratio (SNR) for the VLC connectivity affected by sand particles when the visibility is 5 Km	85
4.24	The bit error rate (BER) for the VLC connectivity affected by sand particles when the visibility is 5 Km	85
4.25	The received power for the VLC affected by sand particles when the visibility is 1 Km	87

Figure Number	Subject	Page Number
4.26	The signal to noise ratio (SNR) for the VLC connectivity affected by sand particles when the visibility is 1 Km	88
4.27	The bit error rate (BER) for the VLC connectivity affected by sand particles when the visibility is 1 Km	88
4.28	The received power for the VLC affected by sand particles when the visibility is 0.1 Km	90
4.29	The signal to noise ratio (SNR) for the VLC connectivity affected by sand particles when the visibility is 0.1 Km	91
4.30	The bit error rate (BER) for the VLC connectivity affected by sand particles when the visibility is 0.1 Km	91
4.31	The received power for the VLC affected by gravel particles when the visibility is 5 Km	94
4.32	The signal to noise ratio (SNR) for the VLC connectivity affected by gravel particles when the visibility is 5 Km	94
4.33	The bit error rate (BER) for the VLC connectivity affected by gravel particles when the visibility is 5 Km	95
4.34	The received power for the VLC affected by gravel particles when the visibility is 1 Km	97

Figure Number	Subject	Page Number
4.35	The signal to noise ratio (SNR) for the VLC connectivity affected by gravel particles when the visibility is 1 Km	97
4.36	The bit error rate (BER) for the VLC connectivity affected by gravel particles when the visibility is 1 Km	98
4.37	The received power for the VLC affected by gravel particles when the visibility is 0.1 Km	100
4.38	The signal to noise ratio (SNR) for the VLC connectivity affected by gravel particles when the visibility is 0.1 Km	100
4.39	The bit error rate (BER) for the VLC connectivity affected by gravel particles when the visibility is 0.1 Km	101
4.40	Comparison of the received power for different density Clay and Sand particle sandstorm	103
4.41	Comparison of the received power for different density Gravel and Silt particle sandstorm	104
4.42	Comparison of the signal to noise ratio (SNR) for different density Clay and Sand particle sandstorm	105
4.43	Comparison of the signal to noise ratio (SNR) for different density Gravel and Silt particle sandstorm	105

Figure Number	Subject	Page Number
4.44	Comparison of the bit error rate (BER) for different density Clay and Sand particle sandstorm	106
4.45	Comparison of the bit error rate (BER) for different density Gravel and Silt particle sandstorm	107

List of Appendixes

Appendix Number	Appendix
A	Simulations Results

Chapter One

Introduction

1.1	Research Problem
1.2	Research Questions
1.3	The Objectives of Research
1.4	Significance of the Research
1.5	The limitations of the Research
1.6	Research Terminology

Chapter One: Introduction

In the last few years, the need for wireless connection has increased due to the development in the social media, home entertainment and the mobile applications. Although the radio band is available, it is currently congested and it cannot cover all the needs in wireless connection. In addition, the distributions of radio waves generate a new type of pollution which called "electromagnetic pollution". Moreover, Wi-Fi technology has some limitations in some applications; therefore, it cannot be used in many places. For example, Wi-Fi is not suitable in hospitals, airplanes, hazardous environments, and underwater submarine (Jaiswal & Chopade, 2013; George et al., 2014). Besides, the main problem that is facing Wi-Fi in our countries is the interference and the drop of the signal. These problems can be noticed in offices as well as in the home. The main cause of these problems is the nature of our environments. In addition, the nature of the materials used to construct our buildings which consist mainly of blocks and cement that do not allow the signal to pass-through. Moreover, the cost of providing Wi-Fi Access point everywhere makes the researchers look for better and cost-effective solutions.

Wi-Fi is used indoor and outdoor, but nowadays the use of Wi-Fi outdoor has been reduced and replaced with different technologies such as 4G LTE (Long Term Evolution) and mobile WiMax (Worldwide interoperability for Microwave Access) technologies. Both technologies have the same advantage which is providing better bandwidth and connectivity and both have the same drawback (Retnasothie et al., 2006; Santhi et al., 2003). The main disadvantage for both technologies is the need for more power to provide a better signal (Vaughan-Nichols, 2008). Moreover, both technologies produce strong interference (Yang-Yang Li

& Sousa, 2010). Therefore, researchers search for an alternative solution to cover the limitations found in radio communication. Moreover, the alternative solution should be cost effective and produce green technology (Greentech). Although Infrared (IR), which is a light with long wavelength that make it in-visible consider as one of the optical wireless communication and it was used to connect devices in different buildings in the past, one of the main problems in this technology is that IR is affected by the weather. In addition, infrared is not suitable to be used inside the buildings because it cannot connect multiple devices at the same time and it needs line-of-sight when it is connected.

The researchers start to investigate in the visible light as new innovation for optical wireless communication (OWC). The researchers have found that visible light is the alternative solution for the radio waves because of its availability in home and streets and also it has very high bandwidth. In addition, it has free license's fees and it does not need for new infrastructure so it is cost-effective. Moreover, it is not producing electromagnetic pollution so it is Greentech (Jaiswal & Chopade, 2013).

Researchers propose visible light communication (VLC) which also known as Light Fidelity (LIFI) as the alternative solution for the radio wave limitations. VLC can be used in the bidirectional wireless network as well as data broadcasting. Moreover, VLC provides high-speed communication. In 2011, the Institute of Electrical and Electronics Engineers (IEEE) announce IEEE 802.15.7 as the international standard for the VLC (Jaiswal & Chopade, 2013).

The idea of VLC is to pulse the light at very high speed, therefore, it needs a light which has this feature without damaging the light itself. Therefore, researchers have focused on the light emitting diodes (LED) to

benefit from its feature which includes the high-speed pulsing without affecting the light itself and it is not noticeable by human eye.

A light-emitting diode (LED) is a healthy product and one of the Greentech because it does not contain mercury or lead. In addition, carbon footprint and waste are reduced due to the use of LED (George et al., 2014). LED was proposed for remote-control circuits by using Infrared LEDs and until now it is used.

Besides, the best advantage of the LEDs light in comparison to the ordinary light is that it is 50 to 90% lower energy consumption. In addition, it reduces the maintenance cost of the infrastructure because it has longer lifetime comparing to the ordinary light. Moreover, LED has better response time (45ns) comparing to the ordinary lights (Edgar & close, 1998). Therefore, LED can be used in many applications such as aviation lighting, automotive headlamps, advertising, traffic signals and others. As a result, researchers have proposed the LEDs for the VLC to make use of it infrastructure and features. By using LED for VLC, we can decrease the electromagnetic pollution and implementing Greentech.

1.1 Research Problem

Most of the researches focused on the use of VLC for indoor purpose. In addition, some researchers studied the effect of fog and the traditional lights on the outdoor model of the VLC (Kumar et al., 2011). Some of the previous researches simulated the use of VLC, whereas the others implemented an experimental model inside the LAB. The purpose of this research is to examine the VLC technology for outdoor use and fill the gap in the previous research by studying the effect of different weather influence not addressed by researchers such as sandstorm which is present in the Arab Gulf region.

1.2 Research Questions

This thesis aims at addressing the following research questions:

- How much is the drop in the signal strength for the Visible Light Communication (VLC) technology when it is affected by the sandstorm as one of the weather influences?
- Does the sand and dust storm affect the VLC coverage distance?

1.3 The Objectives of Research

This research aims to achieve the following objectives:

- First, it aims to simulate the use of VLC for vehicle-to-road communication. This simulation considers the traffic lights as the transmitter to broadcast information to vehicles which are considered as the receivers.
- Second, it aims to contribute to the past literature through simulating the VLC technology with the sand storm as a weather influence and investigate the effect of sandstorms on VLC transmission.
- Finally, it aims to seek new findings which can be beneficial for different places in the world.

1.4 Significance of the Research

The research in the field of VLC technology is new and it is open for more investigation. Therefore, this research aims to investigate the weather influences such as sand and dust storm on outdoor VLC vehicle to road communication and fill the gap in the literature as little research has been conducted for outdoor applications. Most of the VLC research which has been implemented before focused on the laboratory

experiments and there is few researchers studied this technology in the commercial field (Liu et al., 2011; Sagotra & Aggarwal, 2013). There are many areas that can benefit from such technology in the commercial sector. Only some of these areas researchers started to investigate such as vehicle-to-road communication and indoor positioning system which is under investigation by Nakagawa Laboratory (Kim et al., 2011; Lee et al., 2012), COWA at Penn State (Panta & Armstrong, 2012; Horikawa et al., 2003; Yoshino et al., 2008; Zhang & Kavehrad, 2012) and others.

VLC is a suitable solution for sensitive places where radio waves are not recommended or prohibited such as hospitals and airplanes. Moreover, VLC is difficult to be hacked because it transmits the data in a safety manner. In addition, VLC produces faster connectivity than Wi-Fi (Jaiswal & Chopade, 2013; George et al., 2014). Most of the researchers nowadays have focused on the VLC as indoor GPS system because it provides accuracy higher than radio waves.

This research will fill this gap through providing a simulation methodological approach through studying outdoor vehicle-to-road communication and the effect of dust and sandstorm on it.

1.5 The Limitations of Research

This research simulates the weather influences on the VLC technology. In addition, it focuses on the mineral sandstorm such as clay, silt, sand, and gravel because it frequently happens in the Arab Gulf countries. Although, there are different types of dust storm happens worldwide, this research does not investigate organic and vegetable dust, chemical dust, and metallic dust. Moreover, the researcher focuses on the red Led light when the car stops and does not study the green Led light due to the speed of the car while moving. Besides, since the researcher

investigates the red LED light, the receiver needs to have a red optical filter which makes the investigation in a different colour in the same time is a little bit complicated. The study does not investigate the maximum number of cars that the system can handle. In addition, the researcher does not consider the interference of the cars brake light on the system. Finally, due to the limitation to investigate the system in the real world, due to the lack of the equipment and the laboratory, the theoretical calculation has not been compared with the practical implementation.

1.6 Research Terminology

This section aims to present the main research terminology.

To start with, optical wireless communication (**OWC**) is the technology that used the light such as visible, infrared (IR), or ultraviolet (UV) as a data communication medium to carry a signal. OWC system operates in a different band such as visible light communication (VLC) which operates in visible band (400 to 700 nm) (Jaiswal & Chopade, 2013). And infrared operates at the near IR band (750 to 1600nm) which is used in point-to-point communication and known as the free space optical (FSO) systems.

Visible light communication (**VLC**) which also known as Light Fidelity (LIFI) is the light with a frequency between 400THz and 800THz and has a wavelength between 400nm to 700nm. This light is used as a transmitter by flashing the light at speeds undetectable by the human eye without affecting on the light itself and the best light for this is the LEDs light (Jaiswal & Chopade, 2013).

Moreover, the following various terminologies are used:

- A light-emitting diode (**LED**) is a two-lead semiconductor light

- 4G **LTE** is Long Term Evolution.
- **WiMax** is worldwide interoperability for Microwave Access.
- **Greentech** is Green technology.
- Infrared (**IR**) is a light with long wavelength that make it invisible, and used to connect devices in different buildings in the past.
- **IEEE** is Institute of Electrical and Electronics Engineers.
- **FSO** is Free-space optical.
- On-off keying (**OOK**) is to switch the light on and off. This technique is the simplest modulation technique which represents the digital data.
- Pulse width modulation (**PWM**) is one of the modulation techniques for digital data. This module uses the duration of pulses to send the information.
- Pulse position modulation (**PPM**) is one of the modulation techniques which use the pulse position to encode the data within the frame.
- Variable Pulse Position Modulation (**VPPM**) is one of the modulation techniques which is the same as PPM. In addition, this modulation uses the pulse width to control the lighting dimming.
- Colour shift keying (**CSK**) is one of the modulation techniques which can be used when the LEDs is of RGB types.
- Orthogonal Frequency Division Multiplex (**OFDM**) is one of the modulation techniques that produce low rate sub-streams from splitting the high data rate serial.
- **Attocell** is an optical Access Point.
- **RSSI** is the relative received signal strength in a wireless environment. This technology is used in positioning systems.

- Time of arrival (**TOA** or **ToA**), is the time when the radio signal travels between the single transmitter and single receiver. This technology is used in positioning systems.
- Time Difference of Arrival (**TDOA**), is a technology used in positioning systems based on determining the mobile phone positing from the cell towers.
- The Angle of Arrival **(AoA)** is a technology used in positioning systems to find the direction by measuring the TDOA.

Chapter Two

Literature Review

2.1	Background and History
2.2	Introducing the Concept of VLC
2.3	Development of Modulation Techniques
2.4	VLC Applications
2.5	Improvement in Transmitters and Receivers
2.6	Indoor VLC Studies
2.7	Outdoor Studies for VLC Application
2.8	Summary

Chapter Two: Literature Review

This chapter aims to review the research works and studies related to the VLC topic to provide an academic background that can help in analyzing the research findings. This chapter started with providing a background and a historical framework of the use of Visible Light Communication (VLC) then, the chapter is divided into six divisions. The first division is the introduction of the concept through offering the main descriptive studies in the field of VLC. The second division is the development of modulation techniques. The third division is reviewing the different applications of the concept. The fourth division is outlining how to improve the connectivity by investigating the improvement in transmitters and receivers. The fifth division is reviewing different indoor studies for VLC. The sixth division is outlining different outdoor studies for VLC application. Finally, a summary of the key conclusions that include the most beneficial ideas is presented.

2.1 Background and History

Several studies discussed the significance and applications of using Visual Light Communication (VLC) technology. For instance, Ball and Tien stated that the development of the wireless communication equipment made reaching the internet easier than before. There was a need to provide high speed and more reliable network with large area coverage in social media era which led to the emergence of the fourth generation mobile network (Ball & Tien, 2012). The main advantage of VLC technology, which makes it cost-effective, is that there is no need to implement a new infrastructure for it as we can make use of the existing light infrastructure that uses Light Emitting Diode (LED) bulb.

Nowadays, LEDs have been deployed in many places such as indoor lighting equipment, traffic lights, car indicator, displays and so on because they have a long life, low power consumption and small volume (Wang et al., 2012).

Historically, the use of VLC started when Alexander Graham Bell in 1880 tried to transfer a voice signal on a beam of light (Sagotra & Aggarwal, 2013). Bell's idea was to create photo phone by vibrating mirror with a certain mechanism and focused sunlight on it. The receiver will receive the vibrated beam and transfer the received signal back to a voice signal. Bell succeeded to transfer the light from one point into another. On the other hand, Bell failed to generate a frequency which could be used as a carrier. In addition, he found that the fog and the rain are other obstacles which made him stop his innovation (Sagotra & Aggarwal, 2013).

Since 1880 when Alexander Graham Bell decided to stop the investigation in the VLC, no one starts any investigation in the same area. In 2003, Nakagawa Laboratory, in Keio University in Japan, started an investigation in Bell innovation by studying LED light as a currier for data and since then the attention in the VLC increased and new investigations have been started by other researchers. Researchers in Siemens and Fraunhofer Institute transmitted data at 500Mbps over 5 meters length in 2010. Besides, at the beginning of 2013, Oledcomm Company started marketing their products and solutions in the VLC and became the first European company that market the VLC for commercial use (Jaiswal & Chopade, 2013). Moreover, Engineering and Physical Sciences Research Council (EPSRC) in the United Kingdom funded a project named Ultra-parallel visible light communications (UP-VLC) with an amount of £4.6 million. This project consists of "partnership

between 6 research groups at 5 institutions" running from October 2012 to September 2016 and led by professor M.D. Dawson in the University of Strathclyde and mentored by Professor P. Blood in Cardiff University. The idea of this project is to achieve ultra-high data density by improving the VLC hardware through investigating the use of arrays of LEDs and control it by CMOS ("Ultra-Parallel Visible Light Communications (UP-VLC)", n.d.; Harris, 2013).

2.2 Introducing the Concept of VLC

Several scholars provided different frameworks to explain the concept of the VLC. This section aims to review the main studies that described the technology of Visible Light Communication.

To start with, Kavehrad (2007) followed the descriptive methodology framework to outline the use of an optical wireless network to provide the internet for the room. The author explained the use of infrared as an optical wireless system and how it could operate. In addition, the author explained the white LED and how we could benefit from it for data transmission and illumines of the room. Moreover, the author noted that LED had a long life and consumed lower power.

Hu et al. (2007) proposed red laser diode as visible light for free-space optical (FSO) communication. They followed experimental methodology framework by conducting some experiments on using low power red laser diode. Theoretically, they achieved data rate 100Mb/s for range 300m. Whereas, practically in the experiment, they achieved data range 10Mb/s for coverage of 300m.

O'Brien et al. (2008a) followed the descriptive methodology framework by studying and summarizing the "Visible light

communication challenges and possibilities". In addition, the researchers listed the possible applications that can be benefited from VLC (i.e. signboards, signal lights, and positioning system). The researchers explained the components of the VLC such as the transmitter, the receiver, and the medium. The researchers ended their study with the challenges such as how to achieve high data rate, two-way communications, and the regulation.

Borogovac et al. (2011) have studied the possibility of communication when the light is off by following the theoretical and experimental methodology framework. The researchers explained that VLC needs illumination to establish the connection and when the lights is off there is no illumination; therefore, there is no connection. The researchers analyze the minimum possible illumination which is required to have a connection. In addition, they calculated the accepted illumination by the user that makes him feel that the light is in off state. They conclude that the connectivity is possible and they can achieve proper data rate with low light illumination.

Elgala et al. (2011) followed the descriptive methodology framework to explain the possibility and the modulation of the indoor optical wireless communication. Although IR LEDs used for communication, the researchers explained that white LEDs provided communication and lighting. Researchers listed and explained the components which could be used for the indoor optical wireless system. In addition, the researchers stated the airplanes as a typical scenario for the future wireless network. Moreover, the researchers explained different modulation techniques (i.e. Single carrier pulse modulation, and multiple subcarrier modulation). Finally, the researchers concluded that further

studies are needed for optical communication techniques using LEDs before it can be used commercially.

Lee (2011) outlined the VLC components and configuration. In addition, Lee summarized the recent development, technical issues, and research results. The researchers followed the descriptive methodology framework to describe VLC transmitter and receiver. Moreover, Lee illustrated some of the components and the standardizations of the VLC.

Mishra and Salian (2011) outlined the concept of the VLC through conducting an experiment. In addition, they aimed to explain how the application could benefit from VLC through receiving wireless internet. Therefore, they followed an experiential methodology framework to explain the concept by implementing a prototype. They noticed from their experiments that visible light is excellent and low-cost medium to transfer the Data. Besides, they concluded that LEDs is the best available technology that can be used to implement VLC technology for current and future purpose because it could provide an efficient, clean communication. In addition, they listed some of the applications that could benefit from VLC such as the airplane, personal networks, mobile communications, and petrochemical plant.

Vucic and Langer (2012) outlined the concept of VLC by following descriptive methodology framework. The researchers started their study by explaining that modulation was the main challenge that is facing the researchers to achieve high data rate. In addition, the researchers explained how other researchers had come up with new or modified modulation techniques (i.e. OFDM, MIMO, and WDM) to solve this problem. Moreover, they discussed the use of image sense instead of the

photodiode in the receiver side. Additionally, they reviewed the use of VLC in underwater communication.

Jaiswal and Chopade (2013) used the descriptive methodology framework to explain the VLC. The researchers started with defining the VLC (Li-Fi) as the communication technique which uses the LEDs illumination to transmit the data without the need of fibre. They stated that the VLC Protocol is standardized by IEEE in 2011 as IEEE 802.15. In addition, the researchers explained the way of how VLC is working. Moreover, they described the differences between the VLC technology and the other wireless technology. Besides, they listed and explained some of the main applications that VLC could be used such as medical, airline, sensitive area, and underwater. The researchers concluded their study stating the advantages of the VLC such as the high data rate, security, solving the saturation in the radio frequency and making every light as a free access point. In addition, they explained the limitations of the VLC such as the fact that the transmission can occur when there is a line of sight and the drop of the line when any obstacles pass through the channel.

Tsonev et al. (2013a) followed descriptive methodology framework by summarizing some of the research related to wireless networking. In addition, they explained some of the modulation used for VLC. Moreover, they explained the up-line concept using radio frequency and infrared frequency. Besides, they explained the concept of optical "attocell".

George et al. (2014) aimed to explain the concept of VLC by using the descriptive methodology framework as well. They started by defining the VLC as "a short-range optical wireless communication using LEDs

for illumination and communication simultaneously "... VLC is the technology which utilizes the visible light source as a signal transmitter, the air as a transmission medium, and the appropriate photodiode as a signal receiving component...". The researchers compared VLC with other optical wireless communication such as radio-wave and infrared from a different perspective (i.e. efficiency, capacity, cost, safety, security, human health, distance, and application). In addition, they explained the modulation technique which is used for VLC and the main challenges. Besides, researchers listed the key applications which could we benefit from VLC such as aviation, hazardous environments, hospitals, and underwater communications.

2.3 Development of Modulation Techniques

Various studies aimed to improve the data rate and the performance of the VLC through investigating in the modulation technique.

For example, Afgani et al. (2006) followed the theoretical framework that was supported with the experimental methodology framework to study the use of Orthogonal Frequency Division Multiplex (OFDM) for intensity modulation in VLC. The researchers developed a prototype by using two digital signal processing boards (DSP) and one LED. The researchers compared the theoretical framework to the experimental results by using a Matlab simulation and found that they were almost the same. The researchers noticed that 10^{-3} bit error rate (BER) could be achieved for indoor VLC that is interfering with another light source when OFDM used for one LED and the distance is one meter. Although the high peak to average ratio (PAR) considered as a disadvantage in radio-wave communication for OFDM modulation, the researchers found that it was an advantage for VLC.

Elgala et al. (2007) used the experimental methodology framework to study the use of white LEDs for OFDM modulation in Visible Light Communication. The researchers implemented a prototype to evaluate the performance for the indoor application. They used two digital signal processing (DSP) boards, one for the transmitter (Tx) and the other for the receiver (Rx). Moreover, they used Matlab and Simulink for the algorithms and the coding of the DSP boards. The researchers implemented the experiment in direct LOS (line-of-sight) and concluded that OFDM could be used for transmission. Moreover, a bit error rate (BER) 10^{-5} at the maximum distance of 90cm could be achieved by using Quadrature Phase Shift Keying (QPSK) modulation.

Grubor et al. (2007) used a theoretical methodology framework to investigate indoor high-speed data rate VLC system. The researchers started their work by assuming a medium office room with standard illumination and with commercial LEDs and photodiodes. In addition, the researchers used baseband and discrete multi-tone (DMT) modulation in their work. The researcher's achieved about 200Mb/s in their investigation.

Elgala et al. (2009) attempted to achieve good illumine and signals to noise ratio (SNR) for indoor broadcasting VLC through using OFDM. The researchers followed the experiential methodology framework for their study. The researchers started their study by describing different modulation techniques. In addition, the researchers developed a prototype by using nine LEDs and two DSP to measure illumine and the SNR of OFDM modulation. The measured illumine was compared with the standard illumine (500lux) which was required for offices and they found that it was bellowed the required standard. In addition, the researchers

found that when the array of LEDs was increased, the SNR and illumine became better.

Bai et al. (2010) aimed to achieve high capacity communication and flexible dimming. Therefore, the researchers proposed new modulation which is overlapping pulse-position modulation (OPPM) and followed a theoretical methodology framework to compare it with On/Off Keying (OOK) modulation and variable PPM modulation. The researchers compared the proposed modulation with the other modulation in "dimming range, flicker severity index, cut-off data rate, and power and bandwidth efficiencies". They noticed that OPPM flicker was less than the other modulation techniques. Whereas, OPPM requires more power to achieve the OOK BER. Moreover, OPPM had more brightness and provided higher dimming range and cut-off data. The researchers concluded that the proposed modulation performed better than the other modulation techniques.

Wang et al. (2011) aimed to improve the performance in multi-level quadrature amplitude modulation (M-QAM) OFDM signal. Therefore, the researchers followed a simulation methodology framework to study indoor VLC. The researchers assumed high absorption from the floor and walls in the LOS simulation. The researchers aimed to improve the SNR and receive the maximum power at the photo-detector; therefore, the researchers used Newton method to find the tilting angle. The researchers found that when 12W was used as a launching power for one LED source, the maximum improvement in spectral efficiency was 0.44bit/s/Hz. Whereas, when there were four LEDs, the maximum improvement was 0.21bit/s/Hz.

Stefan et al. (2011) attempted to study the BER performance of OFDM system with considering the LED nonlinearity effects by the experiment. Therefore, they followed experimental methodology framework by using digital signal processing (DSP) with field-programmable gate array (FPGA). Moreover, the researchers used high-power IR LED and Silicon PIN photodiode. The researchers found that when the LED was an operating point set in the proper way, the BER performance was improved. Besides, a poor BER performance was recorded due to the clipping of OFDM signal lower peaks which was caused by low bias currents. Additionally, an improvement in BER performance in some cases was recorded when the bias currents were higher than the IR LED recommended values.

Ghimire et al. (2011) followed theoretical methodology framework by proposing an algorithm for "Time and Frequency Synchronization in Optical Wireless OFDM Networks". The researchers studied the synchronization of OFDM system in the optical wireless network which used intensity modulation (IM) /direct detection (DD). The researchers explained that the bottleneck in optical wireless is the analogue front-end bandwidth, and they stated that their proposed algorithm solve that bottleneck. In addition, the performance of synchronized system was increased by using the proposed algorithm. Moreover, the researchers stated that their proposed algorithm was easy to be implemented in digital hardware.

Dimitrov et al. (2012) studied different types of carrier transmissions for OWC such as PPM, Pulse-amplitude modulation (PAM), quadrature amplitude modulation (QAM) direct-current biased optical OFDM (DCO-OFDM) and asymmetrically clipped optical OFDM (ACO-OFDM). In addition, the researchers proposed a signal shaping

frameworks to make those carrier transmissions fitting the optical power constraints. Signal-to-noise ratio (SNR) requirement and spectral efficiency were compared to the OWC by following theoretical methodology framework. The researchers found that the proposed framework reduced the required electrical SNR. In addition, DCO-OFDM and ACO-OFDM showed more spectral efficiency when the DC bias power was neglected. The researchers noticed that PAM and PPM were lower SNR due to the DC bias.

González (2012) outlined the benefits and the drawbacks of multiple input, multiple output OFDM (MIMO-OFDM) in optical wireless communication. In addition, multi-user LS detection was studied when it was combined with OFDM and angle-diversity receivers. Therefore, the author followed a descriptive and simulation methodology framework. The author noticed that the use of multi-user LS detection increased the accuracy by finding the receiving user which led to improving the performance. Moreover, the author concluded that such a scheme can improve the capacity of VLC networks.

Khalid et al. (2012) attempted to achieve a data rate of 1Gb/s with the consideration of the power amplifier and the nonlinearity of the LED. The researcher's proposed algorithm and followed the experimental methodology framework to demonstrate their work. In addition, to maximize the capacity, the researchers studied the effect of the quantity of the subcarriers. The researchers achieved a data rate of 1Gb/s after using optimized discrete multi-tone modulation technique in standard illumines. Besides, they achieved 640 Mb/s with lower luminance.

Moon and Jung (2012) aimed to achieve high data rate and reduce the BER by proposing a new modulation which they called "multi-coded

variable pulse position modulation (MC-VPPM) for visible light communication systems". The researchers followed a simulation methodology framework to study the proposed modulation which is based on "Pulse Width Modulation (PWM) and Pulse Position Modulation (PPM)". The researchers achieved an enhancement in the data rate by using "orthogonal codes to multi-coded the PWM and PPM". In addition, the researchers noticed an improvement in the BER.

Cossu et al. (2012a) attempted to achieve high data rate by using RGB LEDs. Therefore, the researchers followed the experimental methodology framework to test the data rate for indoor VLC for a distance of 30cm. The researchers implemented two different scenarios: one with Discrete Multi-Tone (DMT) modulation and the other with wavelength division multiplexing (WDM) modulation. The researchers noticed that 1.5Gbit/s could be achieved by using DMT modulation for distance 30cm. In addition, they achieved 3.4Gbit/s for the same distance when they used WDM modulation. Moreover, they noticed that the BER for both scenarios was below the Forward Error Correction (FEC) limit.

Tsonev et al. (2013b) followed the analytical methodology framework for "Complete Modeling of Nonlinear Distortion in OFDM-based Optical Wireless Communication". The researchers used Bussgang theorem for the theoretical background. The researchers provide a novel method which "describes how a closed-form analytical expression for the system bit error rate can be obtained for an arbitrary memory-less distortion". In addition, the researchers studied different types of OFDM modelling such as "direct-current biased optical OFDM (DCO-OFDM), asymmetrically clipped optical OFDM (ACO-OFDM), pulse-amplitude-modulated discrete multi-tone modulation (PAM-DMT), and unipolar orthogonal frequency division multiplexing (U-OFDM)". The researchers

compared their theory with Monte Carlo simulations and found that the results were almost the same. The researchers were concluded that their theory is better than conduction Monte Carlo simulation because of the cost. In addition, researchers found that their theory estimated the system performance faster and the accuracy was high.

Ren et al. (2013) proposed a new modulation technique which is based on OOK and PAM modulation and called it m-ray return-to-zero optical pulse modulation (MRZOPAM). The researchers followed theoretical methodology framework to study the proposed technique. The researchers noticed that the proposed technique had the ability to achieve high data rate. In addition, they noticed that it could control the dimming and the flicker mitigation. Besides, the researchers concluded that MRZOPAM achieved high data rate and improvement in the BER performance.

González et al. (2014) proposed MIMO-OFDM for multi-user VLC. In addition, to specify each user information, the authors compared the capacity of non-imaging and imaging reception. Thus, the authors followed a descriptive and simulation methodology framework. The authors noticed that in joint detection scenario there was an improvement in the SNR for the imaging receivers. Moreover, a decreased in the performance was noticed for a non-imaging receiver when it was in the centre of the room. The authors concluded that the imaging receivers are the suitable solution for multi-user VLC.

2.4 VLC Applications

Several scholars studied different VLC application. For example, Kumar et al. (2006) studied "Visible light communication for advanced Driver Assistant Systems (VIDAS)" theoretically. The researchers

followed a simulation methodology framework by implementing simulation and analyzing the results. The researchers noticed that the front end receiver needed to enhance the performance. Therefore, they studied the transmission range of 100m and optimized the design parameters. The researchers concluded that their proposed design was suitable for different packet sizes and distances. Moreover, they called for future work to develop a prototype that could transmit a data rate of 1Mbps and had BER less than 10^{-6}.

Kavehrad and Amirshahi (2006) proposed a suitable channel model for VLC and broadband power-line (BPL). In addition, the researchers calculated the transmission capacity value for both techniques. The researchers followed an experimental methodology framework in their investigation by implementing VLC system. The researchers noticed that a high transmission capacity was offered by medium and low voltage grids of the power-line. Moreover, it was noticed that performance was reduced due to the reflection caused by mismatches throughout. Although signal distortion could appear due to optical path difference, the researchers noticed high data rate which was equal to 1Gbps. The researchers concluded that home network could benefit from combining these two technologies.

Liu et al. (2011) experimented VLC vehicle-to-road applications under certain conditions to find if there was any effect in the VLC communication. These experiments focused on the interference and the flexibility to other visible light noise. The researchers followed an experimental methodology framework by proposing a prototype and using Matlab for coding the modulation. They noticed that VLC was flexible to the interference from the other source of lighting when the receiver received the signal from narrow-angle. In addition, the

researchers examined if the network had satisfied the required performance when the VLC network faced normal and heavy usage. At the end, they noticed that VLC could operate in such conditions without affecting the performance.

Pu and Hu (2012) stated that the screens and cameras were widely used in recent years. Although it was possible to establish communication between screens and cameras by using VLC system, the researchers noticed that frame synchronization issues appeared. The researchers proposed an algorithm and developed a prototype for a connection between laptop and phone by following a practical methodology framework. The researchers used the laptop as a transmitter through the display and they used the phone camera as a receiver. The researchers noticed that a smooth code with higher throughputs achieved.

Lee et al. (2012) aimed to achieve "evaluation of visible light communication channel delay profiles for automotive applications". Therefore, the researchers followed a simulation methodology framework to design two different scenarios. The researchers used CATIA V5 tool to simulate crossroad and metropolitan street scenarios. In addition, LightTools software was used to trace the light beam in "vehicle-to-vehicle and vehicle-to-infrastructure (V2I) communication links". The researchers found that when the multiple lines of sight linked were increased and non-line of sight was less, the delay profiling happened. Moreover, they found that visible light was more reflective and diffused in V2I link in the metropolitan scenarios which increased the channel delay profile.

He et al. (2013) aimed to broadcast high-quality audio and video via VLC. The researchers followed the practical methodology framework to

examine their aim. The researchers developed prototype of video and audio broadcasting system and implemented same experiments for different distances. The researchers concluded that their goal could be achieved to maximum distance of 3m. In addition, they concluded that they could improve the performance by adding lens between the transmitter and the receiver.

Abualhoul et al. (2013) followed the simulation and experimental methodology framework to study the feasibility of using VLC in platoon control. The researchers built a complete VLC model and calculated the effect of inter-vehicle distance, background noise, and incidence angle on BER. In addition, the researchers developed a Matlab/Simulink model to study the performance of platooning control. The researchers found that they could achieve up to 7m when there was line of sight and road curvature up to 60 degrees. In addition, it was noticed that the performance and the processing time of the proposed lateral controller was good and it reached maximum error of 20cm.

Nguyen and Jang (2013) attempted to improve the accuracy of positioning system by proposing a new technique using VLC. The researchers followed a simulation methodology framework to achieve their goal. The researchers explained different types of localization techniques (i.e. received signal strength indication "RSSI", time of arrival "TOA", time difference of arrival "TDOA", and angle of arrival "AOA") and discussed their proposed technique which was based on three-dimensional positioning techniques using indoor VLC. The result of the proposed technique made improvement in the performance and accuracy.

Hapani et al. (2013) aimed to transmit an image via secured VLC, therefore, they used experimental methodology framework by designing a

prototype. The components of this prototype were: microcomputer, photodiode, LEDs and Matlab for converting the image to binary. The researchers explained that it was difficult for the intruder to capture the signal due to the natural of the light because the light could not pass through the wall. In addition, to make the signal more secure, the researchers proposed a steganography with password sharing to add one more layer of the security. The proposed technique was useful when the secured data was needed to be shared and there were many users sharing the same VLC network. The researchers concluded that VLC was a secure network because it was within the same area. Moreover, they found that using steganography increased the security of the VLC.

Gupta and Sharma (2014) followed an experimental methodology framework to study the use of VLC in vehicle-to-vehicle data broadcasting. The researchers started their work with outlining the application that is benefited from VLC and the challenges of the VLC. The researchers developed a prototype by using Arduino interface to develop vehicle-to-vehicle visible light communication. The researchers implemented a feasibility study to check if the prototype worked under working conditions. The researchers noticed that when the receiver had a narrow field of view, it was more flexible to the noise from sunlight as well as legacy lighting. The researchers concluded that the proposed system could help lowering the probability of traffic accident by detecting the incident and providing early warnings.

Abualhoul et al. (2014) aimed at "Enhancing the field of view limitation of Visible Light Communication-based platoon". Therefore, they followed the simulation methodology framework and proposed a new method for the enhancement of Field of View (FOV). Matlab/Simulink was used for the simulation of four vehicles using VLC

and positioning system. The researchers proposed different scenarios to test their method and noticed that their method found a solution for optical incidence and irradiance angles efficiency. Moreover, they concluded that the receiver FOV was not limiting the VLC-based platoon.

Iannucci and Pini (2014) followed a descriptive methodology framework to outline the benefits of VLC in the "smart city". They explained that VLC provided a set of tools which could "increase the quality of life in an urban environment". In addition, they explained that citizens could access the information and services easily. Moreover, they reviewed the financial profits of using such technology.

Kumar (2014) proposed "A traffic information broadcast system for road safety applications" system by using a theoretical methodology framework. Kumar investigated the feasibility of using VLC for broadcasting the information for road safety applications by studying the experiment results from a case study. Moreover, Kumar outlined the integration of the VLC with the intelligent transportation system (ITS) and explained the VLC reference model architecture. Finally, Kumar concluded that his proposed system was feasible.

2.5 Improvement in Transmitters and Receivers

Several scholars aim to enhance the connectivity and improve the performance by an investigation in the enhancement of VLC transmission and receiving.

For instance, O'Brien et al. (2008b) described the possibility and the challenges to achieve 100Mb/s through different approaches. In addition, the researchers illustrated the configuration and performance of VLC. The researchers followed the descriptive and experimental methodology

framework to outline their aims. The researchers checked the possibility of achieving 100Mb/s by simulating the BER against the data rate and they concluded that 72Mb/s could be achieved by equalized LED array. The researchers followed different approaches to increase the data rate and achieve 100Mb/s data rate. The first approach that researchers followed was to use an optical filter, whereas, the second approach was to use multilevel modulation schemes. The third approach was to combine numbers of LED together in an array, but this approach had disadvantages which was the alignment of the array. The researchers concluded that more than 100Mb/s could be achieved by using the second approach. Finally, the researchers outlined the challenges that were facing the VLC such as the uplink, the regulation, and the standardization.

Cui et al. (2010) followed a theoretical methodology framework and support it with experimental methodology framework to study the line of sight of the VLC. The researchers started their study with illustrating the issues of the line of sight for indoor VLC. The researchers conducted a simulation to examine the theoretical framework. In addition, the researchers studied how to achieve the best performance for the practical design by implementing a prototype and the use of optimization method using image sensor instead of the photodiode. The researcher compared the results of the simulation and the practical and noticed that they were close to each other.

Borogovac et al. (2010) aimed to achieve a high data rate and reduce the distortion on the indoor VLC. The researchers proposed a new idea to use the spotlight by using a theoretical methodology framework. The researchers explained that the idea of using spotlighting was to reduce FOV which would focus the beam of the light in a smaller area. Therefore, a number of users using the same source would be decreased

and illumine would be focused. The researchers concluded that by using spotlighting, they could increase the data rate and decreased the channel distortion. Moreover, they noticed that their idea reduced the interfering link between the users. Besides, they proposed a hybrid solution which could combine the high data rate in the critical area with wide coverage by combining the spotlighting with the normal LEDs.

Kumar and Lourenco (2010) aimed to study the use of LEDs in VLC system and to outline high-brightness (HB) LEDs and its performance and features (i.e. bandwidth virtually unlimited, cheap TX and RX, secure, safe, and not interface with other RF devices). Therefore, they followed a theoretical methodology framework. The researchers concluded that LEDs was suitable to be used for indoor and outdoor VLC because it provided illumination and data transmission. Moreover, they concluded that although VLC was facing some challenges, the results in such technology were promising for future development.

Uddin et al. (2011) proposed a method to keep the receiver's output current stay the same and reduce the performance variation in VLC when multicolour channels were used. The researches followed a theoretical methodology framework and supported it with simulation methodology framework by using Matlab. The researchers studied SNR, BER, output current, and outage probability for three colour channels which is red, green, and blue. The simulation showed that the performance variation was reduced; therefore, the researchers achieved their goals.

Ball and Tien (2012) proposed and tested a high standard VLC hardware which would help the researcher and the industry investigation to develop a high level of VLC in their research. The researchers used the experiment methodology framework. They developed a prototype and

demonstrated indoor VLC which achieved 3 Mbps at 2.6m by using their hardware with USRP2 software-defined radio.

Le et al. (2012) aimed to propose a "Dynamic Channel Selection Scheme for IEEE 802.15.7 Visible Light Communication" by following the experimental methodology framework. The researcher explained that the channel in VLC was depending on the wavelength colour. Therefore, they proposed a colour channel selection scheme which enhanced the physical layer and they called it as "virtual cognitive MAC". The researchers concluded that the BER of the channel enhanced was more than 20% when they used the proposed scheme. In addition, the proposed scheme increased the SNR when it was compared to fix colour channel and it improved the system performance.

Lin et al. (2012) attempted to simplify the installation of VLC; therefore, they followed the experimental methodology framework. The researchers proposed wavelength-division-multiplexing (WDM) VLC using laser pointer lasers (LPLs). Morcover, an adaptive filter and preamplifier were used to achieve $<10^{-9}$ BER at 10m/500Mbps. Besides, the researchers achieved high data rate. The researchers demonstrated that their proposed WDM VLC was easy and simple for installation.

Kizilirmak (2013) followed an experimental methodology framework to examine the "Impact of repeaters on the performance of indoor visible light communications". In addition, the performance of a bit error rate for PPM was evaluated by simulation and analytical calculations. The experimental study was conducted by placing a repeater on the desk to repeat the signals which resulted in improving the luminance and BER performance. In addition, this repeater improved the communication when the shadows appeared in the channel.

Ghassemlooy et al. (2013) aimed to achieve a high data rate in indoor VLC. The researchers followed an experiment methodology framework by using LED, low-bandwidth organic photo-detector and equalizer. In addition, Matlab was used to translate the OOK data format which was generated by Matlab into 4-PPM code. The researchers used Matlab to implement the artificial neural network (ANN) equalizer. Moreover, "Levenberg–Marquardt back-propagation algorithm" was used to train the ANN. The researchers found that 4-PPM modulation achieved 200kbits/s without the equalizer. Whereas, it achieved 3.75Mbits/s when the equalizer was used. Besides, 200kbits/s was achieved for OOK modulation without the equalizer and 2.8Mbits/s with the equalizer. The researchers concluded that indoor VLC using organic photo-detector with ANN equalizer could achieve high data rate.

Butala et al. (2013) proposed a "modified singular value decomposition VLC (SVD-VLC) MIMO system" to maximize the capacity of LEDs. Therefore, the researchers followed a theoretical methodology framework to study the maximum data rate without affecting the illumination. The proposed design considered MIMO VLC channel with imaging receiver. The researcher calculated and compared the upper bound on the capacity of the LEDs using SVD-VLC and single-input single-output (SISO) channels and found that SVD-VLC offers large capacity gains.

Chun et al. (2014) used "Blue GaNμLED and Fluorescent Polymer" in VLC to achieve a high data rate. Therefore, they followed an experimental methodology framework by proposing a new schema. The idea of their schema was to generate white light which could be used for illumination and communication from "blue GaNμLED and a yellow fluorescent copolymer". The researcher noticed in their demonstration

that 1.65 Gb/s could be achievable for distance 3cm using DCO-OFDM modulation.

2.6 Indoor VLC Studies

Several scholars have studied the indoor VLC from different angles. For instance, Lo (2004) aimed to examine the configuration and the features of VLC. Therefore, an experimental methodology framework was conducted. The author investigated in data rate, transmission distance, and transmitter field of the view. In addition, the author tested broadcasting music by using his prototype. The author concluded that a transmission of data rate 100 kHz for distance 170cm could be achieved. In addition, the transmission happened when the direction of field of view was 160° and the radius was 1.7m.

Wu and Little (2010) aimed to achieve a reasonable data rate for multiple access line of sight VLC system. Therefore, they followed a simulation methodology framework and proposed two communication protocols and a hexagonal physical device design. Those protocols were point-to-point and point-to-host. The researchers found that the proposed protocols were good for different approaches and applications. When a high data rate was required, the point-to-point protocol was suitable and when average data rate was required, a peer-to-host protocol was the suitable one. Moreover, the researchers found that peer-to-host protocol was simpler and easier to implement.

Nguyen et al. (2010) followed the experimental methodology framework to calculate the "illumination distribution, root mean square (RMS) delay spread, and received signal wave-form". Therefore, Matlab and Simulink were used to simulate indoor VLC. The researchers started their work by outlining the modelling of physical structure, RMS, and the

luminance performance. The researchers assumed the physical parameters for the simulation and analyzed the received signal at the bottom surface. Moreover, direct and reflected illumination was calculated using the program. The researchers concluded that they needed more practical parameters and different modulation to consider.

Aschenbrenner (2010) said that a demonstration was conducted by a team of researchers from Siemens and Fraunhofer Institute for Telecommunications (Heinrich Hertz Institute in Berlin). The team followed the experimental methodology framework to investigate in VLC. The author concluded that the team achieved a 500 Mbit/s with a white LED over a distance of 5 meters (16 ft), and 100 Mbit/s over longer distance using five LEDs.

Wang et al. (2012) aimed to study the relationship between the BER and communication distance by conducting an experiment. The researchers followed an experimental methodology framework by proposing an indoor prototype for point-to-point connection and analyzing the results for different distance. In addition, the researchers considered the effect of background light in their experiment. A distance of 1.5m and with data rate of 111.607bit/s was achieved when the illumination was 40lx. Moreover, the researchers concluded that the best distance with lower BER was 85cm. Whereas, the BER is increased when the distance was longer than 90cm.

Ab-Rahman et al. (2012) aimed to study the external factor which affected the indoor VLC mainly the SNR. Therefore, they followed the simulation methodology framework by using MathCAD tools in their study. The performance of single source calculated and the results were analyzed. The researchers found that when the SNR was at the minimum

(15dB), the maximum accepted distance was 3.0785m with angle of incident equal to 56.989°. Moreover, the researcher's explained that theoretically the minimum accepted SNR value was 15dB in the wireless communication. The researchers concluded that the system needed to be optimized to improve the performance and make the system more reliable.

Nguyen et al. (2012) aimed to study the effect of using LED emission cross-sections on VLC systems. The researchers followed a simulation methodology framework to simulate the indoor VLC by using Matlab/Simulink software. Fluctuation in the illumination and optical power distribution were studied by proposing LED emission cross-sections and comparing the result to circular LED. In addition, RMS delay spread and the data rate were compared. The researchers found that emission cross-sections LEDs had less fluctuation than the circular LED. Moreover, the researchers found an increase in RMS delay spread and a decrease in data rate in delay emission cross-sections LEDs. Finally, the researchers concluded that emission cross-sections LEDs were suitable for indoor VLC.

Schmid et al. (2012) aimed to investigate in bidirectional VLC system. Therefore, they followed an experimental methodology framework by using microcontroller and LED in both sides. In addition, microcontroller was used to synchronize the connection which would lead to achieve a bidirectional communication. The researchers achieved their goal and concluded that their proposed idea provided a low data rate and a low power system.

Zhang et al. (2012) aimed to investigate in the impulse and frequency response of VLC diffuse channels. Therefore, the researchers

followed an experiential methodology framework by conducting an experiment on short pulse and frequency sweep techniques. In addition, the researchers investigated the receiver FOV and angle on 3dB bandwidth channel. The researches noticed that 1.8ns was the impulse response and 63MHz was the 3dB bandwidth channel. Moreover, it was noticed that the bandwidth was decreased when the receiver was pointing the optical sources. In addition, 3dB bandwidth channel was decreased when FOV was wider.

Cossu et al. (2012b) followed experimental framework by conducting indoor VLC experiment using RGB LEDs with DMT modulation to test the achievable data rate between two different distances. They noticed that when the distance between the receiver and the transmitter was 2.5m, they achieved 780Mbit/s. Whereas, when the distance was 4m, they achieved 570Mbit/s. They concluded that the distance had effect on the VLC connectivity as it reduced the data rate but the BER was within the effective range.

Schmid et al. (2013) aimed to study the bidirectional VLC ad-hoc network; therefore, they proposed "a software-based VLC physical layer (PHY) and a VLC medium access control layer (MAC)". The researchers followed an experimental methodology framework by developing a prototype using microcontroller. Moreover, to improve the reliability, time synchronization was proposed. The researchers explained that VLC ad-hoc network was suitable for specific areas. The researchers noticed that the data rate was less than 1Mb/s for distance not more than 2m. They approved that such a network was useful for "sensor networks, home networks, smart illumination, or when connecting consumer devices like smart toys".

Ali and Zhang (2013) aimed to provide the best coverage area. Therefore, they investigated in finding the best location for single and multiple LED. In addition, they aimed to gain the minimum accepted received power from those LEDs for indoor VLC. Therefore, the researchers followed a simulation methodology framework for line of sight of VLC by simulation program using Matlab. Moreover, the expected received power was theoretically calculated and the results were studied to get the relationship between the distance and the signal quality. The researchers used the program to calculate the required LED to cover the room areas. In addition, this program was used to calculate the distance between LEDs and the area of illumination. The researchers achieved 1×10^{-4}mW received power for single transmitter at area 27.5m^2 and the height of 5m. The researchers concluded that the power decreased when the distance of the light was increased.

Videv and Haas (2014) aimed to examine spatial shift keying (SSK) VLC system. Therefore, they followed an experimental methodology framework by using a field programmable gate array (FPGA) board. The researchers evaluated the SSK and noticed all the challenges. In addition, below than 2×10^{-3}BER was achieved during the experiment. Moreover, the researchers noticed that the main challenges in SSK were keeping the separation between the received symbols stay the same. Therefore, they proposed a solution for this problem by using polarization filters at both ends. Moreover, they reduce the overlap in FOV by placing the photodiode and the LEDs at a proper positing.

2.7 Outdoor Studies for VLC Application

Several scholars studied the use of VLC for outdoor application. In addition, some of them studied the effect of weather influences such as fog, haze, and interference with sunlight.

For instance, Hu et al. (2007) followed experimental methodology framework by examining the use of the visible red light laser. They noticed that when the visible red light laser was used for free-space optical, that there was some attenuation in the power received. This attenuation was caused by the absorption and the scattering of the atmosphere which caused to lose some data. They concluded that the attenuation of the light was due to gas molecules and aerosol particles.

Mahalati and Kahn (2012) studied the effect of haze, fog and rain which were considered under weather influences on the FSO links using imaging receivers. They followed experimental framework in their research. They studied the link attenuation and the image blooming and noticed that when the fog was heavy or medium the attenuation increased and there was image blooming. Moreover, they found that when the fog was light, the attenuation was less but there was image blooming affecting the performance of the link.

Beshr et al. (2012) followed experimental framework by conducting different experiments around the world to study the effect of the sunlight on VLC in different locations. They examined the performance, the BER and the SNR of the VLC in Cairo and Glasgow during the year, and noticed that there was a different effect of the sunlight on the VLC. They found that sunlight in Cairo had more effect on the VLC than Glasgow during summer. In addition, they noticed that when the sunlight in

summer at the maximum intensity, the performance, and the SNR decreased and the BER increased.

Kumar (2013) presented in IEEE Wireless Communications and Networking Conference an introduction about VLC concept and challenges. Moreover, he presented a case study about safety application for outdoor VLC. He followed experimental framework in his case study to investigate the VLC challenges such as distance and sunlight. He noticed that when the distance increased, the average power received decreased. In addition, he found the BER increased, when the distance increased and the increase was more during the day time than night time due to the sun.

2.8 Summary

To conclude, the previous studies focused on some main points that can be summarized as followings:

- Visible Light Communication is feasible with some main challenges such as LOS, uplink, regulation, and the standardization (George et al., 2014; Jaiswal & Chopade 2013; O'Brien et al., 2008a; Borogovac et al., 2011).
- VLC is applicable for some critical environments such as aviation, hazardous environments, hospitals, and underwater communications (George et al., 2014; Jaiswal & Chopade 2013; Mishra & Salian, 2011).
- VLC has some main advantages such as cost-effective, efficient, safety, high data rate and green technology that has no effect on human health (George et al., 2014).

- High data rate can be achieved with different modulation techniques such as OFDM, optimized discrete multi-tone, TDM, 4-PPM (Afgani et al., 2006; Elgala et al., 2011; Khalid et al., 2012; Grubor et al., 2007; Ghassemlooy et al., 2013).
- An improvement in the performance is noticed with different modulation techniques such as OFDM, MC-VPPM, OPPM,M-QAM, DCO-OFDM and ACO-OFDM (Elgala et al., 2007; Tsonev et al., 2013b; Ghimire et al., 2011; Moon & Jung, 2012; Bai et al., 2010; Wang et al., 2011; Dimitrov et al., 2012).
- An improvement in the performance (i.e. data rate, and bit error rate) is noticed due to improvement in the transmitter and the receiver (Kizilirmak, 2013; O'Brien et al., 2008b; Elgala et al., 2009; He et al., 2013; Uddin et al., 2011; Borogovac et al., 2010; González, 2012; González et al., 2014).
- There is a direct inverse relationship between distance and power (Ali & Zhang, 2013).
- VLC is feasible and can be used in platoon control, position system, advanced driver assistant systems, and vehicle-to-vehicle and vehicle-to-infrastructure data broadcasting (Abualhoul et al., 2013; Kumar et al., 2006; Nguyen & Jang, 2013; Lee et al., 2012).
- VLC is secure because it cannot pass through the wall (Hapani et al., 2013).
- More than 1Gbit can be achieved by using different modulation with RGB LEDs (Cossu et al., 2012a; Chun et al., 2014).
- Bidirectional VLC system is feasible (Schmid et al., 2012).
- Weather influences such as fog, rain, and haze affect the performance of the VLC (Hu et al., 2007; Mahalati and Kahn, 2012).

- Sunlight has a different effect on the performance of the VLC based on the time and the location worldwide (Beshr et al., 2012; Kumar, 2013).
- Bit rate is dependent on the distance and limited by modulation used and LEDs response time (Kumar, 2014).
- OOK and VPPM modulation are standardised by IEEE for VLC, whereas, OFDM, OPPM, and WDM are not. In addition, OOK, VPPM, and OPPM provide more luminance, whereas, OFDM needs more array of LEDs to provide the same luminance. Moreover, OFDM and WDM perform better than OOK, VPPM, and OPPM. Besides, OOK and VPPM have lower bit rate, whereas, OFDM, OPPM, and WDM have higher bit rate (Elgala et al., 2007; Elgala et al., 2009; Bai et al., 2010; Cossu et al., 2012a).

We got to benefit from listing and discussing the previously done research that set the key background and applications of Visible Light Communication. It gives significant theoretical insights that are important in implementing the research and analyzing the findings. Besides, the literature on weather influence on VLC gives the researcher a beneficial background to conduct his research. Moreover, the researcher benefit from the research that used a simulation methodology approach from different aspects as the researcher aims to use simulation methodology as well. Hopefully, this research will get use of the previous literature and contribute to the VLC research by tackling a VLC area that was not addressed by previous research as it is studying the effect of sandstorm on V2LC VLC communication.

Chapter Three

Methodology

3.1	Research Methods	
3.2	Research Model and Tools	
3.3	Research Approach	
3.4	Research Procedures	
	3.4.1	Theoretical Background
	3.4.2	The Simulation Equation
	3.4.3	Noise Effect Calculation
	3.4.4	VLC Modulation

Chapter Three: Methodology

The research on the field of Visible Light Communication (VLC) technology is new and it is open for more investigation. Therefore, this research aims to investigate the weather influences on outdoor VLC and fill the gap in the literature as little research has been conducted in this area. Most of the past research on VLC has focused on the laboratory and there is few research that studied this technology in the commercial field (Liu et al., 2011; Sagotra & Aggarwal, 2013). There are many areas that can benefit from such a technology in the commercial sector but only some of these areas the researchers started to investigate such as vehicle-to-road communication and indoor positioning system which is under investigation by Nakagawa Laboratory (Kim et al., 2011; Lee and Kavehrad, 2012), COWA at Penn State (Panta & Armstrong, 2012; Horikawa et al., 2003; Yoshino et al., 2008; Zhang & Kavehrad, 2012) and others. This chapter aims to outline the research methodology used in this thesis and the tools used.

3.1 Research Methods

This thesis is based on a theoretical and simulation framework. A simulation for vehicular to road VLC (V2LC) system application has been conducted on different sandstorm conditions.

It is noticed that the past research used three key approaches when using the simulation methodology. The first approach focused on the improvement of the VLC hardware. The second approach focused on testing VLC applications. Whereas, the third approach focused on the improvement of the VLC modulation. This research will take the second approach that has focused on testing the VLC applications. This will be

achieved through investigating VLC technology by simulating the vehicular to road VLC (V2LC) application to study the effect of the Arab Gulf environment and weather on VLC technology. The main contribution of this research is to fill the gap in the literature as no research is conducted to study the effect of sandstorm on the use of VLC which is an important weather influence in the Arab Gulf region.

3.2 Research Model and Tools

The original aim of the research is to conduct a simulation and implement a prototype to examine the VLC in the real life but due to the lack of the availability of the testing Lab and equipment, the researcher focused on a simulation approach using MATLAB R2013a. The idea of the V2LC application is based on Kumar et al. (2006) research that proposed V2LC application. This application uses the traffic light as the transmitter and the car as the receiver as shown in Figure 3.1. The used simulation approach is based on implementing the proposed application of Kumar et al. and investigating the effect of weather influences of sand and dust storms on this application. The researcher investigates the red led traffic light as the transmitter. Besides, the simulation design uses traffic light with the height of 3 meters and the distance between the receiver and the traffic light is 2.05 meter height. Moreover, the simulation design range is 10 meters for the road width and 500 meters for the road length. In addition, the researcher fixes the temperature in the simulation on 32°. Different simulation scenarios are conducted to examine the VLC in different weather influences as follow:

1. Simulating VLC on clear weather.
2. Simulating VLC on a low, medium, and high-density sand and dust storm.

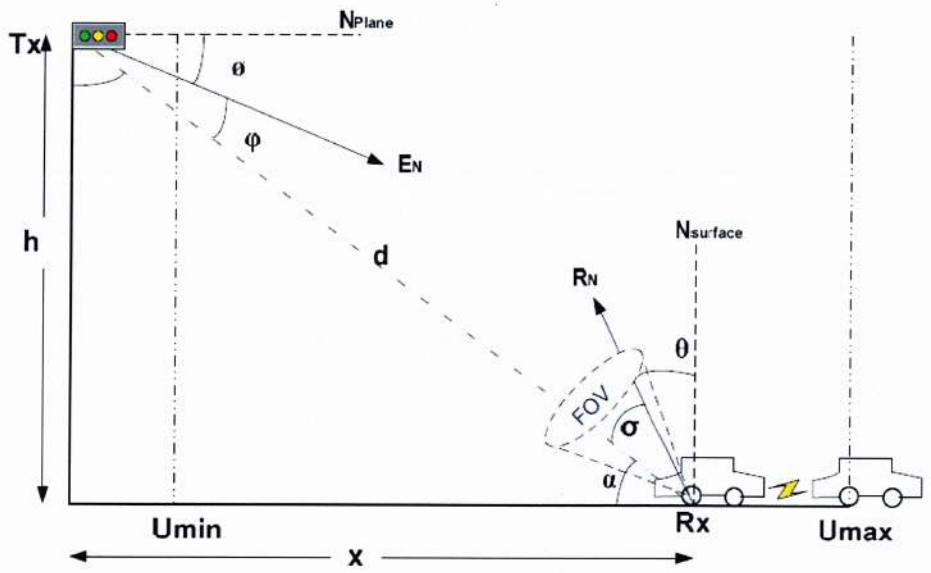


Figure (3.1)

Kumar et al. V2LC proposed application (Kumar et al., 2006)

3.3 Research Approach

Simulation is a powerful tool that helps researchers investigate and find solutions to different problems. It can answer the question "what will happen if I did this" which is beneficial to study different scenarios. Moreover, the simulation approach depends on the data inputs and the theoretical equation. When the researcher uses mathematical equations with realistic and accurate data, the results will be the same as the experiments (Sargent, 2005). The simulation approach has been used by different researchers in developing their proposed modulation techniques such as OFDM modulation, M-QAM, and MC-VPPM (Afgani et al., 2006; Wang et al., 2011; Moon & Jung, 2012). In addition, simulation was used in studying the VLC application such as advanced Driver Assistant Systems, channel delay profiles for automotive applications, platoon control, and three-dimensional positioning techniques (Kumar et al., 2006; Lee et al., 2012; Abualhoul et al., 2013; Nguyen & Jang, 2013).

Moreover, other researchers used the simulation approach to improving the use of transmitters and the receivers such as Cui et al. (2010) who used image sensor for VLC receivers. In addition, Uddin et al. (2011) proposed a method to keep the receiver output current stay the same and reduce the performance variation in VLC when multicolour channels were used. Besides, Kizilirmak (2013) studied the impact of repeaters on the performance of indoor VLC. Additionally, the simulation was used to implement an indoor VLC (Wu and Little, 2010; Nguyen et al., 2010; Ab-Rahman et al., 2012).

3.4 Research Procedures

To implement a correct simulation approach, the researcher starts first to study the theoretical background of the problem and derive a mathematical equation that represents the behaviour of the system. Secondly, the researcher writes a simulation program that uses the derived equation with different parameters and then derives the output. The simulation starts by converting the derived mathematical equation into MATLAB code. Both input and output parameters are defined for each scenario.

3.4.1 Theoretical Background

Visible light communication is operated on the visible light which wavelength is between 400nm to 700nm. Therefore, the researcher needs to consider all the influences that affect the visible light and to define the methods for calculating these influences. One of these influences is the dust and sandstorm which happens in the dry climate and desert area. Moreover, sandstorm can occur even in other areas due to the dust and sand movements with the heavy wind which create a phenomenon named sandstorm wall as shown in Figure 3.2 ("Dust", 2011).

In addition, the researcher seeks to find the parameters which could be used in the calculation methods before planning the communications approach. Therefore, based on the past literature, the thesis studies and uses some of the communication methods which other researchers used in their simulation.

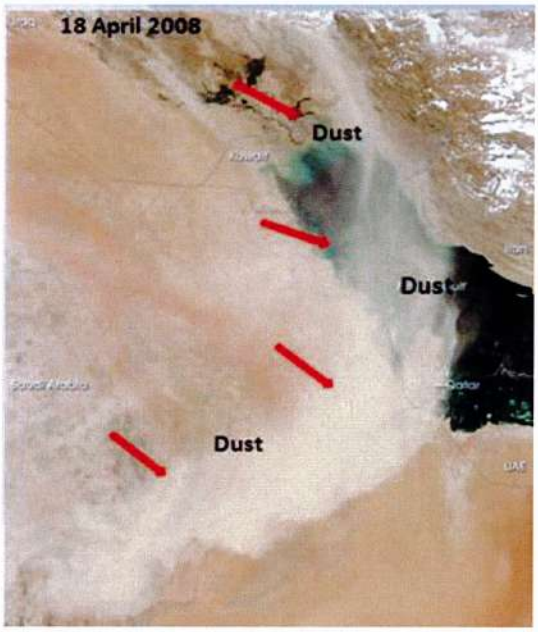


Figure (3.2)

Sandstorm wall ("Dust", 2011).

Sand and dust storm can be defined as the phenomenon which is caused by the turbulent and strong wind when it happens on dry climate or desert to move the loose soil. This weather phenomenon affects the horizontal visibility and reduces it to less than 1 Km. Due to the Arab Gulf dry climate and the Empty Quarter Desert in Saudi Arabia, the Arab Gulf countries are affected frequently by sand and dust storm according to The Ministry Of Transportation, Bahrain Meteorological Directorate as shown in Figure 3.3, 3.4, and 3.5 ("Dust", n.d.).

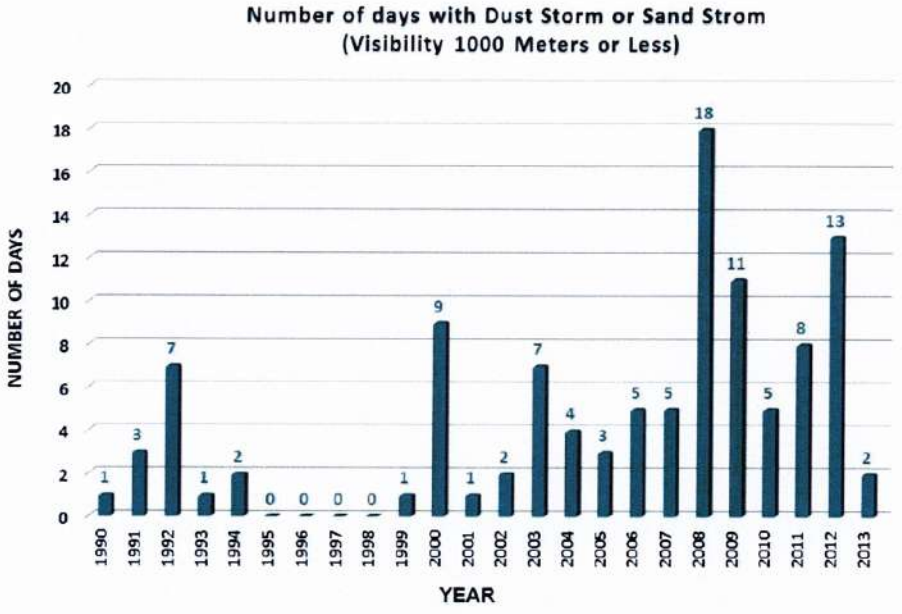


Figure (3.3)

Number of days with dust storm or sand storm when visibility 1Km or less ("Dust", n.d.).

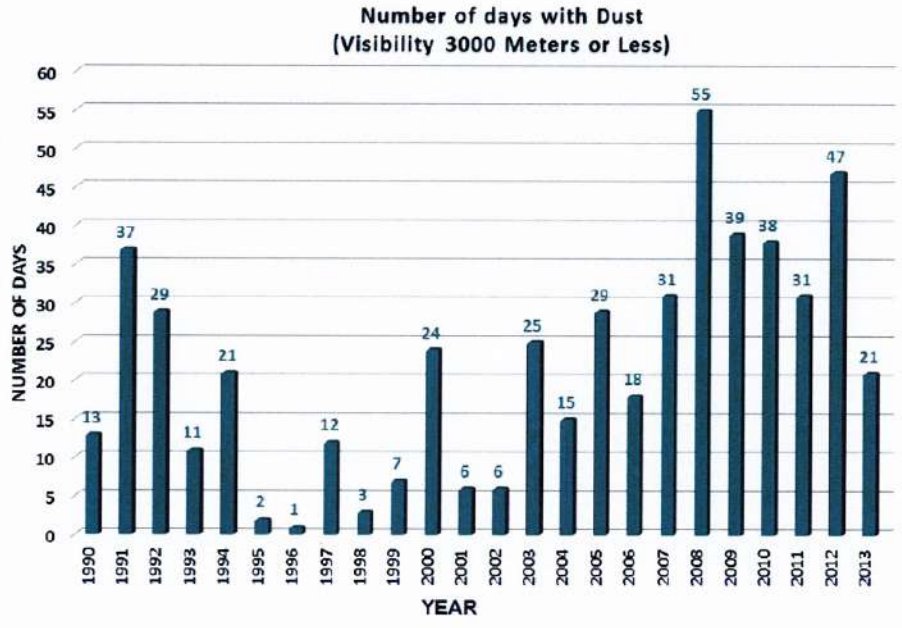


Figure (3.4)

Number of days with dust storm or sand storm when visibility between 1Km and 3Km ("Dust", n.d.).

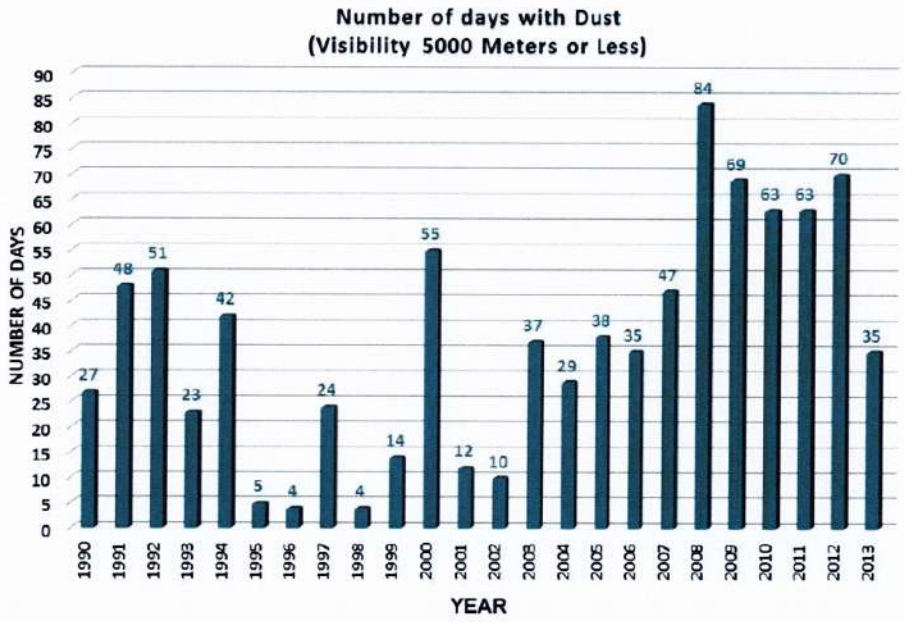


Figure (3.5)

Number of days with dust storm or sand storm when visibility between 3Km and 5Km ("Dust", n.d.).

Moreover, Arab Gulf countries are affected by three main types of dust and sand storm which come from Iraq, Iran, and Empty Quarter Desert in Saudi Arabia. There are different types of dust such as mineral dust which contains quartz sand, calcite, and loess. The other type of dust is metallic dust which contains lead, cadmium, nickel, and beryllium. Moreover, chemical dust is another type of dust which contains bulk chemicals and pesticides. Besides, organic and vegetable dust is considered as other types of dust which contains flour, wood, cotton, and tea. The biohazard is the last types of dust which contains viable particles, moulds, and spores (Péwé & "American Association for the Advancement of Science", 1981; "World Health Organization", 1999). The Arab Gulf countries are affected by mineral dust which mainly contains clay particles that have a size less than 2 microns and silt particles that have a size between 2 to 74 microns. In addition, they are

affected by sand and gravel particles that have a size larger than 74 microns ("Dust", 2011).

3.4.2 The Simulation Equation

Visible light communication consists of a transmitter which is the LED and a receiver which is the photodiode. Photodiode converts the received illumines into current; therefore, the researcher needs to study the power received to calculate the signal power. From the past literature, researchers used the following equation to study the power gain in the receiver (P_r) (Uddin et al., 2011):

$$P_r = P_t.\frac{(m_l+1)A}{2\pi d^2} cos^{m_l}(\theta).T_s(\Psi).g(\Psi).cos(\Psi), 0 \leq \Psi \leq \Psi_{con} \qquad (1)$$

Where:

P_t: Transmitted power from a LED.

m_l: Order of Lambertian emission.

A: Photo-detector area.

d: Distance between transmitter and receiver.

θ: Angle of irradiance.

Ψ: Angle of incidence.

$T_s(\Psi)$: Signal transmission coefficient of an optical filter.

$g(\Psi)$: Gain of an optical concentrator.

Ψ_{con}: Receiver field of view (FOV).

$$m_l = -\frac{ln(2)}{ln(cos\,\Phi_{1/2})} \qquad (2)$$

Where:

$\Phi_{1/2}$: Transmitter half power angle

$$g(\Psi) = \begin{cases} \frac{n^2}{sin^2\Psi_{con}}, & 0 \leq \Psi \leq \Psi_{con} \\ 0, & 0 \geq \Psi_{con} \end{cases} \qquad (3)$$

Where:

n: Internal refractive index of the optical concentrator.

3.4.3 Noise Effect Calculation

It is noticed from the past literature that some researchers used white Gaussian noise to calculate the noise in the receiver's side. Whereas, other researchers used shot noise with the thermal noise to calculate the total noise. In the thesis, the researcher used the following equation which takes into consideration both the thermal and shot noise to calculate the photo-detector current (Uddin et al., 2011):

$$I(t) = \gamma P_i(t) \otimes h(t) + N(t) \qquad (4)$$

Where:

$I(t)$: Photo-detector current.

γ : Photosensitivity of the photo-detector (in A/W).

$P_i(t)$: Instantaneous input power.

$\otimes$: Denotes linear convolution.

h(t): Resembles the impulse response.

$N(t)$: Total noise

$$N = \partial^2 s + \partial^2 th \qquad A^2 \quad (5)$$

Where:

N: Sum of the both shot and thermal noise.

∂s: Shot noise.

∂th: Thermal noise

Shot noise is the combination of both the vehicle rear LEDs and the surrounding lights from other resources during the day time and it can be calculated using the following equation (Uddin et al., 2011):

$$\partial^2 s = 2q\gamma\left(P_{r\,signal}\right)B + 2q\gamma.P_{bg}I_2B \qquad A^2 \ (6)$$

Where:

q: Electronic charge.

B: Equivalent noise rectangular transmitter pulse shape.

P_{bg}: Background noise power.

The following equation can be used for the thermal noise (Petković et al., 2014; Teich & Saleh, 1991; Mahalati & Kahn, 2012):

$$\partial^2 th = \frac{4kT_kB}{R} \qquad A^2 \ (7)$$

Where:

k: Boltzmann's constant.

T_k: Temperature in Kelvin.

B: Bandwidth.

R: Shunt Resistance.

3.4.4 VLC Modulation

The researcher noticed that there are different modulation approaches that can be used to implement the VLC. Elgala et al. (2011), Vucic and Langer (2012), Tsonev et al. (2013b) explained the possibility and the modulation of VLC. In addition, Afgani et al. (2006), Elgala et al. (2007), Bai et al. (2010), Wang et al. (2011), Di Renzo et al.(2014) and other researchers investigated the VLC modulation such as OOK, M-

QAM, OPPM, spatial modulation for MIMO, and OFDM. In this research, the OOK modulation is chosen because it provides more luminance, standardised by IEEE, and it is more practical to implement. Besides, the calculation of the BER depends on the modulation used. As the researcher is using OOK modulation, the following equation is applicable for the BER and the SNR (Uddin et al., 2011):

$$BER = Q\left(\sqrt{SNR}\right) \quad (8)$$

$$Q(x) = \frac{1}{2\pi}\int_{x}^{\infty} e^{-y^2/2}dy \quad (9)$$

$$SNR = \frac{S}{N} \quad (10)$$

Where S is signal and N is total background noise (Gupta and Sharma, 2014).

$$S = \gamma^2 P_r^2 \qquad A^2 \quad (11)$$

Where:

P_r: Power received in the photodiode.

γ: Photosensitivity of the photo-detector (in A/W).

Furthermore, the performance of the VLC can be affected by the sunlight when the sun beams in the same direction of the visible light link. In addition, VLC connectivity is affected by the weather influences. Those influences consist of molecular species and aerosols which are a small suspended particle. In addition, these influences cause absorption, scattering, and scintillation for the light. Moreover, they reduce the power of the illumine which causes attenuation. This attenuation affects the received power in the photodiode. Therefore, the researcher investigated

the light attenuation to calculate the actual received power in the photodiode. Chen (1975) studied the attenuation of electromagnetic radiation by haze, fog, clouds, and rain. In addition, Buys and Janssen (1981) used the Beer Lambert-Bouguer's law to calculate the attenuations in the lights when there are rain and snow. Moreover, Tamošiūnaitė et al. (2011) used the Beer Lambert-Bouguer's law to calculate the atmospheric attenuation due to humidity. Therefore, in this thesis, the researcher decides to use Beer Lambert-Bouguer's law as well in the calculation to get a benefit of the previous studies in every proposed scenario.

$$P_r = P_t \cdot e^{(-l\varepsilon)} \qquad (12)$$

Where:

P_t: Transmitted power.

P_r: Received power.

l: Distance between the transmitter and the receiver.

ε: Extinction coefficient.

To simplify the Beer Lambert-Bouguer's law, the researcher starts investigating it in the way of producing the extinction coefficient ε. The researcher finds that Rayleigh scattering (molecular scattering), aerosol absorption, and aerosol scattering (Mie scattering) are producing the extinction coefficient. Therefore, the researcher starts studying each scattering and absorption separately to use it in the calculation in the thesis.

The attenuation from the Rayleigh scattering is based on the interaction between the light illumine and the atmosphere particles and gases which are smaller than the wavelength (Taylor, 2000; "P.1817",

2012). The Rayleigh scattering produced an extinction coefficient as follows:

$$\beta_m(\lambda) = \frac{24\pi^3}{\rho\lambda^4} 10^3 \left(\frac{[n(\lambda)]^2 - 1}{[n(\lambda)]^2 + 2}\right)\left(\frac{6 + 3\delta}{6 - 7\delta}\right) \qquad (13)$$

Where:

$\beta_m(\lambda)$: Molecular scattering coefficient (km^{-1})

λ: Wavelength (μm)

ρ: Molecular density (m^{-3})

δ: Depolarization factor of the air ($\cong 0.03$)

$n(\lambda)$: Refractive index of air.

An approximate value of $\beta_m(\lambda)$is:

$$\beta_m(\lambda) = A\lambda^{-4} \qquad (14)$$

Where:

$$A = 1.09 * 10^{-3} \frac{P}{P_0} \frac{T_0}{T} \quad km^{-1}m^4 \qquad (15)$$

And

P: Atmospheric pressure (mbar).

P_0: 1013 mbar.

T: Atmospheric temperature (K).

T_0: 273.15 K.

In addition, aerosol absorption is based on the interaction between the illumine with a solid or liquid particles such as ice, dust, smoke, and fog which is available in the atmosphere (Taylor, 2000; "P.1817", 2012). These particles flow in the atmosphere or fall with very low speed. Besides, their sizes are usually between 10^{-2} and 100μm ("P.1817",

2012). The following equation shows how the extinction coefficient is calculated from the aerosol absorption:

$$\alpha_n(\lambda) = 10^5 \int_0^\infty Q_a\left(\frac{2\pi r}{\lambda}, n''\right)\pi r^2 \frac{dN(r)}{dr} dr \qquad km^{-1} \quad (16)$$

Where:

λ: Wavelength (μm).

$dN(r)/dr$: Particle size distribution per unit of volume (cm^{-4}).

n'': Imaginary part of the refractive index, n, of the considered aerosol.

r: Radius of the particles (cm).

$Q_a(2\pi r/\lambda, n'')$: Absorption cross-section for a given type of aerosol.

Moreover, when the particles size is less than or equal to the wavelength of the beam light, a scattering for the beam light occurred which is called Mie scattering. In addition, to calculate the extinction coefficient for the Mie scattering the following equation can be used:

$$\beta_n(\lambda) = 10^5 \int_0^\infty Q_d\left(\frac{2\pi r}{\lambda}, n'\right)\pi r^2 \frac{dN(r)}{dr} dr \qquad km^{-1} \quad (17)$$

Where:

λ: Wavelength (μm).

$dN(r)/dr$: Particle size distribution per unit of volume (cm^{-4}).

n': Real part of the refractive index n of the aerosol.

r: Radius of the particles (cm).

$Q_d(2\pi r/\lambda, n')$: Scattering cross-section for a given type of aerosol.

The attenuation of the aerosol scattering and absorption is difficult to expect due to the concentration, composition and the sizes of the particles. Therefore, the researcher decided to use those mathematical equations to calculate the effect of sand and dust storm particles on VLC.

Additionally, the aerosol absorption and scattering depend on the particles refractive index and illumine wavelength. Therefore, the researcher started investigating the particles sizes for each scenario and the refractive index of those particles. Moreover, it is noticed that refractive index consists of two parts: the first part is the real n' which is responsible for the scattering; and the second part is the imaginary n'' which is responsible for the absorption ("P.1817", 2012).

Finally, to solve equation (16) and (17), the researcher needs to find the sand and dust storm density. Therefore, the researcher investigates how they can calculate the density and it is found that the previous researchers used the visibility to determine the density as follows (Chu, 1979; Alhaider, 1986; Goldhirsh, 2001; Elabdin et al., 2008; Elshaikh et al., 2009):

$$V = \frac{5.5 \times 10^{-4}}{N a_e^2} \qquad km \quad (18)$$

Where:

a_e: Equivalent particle radius (m).

N: Particle density (number of particles/m^3).

From visibility the researcher can get the density as follows:

$$N = \frac{5.5 \times 10^{-4}}{V a_e^2} \qquad m^{-3} \quad (19)$$

Chapter Four

Results, Discussion and Recommendations

4.1	Simulation Scenarios
	4.1.1 Experiment 1: Simulate Clear Weather
	4.1.2 Experiment 2: Simulate the Effect of Clay Particles on VLC
	4.1.3 Experiment 3: Simulate the Effect of Silt Particles on VLC
	4.1.4 Experiment 4: Simulate the Effect of Sand Particles on VLC
	4.1.5 Experiment 5: Simulate the Effect of Gravel Particles on VLC
4.2	Discussion of the Results

Chapter Four: Results, Discussion and Recommendations

This research studies the effect of sand and dust storms on the visible light communication through simulating the transmitted and received light through different types of sandstorms. Although the investigation on VLC started since 2003 in Japan, no research to the best of our knowledge has investigated the influence of the sandstorm on the VLC, a phenomena that is frequently occurring in the Arab Gulf countries, Middle East and other parts of the world. In addition, most of the previous researchers focused on the use of the VLC for indoor purpose and only a few researchers studied the effect of weather influence on VLC such as the effect of fog and thc effect of the sun on the transmission.

This research focuses on the effect of sandstorm on VLC. The researcher first starts studying the types of the sandstorm that are popular in the Gulf region. According to dust research report which was published by National Center of Meteorology and Seismology (NCMS) in the United Arab Emirates, Gulf countries are affected by sandstorms that are originating from the Kingdom of Saudi Arabia, Iraq, and Iran ("Dust", 2011). The sandstorms which came from these areas contain four types of particles and these particles are clay, silt, sand, and gravel.

Based on this study, the researcher starts the research by investigating the effect of the sandstorm on the VLC when the sandstorm contains one of these particles types. In addition, the researcher conducts different simulation experiments for these particles with different scenarios. Due to the scattering and the absorption of the light when there

is a sandstorm, the research takes the 500 meters distance between the transmitter and the receiver as a pattern for the research. Moreover, the researcher considered the density, radius, and the refractive index of the particles in the research because they affect the transmission as well. Besides, to calculate the density of the particles, the researcher has to study the road visibility. Therefore, the researcher focuses in the thesis on studying the effect of the sandstorm and dust storm by knowing the visibility, radius, and the refractive index of the particles.

4.1 Simulation Scenarios

The researcher conducts five different experiments that included different simulation scenarios to investigate the effect of the sandstorm and dust storm on the VLC. These experiments are based on the proposed simulation scenarios in chapter three and the experiments are as follow:

- Experiment 1: Simulating VLC in clear weather.
- Experiment 2: Simulating VLC in the storm that has low, medium, and high density clay particles.
- Experiment 3: Simulating VLC in the storm that has low, medium, and high density silt particles.
- Experiment 4: Simulating VLC in the storm that has low, medium, and high density sand particles.
- Experiment 5: Simulating VLC in the storm that has low, medium, and high density gravel particles.

The researcher chooses these experiments based on the study of National Centre of Meteorology and Seismology (NCMS) in the United Arab Emirates which mentions the types of the particles that are affecting the Arab Gulf countries during the time of the sandstorm. In addition, the

researcher fixes the simulation temperature at 32° based on the average temperature which is noticed by NCMS (see Appendix A Table A.1 for the calculated distance for the simulations scenarios).

4.1.1 Experiment 1: Simulation of Clear Weather

The first experiment simulates the effect of the oxygen molecular when the weather is clear and the visibility is 10 Km and the other input parameters as shown in Table 4.1. The parameters used to simulate clear atmosphere are based on several past studies (Edgar & Close, 1998; "Dust", 2011; Hong et al., 2008; "Periodic table", n.d.; Uddin et al., 2011; "Photovoltaic Series", n.d.; Otas et al., 2012; Ab-Rahman, 2012; Lo, 2004; Abualhoul, 2013).

Table (4.1)

The parameters used to simulate clear atmosphere

LED Power	30 mW
Number Of LED	620
Receiver area, A	9e-5 m^2
Distance between source and receiver	2.05 m
dimension in meter	lx=500 m ly=10 m lz=3 m
Field of view of a receiver, FOV	60°
Semi-angle at half power	60°
Photodiode responsibility	0.43 A/W
Gain of an optical filter, Ts	1
Refractive index of a lens at a Photodiode	1.5
Boltzmann's constant, k	$1.3806488X10^{-23}$ J/K
Fix temperature	273.15 K
Fix pressure	1013 mbar

Medium refractive index (Air)	1.003+0i
Electronic charge, q	1.602176487e-19 C
Background Power	0.009444 w
Bandwidth	$10X10^{6}$ Hz
Shunt Resistance, R	$20X10^{6}$ omh
Red LED Light wave	0.644 um
Visibility	**10 km**
Atmospheric pressure	**1017 mbar**
Atmospheric temperature	32 °C = 305.15 K
Particle refractive index	**1.000271+0i**
Particle radius	**$4.8X10^{-9}$ cm**

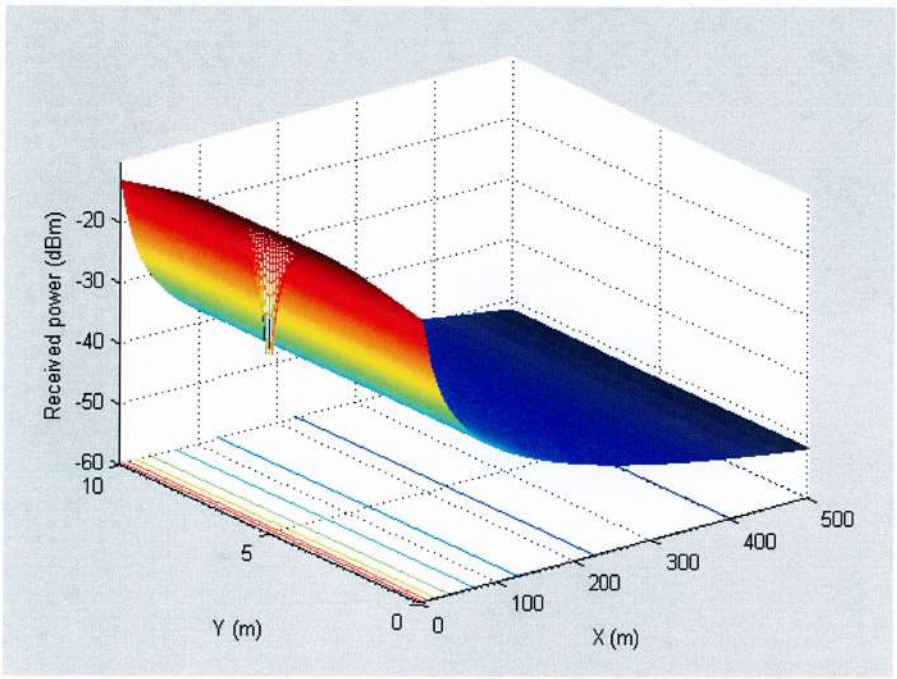


Figure (4.1)

The received power when the weather condition is clear atmosphere

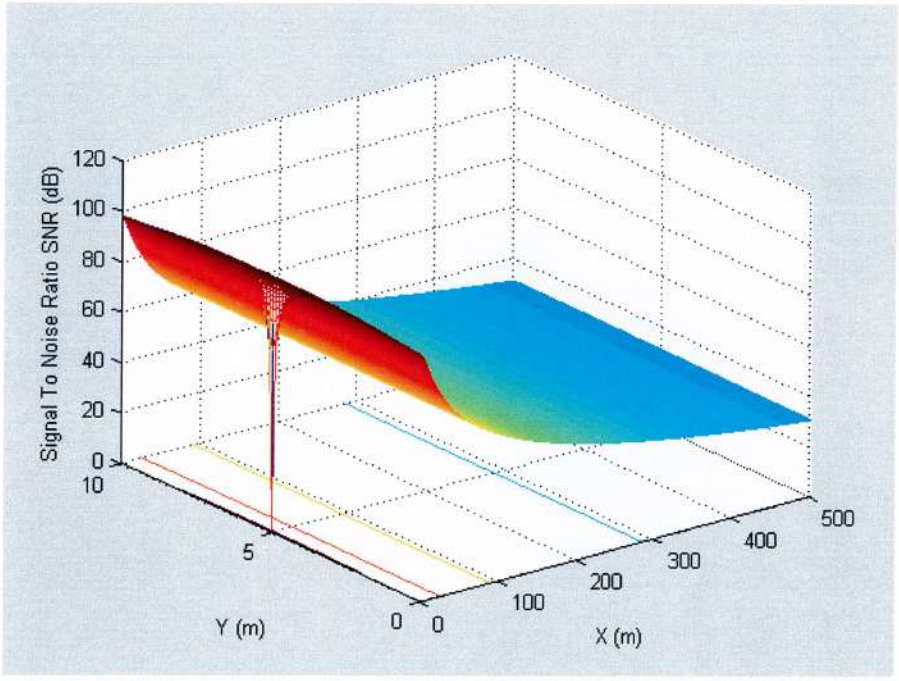


Figure (4.2)

The signal to noise ratio (SNR) when the weather condition is clear atmosphere

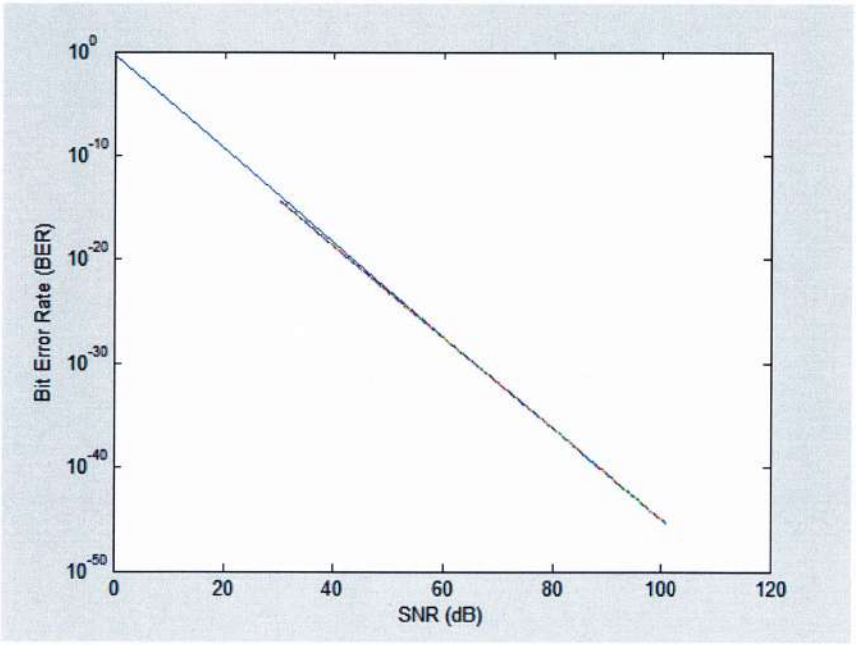


Figure (4.3)

The bit error rate (BER) when the weather condition is clear atmosphere

After conducting the first simulation scenario when the visibility is 10 Km and the weather is clear, the researcher notices that there are two different degradations in the power received. The first degradation in the power received is due to the distance increase. It is noticed that when the distance between the transmitter and the receiver is 2.864m, the power received is (-10.221) dBm, the signal to noise ratio SNR is (100) dB and the bit error rate BER was (4.6E-46). Whereas, when the distance reaches 500 m, the power received reaches (-51.955) dBm and the SNR is (30.114) dB and the BER records (4.2E-15) as shown in Figure 4.1, 4.2, and 4.3 (see Appendix A Table A.2, A.3, and A.4 for the simulation results). The second degradation in the power received is due to the weakness of the signal in the short distance when the line of sight decreases. The researcher notices that when the distance between the transmitter and the receiver decreases less than 2.864 m, the power received decreases to less than (-10.221) dBm. For example, the researcher notices that the power received reaches -12.287 dBm when the distance is 2.281 m, and the SNR reaches 98.617 dB which causes the BER to increase up to 4.2E-45. Moreover, when the distance between the transmitter and the receiver reaches 2.05, the researcher notices that there is no power received, the SNR reaches 0 dB, and the BER reaches the maximum 5.0E-01. This is because there is no line of sight as shown in Figure 4.1, 4.2, and 4.3 (see Appendix A Table A.2, A.3, and A.4 for the simulation results).

4.1.2 Experiment 2: Simulation of the Effect of Clay Particles on VLC

The second experiment simulates the effect of the clay particles on the VLC with different sandstorm visibility scenarios (Alexander et al.,

2013; "Dust", 2011). The first scenario is for simulating low density clay particles sandstorm when the visibility is 5 Km as shown in Table 4.2.

Table (4.2)

The parameters used to simulate clay (Montmorillonite) particles with the visibility 5 Km

Visibility	**5 km**
Atmospheric pressure	**1000 mbar**
Particle refractive index	**1.523 + i3.8E–5**
Particle radius	**1X10^{-4} cm**

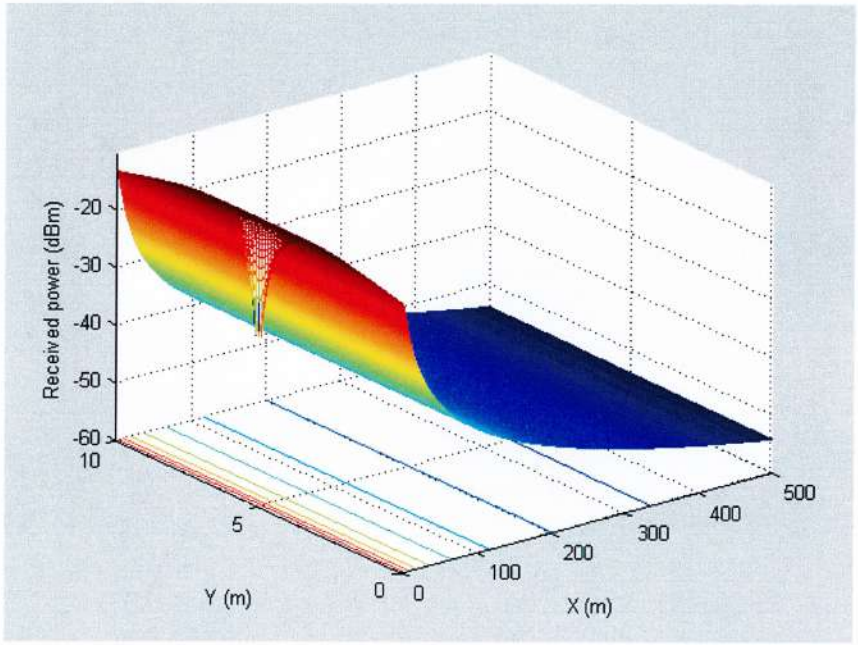


Figure (4.4)

The received power for the VLC affected by clay particles when the visibility is 5 Km

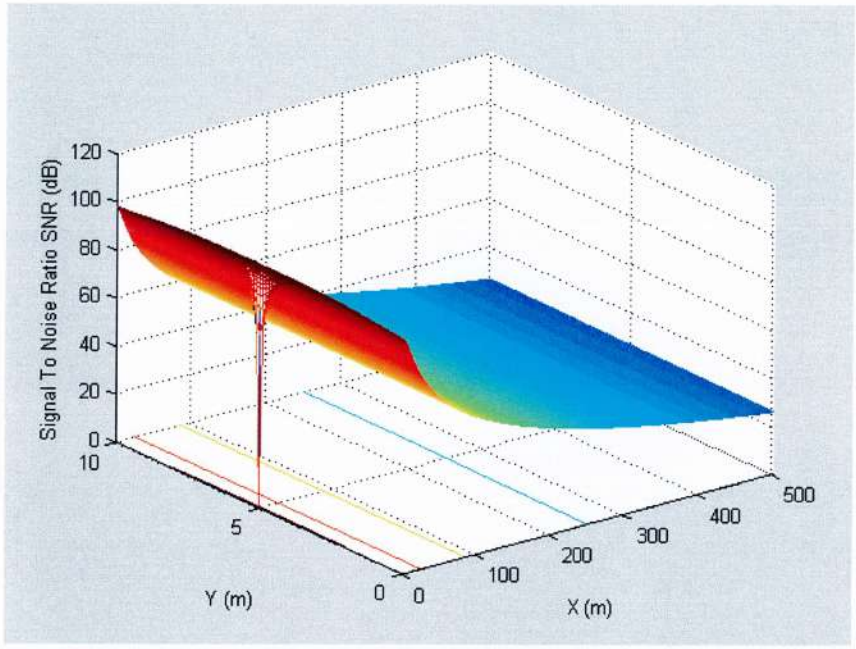


Figure (4.5)

The signal to noise ratio (SNR) for the VLC connectivity affected by clay particles when the visibility is 5 Km

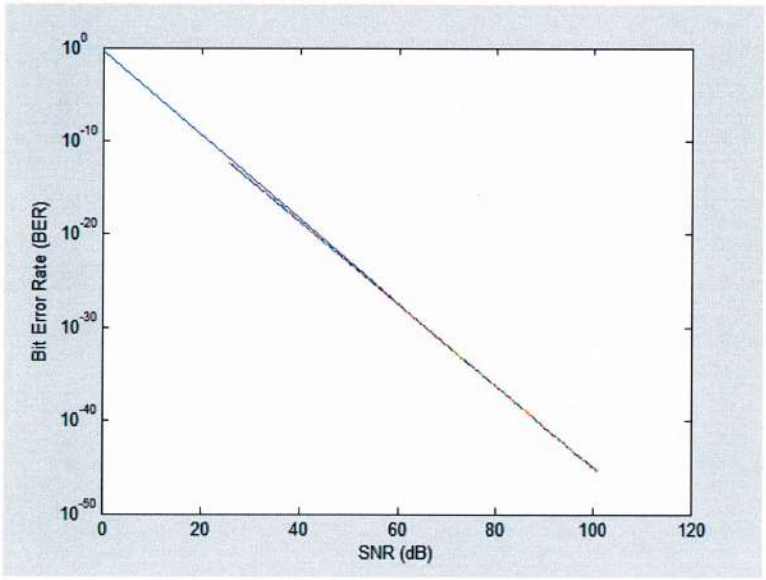


Figure (4.6)

The bit error rate (BER) for the VLC connectivity affected by clay particles when the visibility is 5 Km

The first scenario simulates the effect of low density sandstorm with clay particle on the VLC. The result of the simulation when the visibility is 5 Km shows that there are two different degradations in the power received. The first degradation in the power received is due to the distance increases and the effect of clay particle density. It is noticed that when the distance between the transmitter and the receiver is 2.864m, the power received is -10.234 dBm, the signal to noise ratio SNR is 100 dB and the bit error rate BER was 4.6E-46. Whereas, when the distance reaches 500m, the power received reaches -54.166 dBm and the SNR is 25.694 dB and the BER records 3.8E-13 as shown in Figure 4.4, 4.5, and 4.6 (see Appendix A Table A.5, A.6, and A.7 for the simulation results). The second degradation in the power received is due to the weakness of the signal in the short distance when the line of sight decreases. The researcher notices that when the distance between the transmitter and the receiver is 2.281 m, the power received comes down to -12.297 dBm. In addition, the researcher notices that SNR reaches 98.606 dB which causes the BER to increase up to 4.2E-45. Moreover, when the distance between the transmitter and the receiver reaches 2.05, the researcher notices that there is no power received, the SNR reaches 0 dB, and the BER reaches the maximum 5.0E-01. This is because there is no line of sight as shown in Figure 4.4, 4.5, and 4.6 (see Appendix A Table A.5, A.6, and A.7 for the simulation results).

The second scenario simulates the effect of medium density clay particles sandstorm on the VLC when the road visibility is 1 Km as shown in Table 4.3.

Table (4.3)

The parameters used to simulate clay (Montmorillonite) particles with visibility 1 Km

Visibility	**1 km**
Atmospheric pressure	**700 mbar**
Particle refractive index	**1.523 + i3.8E–5**
Particle radius	**$1X10^{-4}$ cm**

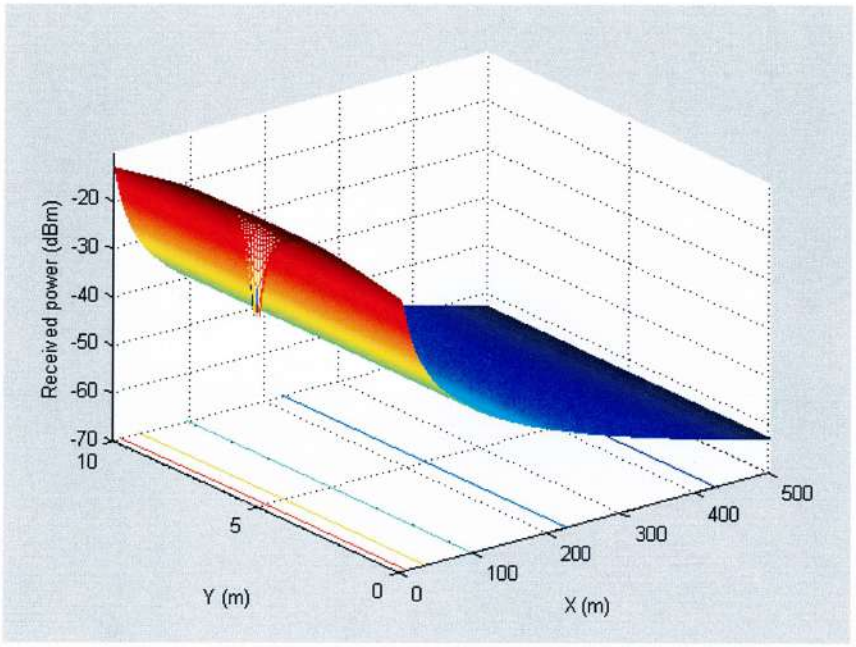


Figure (4.7)

The received power for the VLC affected by clay particles when the visibility is 1 Km

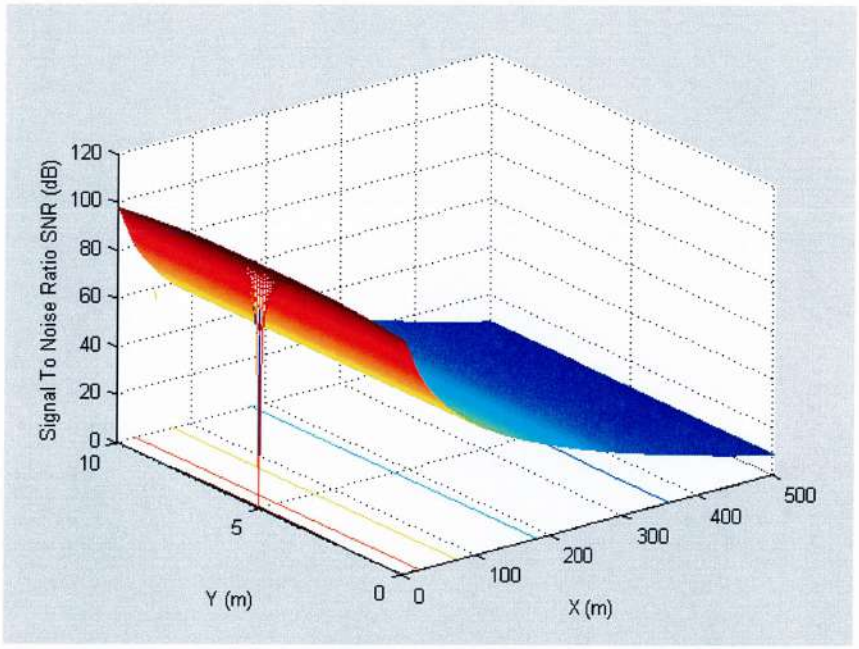


Figure (4.8)

The signal to noise ratio (SNR) for the VLC connectivity affected by clay particles when the visibility is 1 Km

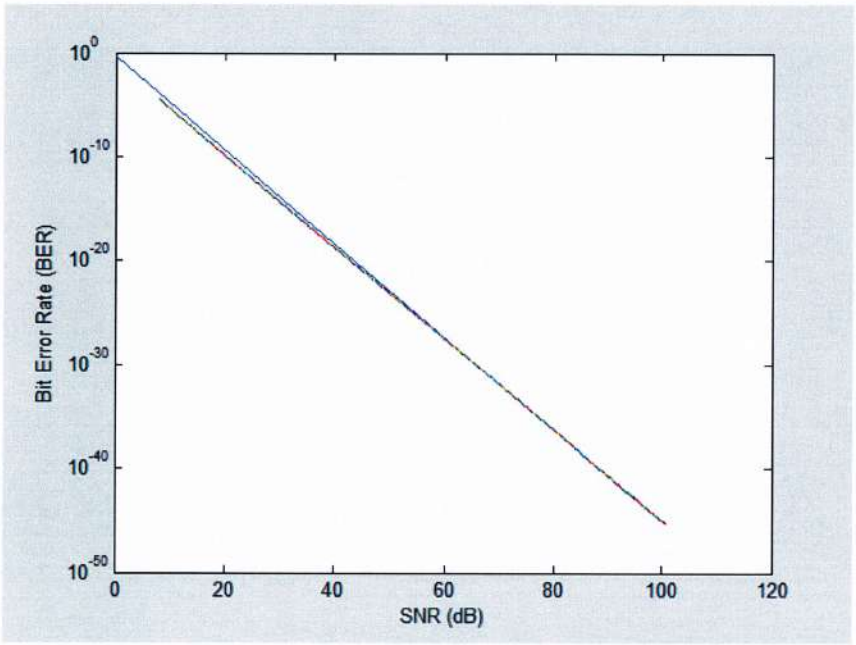


Figure (4.9)

The bit error rate (BER) for the VLC connectivity affected by clay particles when the visibility is 1 Km

The second scenario simulates the effect of the medium sandstorm with clay particles on the VLC. The result of the simulation when the visibility is 1 Km shows that there are two different degradations in the power received. The first degradation in the power received is due to the distance increase and the effect of clay particle density. The researcher notices that when the distance between the transmitter and the receiver is 2.864m, the power received is -10.284 dBm, the signal to noise ratio SNR is 100 dB and the bit error rate BER was 4.9E-46. As Ab-Rahman et al. (2012) noticed that the minimum acceptable SNR is 15 dB, therefore the minimum achievable power received in this research is -59.936 dBm at distance 425 m and the BER records 5.2E-08 as it is shown in Figure 4.7, 4.8, and 4.9 (see Appendix A Table A.8, A.9, and A.10 for the simulation results). The second degradation in the power received is due to the weakness of the signal in the short distance when the line of sight decreases. The researcher notices that when the distance between the transmitter and the receiver is 2.281 m, the power received comes down to -12.337 dBm. In addition, the researcher notices that SNR reaches 98.562 dB which causes the BER to increases up to 4.4E-45. Moreover, when the distance between the transmitter and the receiver reaches 2.05, the researcher notices that there is no power received, the SNR reaches 0 dB, and the BER reaches the maximum 5.0E-01. This is because there is no line of sight as shown in Figure 4.7, 4.8, and 4.9 (see Appendix A Table A.8, A.9, and A.10 for the simulation results).

The third scenario simulates the effect of heavy density clay particles sandstorm on the VLC when the road visibility is 0.1 Km as shown in Table 4.4.

Table (4.4)

The parameters used to simulate clay (Montmorillonite) particles with visibility 0.1 Km

Visibility	**0.1 km**
Atmospheric pressure	**500 mbar**
Particle refractive index	**1.523 + i3.8E–5**
Particle radius	**$1X10^{-4}$ cm**

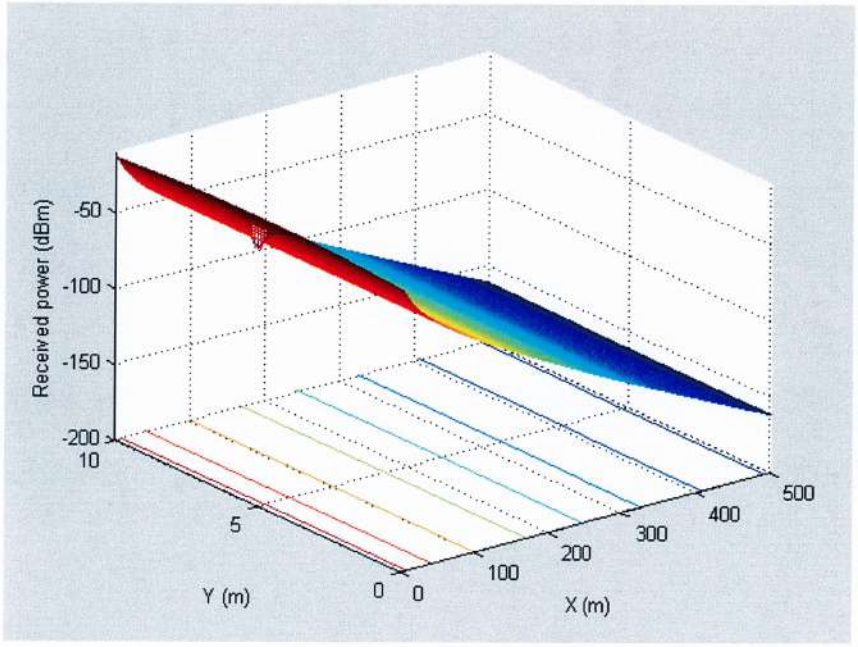


Figure (4.10)

The received power for the VLC affected by clay particles when the visibility is 0.1 Km

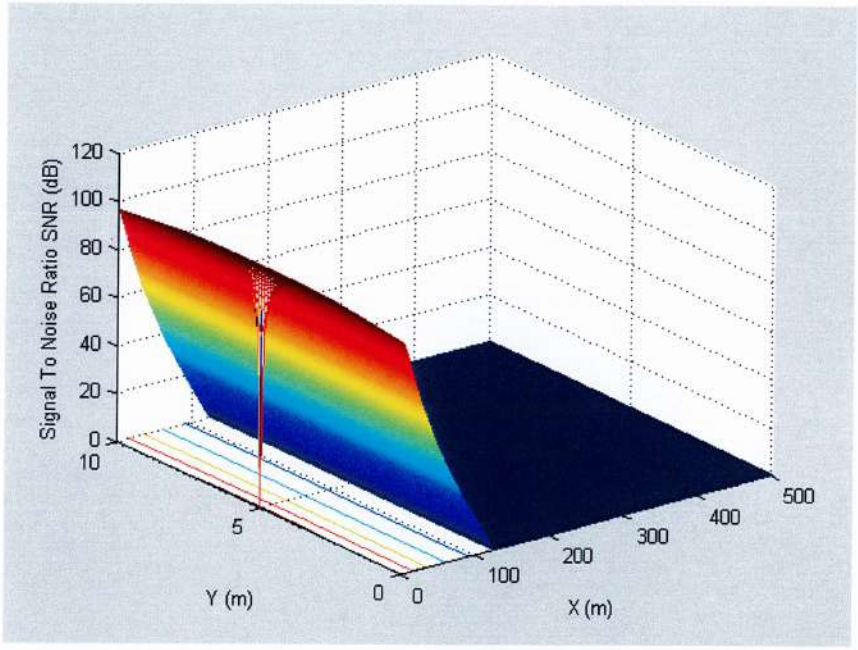


Figure (4.11)

The signal to noise ratio (SNR) for the VLC connectivity affected by clay particles when the visibility is 0.1 Km

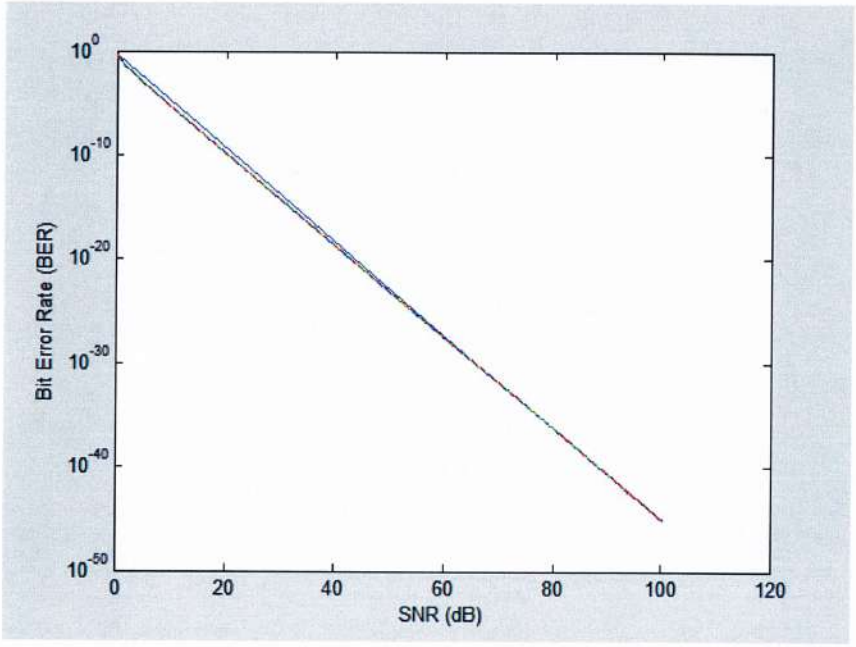


Figure (4.12)

The bit error rate (BER) for the VLC connectivity affected by clay particles when the visibility is 0.1 Km

The third scenario simulates the effect of the heavy sandstorm with clay particles on the VLC. The result of the simulation when the visibility is 0.1 Km shows that there are two different degradations in the power received. The first degradation in the power received is due to the distance increase and the effect of clay particle density. The researcher notices that when the distance between the transmitter and the receiver is 2.864m, the power received is -10.854 dBm, the signal to noise ratio SNR is 100 dB and the bit error rate BER is 9.0E-46. As Ab-Rahman et al. (2012) noticed that the minimum acceptable SNR is 15 dB, therefore the minimum achievable power received in this research is above -60.084 dBm at distance between 75 m and 100 m and the BER records 7.0E-08 at 100 m as shown in Figure 4.10, 4.11, and 4.12 (see Appendix A Table A.11, A.12, and A.13 for the simulation results). Besides, it is noticed that when the distance between the transmitter and the receiver is 500 m, the power received is down to -162.514dBm due to the particle density which causes the SNR to reach 0 dB and the BER to 5.0E-01. The second degradation in the power received is due to the weakness of the signal in the short distance and the clay particle density when the line of sight decreases. The researcher notices that when the distance between the transmitter and the receiver is 2.281 m, the power received is down to -12.791 dBm. In addition, the researcher notices that SNR reaches 98.068 dB which causes the BER to increase up to 7.3E-45. Moreover, when the distance between the transmitter and the receiver reaches 2.05, the researcher notices that there is no power received, the SNR reaches 0 dB, and the BER reaches the maximum 5.0E-01. This is because there is no line of sight as shown in Figure 4.10, 4.11, and 4.12 (see Appendix A Table A.11, A.12, and A.13 for the simulation results).

The researcher notices from these three different scenarios for the clay particles that the particles radius, density (number of particles per cubic meter), and refractive index affect the connectivity. The researcher notices that when the number of particles increases, the density increases and causes the visibility to decrease. In addition, the researcher notices that the maximum distance with the minimum acceptable SNR 15 dB for high density sandstorm is below 100 m and it is noticed that when the storm is medium density, the maximum distance is 425 m. Moreover, when the SNR reaches the minimum acceptable value which is 15 dB, the researcher notices that the bit error rate increases and reaches 7.0E-08 for high density and 5.2E-08 for medium density.

4.1.3 Experiment 3: Simulation of the Effect of Silt Particles on VLC

The third experiment simulates the effect of the silt particles on the VLC with different sandstorm density and visibility scenarios ("Instruments", 1997; "Refractive Index Database", n.d.). The first scenario is when the road visibility is 5 Km as shown in Table 4.5.

Table (4.5)

The parameters used to simulate silt particles with visibility 5 Km

Visibility	**5 km**
Atmospheric pressure	**1000 mbar**
Particle refractive index	**1.4718+0i**
Particle radius	**$36X10^{-4}$ cm**

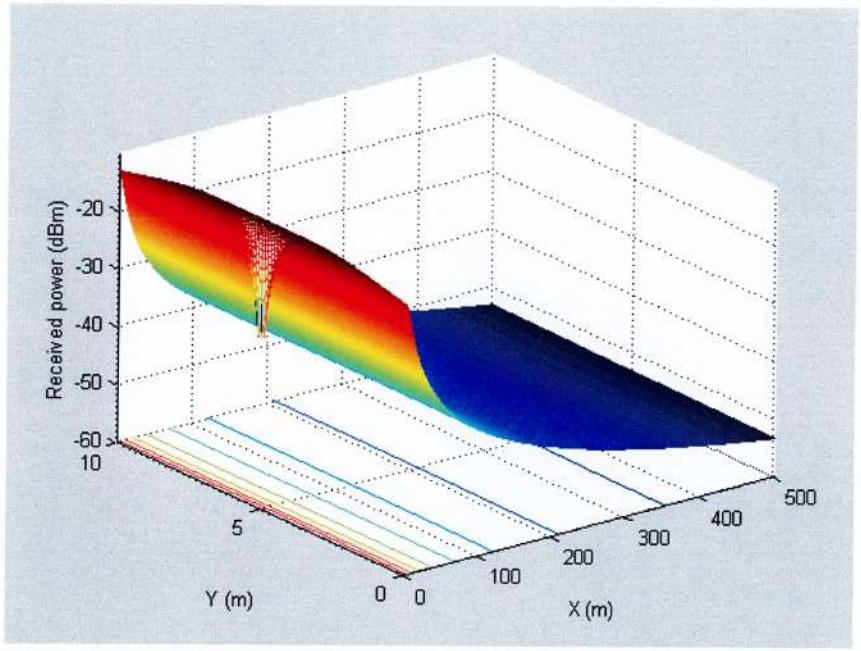


Figure (4.13)

The received power for the VLC affected by silt particles when the visibility is 5 Km

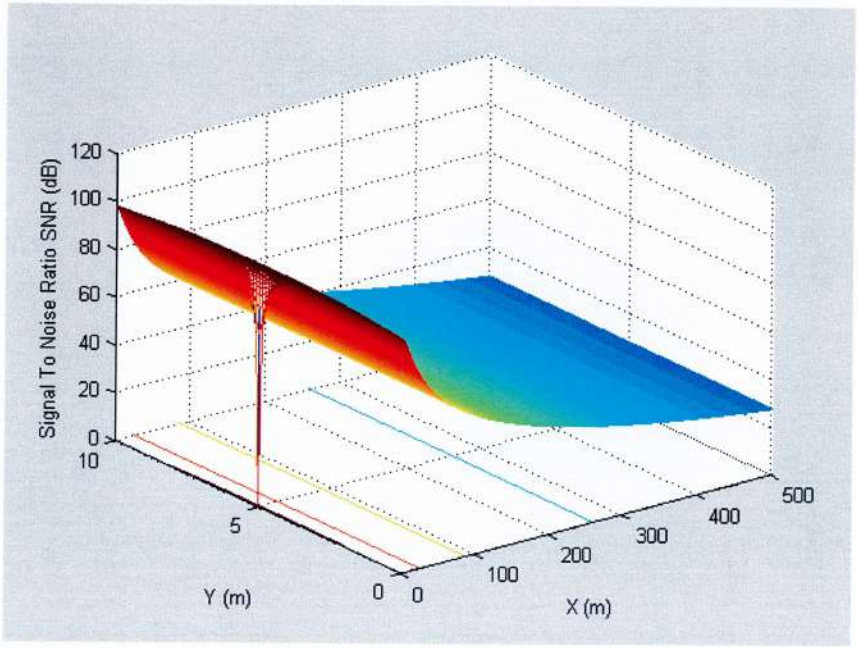


Figure (4.14)

The signal to noise ratio (SNR) for the VLC connectivity affected by silt particles when the visibility is 5 Km

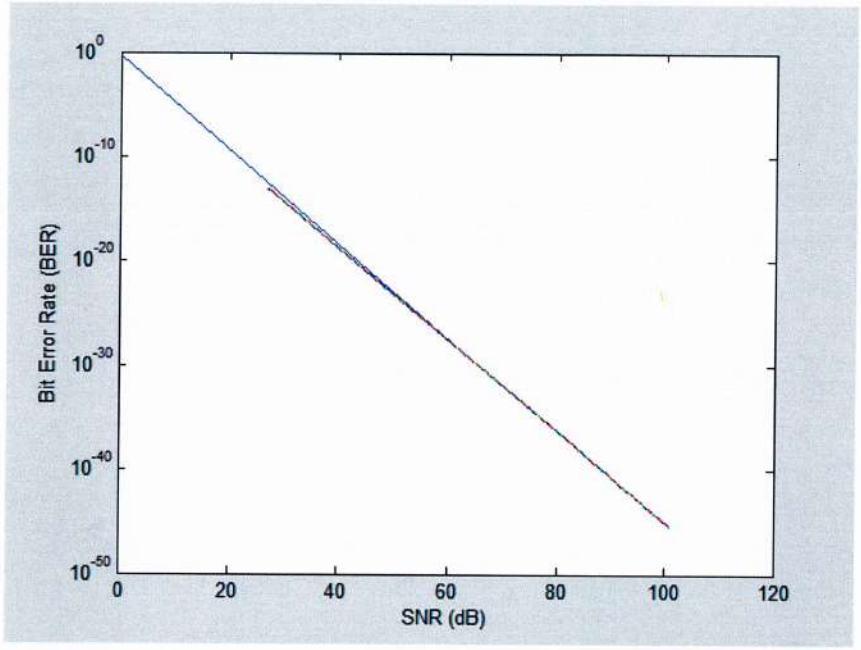


Figure (4.15)

The bit error rate (BER) for the VLC connectivity affected by silt particles when the visibility is 5 Km

The first scenario simulates the effect of the low density sandstorm with silt particle on the VLC. The result of the simulation when the visibility is 5 Km shows that there are two different degradations in the power received. The first degradation in the power received is due to the distance increase and the effect of silt particle density. It is noticed that when the distance between the transmitter and the receiver is 2.864m, the power received is -10.230 dBm, the signal to noise ratio SNR is 100 dB and the bit error rate BER is 4.6E-46. Whereas, when the distance reaches 500m, the power received reaches -53.496 dBm and the SNR is 27.032 dB and the BER records 9.7E-14 as shown in Figure 4.13, 4.14, and 4.15 (see Appendix A Table A.14, A.15, and A.16 for the simulation results). The second degradation in the power received is due to the weakness of the signal in the short distance when the line of sight decreases. The researcher notices that when the distance between the transmitter and the

receiver is 2.281 m, the power received is down to -12.294 dBm. In addition, the researcher notices that SNR reaches 98.609 dB which causes the BER to increase up to 4.2E-45. Moreover, when the distance between the transmitter and the receiver reaches 2.05, the researcher notices that there is no power received, the SNR reaches 0 dB, and the BER reaches the maximum 5.0E-01. This is because there is no line of sight as shown in Figure 4.13, 4.14, and 4.15 (see Appendix A Table A.14, A.15, and A.16 for the simulation results).

The second scenario simulates the effect of medium density silt particles sandstorm on the VLC when the road visibility is 1 Km as shown in Table 4.6.

Table (4.6)

The parameters used to simulate silt particles with visibility 1 Km

Visibility	**1 km**
Atmospheric pressure	**700 mbar**
Particle refractive index	**1.4718+0i**
Particle radius	**$36X10^{-4}$ cm**

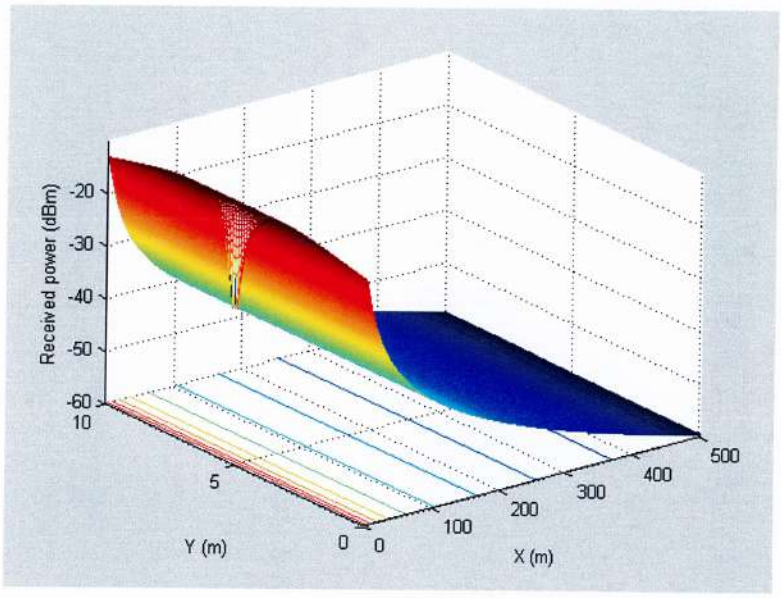


Figure (4.16)

The received power for the VLC affected by silt particles when the visibility is 1 Km

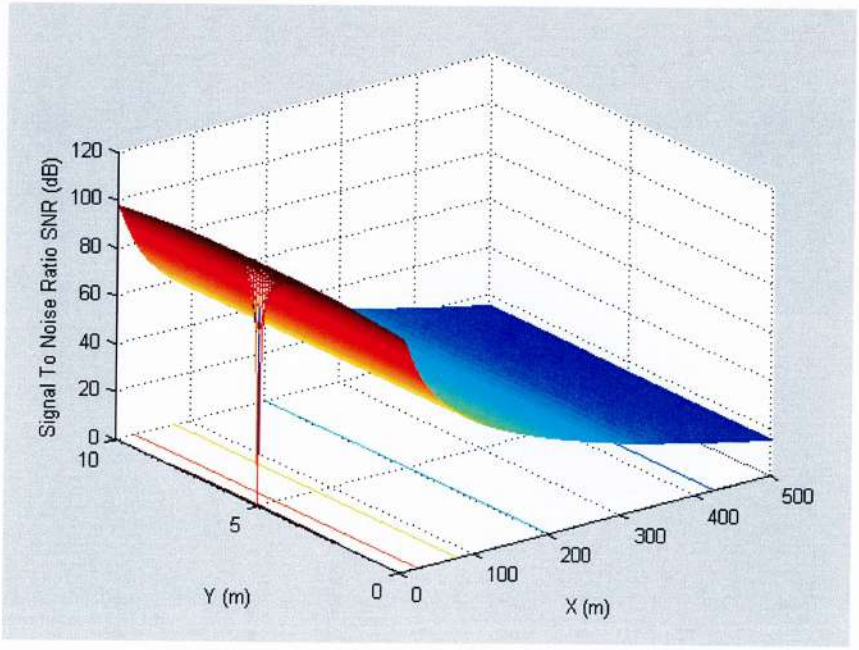


Figure (4.17)

The signal to noise ratio (SNR) for the VLC connectivity affected by silt particles when the visibility is 1 Km

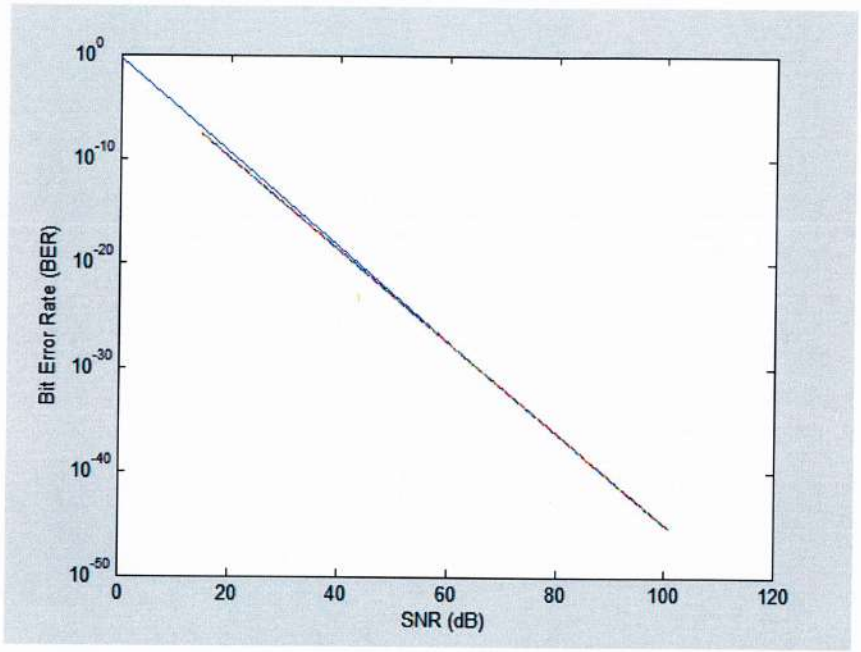


Figure (4.18)

The bit error rate (BER) for the VLC connectivity affected by silt particles when the visibility is 1 Km

The second scenario simulates the effect of the medium sandstorm with silt particles on the VLC. The result of the simulation when the visibility is 1 Km shows that there are two different degradations in the power received. The first degradation in the power received is due to the distance increase and the effect of silt particle density. The researcher notices that when the distance between the transmitter and the receiver is 2.864 m, the power received is -10.265 dBm, the signal to noise ratio SNR is 100 dB and the bit error rate BER is 4.8E-46. As Ab-Rahman et al. (2012) noticed that the minimum acceptable SNR is 15 dB, therefore the minimum achievable power received in this research is -59.661 dBm at distance 500 m and the BER records 2.9E-08 as shown in Figure 4.16, 4.17, and 4.18 (see Appendix A Table A.17, A.18, and A.19 for the simulation results). The second degradation in the power received is due to the weakness of the signal in the short distance when the line of sight

decreases. The researcher notices that when the distance between the transmitter and the receiver is 2.281 m, the power received is down to -12.322 dBm. In addition, the researcher notices that SNR reaches 98.578 dB which causes the BER to increase up to 4.4E-45. Moreover, when the distance between the transmitter and the receiver reaches 2.05, the researcher notices that there is no power received, the SNR reaches 0 dB, and the BER reaches the maximum 5.0E-01. This is because there is no line of sight as shown in Figure 4.16, 4.17, and 4.18 (see Appendix A Table A.17, A.18, and A.19 for the simulation results).

The third scenario simulates the effect of heavy density silt particles sandstorm on the VLC when the road visibility is 0.1 Km as shown in Table 4.7.

Table (4.7)

The parameters used to simulation silt particles with visibility 0.1 Km

Visibility	**0.1 km**
Atmospheric pressure	**500 mbar**
Particle refractive index	**1.4718+0i**
Particle radius	**$36X10^{-4}$ cm**

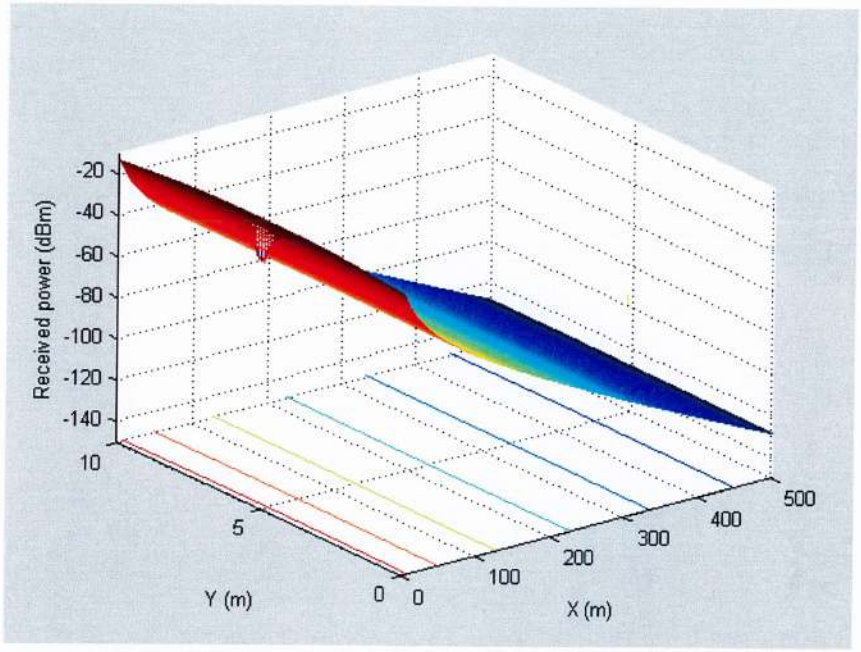


Figure (4.19)

The received power for the VLC affected by silt particles when the visibility is 0.1 Km

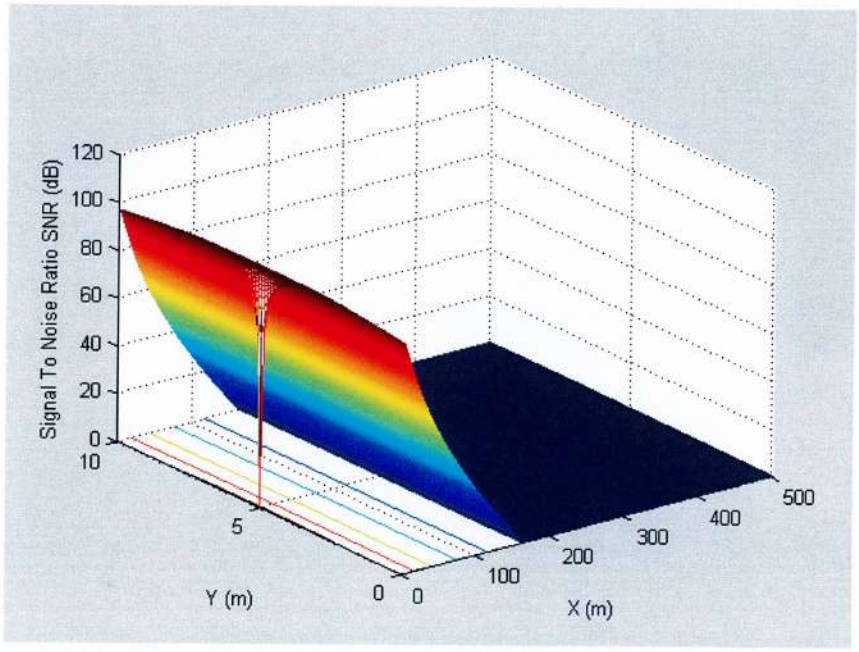


Figure (4.20)

The signal to noise ratio (SNR) for the VLC connectivity affected by silt particles when the visibility is 0.1 Km

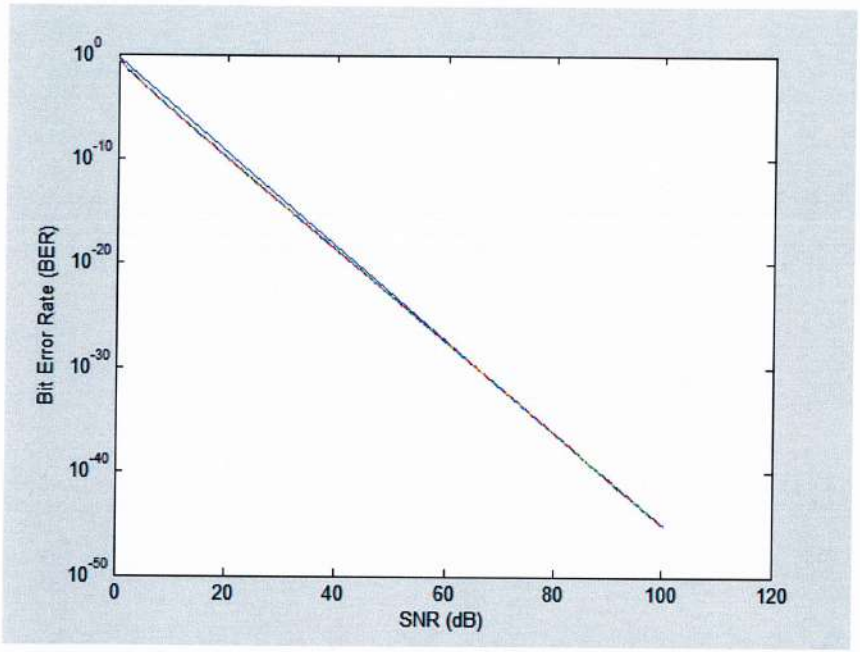


Figure (4.21)

The bit error rate (BER) for the VLC connectivity affected by silt particles when the visibility is 0.1 Km

The third scenario simulates the effect of the heavy sandstorm with silt particles on the VLC. The result of the simulation when the visibility is 0.1 Km shows that there are two different degradations in the power received. The first degradation in the power received is due to the distance increase and the effect of silt particle density. The researcher notices that when the distance between the transmitter and the receiver is 2.864m, the power received is -10.663 dBm, the signal to noise ratio SNR is 100 dB and the bit error rate BER is 7.3E-46. As Ab-Rahman et al. (2012) noticed that the minimum acceptable SNR is 15 dB, therefore the minimum achievable power received in this research is below -59.183 dBm at distance between 125 m and 150 m and the BER records 1.1E-08 at 125 m as shown in Figure 4.19, 4.20, and 4.21 (see Appendix A Table A.20, A.21, and A.22 for the simulation results). Besides, it is noticed that when the distance between the transmitter and the receiver is 500 m,

the power received is down to -129.055dBm due to the particle density which causes the SNR to reach 0 dB and the BER to 5.0E-01. The second degradation in the power received is due to the weakness of the signal in the short distance and the silt particle density when the line of sight decreases. The researcher notices that when the distance between the transmitter and the receiver is 2.281 m, the power received is down to -12.639 dBm. In addition, the researcher notices that SNR reaches 98.235 dB which causes the BER to increase up to 6.2E-45. Moreover, when the distance between the transmitter and the receiver reaches 2.05, the researcher notices that there is no power received, the SNR reaches 0 dB, and the BER reaches the maximum 5.0E-01. This is because there is no line of sight as shown in Figure 4.19, 4.20, and 4.21 (see Appendix A Table A.20, A.21, and A.22 for the simulation results).

The researcher notices from these three different scenarios for the silt particles that the particles radius, density (number of particles per cubic meter), and refractive index affect the connectivity. The researcher noticed that when the number of particles increases, the density increases and causes the visibility to decrease. In addition, the researcher notices that the maximum distance with the minimum acceptable SNR 15 dB for high density sandstorm is between 125 m and 150m. Besides, it is noticed that when the storm is medium density, the maximum distance is 500 m. Moreover, when the SNR reaches the minimum acceptable which is 15 dB, the researcher notices that the bit error rate increases and reaches 1.1E-08 for high density and 2.9E-08 for medium density.

4.1.4 Experiment 4: Simulate of the Effect of Sand Particles on VLC

The forth experiment simulates the effect of the sand particles on the VLC with different sandstorm density and visibility scenarios (Hong et

al., 2008). The first scenario is for low density sandstorm with a road visibility of 5 Km as shown in Table 4.8.

Table (4.8)

The parameters used to simulate sand particles with visibility 5 Km

Visibility	**5 km**
Atmospheric pressure	**1000 mbar**
Particle refractive index	**2.288-0.0568i**
Particle radius	**$74X10^{-4}$ cm**

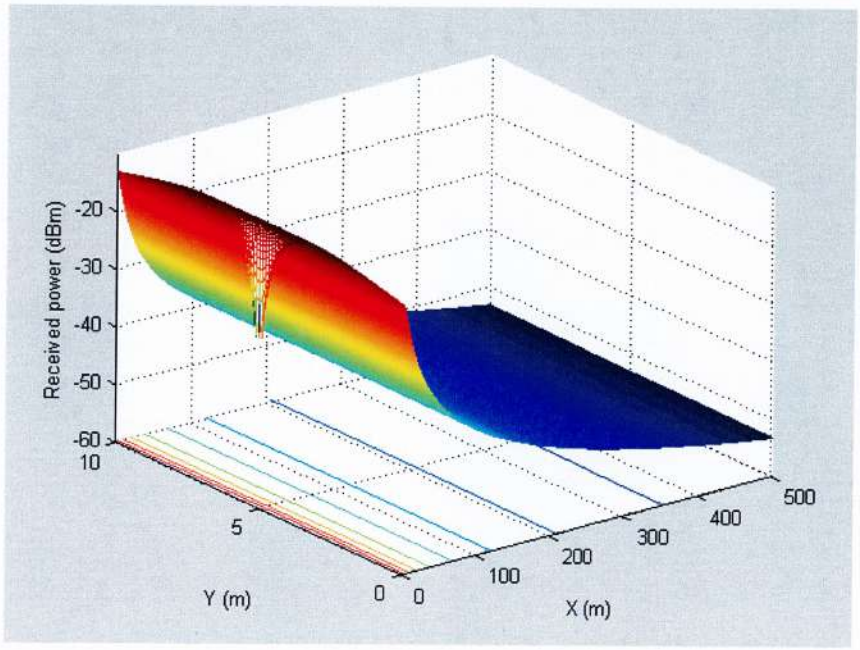


Figure (4.22)

The received power for the VLC affected by sand particles when the visibility is 5 Km

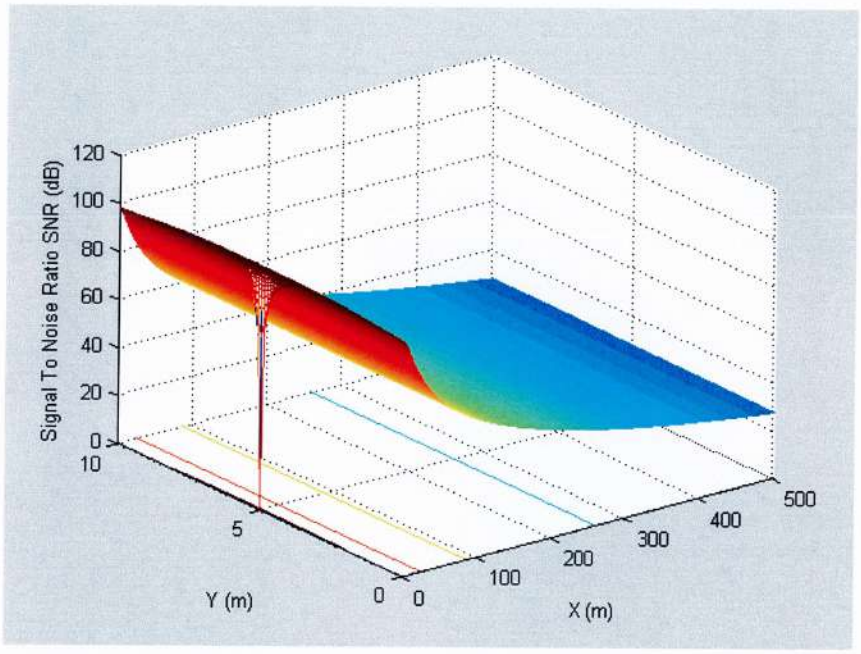


Figure (4.23)

The signal to noise ratio (SNR) for the VLC connectivity affected by sand particles when the visibility is 5 Km

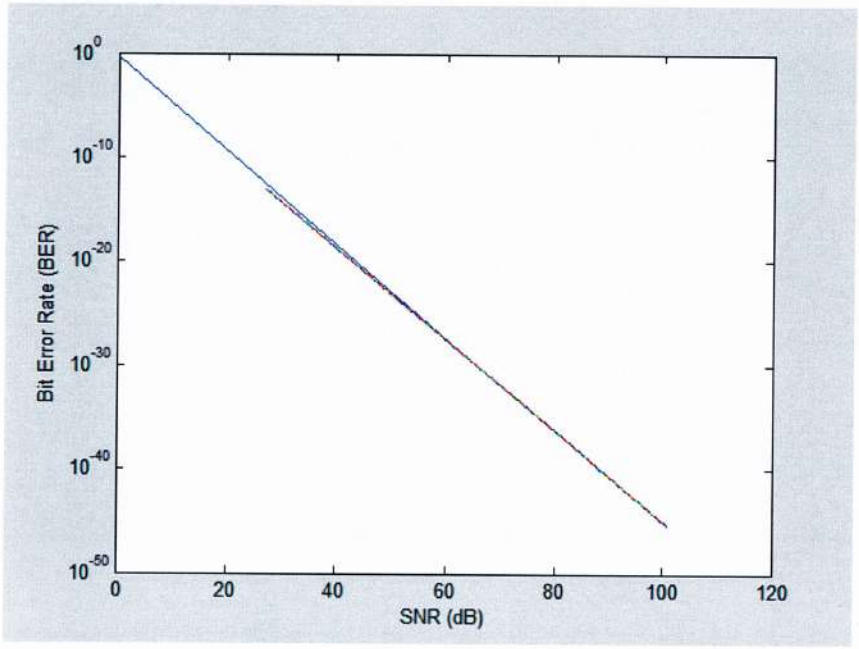


Figure (4.24)

The bit error rate (BER) for the VLC connectivity affected by sand particles when the visibility is 5 Km

The first scenario simulates the effect of the low density sandstorm with sand particle on the VLC. The result of the simulation when the visibility is 5 Km shows that there are two different degradations in the power received. The first degradation in the power received is due to the distance increase and the effect of sand particle density. It is noticed that when the distance between the transmitter and the receiver is 2.864m, the power received is -10.230 dBm, the signal to noise ratio SNR is 100 dB and the bit error rate BER is 4.6E-46. Whereas, when the distance reaches 500m, the power received reaches -53.475 dBm and the SNR is 27.076 dB and the BER records 9.3E-17 as shown in Figure 4.22, 4.23, and 4.24 (see Appendix A Table A.23, A.24, and A.25 for the simulation results). The second degradation in the power received is due to the weakness of the signal in the short distance when the line of sight decreases. The researcher notices that when the distance between the transmitter and the receiver is 2.281 m, the power received is down to -12.294 dBm. In addition, the researcher notices that SNR reaches 98.609 dB which causes the BER to increase up to 4.2E-45. Moreover, when the distance between the transmitter and the receiver reaches 2.05, the researcher notices that there is no power received, the SNR reaches 0 dB, and the BER reaches the maximum 5.0E-01. This is because there is no line of sight as shown in Figure 4.22, 4.23, and 4.24 (see Appendix A Table A.23, A.24, and A.25 for the simulation results).

The second scenario simulates the effect of the sand particles on the VLC when the road visibility is 1 Km as shown in Table 4.9.

Table (4.9)

The parameters used to simulate sand particles with visibility 1 Km

Visibility	**1 km**
Atmospheric pressure	**700 mbar**
Particle refractive index	**2.288-0.0568i**
Particle radius	**$74X10^{-4}$ cm**

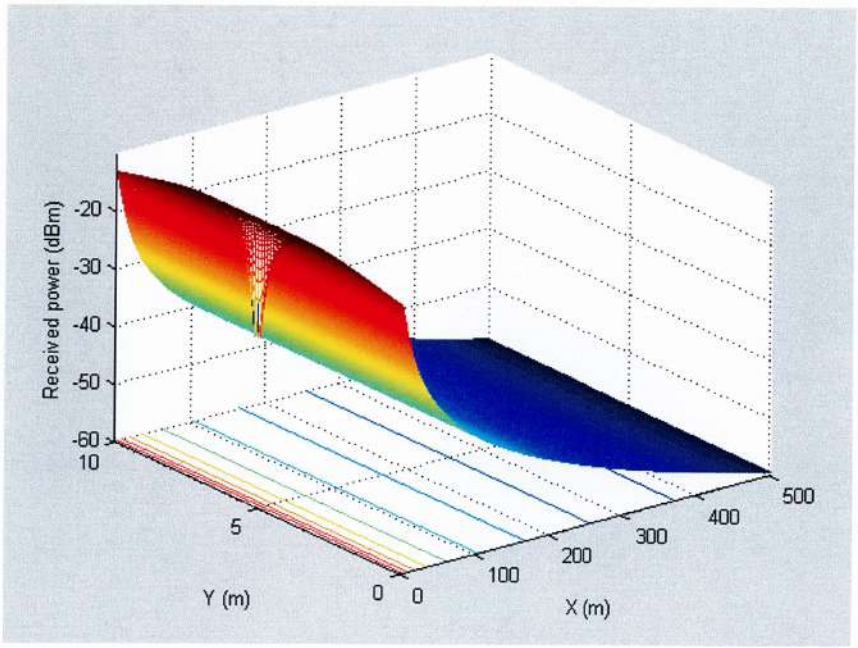


Figure (4.25)

The received power for the VLC affected by sand particles when the visibility is 1 Km

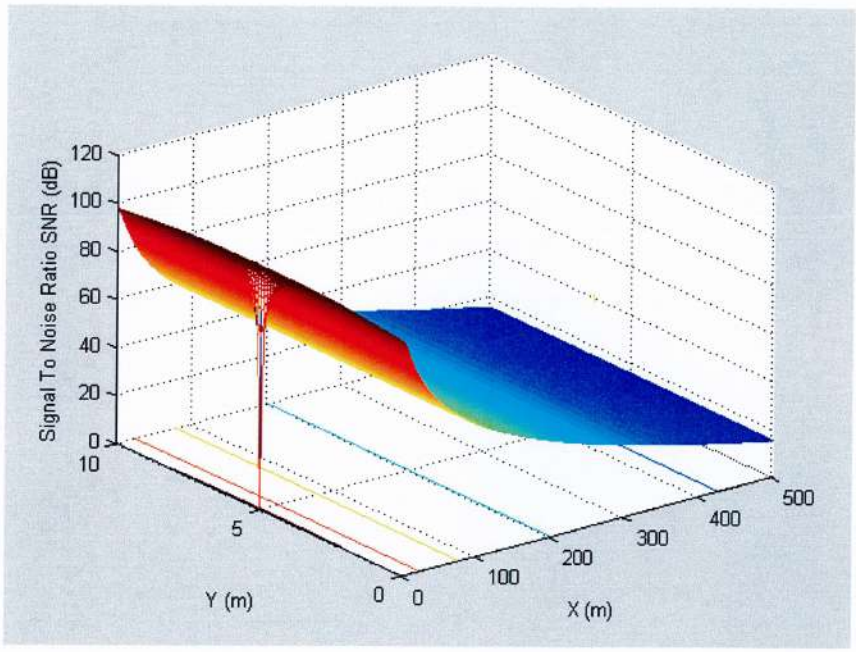


Figure (4.26)

The signal to noise ratio (SNR) for the VLC connectivity affected by sand particles when the visibility is 1 Km

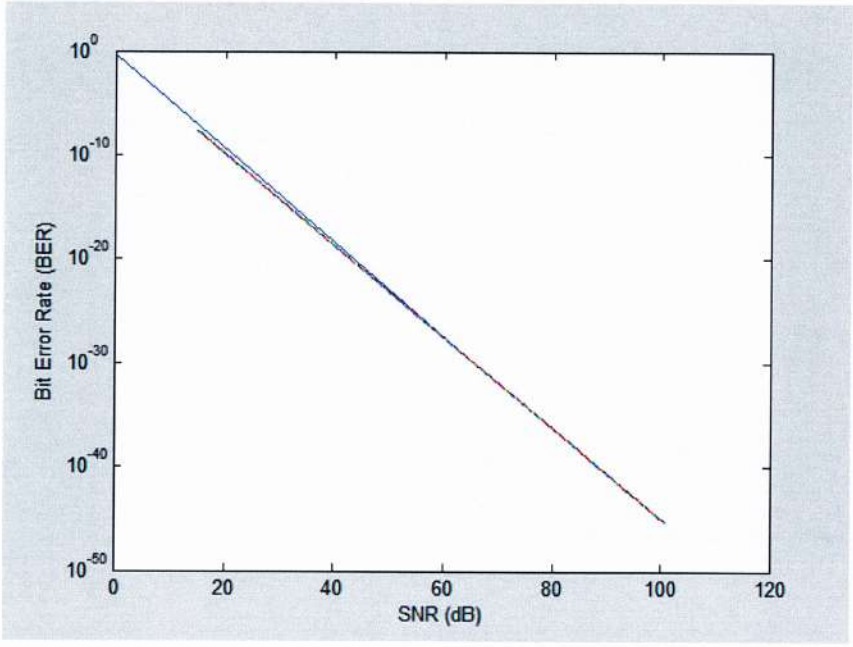


Figure (4.27)

The bit error rate (BER) for the VLC connectivity affected by sand particles when the visibility is 1 Km

The second scenario simulates the effect of the medium sandstorm with sand particles on the VLC. The result of the simulation when the visibility is 1 Km shows that there are two different degradations in the power received. The first degradation in the power received is due to the distance increase and the effect of sand particle density. The researcher notices that when the distance between the transmitter and the receiver is 2.864 m, the power received is -10.265 dBm, the signal to noise ratio SNR is 100 dB and the bit error rate BER is 4.8E-46. As Ab-Rahman et al. (2012) noticed that the minimum acceptable SNR is 15 dB, therefore the minimum achievable power received in this research is -59.551 dBm at distance 500 m and the BER records 2.3E-08 as shown in Figure 4.25, 4.26, and 4.27 (see Appendix A Table A.26, A.27, and A.28 for the simulation results). The second degradation in the power received is due to the weakness of the signal in the short distance when the line of sight decreases. The researcher notices that when the distance between the transmitter and the receiver is 2.281 m, the power received is down to -12.322 dBm. In addition, the researcher notices that SNR reaches 98.579 dB which causes the BER to increase up to 4.4E-45. Moreover, when the distance between the transmitter and the receiver reaches 2.05, the researcher notices that there is no power received, the SNR reaches 0 dB, and the BER reaches the maximum 5.0E-01. This is because there is no line of sight as shown in Figure 4.25, 4.26, and 4.27 (see Appendix A Table A.26, A.27, and A.28 for the simulation results).

The third scenario simulates the effect of heavy density sand storm that contains sand particles on the VLC when the road visibility is 0.1 Km as shown in Table 4.10.

Table (4.10)

The parameters used to simulate sand particles with visibility 0.1 Km

Visibility	**0.1 km**
Atmospheric pressure	**500 mbar**
Particle refractive index	**2.288-0.0568i**
Particle radius	**$74X10^{-4}$ cm**

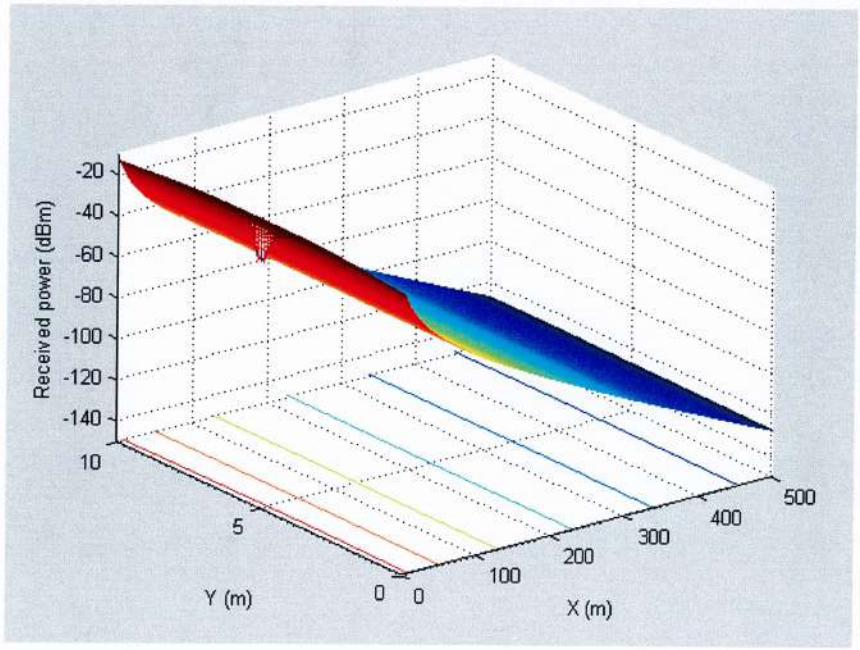


Figure (4.28)

The received power for the VLC affected by sand particles when the visibility is 0.1 Km

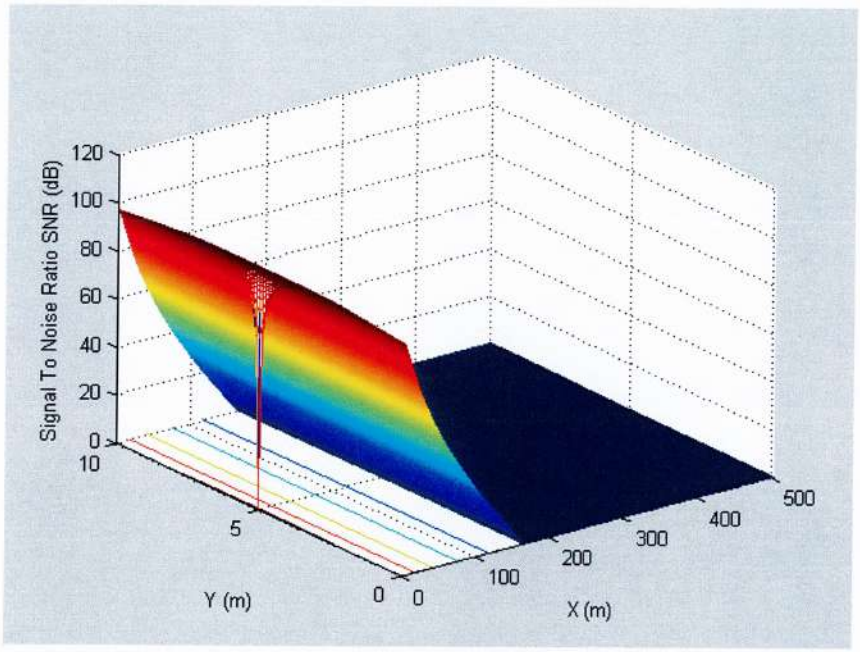


Figure (4.29)

The signal to noise ratio (SNR) for the VLC connectivity affected by sand particles when the visibility is 0.1 Km

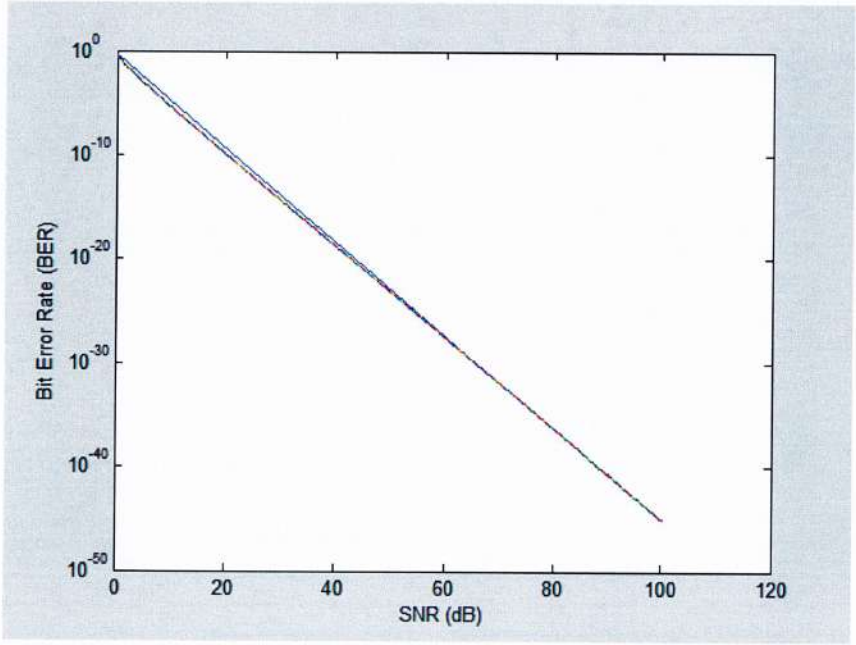


Figure (4.30)

The bit error rate (BER) for the VLC connectivity affected by sand particles when the visibility is 0.1 Km

The third scenario simulates the effect of the heavy sandstorm with sand particles on the VLC. The result of the simulation when the visibility is 0.1 Km shows that there are two different degradations in the power received. The first degradation in the power received is due to the distance increase and the effect of sand particle density. The researcher notices that when the distance between the transmitter and the receiver is 2.864 m, the power received is -10.656 dBm, the signal to noise ratio SNR is 100 dB and the bit error rate BER is 7.3E-46. As Ab-Rahman et al. (2012) noticed that the minimum acceptable SNR is 15 dB, therefore the minimum achievable power received in this research is below -58.909 dBm at distance between 125 m and 150 m and the BER records 6.2E-09 at 125 m as shown in Figure 4.28, 4.29, and 4.30 (see Appendix A Table A.29, A.30, and A.31 for the simulation results). Besides, it is noticed that when the distance between the transmitter and the receiver is 500 m, the power received is down to -127.959dBm due to the particle density which causes the SNR to reach 0 dB and the BER to 5.0E-01. The second degradation in the power received is due to the weakness of the signal in the short distance and the sand particle density when the line of sight decreases. The researcher notices that when the distance between the transmitter and the receiver is 2.281 m, the power received is down to -12.634 dBm. In addition, the researcher notices that SNR reaches 98.240 dB which causes the BER to increase up to 6.1E-45. Moreover, when the distance between the transmitter and the receiver reaches 2.05, the researcher notices that there is no power received, the SNR reaches 0 dB, and the BER reaches the maximum 5.0E-01. This is because there is no line of sight as shown in Figure 4.28, 4.29, and 4.30 (see Appendix A Table A.29, A.30, and A.31 for the simulation results).

The researcher finds from these three different scenarios for the sand particles that the particles radius, density (number of particles per cubic meter), and refractive index affect the connectivity. The researcher notices that when the number of particles increases, the density increases and causes the visibility to decrease. In addition, the researcher notices that the maximum distance with the minimum acceptable SNR 15 dB for high density sandstorm is between 125 m and 150 m. Besides, it is noticed that when the storm is medium density, the maximum distance is 500 m. Moreover, when the SNR reaches the minimum acceptable value which is 15 dB, the researcher notices that the bit error rate increases and reaches 6.2E-09 for high density and 2.3E-08 for medium density.

4.1.5 Experiment 5: Simulation of the Effect of Gravel Particles on VLC

The Fifth experiment simulates the effect of the gravel particles on the VLC with different sandstorm density and visibility scenarios ("Refractive index database", n.d.). The first scenario is for low density storm when the road visibility is 5 Km as shown in Table 4.11.

Table (4.11)

The parameters used to simulate gravel particles with visibility 5 Km

Visibility	**5 km**
Atmospheric pressure	**1000 mbar**
Particle refractive index	**1.550 + i1.0E–4**
Particle radius	**$74X10^{-4}$ cm**

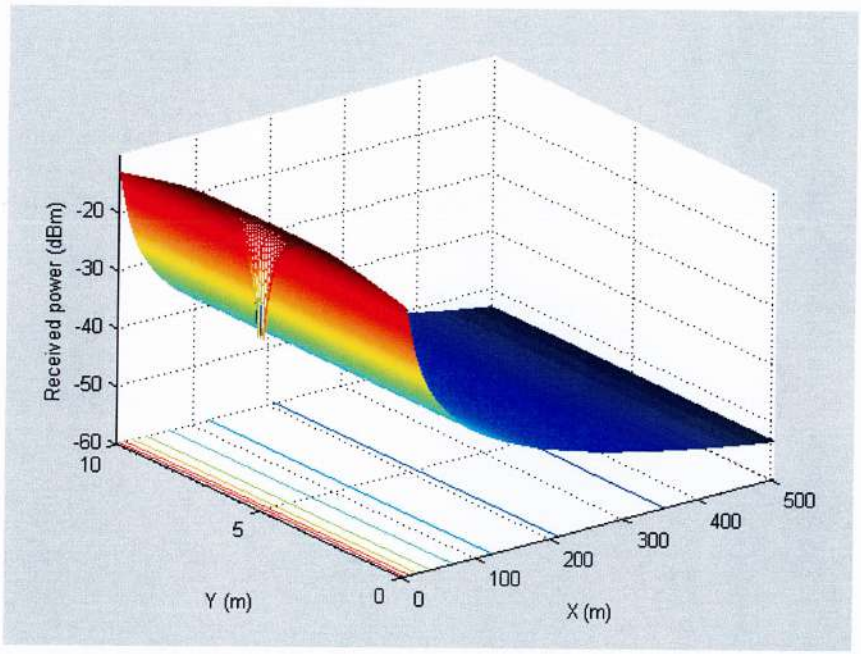


Figure (4.31)

The received power for the VLC affected by gravel particles when the visibility is 5 Km

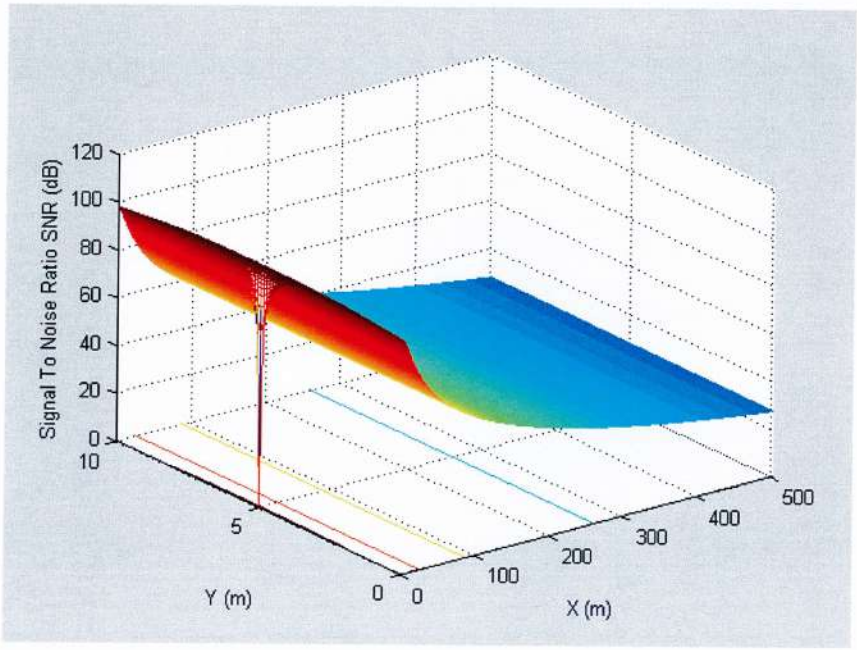


Figure (4.32)

The signal to noise ratio (SNR) for the VLC connectivity affected by gravel particles when the visibility is 5 Km

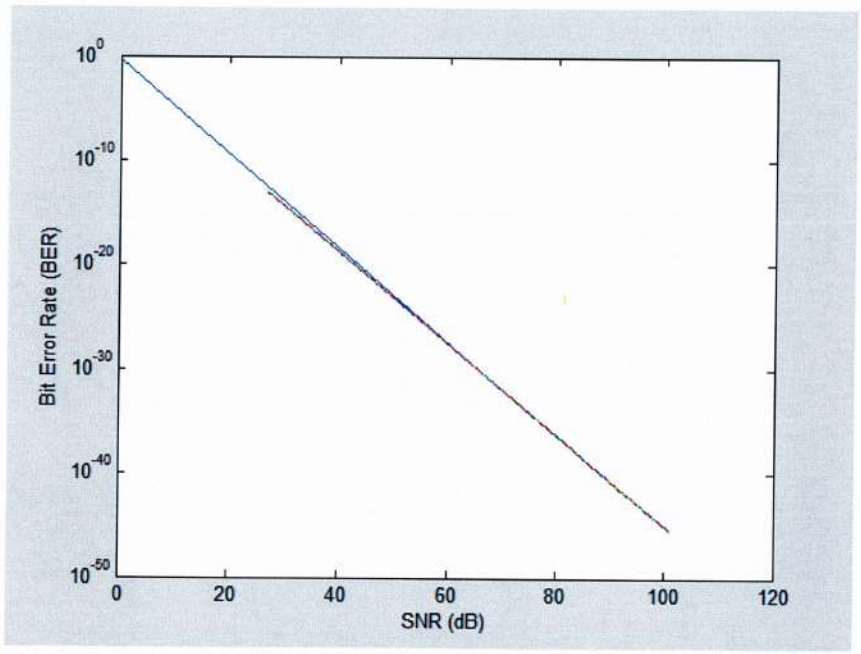


Figure (4.33)

The bit error rate (BER) for the VLC connectivity affected by gravel particles when the visibility is 5 Km

The first scenario simulates the effect of the low density sandstorm with gravel particle on the VLC. The result of the simulation when the visibility is 5 Km shows that there are two different degradations in the power received. The first degradation in the power received is due to the distance increase and the effect of gravel particle density. It is noticed that when the distance between the transmitter and the receiver is 2.864m, the power received is -10.230 dBm, the signal to noise ratio SNR is 100 dB and the bit error rate BER is 4.6E-46. Whereas, when the distance reaches 500m, the power received reaches -53.479 dBm and the SNR is 27.067 dB and the BER recorded 9.4E-14 as shown in Figure 4.31, 4.32, and 4.33 (see Appendix A Table A.32, A.33, and A.34 for the simulation results). The second degradation in the power received is due to the weakness of the signal in the short distance when the line of sight decreases. The researcher notices that when the distance between the

transmitter and the receiver is 2.281 m, the power received is down to -12.294 dBm. In addition, the researcher notices that SNR reaches 98.609 dB which case the BER to increase to 4.2E-45. Moreover, when the distance between the transmitter and the receiver reaches 2.05, the researcher notices that there is no power received, the SNR reaches 0 dB, and the BER reaches the maximum 5.0E-01. This is because there is no line of sight as shown in Figure 4.31, 4.32, and 4.33 (see Appendix A Table A.32, A.33, and A.34 for the simulation results).

The second scenario simulates the effect of medium density gravel particles sandstorm on the VLC when the road visibility is 1 Km as shown in Table 4.12.

Table (4.12)

The parameters used to simulate gravel particles with visibility 1 Km

Visibility	**1 km**
Atmospheric pressure	**700 mbar**
Particle refractive index	**1.550 + i1.0E–4**
Particle radius	**$74X10^{-4}$ cm**

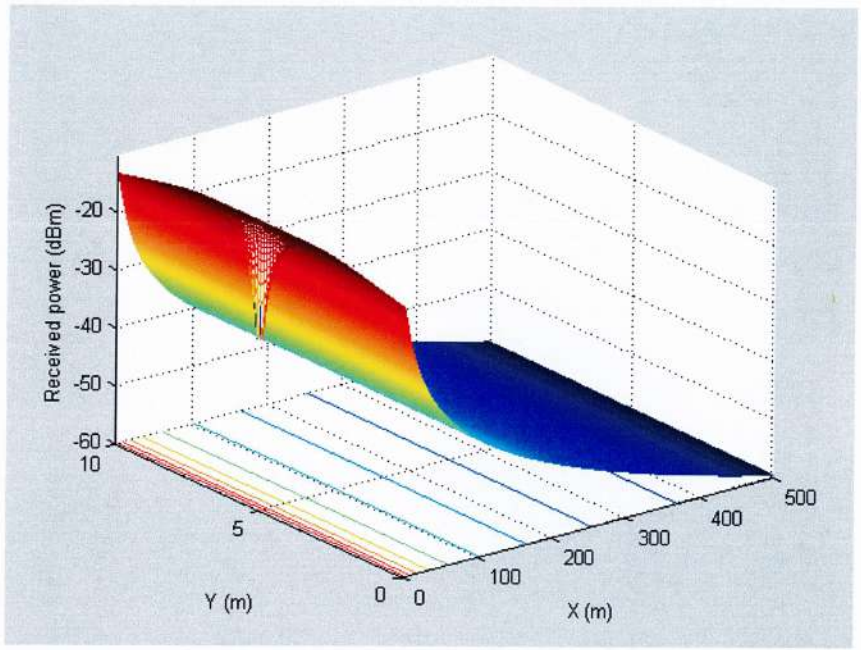


Figure (4.34)

The received power for the VLC affected by gravel particles when the visibility is 1 Km

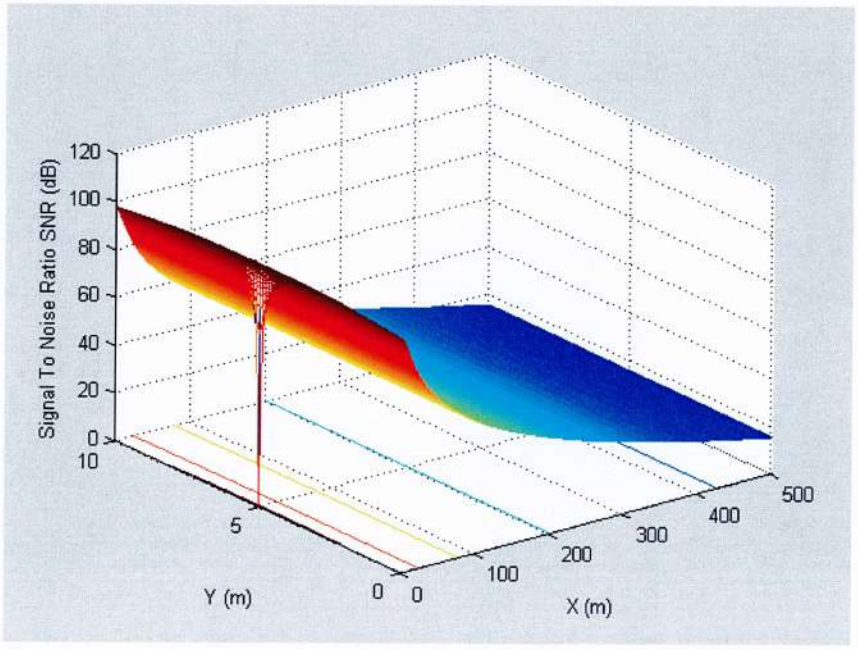


Figure (4.35)

The signal to noise ratio (SNR) for the VLC connectivity affected by gravel particles when the visibility is 1 Km

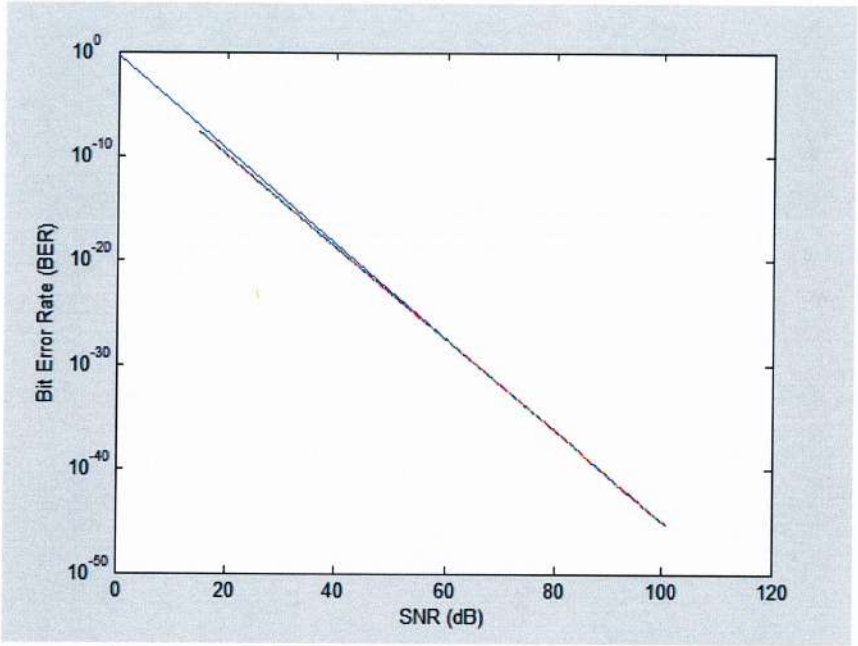


Figure (4.36)

The bit error rate (BER) for the VLC connectivity affected by gravel particles when the visibility is 1 Km

The second scenario simulates the effect of the medium sandstorm with gravel particles on the VLC. The result of the simulation when the visibility is 1 Km shows that there are two different degradations in the power received. The first degradation in the power received is due to the distance increase and the effect of gravel particle density. The researcher notices that when the distance between the transmitter and the receiver is 2.864m, the power received is -10.265 dBm, the signal to noise ratio SNR is 100 dB and the bit error rate BER is 4.8E-46. As Ab-Rahman et al. (2012) noticed that the minimum acceptable SNR is 15 dB, therefore the minimum achievable power received in this research is -59.572 dBm at distance 500 m and the BER records 2.4E-08 as shown in Figure 4.34, 4.35, and 4.36 (see Appendix A Table A.35, A.36, and A.37 for the simulation results). The second degradation in the power received is due to the weakness of the signal in the short distance when the line of sight

decreases. The researcher notices that when the distance between the transmitter and the receiver is 2.281 m, the power received is down to -12.322 dBm. In addition, the researcher notices that SNR reaches 98.579 dB which causes the BER to increase up to 4.4E-45. Moreover, when the distance between the transmitter and the receiver reaches 2.05, the researcher notices that there is no power received, the SNR reaches 0 dB, and the BER reaches the maximum 5.0E-01. This is because there is no line of sight as shown in Figure 4.34, 4.35, and 4.36 (see Appendix A Table A.35, A.36, and A.37 for the simulation results).

The third scenario simulates the effect of heavy density gravel particles sandstorm on the VLC when the road visibility is 0.1 Km as shown in Table 4.13.

Table (4.13)

The parameters used to simulation gravel particles with visibility 0.1 Km

Visibility	**0.1 km**
Atmospheric pressure	**500 mbar**
Particle refractive index	**1.550 + i1.0E–4**
Particle radius	**$74X10^{-4}$ cm**

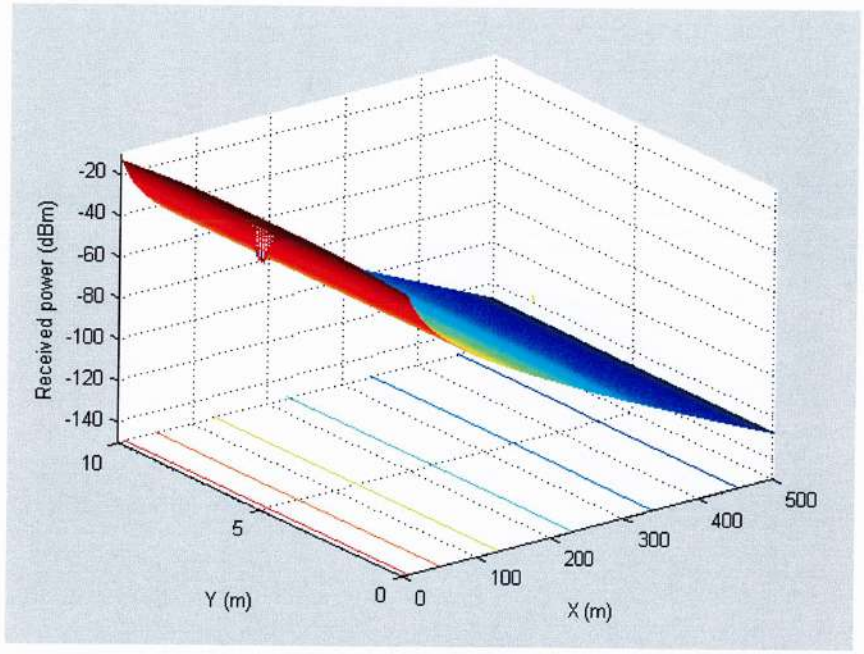


Figure (4.37)

The received power for the VLC affected by gravel particles when the visibility is 0.1 Km

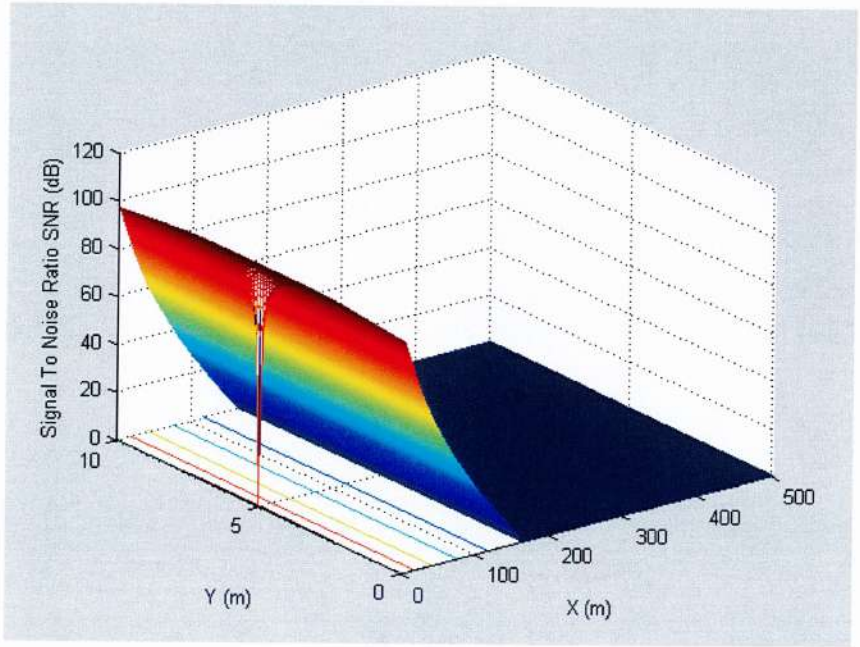


Figure (4.38)

The signal to noise ratio (SNR) for the VLC connectivity affected by gravel particles when the visibility is 0.1 Km

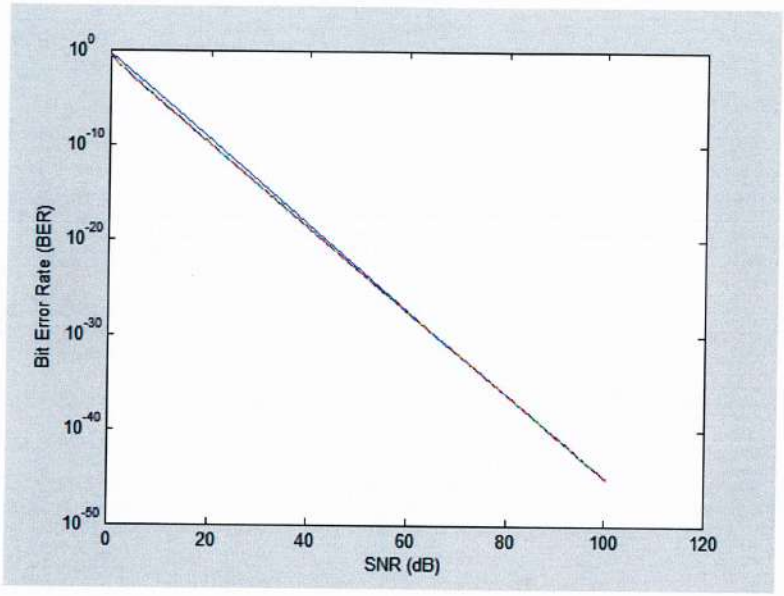


Figure (4.39)

The bit error rate (BER) for the VLC connectivity affected by gravel particles when the visibility is 0.1 Km

The third scenario simulates the effect of the heavy sandstorm with gravel particles on the VLC. The result of the simulation when the visibility is 0.1 Km shows that there are two different degradations in the power received. The first degradation in the power received is due to the distance increase and the effect of gravel particle density. The researcher notices that when the distance between the transmitter and the receiver is 2.864m, the power received is -10.658 dBm, the signal to noise ratio SNR is 100 dB and the bit error rate BER is 9.2E-46. As Ab-Rahman et al. (2012) noticed that the minimum acceptable SNR is 15 dB, therefore the minimum achievable power received in this research is below -58.960 dBm at distance between 125 m and 150 m and the BER records 6.9E-09 at 125 m as shown in Figure 4.37, 4.38, and 4.39 (see Appendix A Table A.38, A.39, and A.40 for the simulation results). Besides, it is noticed that when the distance between the transmitter and the receiver is 500 m, the power received is down to -128.164 dBm due to the particle density

which causes the SNR to reach 0 dB and the BER to 5.0E-01. The second degradation in the power received is due to the weakness of the signal in the short distance and the gravel particle density when the line of sight decreases. The researcher notices that when the distance between the transmitter and the receiver is 2.281 m, the power received is down to -12.635 dBm. In addition, the researcher notices that SNR reaches 98.239 dB which causes the BER to increase up to 6.1E-45. Moreover, when the distance between the transmitter and the receiver reaches 2.05, the researcher notices that there is no power received, the SNR reaches 0 dB, and the BER reaches the maximum 5.0E-01. This is because there is no line of sight as shown in Figure 4.37, 4.38, and 4.39 (see Appendix A Table A.38, A.39, and A.40 for the simulation results).

The researcher notices from these three different scenarios for the gravel particles that the particles radius, density (number of particles per cubic meter), and refractive index affect the connectivity. The researcher notices that when the number of particles increases, the density increases and causes the visibility to decrease. In addition, the researcher notices that the maximum distance with the minimum acceptable SNR 15 dB for high density sandstorm is between 125 m and 150 m. Besides, it is noticed that when the storm is medium density the maximum distance is 500 m. Moreover, when the SNR reaches the minimum acceptable which is 15 dB, the researcher notices that the bit error rate increases and reaches 6.9E-09 for high density and 2.4E-08 for medium density.

To summarize the thesis results, Figure 4.40, 4.41, and Table 4.14 show the comparison of the received power for the different sandstorm types with different density. In addition, Figure 4.42, 4.43 and Table 4.15 show a comparison for the SNR for different sandstorms types with

different density. Moreover, Figure 4.44, 4.45 and Table 4.16 compares the BER for different sandstorm types with different density.

Table (4.14)

Comparison of the received power for different sandstorm particles

Type of Sandstorm	Low density		Medium density		High density	
	Min dBm	Max dBm	Min dBm	Max dBm	Min dBm	Max dBm
Clay	-54.166	-10.233	-63.008	-10.284	-162.514	-10.854
Silt	-53.497	-10.230	-59.662	-10.265	-129.055	-10.663
Sand	-53.475	-10.230	-59.552	-10.265	-127.959	-10.656
Gravel	-53.479	-10.230	-59.573	-10.265	-128.164	-10.658

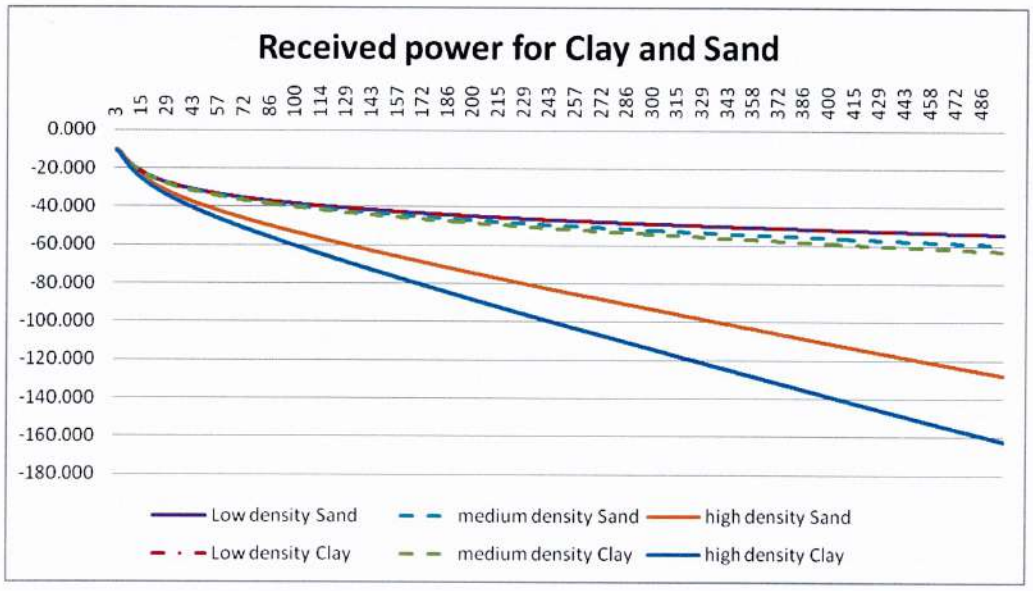


Figure (4.40)

Comparison of the received power for different density Clay and Sand particle sandstorm

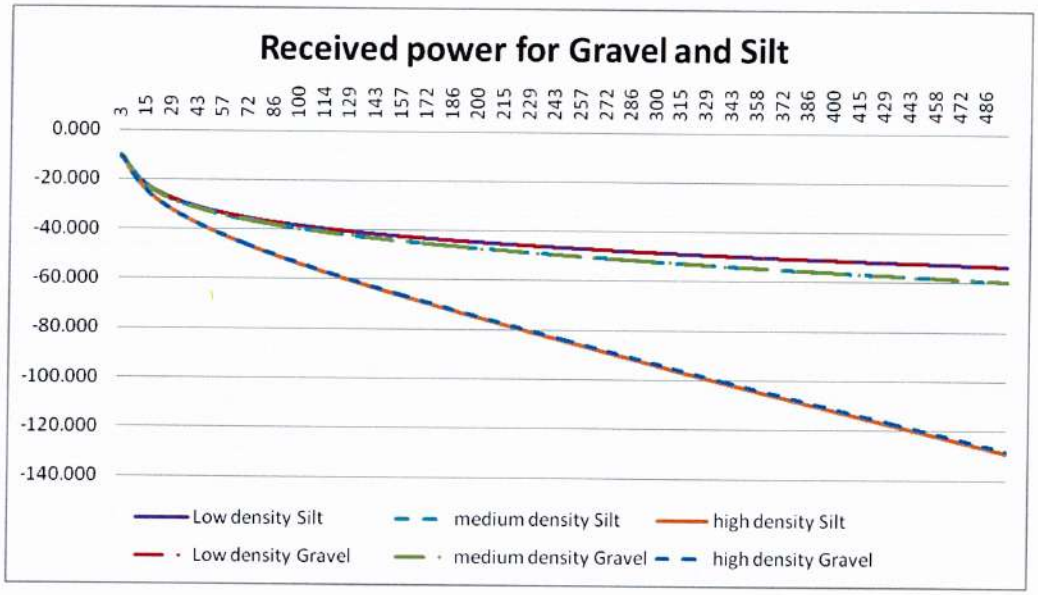


Figure (4.41)

Comparison of the received power for different density Gravel and Silt particle sandstorm

Table (4.15)

Comparison of the Signal to Noise Ratio (SNR) for different sandstorm particles

Type of Sandstorm	Low density		Medium density		High density	
	Min dB	Max dB	Min dB	Max dB	Min dB	Max dB
Clay	25.693	100.807	8.0124	100.754	0	100.151
Silt	27.031	100.811	14.704	100.774	0	100.354
Sand	27.071	100.811	14.923	100.774	0	100.361
Gravel	27.066	100.811	14.882	100.774	0	100.359

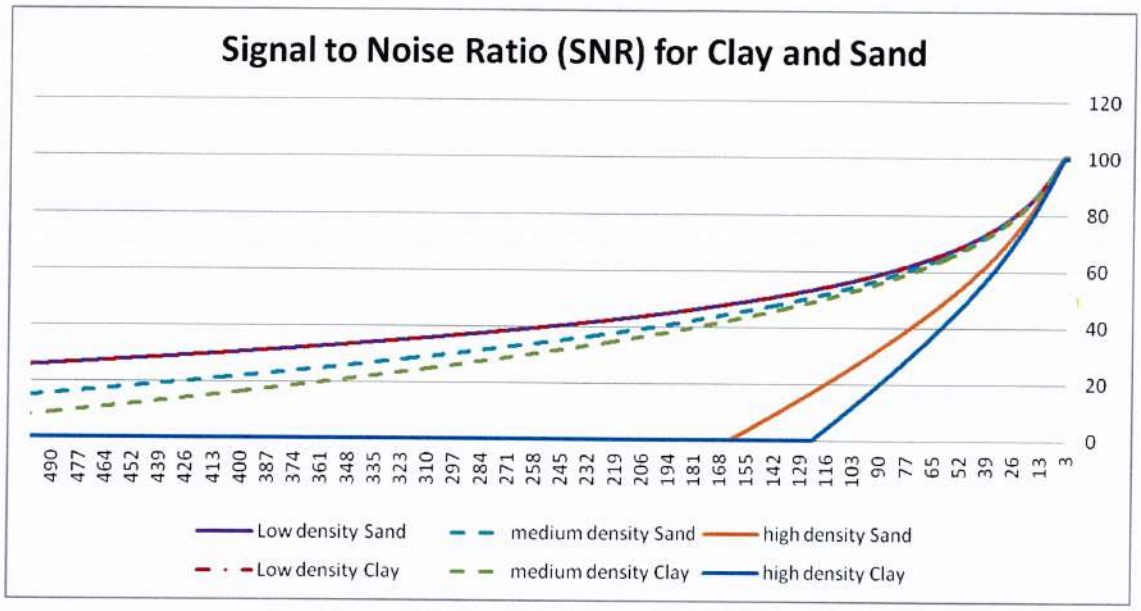


Figure (4.42)

Comparison of the signal to noise ratio (SNR) for different density Clay and Sand particle sandstorm

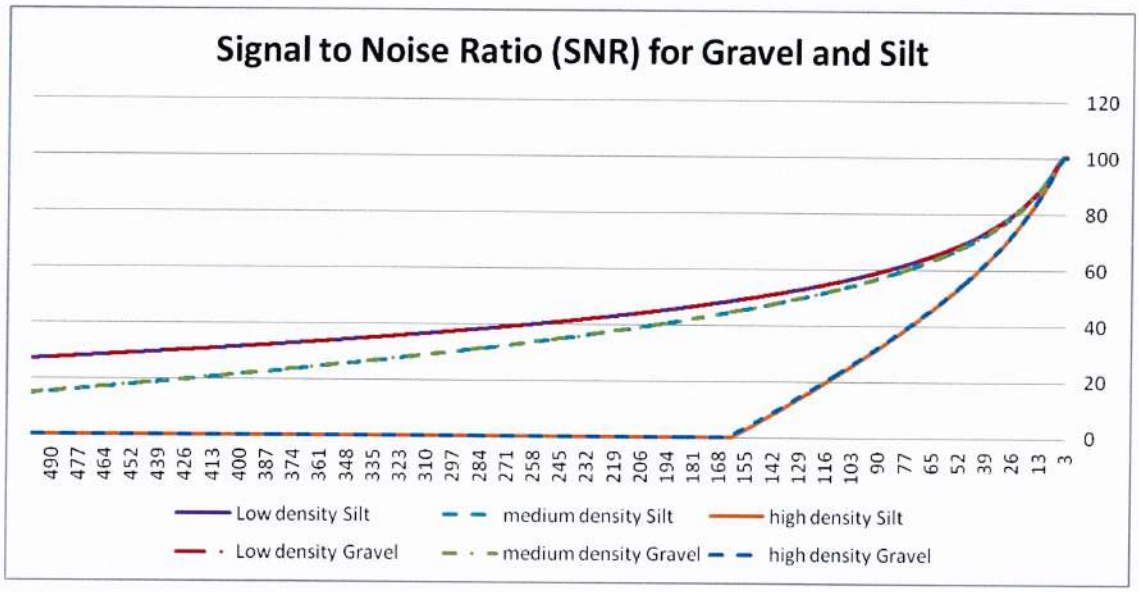


Figure (4.43)

Comparison of the signal to noise ratio (SNR) for different density Gravel and Silt particle sandstorm

Table (4.16)

Comparison of the Bit Error Rate (BER) for different sandstorm particles

Type of Sandstorm	Low density		Medium density		High density	
	Min	Max	Min	Max	Min	Max
Clay	3.794e-13	4.642e-46	3.126e-05	4.897e-46	0.500	8.972e-46
Silt	9.716e-14	4.623e-46	2.933e-08	4.799e-46	0.500	7.316e-46
Sand	9.292e-14	4.622e-46	2.339e-08	4.796e-46	0.500	7.268e-46
Gravel	9.370e-14	4.622e-46	2.440e-08	4.796e-46	0.500	7.277e-46

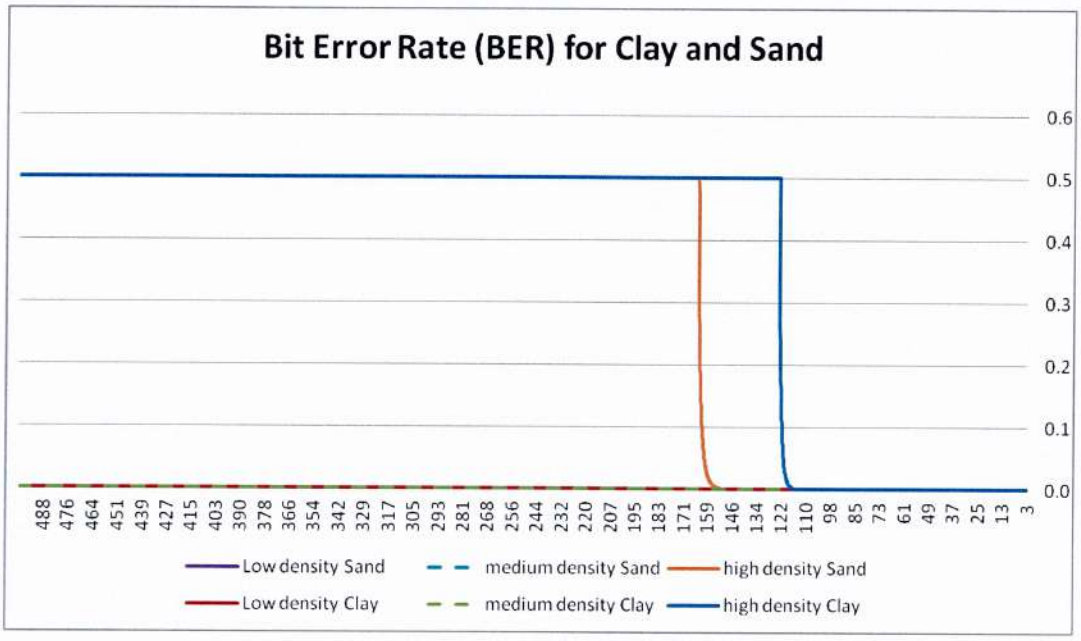


Figure (4.44)

Comparison of the bit error rate (BER) for different density Clay and Sand particle sandstorm

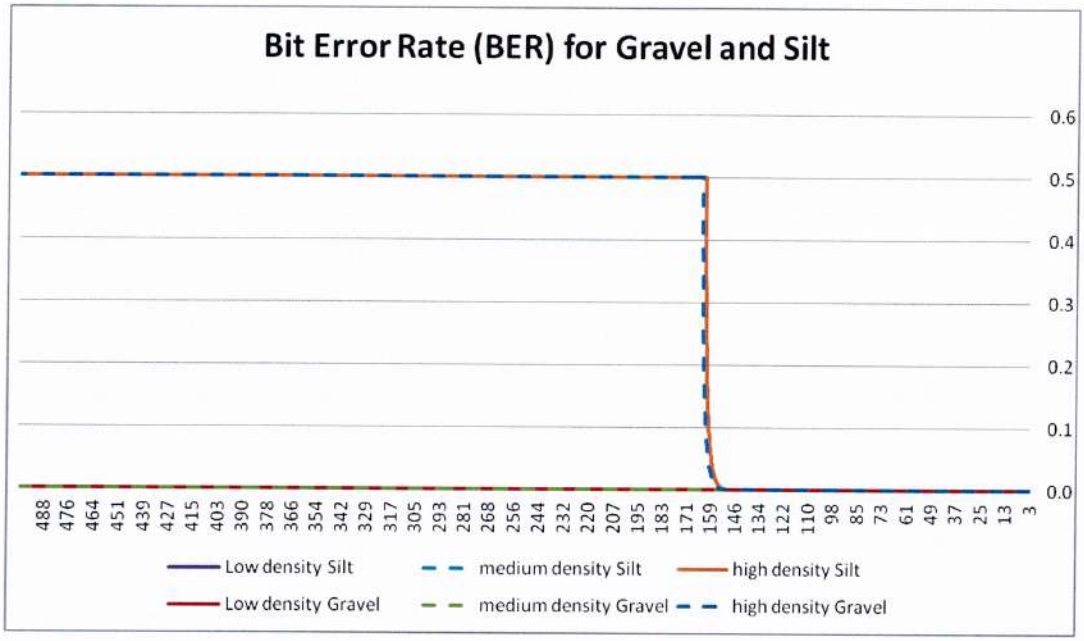


Figure (4.45)

Comparison of the bit error rate (BER) for different density Gravel and Silt particle sandstorm

From Tables 4.15, 4.15, and 4.16 the researcher deduces that clay sandstorm has the most severe effect on VLC connectivity and performance when the sandstorm has high density.

4.2 Discussion of the Results

After discussing the main results of the simulation experiments, this section provides an analysis of the key research findings.

This thesis finds that one of the main challenges that are facing VLC is the distance between the transmitter and the receiver. This can be noticed from all the experiments and the scenarios. For instance, it is noticed that when the distance between the transmitter and the receiver is 2.864 m, the power received is -10.221 dBm and when the distance increases to 500 m, the power received decreases to -51.955 dBm. In

addition, it is noticed that the weather conditions affect the connectivity as it is recorded -54.166 dBm for low density clay sandstorm, -63.008 dBm for medium density, and -162.514 dBm for high density for 500 m. Similarly, O'Brien et al. (2008b), Borogovac et al. (2011), Jaiswal and Chopade (2013), and George et al. (2014) outlined in their studies that there are different types of challenges that are facing the visible light communication. These challenges are a line of sight, interference with other light sources, range, regulation, and standardization.

O'Brien et al. (2008a), Bai et al. (2010) and other researchers noticed that to achieve good bit error rate, they need to receive more power and this is similar to what the researcher noticed in the research results. The researcher finds that when the distance between the transmitter and the receiver is 2.864 m, the SNR records 100 dB and the BER is 4.6E-46. Besides, when the distance reaches 500 m, the power received for clear atmosphere reaches -51.955 dBm, which causes a decrease in the signal to noise ratio down to 30.113 dB and an increase in the bit error rate up to 4.2E-15. Moreover, it is noticed that the maximum distance that can by achievable for low density clay sandstorm is 500 m and for medium density the minimum acceptable SNR which is 15 dB is at distance 450 m, and for high density is below 100 m. This decrease is due to the attenuation caused by the scattering and absorption of the light and thus the bit error rate increases.

The findings of the distance attenuation is similar to Cossu and his colleagues in (2012b) as it is noticed from different experiments that when the distance between the transmitter and the receiver decreases, the power received increases and the SNR increases and a better BER can be achieved. For instance, it is noticed that when the distance is 2.864 m the power received is recorded around -10 dBm and the SNR is 100 dB and

the BER is 4.6E-46. They noticed in their study that when the distance between the transmitter and the receiver was 1.5 m, they could achieve a better performance and less bit error rate for indoor VLC. In addition, they noticed that when the distance was 4 m, the bit error rate increased and the performances decreased.

The research finds that weather influence is another key challenge that is facing the VLC connectivity. As it is found that sandstorm clay, silt, sand, and gravel particles are reducing the power received and noticed that no other research has outlined the effect of sand and dust storm on the VLC. Hu et al. (2007) noticed that attenuation due to the absorption and scattering of the light is due to the gas molecules and aerosol particles when they studied the use of visible red light laser beam for Free-Space Optical (FSO) communication.

The research finds that when the particles density increases, the visibility decreases and the power received decreases as well which affects the achievable distance. It is noticed when the visibility is between 1 Km and 5 Km, the density of the particles is medium. As a result, the minimum acceptable power received is -59.661 dBm at distance 500 m for silt particle when the visibility is 1 Km. Whereas, it is noticed that in clay particle that when the visibility is 1 Km, the minimum acceptable power received is -59.936 dBm at distance 425 m. In addition, when the visibility decreases below 1 Km, the storm becomes heavy and the density increases and the power received decreases more, which affects the achievable distance. The research finds that when the visibility decreases below 1 Km in the clay particles experiment, the power received decreases to more than the other particles experiments due to the particles radius and refractive index. For instance, the maximum distance that can be achieved for clay particle is between 75 m and 100 m.

Whereas, the maximum distance that can be achieved in silt, sand, and gravel is between 125 m and 150 m. Similar results have been achieved by Hu et al. (2007) when they studied the effect of fog on the visible red light laser beam. As they found that when the visibility decreased below 1 Km, the attenuation increased due to the increase in the fog density.

The researcher notices a similarity between the thesis findings and Mahalati and Kahn's (2012) results when they studied the use of imaging receivers for free-space optical links. They noticed that weather influences such as haze, fog and rain caused attenuation for the connectivity. In addition, they noticed that when there were medium to heavy fog, the attenuation increased. The thesis results show that when the sandstorm density increases, the attenuation increases. For instance, for sand particles sandstorm, when the density is low, the minimum power received at 500m is -53.475 dBm and the SNR is 27.076 dB which makes the BER increase to 9.3E-14. Whereas, when the storm becomes a medium, the minimum power received for the same distance is -59.551 dBm and the SNR is 14.925 dB which makes the BER increase to 2.3E-08. Besides, when the storm becomes heavy, the minimum value of the power received at 500 m is -127.955 dBm and the SNR is 0 dB and the BER reaches 5.0E-01.

The researcher notices that the decrease in the power received is due to the increase of the distance and the sandstorm particles density and radius. Several scholars such as Kumar studied the effect of other weather influences and interference. Kumar presented theoretical information about VLC concept, technology, and challenges and a case study about outdoor safety application in IEEE Wireless Communications and Networking Conference 2013. His result of the case study outlined that

the received average power decreased while distance increased. Moreover, he noticed that the packet error rate increased while distance increased and the increase could be noticed more in day time than night time due to the sunlight.

Beshr and his colleagues (2012) noticed that sunlight had different effects on the VLC based on the seasons and the location worldwide. They found that the attenuation in summer days in Cairo was more than in Glasgow due to the sun position. Whereas, the researcher does not study the effect of the sunlight and the location on VLC due to the effect of the sandstorm on the sunlight.

The researcher notices from the thesis results that the sandstorm as one of the weather influences and the distance between the transmitter and the receiver have an effect on the connectivity. Moreover, the visibility and the radius of the particles have an effect on the connectivity as well. When the road visibility decreases to less than 1 Km, the maximum distance that can be achieved with the minimum acceptable SNR when the particles type is clay is between 75 m and 100 m, and this is due to the noise and the attenuation increase. Liu et al. (2011) and Gupta and Sharma (2014) found in their study for vehicle-to-road and vehicle-to-vehicle data broadcasting that the sunlight as light interference and other light sources have different effects on the VLC. They noticed that when the distance between the receiver and the transmitter was more than 101m and the angle between the receiver and the transmitter was equal to the angle between the receiver and the sunlight, the noise reached the maximum.

The research finds that VLC is applicable during sand and dust storm when the storm is low to the medium using OOK modulation. The

researcher chooses the OOK modulation because it is standardised, provides more luminance, and it is more practical to implement. In addition, this research finds that there is no connectivity or the connectivity reduces when the storm is heavy. This result is similar to Elgala et al. (2011), Vucic and Langer (2012), and Tsonev et al. (2013b) as they explained in their research the possibility and the modulation of VLC. Moreover, the thesis finds that VLC's applicability is due to the use of OOK modulation which has been studied before by Afgani et al. (2006), Elgala et al. (2007), Bai et al. (2010), Wang et al. (2011) in their research for the VLC modulations.

The thesis results show that VLC is applicable to be used for outdoor application as the researcher investigates the use of VLC for vehicle-to-road connectivity. The same investigation for the use of VLC for outdoor application has been investigated by other scholars such as Kumar et al. (2006), Liu et al. (2011), Lee et al. (2012), Abualhoul et al. (2013), Gupta and Sharma (2014), and Kumar (2014). They studied different types of outdoor VLC applications such as vehicle-to-road, and vehicle-to-vehicle applications.

To sum up, the thesis finds that sand storm as one of the weather influences has effect in the VLC connectivity. In the experiments, the researcher examines different types of sandstorm particles which are available in Arab Gulf countries and noticed that all the types have an effect on the VLC. This effect can be noticed by the decrease of the power received and the signal to noise ratio and the increase of the bit error rate. In addition, when the particles density increases and the visibility decreases during the sandstorm, a decrease in the power received and an increase in the bit error rate is noticed. These findings are similar to what Mahalati and Kahn (2012) noticed when they examined

the VLC in fog condition. Moreover, the researcher notices that the distance between the transmitter and the receiver has an effect on the VLC connectivity as well as other researcher's results (O'Brien et al., 2008a; Borogovac et al., 2011; Jaiswal & Chopade, 2013; George et al., 2014).

Chapter Five

Conclusions, Recommendations and Future Work

5.1	Conclusions
5.2	Recommendations and Future Work

Chapter Five: Conclusions, Recommendations and Future Work

5.1 Conclusions

The need for wireless connection has increased due to the development in the social media and mobile application. In addition, the limitation of the Wi-Fi connection in some applications such as hospitals, airplanes, and hazardous environments makes the researchers search for alternative technology. Therefore, visible light has been proposed as a communication technology alternative to Wi-Fi technology in 2003 at Nakagawa Laboratory, in Keio University in Japan. Visible light Communication (VLC) uses the LEDs illumination to transmit the data in the FSO. In addition, this technology is not yet mature and a lot of researchers are doing research in this technology. In 2014, it starts to be available for commercial use for indoor purposes.

It is noticed from studying the previous research that VLC which is also known as Light Fidelity (LIFI) is a possible solution which can be used to work with Wi-Fi to provide the connectivity for many applications, but it has some limitations or challenges. Therefore, some researchers have studied the possibility and the challenges of using VLC and the other have studied the improvement of this technology by investigating the modulation technique, the receiver, and the transmitter improvement. Moreover, other researchers focused on the use of this technology for different types of applications.

In addition, it is pointed out from the previous studies that when the researchers outlined the challenges of the VLC, no research has listed the effect of the sand and dust storm which is an important weather influence

in the Arab Gulf region. Therefore, the contribution of this thesis is to fill this gap in the literature by providing the first research in this field which is based on a theoretical and simulation framework. A mathematical model has been derived for dust and sand particles and is used in the simulation. The simulation is conducted using Vehicular-to-road VLC (V2LC) outdoor application and it aims to study the effect of the sandstorm and dust storm on the use of VLC. Moreover, most of the studies have focused on the applications and improving the VLC for indoor purpose and few studies have investigated the applications and the effect of the sun and the fog for outdoor VLC applications, therefore, the results of this thesis can be beneficial worldwide as it adds new finding to the VLC technology.

This research is conducted using different sandstorms which have different particles size and finds that sandstorm and dust storm affect VLC connectivity according to the density of the sand and dust particles. Moreover, it is noticed that when the road visibility decreases to less than 1Km and the sandstorm particles radius is small, the density of the storm becomes high and the connectivity decreases. For instance, the maximum distance with the minimum acceptable SNR for clay particles is between 75 m and 100m, and for 500 m the power received is recorded -162.514 dBm. The simulation also shows that as the distance between the transmitter and the receiver increases, the connectivity, and the signal to noise ratio decreases. For instance, the maximum power received for the sand particles when the storm is low is -10.230 dBm at 2.864 m and the SNR is 100 dB, and the minimum power received is -53.475 dBm at 500m and the SNR is 27.075 dB. Moreover, it is noticed that the bit error rate increases from 4.6E-46 to 9.3E-14. Finally, the research finds that the type of the sandstorm particles has an effect on the communication as

well. This is because different particles have different refractive indexes which affect the medium by the absorption or reflection of the light. The sandstorm that contains clay among other types of sandstorm is found to be the worst in connectivity because the maximum distance with the minimum acceptable SNR is between 75m and 100m. Whereas, the maximum distance for the silt, sand, and gravel particles is between 125m and 150m. The results of this study show general similarities with past research conducted to investigate the effect of fog and rain on VLC with some extra challenges due to the nature of sandstorm which has different reflection index and particles size as compared with rain and fog. The work of this thesis fills the gap in the current VLC research as it is the first research to study the effect of sand and dust storm on VLC in the Arab Gulf. Moreover, the thesis encourages future research to develop the findings using real prototype system.

5.2 Recommendations and Future Work

According to the Meteorological Directorate at Ministry Of Transportation Kingdom of Bahrain, the maximum number of days per year which the visibility decreases below 1 Km due to the sand and dust storm is 18 days and it is recorded in the year 2008 ("Dust", n.d.). Therefore, the researcher finds that connectivity will be down or there will be low connectivity which is reasonable because the number of days is equivalent to 4.93% of the year. Moreover, it is noticed that the number of days when the visibility decreases below 3 km and above 1 km is 55 days and it is recorded in 2008 as well. The thesis finds that when the visibility is above 1 km, the connectivity will decrease but still there is a connection. Therefore, the researcher recommends using VLC technology

in the Arab gulf countries because it is suitable and the downtime is below 5% in the year.

As a further work, it is useful to investigate more in improving the photodiode. In addition, the researcher recommends doing more investigation to see the effect of replacing the photodiode with an image sensor for outdoor VLC. There is also a need to investigate different outdoor applications of VLC using real prototype system.

Bibliography:

Ab-Rahman, M. S., Shuhaimi, N. I., Azizan, L. A., & Hassan, M. R. (2012). Analytical study of signal-to-noise ratio for visible light communication by using single source. *Journal of Computer Science, 8*(1), 141-144. doi:10.3844/jcssp.2012.141.144.

Abualhoul, M. Y., Marouf, M., Shagdar, O., & Nashashibi, F. (2013). Platooning control using visible light communications: A feasiblitiy study. *16th International IEEE Conference on Intelligent Transportation System (ITSC 2013),* 1535-1540.

Abualhoul, M. Y., Marouf, M., Shag, O., & Nashashibi, F. (2014). Enhancing the field of view limitation of Visible Light Communication-based platoon. *2014 IEEE 6th International Symposium on Wireless Vehicular Communication (WiVeV 2014),* 1-5. Doi:10.1109/WIVEC.2014.6953221.

Afgani, M. Z., Haas, H., Elgala, H., & Knipp, D. (2006). Visible light communication using OFDM. *2nd International Conference on Testbeds and Research Infrastructures for the Development of Networks and Communities, 2006.* 6pp.-134. Doi:10.1109/TRIDNT.2006.1649137.

Alexander, J. M., Laskina, O., Meland, B., Young, M. A., Grassian, V. H., & Kleiber, P. D. (2013). A combined laboratory and modeling study of the infrared extinction and visible light scattering properties of mineral dust aerosol. *Journal of Geophysical Research: Atmospheres,* 118(2), 435-452. doi:10.1029/2012JD018751

Alhaider, M. A. (1986). Radio wave propagation into sandstorms-system design based on ten-years visibility data in Riyadh, Saudi Arabia. *International Journal of Infrared and Millimeter Waves,* 7(9), 1339-1359.

Ali, A. Y., & Zhang, Z. (2013). Received power based area estimation for indoor visible light communication. *Dline Journal, Electronic Devices,* 2(1), 1-8.

Aschenbrenner, N. (2010) 500 Megabits/Second with white led light, [Press release]. Retrieved from: http://www.siemens.com/innovation/pool/en/2010/pdf/e_22_resnews_1002_01-3-4.pdf

Bai, B., Xu, Z., & Fan, Y. (2010). Joint LED dimming and high capacity visible light communication by overlapping PPM. *The 19th Annual Wireless and Optical Communications Conference (WOCC 2010),* 1-5.

Ball, C. & Tien, K. (2012). Design and Development of a Visible Light Communications Link. Retrieved from: https://www.ieee.org/education_careers/education/standards/design_and_develop_of_a_visible_light_communications.pdf

Beshr, M., Andonovic, I., & Hussien, M. (2012). The impact of sunlight on the performance of visible light communication systems over the year. Proc. SPIE 8540, Unmanned/Unattended Sensors and Sensor Networks IX, 85400F. doi:10.1117/12.978935.

Borogovac, T., Rahaim, M., & Carruthers, J. B. (2010). Spotlighting for visible light communications and illumination. *2010 IEEE Globecom Workshops,* 1077-1081.

Borogovac, T., Rahaim, M. B., Tuganbayeva, M., & Little, T. D. (2011). "Lights-off" visible light communications. *2011 IEEE GLOBECOM Workshops (GC Wkshps)*, 797-801.

Butala, P. M., Elgala, H., & Little, T. D. (2013). SVD-VLC: A novel capacity maximizing VLC MIMO system architecture under illumination constraints. *2013 IEEE Globecom Workshops (GC Wkshps)*, 1087-1092.

Buys, J. H., & Janssen, L. H. (1981). Comparison of simultaneous atmospheric attenuation measurements at visible light, mid-infra-red (3–5μm) and millimetre waves (94GHz). *IEE Proceedings H Microwaves, Optics and Antennas IEE Proc.H.Microw.Opt. Antennas UK*, 128(3), 131-136.

Chen, C. C. (1975). Attenuation of electromagnetic radiation by haze, fog, clouds, and rain, Report Prepared for United States Air Force Project Rand, Retrieved from: https://www.rand.org/content/dam/rand/pubs/reports/2006/R1694.pdf.

Chu, T. S. (1979). BSTJ brief: Effects of sandstorms on microwave propagation. *Bell System Technical Journal*, 58(2), 549-555, doi: 10.1002/j.1538-7305.1979.tb02234.x.

Chun, H., Manousiadis, P., Rajbhandari, S., Vithanage, D., Faulkner, G., Tsonev, D., . . . O'brien, D. (2014). Visible Light Communication Using a Blue GaN μLED and Fluorescent Polymer Color Converter. *IEEE Photonics Technology Letters IEEE Photon. Technol. Lett.*, *26*(20), 2035-2038.

Cossu, G., Khalid, A. M., Choudhury, P., Corsini, R., & Ciaramella, E. (2012a). 34 Gbit/s visible optical wireless transmission based on RGB LED. *Opt. Express Optics Express, 20*(26), 501-506.

Cossu, G., Khalid, A. M., Choudhury, P., Corsini, R., & Ciaramella, E. (2012b). Long Distance Indoor High Speed Visible Light Communication System Based on RGB LEDs. *Asia Communications and Photonics Conference*.

Cui, K., Chen, G., Xu, Z., & Roberts, R. D. (2010). Line-of-sight visible light communication system design and demonstration. *2010 7th International Symposium on Communication Systems Networks and Digital Signal Processing (CSNDSP),* 621-625.

Di Renzo, M., Haas, H., Ghrayeb, A., Sugiura, S., & Hanzo, L. (2014). Spatial modulation for generalized MIMO: Challenges, opportunities, and implementation. *Proceedings of the IEEE*, 102(1), 56-103. doi: 10.1109/JPROC.2013.2287851.

Dimitrov, S., Sinanovic, S., & Haas, H. (2012). Signal shaping and modulation for optical wireless communication. *Journal of Lightwave Technology,* 30(9), 1319-1328.

Dust. (n.d.). Retrieved from: http://www.bahrainweather.gov.bh/en/web/guest/dust

Dust. (2011), National centre of Meteorology & Seismology Ministry of Presidential Affairs, Retrieved from: http://www.ncms.ae/ncms-book-details.html?id=05#page/1

Edgar, R., & Close, C. (1998). *Using Light Emitting Diodes in Traffic Signals (No. FHWA-OR-RD-99-04),* Retrieved from: http://www.oregon.gov/odot/td/tp_res/docs/reports/usingleds.pdf.

Elabdin, Z., Islam, M. R., Khalifa, O. O., Raouf, H. E. A., & Salami, M. J. E. (2008). Development of mathematical model for the prediction of microwave signal attenuation due to duststorm. *2008 International Conference on Computer and Communication Engineering,* 1156-1161.

Elgala, H., Mesleh, R., & Haas, H. (2009). Indoor broadcasting via white LEDs and OFDM. *IEEE Transactions on Consumer Electronics,* 55(3), 1127-1134.

Elgala, H., Mesleh, R., & Haas, H. (2011). Indoor optical wireless communication: potential and state-of-the-art. *IEEE Communications Magazine,* 49(9), 56-62.

Elgala, H., Mesleh, R., Haas, H., & Pricope, B. (2007). OFDM visible light wireless communication based on white LEDs. *IEEE 65th Vehicular Technology Conference, 2007. VTC2007-Spring,* 2185-2189. doi: 10.1109/VETECS.2007.451

Elshaikh, Z. E. O., Islam, M. R., Khalifa, O. O., & Abd-El-Raouf, H. E. (2009). Mathematical model for the prediction of microwave signal attenuation due to duststorm. *Progress In Electromagnetics Research M, 6,* 139-153.

George, J. J., Mustafa, M. H., Osman, N. M., & Ahmed, N. H. (2014). A Survey on Visible Light Communication. *International Journal Of Engineering And Computer Science,* 3(2), 3805-3808.

Ghassemlooy, Z., Haigh, P. A., Arca, F., Tedde, S. F., Hayden, O., Papakonstantinou, I., & Rajbhandari, S. (2013). Ghassemlooy, Z., Haigh, P., Arca, F., Tedde, S., Hayden, O., Papakonstantinou, I., & Rajbhandari, S. (2013). Visible light communications: 375 Mbits/s

data rate with a 160 kHz bandwidth organic photodetector and artificial neural network equalization [Invited]. *Photon. Res. Photonics Research,* 1(2), 65-68.

Ghimire, B., Stefan, I., Elgala, H., & Haas, H. (2011). Time and frequency synchronisation in optical wireless OFDM networks. *2011 IEEE 22nd International Symposium on Personal Indoor and Mobile Radio Communications,* 819-823.

Goldhirsh, J. (2001). Attenuation and backscatter from a derived two-dimensional duststorm model. *IEEE Transactions on Antennas and Propagation, 49*(12), 1703-1711.

González, O. (2012). Multiple-Input Multiple-Output (MIMO) Optical Wireless Communications, *Optical Communication, Dr. Narottam Das (Ed.), ISBN: 978-953-51-0784-2, InTech,* DOI: 10.5772/46079.

González, O., Medina, M. F. G., & Martín, I. R. (2014). Multi-User Visible Light Communications, *Advances in Optical Communication, Dr. Narottam Das (Ed.), ISBN: 978-953-51-1730-8, InTech,* DOI: 10.5772/59053.

Grubor, J., Jamett, O. C., Walewski, J. W., Randel, S., & Langer, K. D. (2007). High-speed wireless indoor communication via visible light. *Information Technology Society -ITG- :Broadband coverage in Germany , ITG Conference 2007,* 203-208.

Gupta, R., & Sharma, A. (2014). Vehicle-To-Vehicle Data Broadcasting Through Visible Light Communication. *IOSR Journal of Electronics and Communication Engineering (IOSR-JECE),* 9(2), 90-95.

Hapani, M., Joshi, M. & Maradia, R. (2013). Secured LIFI (secured visible light communication). *International Journal of Students Research in Technology & Management,* 1(05), 579-584.

Harris S. (2013), Microscopic LEDs could speed up wireless communication, *The Engineer,* Retrieved from: http://www.theengineer.co.uk/sectors/electronics/news/microscopic-leds-could-speed-up-wireless-communication/1015347.article

He, Y., Ding, L., Gong, Y., & Wang, Y. (2013). Real-time audio & video transmission system based on visible light communication. *Optics and Photonics Journal,* 3(02), 153-157.

Hong, G., Yang, P., Weng, F., & Liu, Q. (2008). Microwave scattering properties of sand particles: Application to the simulation of microwave radiances over sandstorms. *Journal of Quantitative Spectroscopy and Radiative Transfer,* 109(4), 684-702.

Horikawa, S., Komine, T., Haruyama, S., and Nakagawa, M. (2003). Pervasive Visible Light Positioning System using White LED Lighting, *Technical Report of IEICE*, 103(719), 93-99.

Hu, G. Y., Chen, C. Y., & Chen, Z. Q. (2007). Free-Space Optical communication using visible light. *Journal of Zhejiang University SCIENCE A*, 8(2), 186-191.

Iannucci, C., & Pini, F. (2014). Li-Fi for a Digital Urban Infrastructure: A Novel Technology for the Smart City. *TeMA Journal of Land Use, Mobility and Environment*. 512-522

Instruments, M. (1997). Sample dispersion and refractive index guide.*Man0079.*

Jaiswal, N. S., & Chopade, P. S. (2013). Review of Li-Fi Technology: New Future Technology-Light Bulb to Access the Internet. *International Journal of Scientific & Engineering Research,* 4(12).

Kavehrad, M. (2007). Broadband room service by light. *Scientific American,* 297(1), 82-87.

Kavehrad, M. (2010). Sustainable energy-efficient wireless applications using light. *IEEE Communications Magazine,* 48(12), 66-73.

Kavehrad, M., & Amirshahi, P. (2006). Hybrid MV-LV Power lines and white light emitting diodes for triple-play broadband access communications. *IEC Comprehensive Report on Achieving the Triple Play: Technologies and Business Models for Success,* 167-178.

Khalid, A. M., Cossu, G., Corsini, R., Choudhury, P., & Ciaramella, E. (2012). 1-Gb/s transmission over a phosphorescent white LED by using rate-adaptive discrete multitone modulation. *IEEE, Photonics Journal,* 4(5), 1465-1473.

Kim, H. S., Kim, D. R., Yang, S. H., Son, Y. H., & Han, S. K. (2011). Indoor positioning system based on carrier allocation visible light communication. *2011 International Quantum Electronics Conference (IQEC) and Conference on Lasers and Electro-Optics (CLEO) Pacific Rim Incorporating the Australasian Conference on Optics, Lasers and Spectroscopy and the Australian Conference on Optical Fibre Technology.*

Kizilirmak, R. C. (2013). Impact of repeaters on the performance of indoor visible light communications. . *Turk J Elec Eng & Comp Sci*

TURKISH JOURNAL OF ELECTRICAL ENGINEERING & COMPUTER SCIENCES, 8(1), 1159-1172.

Kumar Navin (2013). Visible Light Communication: Concept, Technology, Challenges and Possibilities, *2013 IEEE Wireless Communications and Networking Conference, Shanghai, China*. Retrieved from: http://wcnc2013.ieee-wcnc.org/WCNC.T10.Slides.pdf

Kumar Navin (2014). Visible Light Communication Based Traffic Information Broadcasting Systems. *International Journal of Future Computer and Communication,* 2(6), 26-30.

Kumar, N., Nero, L. A. & Aguiar, R. L. (2006). Visible Light Communication for Advanced Driver Assistant Systems, T*he work is part of FCT project VIDAS*. Retrieved from: http://www.av.it.pt/conftele2009/papers/38.pdf

Kumar, N., & Lourenco, N. R. (2010). Led-based visible light communication system: a brief survey and investigation. *Journal of Engineering and Applied Sciences J. of Engineering and Applied Sciences,* 296-307.

Kumar, N., Terra, D., Lourenço, N., Alves, L. N., & Aguiar, R. L. (2011). Visible light communication for intelligent transportation in road safety applications. *2011 7th International Wireless Communications and Mobile Computing Conference,* 1513-1518.

Le, N. T., Choi, S., Cha, J., & Jang, Y. M. (2012) Dynamic Channel Selection Scheme for IEEE 802.15. 7 Visible Light Communication. 3, Retrieved from: http://onlinepresent.org/proceedings/vol3_2012/97.pdf

Lee, Chung Ghiu (2011). Visible Light Communication, *Advanced Trends in Wireless Communications, Dr. MutamedKhatib (Ed.), ISBN: 978-953-307-183-1, InTech,* DOI: 10.5772/16034.

Lee, S., Kwon, J. K., Jung, S. Y., & Kwon, Y. H. (2012). Evaluation of visible light communication channel delay profiles for automotive applications. *EURASIP Journal on Wireless Communications and Networking,* 2012(1), 1-8.

Lee, Y. U., & Kavehrad, M. (2012). Long-range indoor hybrid localization system design with visible light communications and wireless network. *2012 IEEE Photonics Society Summer Topical Meeting Series,* 82-83.

Lin, W. Y., Chen, C. Y., Lu, H. H., Chang, C. H., Lin, Y. P., Lin, H. C., & Wu, H. W. (2012). 10m/500Mbps WDM visible light communication systems. *Optics express,* 20(9), 9919-9924.

Liu, C. B., Sadeghi, B., & Knightly, E. W. (2011). Enabling vehicular visible light communication (V2LC) networks. *Proceedings of the Eighth ACM international workshop on Vehicular inter-networking* , 41-50.

Lo, S. C. (2004). Visible Light Communications. *IEEE Transactions on Consumer Electronics,* 50(1).

Mahalati, R. N., & Kahn, J. M. (2012). Effect of fog on free-space optical links employing imaging receivers. *Optics express,* 20(2), 1649-1661.

Mishra, A. A., & Salian, N. S. (2011). Internet using Visible Light Communication. *IACSIT International Journal of Engineering and Technology,* 3(5).

Moon, H. D., & Jung, S. Y. (2012). Multi-coded variable PPM for high data rate visible light communications. *Journal of the Optical Society of Korea,* 16(2), 107-114.

Nguyen, H. Q., Choi, J. H., Kang, T. G., Lim, S. K., Kim, D. H., Kang, M., & Lee, C. G. (2012). Effect of LED emission cross-section in indoor visible light communication systems. *EURASIP Journal on Wireless Communications and Networking,* 2012(1), 1-11.

Nguyen, H. Q., Choi, J., Kang, M., Ghassemlooy, Z., Kim, D. H., Lim, S., ... & Lee, C. G. (2010). A MATLAB-based simulation program for indoor visible light communication system. *2010 7th International Symposium on Communication Systems Networks and Digital Signal Processing (CSNDSP),* 537-541.

Nguyen, T., & Jang, Y. M. (2013). Highly Accurate Indoor Three-Dimensional Localization Technique in Visible Light Communication Systems. *한국통신학회논문지,* 38(9), 775-780.

O'Brien, D., Zeng, L., Le-Minh, H., Faulkner, G., Walewski, J. W., & Randel, S. (2008a). Visible light communications: Challenges and possibilities. *IEEE 19th International Symposium on Personal, Indoor and Mobile Radio Communications,* 1-5.

O'Brien, D., Le Minh, H., Zeng, L., Faulkner, G., Lee, K., Jung, D., ... & Won, E. T. (2008b). Indoor visible light communications: challenges and prospects. *International Society for Optics and Photonics, Optical Engineering+ Applications,* 709106-709106.

Otas, K., Pakenas, V. J., Vaskys, A., & Vaskys, P. (2012). Investigation of LED Light Attenuation in Fog. *ELECTRONICS AND ELECTRICAL ENGINEERING,* 121(5), 47-52.

P.1817: Propagation data required for the design of terrestrial free-space optical links (2012), *ITU (International Telecommunication Union) is the United Nations specialized agency for information and communication technologies – ICTs,* Retrieved from: http://www.itu.int/rec/R-REC-P.1817-1-201202-I/en

Panta, K. And Armstrong, J., (2012). Indoor localisation using white LEDs, *Electronics Letters*. 48(4), 228-230.

Periodic table. (n.d), Retrieved from: http://www.periodictable.com/Elements/008/data.wt.html

Petković, M. I., Đorđević, G. T., & Milić, D. N. (2014). BER Performance of IM/DD FSO System with OOK using APD Receiver. *Radio Engineering,* 23(1).

Péwé, T. L., & American Association for the Advancement of Science (Eds.). (1981). *Geological Society of America, Desert dust: origin, characteristics, and effect on man*, 186.

Photovoltaic Series. (n.d), Retrieved from http://www.osioptoelectronics.com/

Pu, Qifan, & Hu, Wenjun (2012). Smooth transmission over unsychronized vlc links. *Proceedings of the 2012 ACM conference on CoNEXT student workshop*, 51-52.

Refractive index database. (n.d), Retrieved from: http://refractiveindex.info/

Ren, G., He, S., & Yang, Y. (2013). Improving Bandwidth Efficiency of Indoor Visible Light Communication by M—ary Return-to-zero

Optical Pulse Amplitude Modulation. *Information Technology Journal,* 12(5), 975-982.

Retnasothie, F.E., Ozdemir, M.K., Yucek, T., Celebi, H., Zhang, J., Muththaiah, R. (2006). Wireless IPTV over WiMAX: Challenges and Applications. *WAMICON '06. 2006 IEEE Annual Wireless and Microwave Technology Conference,* 1 - 5.

Sagotra, R. & Aggarwal, R. (2013). Visible light communication. *International Journal of Engineering Trends and Technology,* 4(3), 403-405.

Santhi, K. R., Srivastava, V. K., Senthil Kumaran, G., Butare, A. (2003). Goals of true broad band's wireless next wave (4G-5G). *2003 IEEE 58th Vehicular Technology Conference,* 4, 2317-2321.

Sargent, R. G. (2005). Verification and validation of simulation models. *Proceedings of the 37th conference on Winter simulation* , 130-143.

Schmid, S., Corbellini, G., Mangold, S., & Gross, T. R. (2012). An LED-to-LED Visible Light Communication system with software-based synchronization. *2012 IEEE Globecom Workshops (GC Wkshps),* 1264-1268.

Schmid, S., Corbellini, G., Mangold, S., & Gross, T. R. (2013). LED-to-LED visible light communication networks. *Proceedings of the fourteenth ACM international symposium on Mobile ad hoc networking and computing* , 1-10.

Stefan, I., Elgala, H., Mesleh, R., O'Brien, D., & Haas, H. (2011, May). Optical wireless OFDM system on FPGA: Study of LED

nonlinearity effects. *2011 IEEE 73rd Vehicular Technology Conference (VTC Spring)*, 1-5.

Tamošiūnaitė, M., Žilinskas, M., Tamošiūnas, S., & Tamošiuniene, M. (2011). Atmospheric Attenuation due to Humidity, *Electromagnetic Waves, Prof. VitaliyZhurbenko (Ed.), ISBN: 978-953-307-304-0, InTech*, DOI: 10.5772/21430.

Taylor, A. E. (2000). Illumination fundamentals. *Lighting Research Center, Rensselaer Polytechnic Institute*.

Teich, M. C., & Saleh, B. E. (1991). *Fundamentals of photonics*, 22.

Tsonev, D., Videv, S., & Haas, H. (2013a, December). Light fidelity (Li-Fi): towards all-optical networking. *International Society for Optics and Photonics (SPIE OPTO)*, 900702-900702.

Tsonev, D., Sinanovic, S., & Haas, H. (2013b). Complete modeling of nonlinear distortion in OFDM-based optical wireless communication. *Journal of Lightwave Technology*, 31(18), 3064-3076.

Uddin, M. S., Cha, J. S., Kim, J. Y., & Jang, Y. M. (2011). Mitigation technique for receiver performance variation of multi-color channels in visible light communication. *Sensors*, 11(6), 6131-6144.

Ultra-Parallel Visible Light Communications (UP-VLC). (n.d), Retrieved from: http://www.css.eng.ed.ac.uk/research/up-vlc

Vaughan-Nichols, S.J. (2008). Mobile WiMax: The Next Wireless Battle Ground. *Computer*, 41(6), 16-18.

Videv, S., & Haas, H. (2014, April). Practical space shift keying VLC system. *2014 IEEE Wireless Communications and Networking Conference (WCNC)*, 405-409.

Vucic, J., & Langer, K. D. (2012, March). High-speed visible light communications: State-of-the-art. *Optical Society of America, Optical Fiber Communication Conference*.

Wang, J. Y., Zou, N. Y., Dong, W. A. N. G., Kentaro, I. R. I. E., Zensei, I. H. A., & NAMIHIRA, Y. (2012). Experimental study on visible light communication based on LED. *The Journal of China Universities of Posts and Telecommunications*, 19, 197-200.

Wang, Z., Yu, C., Zhong, W. D., & Chen, J. (2011). Performance improvement by tilting receiver plane in M-QAM OFDM visible light communications. *Optics express*, 19(14), 13418-13427.

World Health Organization. (1999). *Hazard prevention and control in the work environment: airborne dust*.

Wu, Z., & Little, T. (2010, July). Network solutions for the LOS problem of new indoor free space optical system. *2010 7th International Symposium on Communication Systems Networks and Digital Signal Processing (CSNDSP)*, 582-587.

Yang-Yang Li, & Sousa, E.S. (2010). Cognitive uplink interference management in 4G cellular femtocells. *2010 IEEE 21st International Symposium on Personal Indoor and Mobile Radio Communications (PIMRC)*, 1567 -1571.

Yoshino, M., Haruyama, S., Nakagawa, M. (2008) High-accuracy positioning system using visible LED lights and image sensor. *2008 IEEE Radio and Wireless Symposium*, 439-442.

Zhang, W., & Kavehrad, M. (2012). A 2-D indoor localization system based on visible light LED. *2012 IEEE Photonics Society Summer Topical Meeting Series,* 80-81.

Zhang, X., Cui, K., Yao, M., Zhang, H., & Xu, Z. (2012, July). Experimental characterization of indoor visible light communication channels. *2012 8th International Symposium on Communication Systems, Networks & Digital Signal Processing (CSNDSP),* 1-5.

Zhou, X., & Campbell, A. T. (2014, September). Visible light networking and sensing. *Proceedings of the 1st ACM workshop on Hot topics in wireless,* 55-60.

Appendix (A)

Simulations Results

• Result of experiment 1: Simulating VLC in clear weather.
• Result of experiment 2: Simulating VLC in storm that has low, medium, and high density clay particles.
• Result of experiment 3: Simulating VLC in storm that has low, medium, and high density silt particles.
• Result of experiment 4: Simulating VLC in storm that has low, medium, and high density sand particles.
• Result of experiment 5: Simulating VLC in storm that has low, medium, and high density gravel particles.

Table (A.1)

The calculated distances for the simulations

0	25	50	75	100	125	150	175	200	225	250	275	300	325	350	375	400	425	450	475	500
5.404	25.577	50.291	75.194	100.146	125.117	150.097	175.083	200.073	225.065	250.058	275.053	300.049	325.045	350.042	375.039	400.037	425.034	450.032	475.031	500.029
4.945	25.484	50.244	75.163	100.122	125.098	150.081	175.070	200.061	225.054	250.049	275.044	300.041	325.038	350.035	375.033	400.031	425.029	450.027	475.026	500.024
4.495	25.401	50.202	75.135	100.101	125.081	150.067	175.058	200.050	225.045	250.040	275.037	300.034	325.031	350.029	375.027	400.025	425.024	450.022	475.021	500.020
4.056	25.327	50.164	75.110	100.082	125.066	150.055	175.047	200.041	225.037	250.033	275.030	300.027	325.025	350.024	375.022	400.021	425.019	450.018	475.017	500.016
3.634	25.263	50.132	75.088	100.066	125.053	150.044	175.038	200.033	225.029	250.026	275.024	300.022	325.020	350.019	375.018	400.017	425.016	450.015	475.014	500.013
3.233	25.208	50.104	75.070	100.052	125.042	150.035	175.030	200.026	225.023	250.021	275.019	300.017	325.016	350.015	375.014	400.013	425.012	450.012	475.011	500.010
2.864	25.164	50.082	75.055	100.041	125.033	150.027	175.023	200.021	225.018	250.016	275.015	300.014	325.013	350.012	375.011	400.010	425.010	450.009	475.009	500.008
2.540	25.129	50.064	75.043	100.032	125.026	150.022	175.018	200.016	225.014	250.013	275.012	300.011	325.010	350.009	375.009	400.008	425.008	450.007	475.007	500.006
2.281	25.104	50.052	75.035	100.026	125.021	150.017	175.015	200.013	225.012	250.010	275.009	300.009	325.008	350.007	375.007	400.007	425.006	450.006	475.005	500.005
2.110	25.089	50.045	75.030	100.022	125.018	150.015	175.013	200.011	225.010	250.009	275.008	300.007	325.007	350.006	375.006	400.006	425.005	450.005	475.005	500.004
2.050	25.084	50.042	75.028	100.021	125.017	150.014	175.012	200.011	225.009	250.008	275.008	300.007	325.006	350.006	375.006	400.005	425.005	450.005	475.004	500.004
2.110	25.089	50.045	75.030	100.022	125.018	150.015	175.013	200.011	225.010	250.009	275.008	300.007	325.007	350.006	375.006	400.006	425.005	450.005	475.005	500.004
2.281	25.104	50.052	75.035	100.026	125.021	150.017	175.015	200.013	225.012	250.010	275.009	300.009	325.008	350.007	375.007	400.007	425.006	450.006	475.005	500.005
2.540	25.129	50.064	75.043	100.032	125.026	150.022	175.018	200.016	225.014	250.013	275.012	300.011	325.010	350.009	375.009	400.008	425.008	450.007	475.007	500.006
2.864	25.164	50.082	75.055	100.041	125.033	150.027	175.023	200.021	225.018	250.016	275.015	300.014	325.013	350.012	375.011	400.010	425.010	450.009	475.009	500.008
3.233	25.208	50.104	75.070	100.052	125.042	150.035	175.030	200.026	225.023	250.021	275.019	300.017	325.016	350.015	375.014	400.013	425.012	450.012	475.011	500.010
3.634	25.263	50.132	75.088	100.066	125.053	150.044	175.038	200.033	225.029	250.026	275.024	300.022	325.020	350.019	375.018	400.017	425.016	450.015	475.014	500.013
4.056	25.327	50.164	75.110	100.082	125.066	150.055	175.047	200.041	225.037	250.033	275.030	300.027	325.025	350.024	375.022	400.021	425.019	450.018	475.017	500.016
4.495	25.327	50.202	75.135	100.101	125.081	150.067	175.058	200.050	225.045	250.040	275.037	300.034	325.031	350.029	375.027	400.025	425.024	450.022	475.021	500.020
4.945	25.484	50.244	75.163	100.122	125.098	150.081	175.070	200.061	225.054	250.049	275.044	300.041	325.038	350.035	375.033	400.031	425.029	450.027	475.026	500.024
5.404	25.577	50.291	75.194	100.146	125.117	150.097	175.083	200.073	225.065	250.058	275.053	300.049	325.045	350.042	375.039	400.037	425.034	450.032	475.031	500.029

Table (A.2)

The result of received power when the weather condition is clear atmosphere

0	25	50	75	100	125	150	175	200	225	250	275	300	325	350	375	400	425	450	475	500
-13.292	-26.148	-32.001	-35.492	-37.980	-39.913	-41.495	-42.833	-43.992	-45.015	-45.930	-46.758	-47.514	-48.210	-48.854	-49.454	-50.015	-50.542	-51.039	-51.509	-51.955
-12.665	-26.117	-31.993	-35.488	-37.978	-39.912	-41.494	-42.832	-43.991	-45.014	-45.930	-46.758	-47.514	-48.210	-48.854	-49.454	-50.015	-50.542	-51.039	-51.509	-51.955
-12.030	-26.089	-31.986	-35.485	-37.976	-39.911	-41.493	-42.831	-43.991	-45.014	-45.929	-46.758	-47.514	-48.209	-48.854	-49.453	-50.014	-50.542	-51.039	-51.509	-51.955
-11.406	-26.064	-31.979	-35.482	-37.974	-39.910	-41.492	-42.831	-43.991	-45.014	-45.929	-46.757	-47.514	-48.209	-48.853	-49.453	-50.014	-50.542	-51.039	-51.509	-51.955
-10.834	-26.042	-31.974	-35.479	-37.973	-39.909	-41.492	-42.830	-43.990	-45.013	-45.929	-46.757	-47.513	-48.209	-48.853	-49.453	-50.014	-50.541	-51.038	-51.509	-51.955
-10.388	-26.023	-31.969	-35.477	-37.972	-39.908	-41.491	-42.830	-43.990	-45.013	-45.929	-46.757	-47.513	-48.209	-48.853	-49.453	-50.014	-50.541	-51.038	-51.509	-51.955
-10.221	-26.008	-31.965	-35.475	-37.971	-39.907	-41.491	-42.830	-43.990	-45.013	-45.929	-46.757	-47.513	-48.209	-48.853	-49.453	-50.014	-50.541	-51.038	-51.509	-51.955
-10.636	-25.996	-31.962	-35.474	-37.970	-39.907	-41.490	-42.829	-43.989	-45.013	-45.928	-46.757	-47.513	-48.209	-48.853	-49.453	-50.014	-50.541	-51.038	-51.509	-51.955
-12.287	-25.987	-31.960	-35.473	-37.969	-39.907	-41.490	-42.829	-43.989	-45.013	-45.928	-46.757	-47.513	-48.209	-48.853	-49.453	-50.014	-50.541	-51.038	-51.509	-51.955
-16.955	-25.982	-31.958	-35.472	-37.969	-39.906	-41.490	-42.829	-43.989	-45.013	-45.928	-46.757	-47.513	-48.209	-48.853	-49.453	-50.014	-50.541	-51.038	-51.509	-51.955
-∞	-25.980	-31.958	-35.472	-37.969	-39.906	-41.490	-42.829	-43.989	-45.013	-45.928	-46.757	-47.513	-48.209	-48.853	-49.453	-50.014	-50.541	-51.038	-51.509	-51.955
-16.955	-25.982	-31.958	-35.472	-37.969	-39.906	-41.490	-42.829	-43.989	-45.013	-45.928	-46.757	-47.513	-48.209	-48.853	-49.453	-50.014	-50.541	-51.038	-51.509	-51.955
-12.287	-25.987	-31.960	-35.473	-37.969	-39.907	-41.490	-42.829	-43.989	-45.013	-45.928	-46.757	-47.513	-48.209	-48.853	-49.453	-50.014	-50.541	-51.038	-51.509	-51.955
-10.636	-25.996	-31.962	-35.474	-37.970	-39.907	-41.490	-42.829	-43.989	-45.013	-45.928	-46.757	-47.513	-48.209	-48.853	-49.453	-50.014	-50.541	-51.038	-51.509	-51.955
-10.221	-26.008	-31.965	-35.475	-37.971	-39.907	-41.491	-42.830	-43.990	-45.013	-45.929	-46.757	-47.513	-48.209	-48.853	-49.453	-50.014	-50.541	-51.038	-51.509	-51.955
-10.388	-26.023	-31.969	-35.477	-37.972	-39.908	-41.491	-42.830	-43.990	-45.013	-45.929	-46.757	-47.513	-48.209	-48.853	-49.453	-50.014	-50.541	-51.038	-51.509	-51.955
-10.834	-26.042	-31.974	-35.479	-37.973	-39.909	-41.492	-42.830	-43.990	-45.013	-45.929	-46.757	-47.513	-48.209	-48.853	-49.453	-50.014	-50.541	-51.038	-51.509	-51.955
-11.406	-26.064	-31.979	-35.482	-37.974	-39.910	-41.492	-42.831	-43.991	-45.014	-45.929	-46.757	-47.514	-48.209	-48.853	-49.453	-50.014	-50.542	-51.039	-51.509	-51.955
-12.030	-26.064	-31.986	-35.485	-37.976	-39.911	-41.493	-42.831	-43.991	-45.014	-45.929	-46.758	-47.514	-48.209	-48.854	-49.453	-50.014	-50.542	-51.039	-51.509	-51.955
-12.665	-26.117	-31.993	-35.488	-37.978	-39.912	-41.494	-42.832	-43.991	-45.014	-45.930	-46.758	-47.514	-48.210	-48.854	-49.454	-50.015	-50.542	-51.039	-51.509	-51.955
-13.292	-26.148	-32.001	-35.492	-37.980	-39.913	-41.495	-42.833	-43.992	-45.015	-45.930	-46.758	-47.514	-48.210	-48.854	-49.454	-50.015	-50.542	-51.039	-51.509	-51.955

Table (A.3)

The result of signal to noise ratio (SNR) when the weather condition is clear atmosphere

0	25	50	75	100	125	150	175	200	225	250	275	300	325	350	375	400	425	450	475	500
97.519	80.096	69.539	62.820	57.941	54.119	50.981	48.321	46.012	43.973	42.147	40.495	38.985	37.596	36.310	35.112	33.991	32.937	31.944	31.005	30.113
98.206	80.149	69.554	62.827	57.945	54.122	50.983	48.322	46.013	43.974	42.148	40.495	38.986	37.597	36.310	35.112	33.991	32.938	31.944	31.005	30.113
98.894	80.196	69.568	62.834	57.948	54.124	50.985	48.323	46.014	43.975	42.149	40.496	38.986	37.597	36.310	35.112	33.991	32.938	31.945	31.005	30.113
99.564	80.239	69.580	62.839	57.951	54.126	50.986	48.324	46.015	43.975	42.149	40.496	38.987	37.597	36.311	35.113	33.991	32.938	31.945	31.005	30.113
100.173	80.276	69.591	62.844	57.954	54.128	50.987	48.325	46.015	43.976	42.150	40.497	38.987	37.598	36.311	35.113	33.992	32.938	31.945	31.005	30.114
100.644	80.307	69.600	62.848	57.957	54.129	50.988	48.326	46.016	43.976	42.150	40.497	38.987	37.598	36.311	35.113	33.992	32.938	31.945	31.005	30.114
100.820	80.333	69.607	62.852	57.959	54.131	50.989	48.327	46.017	43.977	42.150	40.497	38.988	37.598	36.311	35.113	33.992	32.938	31.945	31.005	30.114
100.383	80.353	69.613	62.854	57.960	54.132	50.990	48.327	46.017	43.977	42.151	40.498	38.988	37.598	36.311	35.113	33.992	32.939	31.945	31.005	30.114
98.617	80.367	69.617	62.856	57.961	54.132	50.991	48.328	46.017	43.977	42.151	40.498	38.988	37.598	36.312	35.113	33.992	32.939	31.945	31.006	30.114
93.307	80.376	69.619	62.857	57.962	54.133	50.991	48.328	46.017	43.977	42.151	40.498	38.988	37.598	36.312	35.113	33.992	32.939	31.945	31.006	30.114
0.000	80.378	69.620	62.858	57.962	54.133	50.991	48.328	46.017	43.977	42.151	40.498	38.988	37.598	36.312	35.113	33.992	32.939	31.945	31.006	30.114
93.307	80.376	69.619	62.857	57.962	54.133	50.991	48.328	46.017	43.977	42.151	40.498	38.988	37.598	36.312	35.113	33.992	32.939	31.945	31.006	30.114
98.617	80.367	69.617	62.856	57.961	54.132	50.991	48.328	46.017	43.977	42.151	40.498	38.988	37.598	36.312	35.113	33.992	32.939	31.945	31.006	30.114
100.383	80.353	69.613	62.854	57.960	54.132	50.990	48.327	46.017	43.977	42.151	40.498	38.988	37.598	36.311	35.113	33.992	32.939	31.945	31.005	30.114
100.820	80.333	69.607	62.852	57.959	54.131	50.989	48.327	46.017	43.977	42.150	40.497	38.988	37.598	36.311	35.113	33.992	32.938	31.945	31.005	30.114
100.644	80.307	69.600	62.848	57.957	54.129	50.988	48.326	46.016	43.976	42.150	40.497	38.987	37.598	36.311	35.113	33.992	32.938	31.945	31.005	30.114
100.173	80.276	69.591	62.844	57.954	54.128	50.987	48.325	46.015	43.976	42.150	40.497	38.987	37.598	36.311	35.113	33.992	32.938	31.945	31.005	30.114
99.564	80.239	69.580	62.839	57.951	54.126	50.986	48.324	46.015	43.975	42.149	40.496	38.987	37.597	36.311	35.113	33.991	32.938	31.945	31.005	30.113
98.894	80.239	69.568	62.834	57.948	54.124	50.985	48.323	46.014	43.975	42.149	40.496	38.986	37.597	36.310	35.112	33.991	32.938	31.945	31.005	30.113
98.206	80.149	69.554	62.827	57.945	54.122	50.983	48.322	46.013	43.974	42.148	40.495	38.986	37.597	36.310	35.112	33.991	32.938	31.944	31.005	30.113
97.519	80.096	69.539	62.820	57.941	54.119	50.981	48.321	46.012	43.973	42.147	40.495	38.985	37.596	36.310	35.112	33.991	32.937	31.944	31.005	30.113

Table (A.4)

The result of bit error rate (BER) when the weather condition is clear atmosphere

0	25	50	75	100	125	150	175	200	225	250	275	300	325	350	375	400	425	450	475	500
1.3E-44	5.1E-37	2.1E-32	1.8E-29	2.5E-27	1.2E-25	2.8E-24	4.2E-23	4.3E-22	3.4E-21	2.1E-20	1.1E-19	5.2E-19	2.1E-18	7.9E-18	2.6E-17	8.3E-17	2.4E-16	6.6E-16	1.7E-15	4.2E-15
6.3E-45	4.9E-37	2.1E-32	1.8E-29	2.5E-27	1.2E-25	2.8E-24	4.1E-23	4.3E-22	3.4E-21	2.1E-20	1.1E-19	5.2E-19	2.1E-18	7.9E-18	2.6E-17	8.2E-17	2.4E-16	6.6E-16	1.7E-15	4.2E-15
3.2E-45	4.6E-37	2.1E-32	1.8E-29	2.5E-27	1.2E-25	2.8E-24	4.1E-23	4.3E-22	3.4E-21	2.1E-20	1.1E-19	5.2E-19	2.1E-18	7.9E-18	2.6E-17	8.2E-17	2.4E-16	6.6E-16	1.7E-15	4.2E-15
1.6E-45	4.4E-37	2.0E-32	1.8E-29	2.5E-27	1.2E-25	2.8E-24	4.1E-23	4.3E-22	3.4E-21	2.1E-20	1.1E-19	5.2E-19	2.1E-18	7.9E-18	2.6E-17	8.2E-17	2.4E-16	6.6E-16	1.7E-15	4.2E-15
8.8E-46	4.3E-37	2.0E-32	1.8E-29	2.5E-27	1.2E-25	2.8E-24	4.1E-23	4.3E-22	3.4E-21	2.1E-20	1.1E-19	5.2E-19	2.1E-18	7.9E-18	2.6E-17	8.2E-17	2.4E-16	6.6E-16	1.7E-15	4.2E-15
5.5E-46	4.2E-37	2.0E-32	1.8E-29	2.5E-27	1.2E-25	2.8E-24	4.1E-23	4.3E-22	3.4E-21	2.1E-20	1.1E-19	5.2E-19	2.1E-18	7.8E-18	2.6E-17	8.2E-17	2.4E-16	6.6E-16	1.7E-15	4.2E-15
4.6E-46	4.0E-37	2.0E-32	1.8E-29	2.5E-27	1.2E-25	2.8E-24	4.1E-23	4.3E-22	3.4E-21	2.1E-20	1.1E-19	5.2E-19	2.1E-18	7.8E-18	2.6E-17	8.2E-17	2.4E-16	6.6E-16	1.7E-15	4.2E-15
7.1E-46	4.0E-37	2.0E-32	1.8E-29	2.5E-27	1.2E-25	2.8E-24	4.1E-23	4.3E-22	3.4E-21	2.1E-20	1.1E-19	5.2E-19	2.1E-18	7.8E-18	2.6E-17	8.2E-17	2.4E-16	6.6E-16	1.7E-15	4.2E-15
4.2E-45	3.9E-37	2.0E-32	1.8E-29	2.5E-27	1.2E-25	2.8E-24	4.1E-23	4.3E-22	3.3E-21	2.1E-20	1.1E-19	5.2E-19	2.1E-18	7.8E-18	2.6E-17	8.2E-17	2.4E-16	6.6E-16	1.7E-15	4.2E-15
8.7E-43	3.9E-37	2.0E-32	1.8E-29	2.5E-27	1.2E-25	2.8E-24	4.1E-23	4.3E-22	3.3E-21	2.1E-20	1.1E-19	5.2E-19	2.1E-18	7.8E-18	2.6E-17	8.2E-17	2.4E-16	6.6E-16	1.7E-15	4.2E-15
5.0E-01	3.9E-37	2.0E-32	1.8E-29	2.5E-27	1.2E-25	2.8E-24	4.1E-23	4.3E-22	3.3E-21	2.1E-20	1.1E-19	5.2E-19	2.1E-18	7.8E-18	2.6E-17	8.2E-17	2.4E-16	6.6E-16	1.7E-15	4.2E-15
8.7E-43	3.9E-37	2.0E-32	1.8E-29	2.5E-27	1.2E-25	2.8E-24	4.1E-23	4.3E-22	3.3E-21	2.1E-20	1.1E-19	5.2E-19	2.1E-18	7.8E-18	2.6E-17	8.2E-17	2.4E-16	6.6E-16	1.7E-15	4.2E-15
4.2E-45	3.9E-37	2.0E-32	1.8E-29	2.5E-27	1.2E-25	2.8E-24	4.1E-23	4.3E-22	3.3E-21	2.1E-20	1.1E-19	5.2E-19	2.1E-18	7.8E-18	2.6E-17	8.2E-17	2.4E-16	6.6E-16	1.7E-15	4.2E-15
7.1E-46	4.0E-37	2.0E-32	1.8E-29	2.5E-27	1.2E-25	2.8E-24	4.1E-23	4.3E-22	3.4E-21	2.1E-20	1.1E-19	5.2E-19	2.1E-18	7.8E-18	2.6E-17	8.2E-17	2.4E-16	6.6E-16	1.7E-15	4.2E-15
4.6E-46	4.0E-37	2.0E-32	1.8E-29	2.5E-27	1.2E-25	2.8E-24	4.1E-23	4.3E-22	3.4E-21	2.1E-20	1.1E-19	5.2E-19	2.1E-18	7.8E-18	2.6E-17	8.2E-17	2.4E-16	6.6E-16	1.7E-15	4.2E-15
5.5E-46	4.2E-37	2.0E-32	1.8E-29	2.5E-27	1.2E-25	2.8E-24	4.1E-23	4.3E-22	3.4E-21	2.1E-20	1.1E-19	5.2E-19	2.1E-18	7.8E-18	2.6E-17	8.2E-17	2.4E-16	6.6E-16	1.7E-15	4.2E-15
8.8E-46	4.3E-37	2.0E-32	1.8E-29	2.5E-27	1.2E-25	2.8E-24	4.1E-23	4.3E-22	3.4E-21	2.1E-20	1.1E-19	5.2E-19	2.1E-18	7.9E-18	2.6E-17	8.2E-17	2.4E-16	6.6E-16	1.7E-15	4.2E-15
1.6E-45	4.4E-37	2.0E-32	1.8E-29	2.5E-27	1.2E-25	2.8E-24	4.1E-23	4.3E-22	3.4E-21	2.1E-20	1.1E-19	5.2E-19	2.1E-18	7.9E-18	2.6E-17	8.2E-17	2.4E-16	6.6E-16	1.7E-15	4.2E-15
3.2E-45	4.4E-37	2.1E-32	1.8E-29	2.5E-27	1.2E-25	2.8E-24	4.1E-23	4.3E-22	3.4E-21	2.1E-20	1.1E-19	5.2E-19	2.1E-18	7.9E-18	2.6E-17	8.2E-17	2.4E-16	6.6E-16	1.7E-15	4.2E-15
6.3E-45	4.9E-37	2.1E-32	1.8E-29	2.5E-27	1.2E-25	2.8E-24	4.1E-23	4.3E-22	3.4E-21	2.1E-20	1.1E-19	5.2E-19	2.1E-18	7.9E-18	2.6E-17	8.2E-17	2.4E-16	6.6E-16	1.7E-15	4.2E-15
1.3E-44	5.1E-37	2.1E-32	1.8E-29	2.5E-27	1.2E-25	2.8E-24	4.2E-23	4.3E-22	3.4E-21	2.1E-20	1.1E-19	5.2E-19	2.1E-18	7.9E-18	2.6E-17	8.3E-17	2.4E-16	6.6E-16	1.7E-15	4.2E-15

Table (A.5)

The result of received power for the VLC affected by clay particles when the visibility is 5 Km

0	25	50	75	100	125	150	175	200	225	250	275	300	325	350	375	400	425	450	475	500
-13.316	-26.262	-32.223	-35.824	-38.423	-40.467	-42.158	-43.607	-44.877	-46.010	-47.036	-47.974	-48.841	-49.647	-50.402	-51.112	-51.784	-52.421	-53.029	-53.610	-54.166
-12.687	-26.230	-32.215	-35.820	-38.420	-40.465	-42.157	-43.606	-44.876	-46.010	-47.035	-47.974	-48.841	-49.647	-50.402	-51.112	-51.784	-52.421	-53.029	-53.609	-54.166
-12.050	-26.201	-32.208	-35.817	-38.418	-40.464	-42.157	-43.605	-44.876	-46.009	-47.035	-47.974	-48.840	-49.647	-50.401	-51.112	-51.783	-52.421	-53.029	-53.609	-54.166
-11.424	-26.176	-32.201	-35.814	-38.417	-40.463	-42.156	-43.605	-44.875	-46.009	-47.035	-47.974	-48.840	-49.647	-50.401	-51.112	-51.783	-52.421	-53.029	-53.609	-54.166
-10.850	-26.153	-32.195	-35.811	-38.415	-40.462	-42.155	-43.604	-44.875	-46.009	-47.035	-47.973	-48.840	-49.646	-50.401	-51.111	-51.783	-52.421	-53.028	-53.609	-54.166
-10.403	-26.134	-32.190	-35.809	-38.414	-40.461	-42.155	-43.604	-44.874	-46.008	-47.034	-47.973	-48.840	-49.646	-50.401	-51.111	-51.783	-52.421	-53.028	-53.609	-54.166
-10.234	-26.119	-32.186	-35.807	-38.413	-40.460	-42.154	-43.604	-44.874	-46.008	-47.034	-47.973	-48.840	-49.646	-50.401	-51.111	-51.783	-52.421	-53.028	-53.609	-54.166
-10.647	-26.107	-32.183	-35.806	-38.412	-40.460	-42.154	-43.603	-44.874	-46.008	-47.034	-47.973	-48.840	-49.646	-50.401	-51.111	-51.783	-52.421	-53.028	-53.609	-54.166
-12.297	-26.098	-32.181	-35.805	-38.412	-40.459	-42.153	-43.603	-44.874	-46.008	-47.034	-47.973	-48.840	-49.646	-50.401	-51.111	-51.783	-52.421	-53.028	-53.609	-54.166
-16.965	-26.093	-32.180	-35.804	-38.411	-40.459	-42.153	-43.603	-44.874	-46.008	-47.034	-47.973	-48.840	-49.646	-50.401	-51.111	-51.783	-52.421	-53.028	-53.609	-54.166
-∞	-26.091	-32.179	-35.804	-38.411	-40.459	-42.153	-43.603	-44.874	-46.008	-47.034	-47.973	-48.840	-49.646	-50.401	-51.111	-51.783	-52.421	-53.028	-53.609	-54.166
-16.965	-26.093	-32.180	-35.804	-38.411	-40.459	-42.153	-43.603	-44.874	-46.008	-47.034	-47.973	-48.840	-49.646	-50.401	-51.111	-51.783	-52.421	-53.028	-53.609	-54.166
-12.297	-26.098	-32.181	-35.805	-38.412	-40.459	-42.153	-43.603	-44.874	-46.008	-47.034	-47.973	-48.840	-49.646	-50.401	-51.111	-51.783	-52.421	-53.028	-53.609	-54.166
-10.647	-26.107	-32.183	-35.806	-38.412	-40.460	-42.154	-43.603	-44.874	-46.008	-47.034	-47.973	-48.840	-49.646	-50.401	-51.111	-51.783	-52.421	-53.028	-53.609	-54.166
-10.234	-26.119	-32.186	-35.807	-38.413	-40.460	-42.154	-43.604	-44.874	-46.008	-47.034	-47.973	-48.840	-49.646	-50.401	-51.111	-51.783	-52.421	-53.028	-53.609	-54.166
-10.403	-26.134	-32.190	-35.809	-38.414	-40.461	-42.155	-43.604	-44.874	-46.008	-47.034	-47.973	-48.840	-49.646	-50.401	-51.111	-51.783	-52.421	-53.028	-53.609	-54.166
-10.850	-26.153	-32.195	-35.811	-38.415	-40.462	-42.155	-43.604	-44.875	-46.009	-47.035	-47.973	-48.840	-49.646	-50.401	-51.111	-51.783	-52.421	-53.028	-53.609	-54.166
-11.424	-26.176	-32.201	-35.814	-38.417	-40.463	-42.156	-43.605	-44.875	-46.009	-47.035	-47.974	-48.840	-49.647	-50.401	-51.112	-51.783	-52.421	-53.029	-53.609	-54.166
-12.050	-26.176	-32.208	-35.817	-38.418	-40.464	-42.157	-43.605	-44.876	-46.009	-47.035	-47.974	-48.840	-49.647	-50.401	-51.112	-51.783	-52.421	-53.029	-53.609	-54.166
-12.687	-26.230	-32.215	-35.820	-38.420	-40.465	-42.157	-43.606	-44.876	-46.010	-47.035	-47.974	-48.841	-49.647	-50.402	-51.112	-51.784	-52.421	-53.029	-53.609	-54.166
-13.316	-26.262	-32.223	-35.824	-38.423	-40.467	-42.158	-43.607	-44.877	-46.010	-47.036	-47.974	-48.841	-49.647	-50.402	-51.112	-51.784	-52.421	-53.029	-53.610	-54.166

Table (A.6)

The result of signal to noise ratio (SNR) for the VLC connectivity affected by clay particles when the visibility is 5 Km

0	25	50	75	100	125	150	175	200	225	250	275	300	325	350	375	400	425	450	475	500
97.493	79.905	69.117	62.171	57.067	53.022	49.662	46.779	44.249	41.988	39.941	38.067	36.336	34.725	33.217	31.798	30.456	29.181	27.967	26.806	25.693
98.182	79.959	69.133	62.179	57.071	53.025	49.664	46.781	44.250	41.989	39.941	38.067	36.336	34.726	33.218	31.798	30.456	29.181	27.967	26.806	25.693
98.873	80.007	69.147	62.185	57.075	53.028	49.666	46.782	44.251	41.990	39.942	38.068	36.337	34.726	33.218	31.799	30.456	29.182	27.967	26.806	25.693
99.545	80.050	69.160	62.191	57.079	53.030	49.667	46.783	44.252	41.990	39.943	38.068	36.337	34.726	33.218	31.799	30.456	29.182	27.967	26.806	25.693
100.156	80.088	69.170	62.196	57.082	53.032	49.669	46.784	44.252	41.991	39.943	38.069	36.337	34.727	33.219	31.799	30.457	29.182	27.967	26.806	25.694
100.629	80.119	69.180	62.201	57.084	53.033	49.670	46.785	44.253	41.991	39.944	38.069	36.338	34.727	33.219	31.799	30.457	29.182	27.968	26.807	25.694
100.807	80.145	69.187	62.204	57.086	53.035	49.671	46.786	44.254	41.992	39.944	38.069	36.338	34.727	33.219	31.799	30.457	29.182	27.968	26.807	25.694
100.371	80.166	69.193	62.207	57.088	53.036	49.671	46.786	44.254	41.992	39.944	38.070	36.338	34.727	33.219	31.800	30.457	29.182	27.968	26.807	25.694
98.606	80.180	69.197	62.209	57.089	53.036	49.672	46.787	44.254	41.992	39.944	38.070	36.338	34.728	33.219	31.800	30.457	29.182	27.968	26.807	25.694
93.296	80.189	69.200	62.210	57.089	53.037	49.672	46.787	44.254	41.993	39.945	38.070	36.338	34.728	33.219	31.800	30.457	29.183	27.968	26.807	25.694
0.000	80.192	69.201	62.210	57.090	53.037	49.672	46.787	44.255	41.993	39.945	38.070	36.338	34.728	33.219	31.800	30.457	29.183	27.968	26.807	25.694
93.296	80.189	69.200	62.210	57.089	53.037	49.672	46.787	44.254	41.993	39.945	38.070	36.338	34.728	33.219	31.800	30.457	29.183	27.968	26.807	25.694
98.606	80.180	69.197	62.209	57.089	53.036	49.672	46.787	44.254	41.992	39.944	38.070	36.338	34.728	33.219	31.800	30.457	29.182	27.968	26.807	25.694
100.371	80.166	69.193	62.207	57.088	53.036	49.671	46.786	44.254	41.992	39.944	38.070	36.338	34.727	33.219	31.800	30.457	29.182	27.968	26.807	25.694
100.807	80.145	69.187	62.204	57.086	53.035	49.671	46.786	44.254	41.992	39.944	38.069	36.338	34.727	33.219	31.799	30.457	29.182	27.968	26.807	25.694
100.629	80.119	69.180	62.201	57.084	53.033	49.670	46.785	44.253	41.991	39.944	38.069	36.338	34.727	33.219	31.799	30.457	29.182	27.968	26.807	25.694
100.156	80.088	69.170	62.196	57.082	53.032	49.669	46.784	44.252	41.991	39.943	38.069	36.337	34.727	33.219	31.799	30.457	29.182	27.967	26.806	25.694
99.545	80.050	69.160	62.191	57.079	53.030	49.667	46.783	44.252	41.990	39.943	38.068	36.337	34.726	33.218	31.799	30.456	29.182	27.967	26.806	25.693
98.873	80.050	69.147	62.185	57.075	53.028	49.666	46.782	44.251	41.990	39.942	38.068	36.337	34.726	33.218	31.799	30.456	29.182	27.967	26.806	25.693
98.182	79.959	69.133	62.179	57.071	53.025	49.664	46.781	44.250	41.989	39.941	38.067	36.336	34.726	33.218	31.798	30.456	29.181	27.967	26.806	25.693
97.493	79.905	69.117	62.171	57.067	53.022	49.662	46.779	44.249	41.988	39.941	38.067	36.336	34.725	33.217	31.798	30.456	29.181	27.967	26.806	25.693

Table (A.7)

The result of bit error rate (BER) for the VLC connectivity affected by clay particles when the visibility is 5 Km

0	25	50	75	100	125	150	175	200	225	250	275	300	325	350	375	400	425	450	475	500
1.3E-44	6.2E-37	3.2E-32	3.5E-29	6.1E-27	3.6E-25	1.1E-23	2.0E-22	2.5E-21	2.5E-20	2.0E-19	1.3E-18	7.7E-18	3.9E-17	1.8E-16	7.6E-16	3.0E-15	1.1E-14	3.7E-14	1.2E-13	3.8E-13
6.5E-45	5.9E-37	3.2E-32	3.5E-29	6.1E-27	3.6E-25	1.1E-23	2.0E-22	2.5E-21	2.5E-20	2.0E-19	1.3E-18	7.7E-18	3.9E-17	1.8E-16	7.6E-16	3.0E-15	1.1E-14	3.7E-14	1.2E-13	3.8E-13
3.2E-45	5.6E-37	3.1E-32	3.5E-29	6.0E-27	3.6E-25	1.1E-23	2.0E-22	2.5E-21	2.5E-20	2.0E-19	1.3E-18	7.6E-18	3.9E-17	1.8E-16	7.6E-16	3.0E-15	1.1E-14	3.7E-14	1.2E-13	3.8E-13
1.7E-45	5.4E-37	3.1E-32	3.5E-29	6.0E-27	3.6E-25	1.1E-23	2.0E-22	2.5E-21	2.5E-20	2.0E-19	1.3E-18	7.6E-18	3.9E-17	1.8E-16	7.6E-16	3.0E-15	1.1E-14	3.7E-14	1.2E-13	3.8E-13
8.9E-46	5.2E-37	3.1E-32	3.5E-29	6.0E-27	3.6E-25	1.1E-23	2.0E-22	2.5E-21	2.5E-20	2.0E-19	1.3E-18	7.6E-18	3.9E-17	1.8E-16	7.6E-16	3.0E-15	1.1E-14	3.7E-14	1.2E-13	3.8E-13
5.6E-46	5.0E-37	3.0E-32	3.4E-29	6.0E-27	3.6E-25	1.1E-23	2.0E-22	2.5E-21	2.5E-20	2.0E-19	1.3E-18	7.6E-18	3.9E-17	1.8E-16	7.6E-16	3.0E-15	1.1E-14	3.7E-14	1.2E-13	3.8E-13
4.6E-46	4.9E-37	3.0E-32	3.4E-29	6.0E-27	3.6E-25	1.1E-23	2.0E-22	2.5E-21	2.5E-20	2.0E-19	1.3E-18	7.6E-18	3.9E-17	1.8E-16	7.6E-16	3.0E-15	1.1E-14	3.7E-14	1.2E-13	3.8E-13
7.2E-46	4.8E-37	3.0E-32	3.4E-29	6.0E-27	3.6E-25	1.1E-23	2.0E-22	2.5E-21	2.5E-20	2.0E-19	1.3E-18	7.6E-18	3.9E-17	1.8E-16	7.6E-16	3.0E-15	1.1E-14	3.7E-14	1.2E-13	3.8E-13
4.2E-45	4.7E-37	3.0E-32	3.4E-29	6.0E-27	3.6E-25	1.1E-23	2.0E-22	2.5E-21	2.5E-20	2.0E-19	1.3E-18	7.6E-18	3.9E-17	1.8E-16	7.6E-16	3.0E-15	1.1E-14	3.7E-14	1.2E-13	3.8E-13
8.8E-43	4.7E-37	3.0E-32	3.4E-29	6.0E-27	3.6E-25	1.1E-23	2.0E-22	2.5E-21	2.5E-20	2.0E-19	1.3E-18	7.6E-18	3.9E-17	1.8E-16	7.6E-16	3.0E-15	1.1E-14	3.7E-14	1.2E-13	3.8E-13
5.0E-01	4.7E-37	3.0E-32	3.4E-29	6.0E-27	3.6E-25	1.1E-23	2.0E-22	2.5E-21	2.5E-20	2.0E-19	1.3E-18	7.6E-18	3.9E-17	1.8E-16	7.6E-16	3.0E-15	1.1E-14	3.7E-14	1.2E-13	3.8E-13
8.8E-43	4.7E-37	3.0E-32	3.4E-29	6.0E-27	3.6E-25	1.1E-23	2.0E-22	2.5E-21	2.5E-20	2.0E-19	1.3E-18	7.6E-18	3.9E-17	1.8E-16	7.6E-16	3.0E-15	1.1E-14	3.7E-14	1.2E-13	3.8E-13
4.2E-45	4.7E-37	3.0E-32	3.4E-29	6.0E-27	3.6E-25	1.1E-23	2.0E-22	2.5E-21	2.5E-20	2.0E-19	1.3E-18	7.6E-18	3.9E-17	1.8E-16	7.6E-16	3.0E-15	1.1E-14	3.7E-14	1.2E-13	3.8E-13
7.2E-46	4.8E-37	3.0E-32	3.4E-29	6.0E-27	3.6E-25	1.1E-23	2.0E-22	2.5E-21	2.5E-20	2.0E-19	1.3E-18	7.6E-18	3.9E-17	1.8E-16	7.6E-16	3.0E-15	1.1E-14	3.7E-14	1.2E-13	3.8E-13
4.6E-46	4.9E-37	3.0E-32	3.4E-29	6.0E-27	3.6E-25	1.1E-23	2.0E-22	2.5E-21	2.5E-20	2.0E-19	1.3E-18	7.6E-18	3.9E-17	1.8E-16	7.6E-16	3.0E-15	1.1E-14	3.7E-14	1.2E-13	3.8E-13
5.6E-46	5.0E-37	3.0E-32	3.4E-29	6.0E-27	3.6E-25	1.1E-23	2.0E-22	2.5E-21	2.5E-20	2.0E-19	1.3E-18	7.6E-18	3.9E-17	1.8E-16	7.6E-16	3.0E-15	1.1E-14	3.7E-14	1.2E-13	3.8E-13
8.9E-46	5.2E-37	3.1E-32	3.5E-29	6.0E-27	3.6E-25	1.1E-23	2.0E-22	2.5E-21	2.5E-20	2.0E-19	1.3E-18	7.6E-18	3.9E-17	1.8E-16	7.6E-16	3.0E-15	1.1E-14	3.7E-14	1.2E-13	3.8E-13
1.7E-45	5.4E-37	3.1E-32	3.5E-29	6.0E-27	3.6E-25	1.1E-23	2.0E-22	2.5E-21	2.5E-20	2.0E-19	1.3E-18	7.6E-18	3.9E-17	1.8E-16	7.6E-16	3.0E-15	1.1E-14	3.7E-14	1.2E-13	3.8E-13
3.2E-45	5.4E-37	3.1E-32	3.5E-29	6.0E-27	3.6E-25	1.1E-23	2.0E-22	2.5E-21	2.5E-20	2.0E-19	1.3E-18	7.6E-18	3.9E-17	1.8E-16	7.6E-16	3.0E-15	1.1E-14	3.7E-14	1.2E-13	3.8E-13
6.5E-45	5.9E-37	3.2E-32	3.5E-29	6.1E-27	3.6E-25	1.1E-23	2.0E-22	2.5E-21	2.5E-20	2.0E-19	1.3E-18	7.7E-18	3.9E-17	1.8E-16	7.6E-16	3.0E-15	1.1E-14	3.7E-14	1.2E-13	3.8E-13
1.3E-44	6.2E-37	3.2E-32	3.5E-29	6.1E-27	3.6E-25	1.1E-23	2.0E-22	2.5E-21	2.5E-20	2.0E-19	1.3E-18	7.7E-18	3.9E-17	1.8E-16	7.6E-16	3.0E-15	1.1E-14	3.7E-14	1.2E-13	3.8E-13

Table (A.8)

The result of received power for the VLC affected by clay particles when the visibility is 1 Km

0	25	50	75	100	125	150	175	200	225	250	275	300	325	350	375	400	425	450	475	500
-13.411	-26.714	-33.113	-37.154	-40.193	-42.679	-44.812	-46.703	-48.414	-49.990	-51.457	-52.838	-54.146	-55.395	-56.591	-57.744	-58.857	-59.937	-60.986	-62.009	-63.008
-12.774	-26.680	-33.103	-37.149	-40.191	-42.677	-44.811	-46.702	-48.414	-49.989	-51.457	-52.837	-54.146	-55.394	-56.591	-57.743	-58.857	-59.937	-60.986	-62.009	-63.008
-12.129	-26.650	-33.095	-37.145	-40.188	-42.676	-44.810	-46.701	-48.413	-49.988	-51.456	-52.837	-54.146	-55.394	-56.591	-57.743	-58.857	-59.936	-60.986	-62.009	-63.007
-11.496	-26.623	-33.088	-37.142	-40.186	-42.674	-44.809	-46.700	-48.412	-49.988	-51.456	-52.837	-54.145	-55.394	-56.590	-57.743	-58.856	-59.936	-60.986	-62.009	-63.007
-10.914	-26.600	-33.082	-37.139	-40.185	-42.673	-44.808	-46.699	-48.412	-49.988	-51.456	-52.836	-54.145	-55.393	-56.590	-57.743	-58.856	-59.936	-60.986	-62.008	-63.007
-10.460	-26.580	-33.076	-37.136	-40.183	-42.672	-44.807	-46.699	-48.411	-49.987	-51.455	-52.836	-54.145	-55.393	-56.590	-57.742	-58.856	-59.936	-60.986	-62.008	-63.007
-10.284	-26.564	-33.072	-37.134	-40.182	-42.671	-44.807	-46.698	-48.411	-49.987	-51.455	-52.836	-54.145	-55.393	-56.590	-57.742	-58.856	-59.936	-60.985	-62.008	-63.007
-10.692	-26.551	-33.068	-37.133	-40.181	-42.671	-44.806	-46.698	-48.411	-49.987	-51.455	-52.836	-54.145	-55.393	-56.590	-57.742	-58.856	-59.936	-60.985	-62.008	-63.007
-12.337	-26.542	-33.066	-37.132	-40.180	-42.670	-44.806	-46.698	-48.410	-49.986	-51.455	-52.836	-54.144	-55.393	-56.590	-57.742	-58.856	-59.936	-60.985	-62.008	-63.007
-17.002	-26.537	-33.065	-37.131	-40.180	-42.670	-44.806	-46.698	-48.410	-49.986	-51.455	-52.835	-54.144	-55.393	-56.590	-57.742	-58.856	-59.936	-60.985	-62.008	-63.007
-∞	-26.535	-33.064	-37.131	-40.180	-42.670	-44.806	-46.697	-48.410	-49.986	-51.454	-52.835	-54.144	-55.393	-56.590	-57.742	-58.856	-59.936	-60.985	-62.008	-63.007
-17.002	-26.537	-33.065	-37.131	-40.180	-42.670	-44.806	-46.698	-48.410	-49.986	-51.455	-52.835	-54.144	-55.393	-56.590	-57.742	-58.856	-59.936	-60.985	-62.008	-63.007
-12.337	-26.542	-33.066	-37.132	-40.180	-42.670	-44.806	-46.698	-48.410	-49.986	-51.455	-52.836	-54.144	-55.393	-56.590	-57.742	-58.856	-59.936	-60.985	-62.008	-63.007
-10.692	-26.551	-33.068	-37.133	-40.181	-42.671	-44.806	-46.698	-48.411	-49.987	-51.455	-52.836	-54.145	-55.393	-56.590	-57.742	-58.856	-59.936	-60.985	-62.008	-63.007
-10.284	-26.564	-33.072	-37.134	-40.182	-42.671	-44.807	-46.698	-48.411	-49.987	-51.455	-52.836	-54.145	-55.393	-56.590	-57.742	-58.856	-59.936	-60.985	-62.008	-63.007
-10.460	-26.580	-33.076	-37.136	-40.183	-42.672	-44.807	-46.699	-48.411	-49.987	-51.455	-52.836	-54.145	-55.393	-56.590	-57.742	-58.856	-59.936	-60.986	-62.008	-63.007
-10.914	-26.600	-33.082	-37.139	-40.185	-42.673	-44.808	-46.699	-48.412	-49.988	-51.456	-52.836	-54.145	-55.393	-56.590	-57.743	-58.856	-59.936	-60.986	-62.008	-63.007
-11.496	-26.623	-33.088	-37.142	-40.186	-42.674	-44.809	-46.700	-48.412	-49.988	-51.456	-52.837	-54.145	-55.394	-56.590	-57.743	-58.856	-59.936	-60.986	-62.009	-63.007
-12.129	-26.623	-33.095	-37.145	-40.188	-42.676	-44.810	-46.701	-48.413	-49.988	-51.456	-52.837	-54.146	-55.394	-56.591	-57.743	-58.857	-59.936	-60.986	-62.009	-63.007
-12.774	-26.680	-33.103	-37.149	-40.191	-42.677	-44.811	-46.702	-48.414	-49.989	-51.457	-52.837	-54.146	-55.394	-56.591	-57.743	-58.857	-59.937	-60.986	-62.009	-63.008
-13.411	-26.714	-33.113	-37.154	-40.193	-42.679	-44.812	-46.703	-48.414	-49.990	-51.457	-52.838	-54.146	-55.395	-56.591	-57.744	-58.857	-59.937	-60.986	-62.009	-63.008

Table (A.9)

The result of signal to noise ratio (SNR) for the VLC connectivity affected by clay particles when the visibility is 1 Km

0	25	50	75	100	125	150	175	200	225	250	275	300	325	350	375	400	425	450	475	500
97.388	79.135	67.421	59.566	53.564	48.627	44.376	40.606	37.188	34.041	31.108	28.348	25.732	23.237	20.844	18.540	16.313	14.154	12.055	10.010	8.012
98.087	79.192	67.438	59.575	53.569	48.630	44.379	40.608	37.189	34.042	31.109	28.349	25.733	23.237	20.845	18.540	16.313	14.154	12.055	10.010	8.013
98.787	79.244	67.454	59.582	53.574	48.633	44.381	40.609	37.191	34.043	31.110	28.350	25.734	23.238	20.845	18.541	16.314	14.155	12.056	10.010	8.013
99.468	79.289	67.468	59.589	53.578	48.636	44.383	40.611	37.192	34.044	31.111	28.351	25.734	23.239	20.846	18.541	16.314	14.155	12.056	10.011	8.013
100.088	79.329	67.480	59.595	53.581	48.638	44.385	40.612	37.193	34.045	31.111	28.351	25.735	23.239	20.846	18.542	16.315	14.156	12.056	10.011	8.014
100.568	79.363	67.490	59.600	53.584	48.640	44.386	40.613	37.194	34.046	31.112	28.352	25.735	23.240	20.847	18.542	16.315	14.156	12.057	10.011	8.014
100.753	79.391	67.499	59.604	53.587	48.642	44.388	40.614	37.195	34.046	31.113	28.352	25.736	23.240	20.847	18.542	16.315	14.156	12.057	10.011	8.014
100.323	79.413	67.505	59.607	53.589	48.643	44.389	40.615	37.195	34.047	31.113	28.353	25.736	23.240	20.847	18.543	16.315	14.156	12.057	10.012	8.014
98.562	79.428	67.510	59.610	53.590	48.644	44.389	40.615	37.196	34.047	31.113	28.353	25.736	23.240	20.847	18.543	16.316	14.156	12.057	10.012	8.014
93.250	79.438	67.513	59.611	53.591	48.645	44.390	40.616	37.196	34.048	31.113	28.353	25.736	23.240	20.847	18.543	16.316	14.156	12.057	10.012	8.014
0.000	79.441	67.514	59.611	53.591	48.645	44.390	40.616	37.196	34.048	31.114	28.353	25.736	23.241	20.847	18.543	16.316	14.156	12.057	10.012	8.014
93.250	79.438	67.513	59.611	53.591	48.645	44.390	40.616	37.196	34.048	31.113	28.353	25.736	23.240	20.847	18.543	16.316	14.156	12.057	10.012	8.014
98.562	79.428	67.510	59.610	53.590	48.644	44.389	40.615	37.196	34.047	31.113	28.353	25.736	23.240	20.847	18.543	16.316	14.156	12.057	10.012	8.014
100.323	79.413	67.505	59.607	53.589	48.643	44.389	40.615	37.195	34.047	31.113	28.353	25.736	23.240	20.847	18.543	16.315	14.156	12.057	10.012	8.014
100.753	79.391	67.499	59.604	53.587	48.642	44.388	40.614	37.195	34.046	31.113	28.352	25.736	23.240	20.847	18.542	16.315	14.156	12.057	10.011	8.014
100.568	79.363	67.490	59.600	53.584	48.640	44.386	40.613	37.194	34.046	31.112	28.352	25.735	23.240	20.847	18.542	16.315	14.156	12.057	10.011	8.014
100.088	79.329	67.480	59.595	53.581	48.638	44.385	40.612	37.193	34.045	31.111	28.351	25.735	23.239	20.846	18.542	16.315	14.156	12.056	10.011	8.014
99.468	79.289	67.468	59.589	53.578	48.636	44.383	40.611	37.192	34.044	31.111	28.351	25.734	23.239	20.846	18.541	16.314	14.155	12.056	10.011	8.013
98.787	79.289	67.454	59.582	53.574	48.633	44.381	40.609	37.191	34.043	31.110	28.350	25.734	23.238	20.845	18.541	16.314	14.155	12.056	10.010	8.013
98.087	79.192	67.438	59.575	53.569	48.630	44.379	40.608	37.189	34.042	31.109	28.349	25.733	23.237	20.845	18.540	16.313	14.154	12.055	10.010	8.013
97.388	79.135	67.421	59.566	53.564	48.627	44.376	40.606	37.188	34.041	31.108	28.348	25.732	23.237	20.844	18.540	16.313	14.154	12.055	10.010	8.012

Table (A.10)

The result of bit error rate (BER) for the VLC connectivity affected by clay particles when the visibility is 1 Km

0	25	50	75	100	125	150	175	200	225	250	275	300	325	350	375	400	425	450	475	500
1.4E-44	1.4E-36	1.8E-31	4.9E-28	2.1E-25	3.1E-23	2.2E-21	1.0E-19	3.2E-18	7.8E-17	1.5E-15	2.5E-14	3.6E-13	4.6E-12	5.4E-11	5.7E-10	5.6E-09	5.2E-08	4.5E-07	3.8E-06	3.1E-05
7.1E-45	1.3E-36	1.8E-31	4.9E-28	2.1E-25	3.0E-23	2.2E-21	1.0E-19	3.2E-18	7.8E-17	1.5E-15	2.5E-14	3.6E-13	4.6E-12	5.3E-11	5.7E-10	5.6E-09	5.2E-08	4.5E-07	3.8E-06	3.1E-05
3.5E-45	1.2E-36	1.7E-31	4.8E-28	2.1E-25	3.0E-23	2.2E-21	1.0E-19	3.2E-18	7.8E-17	1.5E-15	2.5E-14	3.6E-13	4.6E-12	5.3E-11	5.7E-10	5.6E-09	5.2E-08	4.5E-07	3.8E-06	3.1E-05
1.8E-45	1.2E-36	1.7E-31	4.8E-28	2.1E-25	3.0E-23	2.2E-21	1.0E-19	3.2E-18	7.8E-17	1.5E-15	2.5E-14	3.6E-13	4.6E-12	5.3E-11	5.7E-10	5.6E-09	5.2E-08	4.5E-07	3.8E-06	3.1E-05
9.6E-46	1.1E-36	1.7E-31	4.8E-28	2.1E-25	3.0E-23	2.2E-21	1.0E-19	3.2E-18	7.8E-17	1.5E-15	2.5E-14	3.6E-13	4.6E-12	5.3E-11	5.7E-10	5.6E-09	5.2E-08	4.5E-07	3.8E-06	3.1E-05
5.9E-46	1.1E-36	1.7E-31	4.7E-28	2.0E-25	3.0E-23	2.2E-21	1.0E-19	3.2E-18	7.8E-17	1.5E-15	2.5E-14	3.6E-13	4.6E-12	5.3E-11	5.7E-10	5.6E-09	5.2E-08	4.5E-07	3.8E-06	3.1E-05
4.9E-46	1.0E-36	1.7E-31	4.7E-28	2.0E-25	3.0E-23	2.2E-21	1.0E-19	3.2E-18	7.8E-17	1.5E-15	2.5E-14	3.6E-13	4.6E-12	5.3E-11	5.7E-10	5.6E-09	5.2E-08	4.5E-07	3.8E-06	3.1E-05
7.5E-46	1.0E-36	1.6E-31	4.7E-28	2.0E-25	3.0E-23	2.2E-21	1.0E-19	3.2E-18	7.8E-17	1.5E-15	2.5E-14	3.6E-13	4.6E-12	5.3E-11	5.7E-10	5.6E-09	5.2E-08	4.5E-07	3.8E-06	3.1E-05
4.4E-45	1.0E-36	1.6E-31	4.7E-28	2.0E-25	3.0E-23	2.2E-21	1.0E-19	3.2E-18	7.8E-17	1.5E-15	2.5E-14	3.6E-13	4.6E-12	5.3E-11	5.7E-10	5.6E-09	5.2E-08	4.5E-07	3.8E-06	3.1E-05
9.2E-43	1.0E-36	1.6E-31	4.7E-28	2.0E-25	3.0E-23	2.2E-21	1.0E-19	3.2E-18	7.8E-17	1.5E-15	2.5E-14	3.6E-13	4.6E-12	5.3E-11	5.7E-10	5.6E-09	5.2E-08	4.5E-07	3.8E-06	3.1E-05
5.0E-01	9.9E-37	1.6E-31	4.7E-28	2.0E-25	3.0E-23	2.2E-21	1.0E-19	3.2E-18	7.8E-17	1.5E-15	2.5E-14	3.6E-13	4.6E-12	5.3E-11	5.7E-10	5.6E-09	5.2E-08	4.5E-07	3.8E-06	3.1E-05
9.2E-43	1.0E-36	1.6E-31	4.7E-28	2.0E-25	3.0E-23	2.2E-21	1.0E-19	3.2E-18	7.8E-17	1.5E-15	2.5E-14	3.6E-13	4.6E-12	5.3E-11	5.7E-10	5.6E-09	5.2E-08	4.5E-07	3.8E-06	3.1E-05
4.4E-45	1.0E-36	1.6E-31	4.7E-28	2.0E-25	3.0E-23	2.2E-21	1.0E-19	3.2E-18	7.8E-17	1.5E-15	2.5E-14	3.6E-13	4.6E-12	5.3E-11	5.7E-10	5.6E-09	5.2E-08	4.5E-07	3.8E-06	3.1E-05
7.5E-46	1.0E-36	1.6E-31	4.7E-28	2.0E-25	3.0E-23	2.2E-21	1.0E-19	3.2E-18	7.8E-17	1.5E-15	2.5E-14	3.6E-13	4.6E-12	5.3E-11	5.7E-10	5.6E-09	5.2E-08	4.5E-07	3.8E-06	3.1E-05
4.9E-46	1.0E-36	1.7E-31	4.7E-28	2.0E-25	3.0E-23	2.2E-21	1.0E-19	3.2E-18	7.8E-17	1.5E-15	2.5E-14	3.6E-13	4.6E-12	5.3E-11	5.7E-10	5.6E-09	5.2E-08	4.5E-07	3.8E-06	3.1E-05
5.9E-46	1.1E-36	1.7E-31	4.7E-28	2.0E-25	3.0E-23	2.2E-21	1.0E-19	3.2E-18	7.8E-17	1.5E-15	2.5E-14	3.6E-13	4.6E-12	5.3E-11	5.7E-10	5.6E-09	5.2E-08	4.5E-07	3.8E-06	3.1E-05
9.6E-46	1.1E-36	1.7E-31	4.8E-28	2.1E-25	3.0E-23	2.2E-21	1.0E-19	3.2E-18	7.8E-17	1.5E-15	2.5E-14	3.6E-13	4.6E-12	5.3E-11	5.7E-10	5.6E-09	5.2E-08	4.5E-07	3.8E-06	3.1E-05
1.8E-45	1.2E-36	1.7E-31	4.8E-28	2.1E-25	3.0E-23	2.2E-21	1.0E-19	3.2E-18	7.8E-17	1.5E-15	2.5E-14	3.6E-13	4.6E-12	5.3E-11	5.7E-10	5.6E-09	5.2E-08	4.5E-07	3.8E-06	3.1E-05
3.5E-45	1.2E-36	1.7E-31	4.8E-28	2.1E-25	3.0E-23	2.2E-21	1.0E-19	3.2E-18	7.8E-17	1.5E-15	2.5E-14	3.6E-13	4.6E-12	5.3E-11	5.7E-10	5.6E-09	5.2E-08	4.5E-07	3.8E-06	3.1E-05
7.1E-45	1.3E-36	1.8E-31	4.9E-28	2.1E-25	3.0E-23	2.2E-21	1.0E-19	3.2E-18	7.8E-17	1.5E-15	2.5E-14	3.6E-13	4.6E-12	5.3E-11	5.7E-10	5.6E-09	5.2E-08	4.5E-07	3.8E-06	3.1E-05
1.4E-44	1.4E-36	1.8E-31	4.9E-28	2.1E-25	3.1E-23	2.2E-21	1.0E-19	3.2E-18	7.8E-17	1.5E-15	2.5E-14	3.6E-13	4.6E-12	5.4E-11	5.7E-10	5.6E-09	5.2E-08	4.5E-07	3.8E-06	3.1E-05

Table (A.11)

The result of received power for the VLC affected by clay particles when the visibility is 0.1 Km

0	25	50	75	100	125	150	175	200	225	250	275	300	325	350	375	400	425	450	475	500
-14.487	-31.804	-43.121	-52.117	-60.122	-67.577	-74.682	-81.544	-88.229	-94.778	-101.219	-107.574	-113.856	-120.079	-126.250	-132.377	-138.465	-144.519	-150.543	-156.541	-162.514
-13.758	-31.752	-43.102	-52.107	-60.115	-67.572	-74.678	-81.541	-88.226	-94.775	-101.217	-107.572	-113.855	-120.077	-126.248	-132.375	-138.463	-144.518	-150.542	-156.540	-162.513
-13.024	-31.705	-43.085	-52.097	-60.109	-67.567	-74.674	-81.537	-88.223	-94.773	-101.215	-107.570	-113.853	-120.075	-126.247	-132.374	-138.462	-144.517	-150.541	-156.538	-162.512
-12.303	-31.663	-43.071	-52.089	-60.103	-67.562	-74.670	-81.535	-88.221	-94.770	-101.213	-107.568	-113.851	-120.074	-126.245	-132.373	-138.461	-144.515	-150.540	-156.538	-162.511
-11.637	-31.627	-43.058	-52.082	-60.098	-67.559	-74.667	-81.532	-88.218	-94.769	-101.211	-107.566	-113.850	-120.073	-126.244	-132.371	-138.460	-144.515	-150.539	-156.537	-162.510
-11.103	-31.597	-43.047	-52.075	-60.094	-67.555	-74.665	-81.530	-88.217	-94.767	-101.210	-107.565	-113.849	-120.072	-126.243	-132.371	-138.459	-144.514	-150.538	-156.536	-162.510
-10.854	-31.571	-43.038	-52.070	-60.090	-67.553	-74.662	-81.528	-88.215	-94.766	-101.208	-107.564	-113.848	-120.071	-126.243	-132.370	-138.458	-144.513	-150.538	-156.535	-162.509
-11.197	-31.552	-43.031	-52.066	-60.087	-67.551	-74.661	-81.527	-88.214	-94.765	-101.208	-107.563	-113.847	-120.070	-126.242	-132.369	-138.458	-144.513	-150.537	-156.535	-162.509
-12.791	-31.538	-43.026	-52.064	-60.086	-67.549	-74.660	-81.526	-88.213	-94.764	-101.207	-107.563	-113.846	-120.070	-126.242	-132.369	-138.458	-144.512	-150.537	-156.535	-162.508
-17.422	-31.529	-43.023	-52.062	-60.084	-67.549	-74.659	-81.525	-88.213	-94.764	-101.207	-107.562	-113.846	-120.069	-126.241	-132.369	-138.457	-144.512	-150.537	-156.534	-162.508
-∞	-31.527	-43.023	-52.061	-60.084	-67.548	-74.659	-81.525	-88.213	-94.763	-101.206	-107.562	-113.846	-120.069	-126.241	-132.369	-138.457	-144.512	-150.537	-156.534	-162.508
-17.422	-31.529	-43.023	-52.062	-60.084	-67.549	-74.659	-81.525	-88.213	-94.764	-101.207	-107.562	-113.846	-120.069	-126.241	-132.369	-138.457	-144.512	-150.537	-156.534	-162.508
-12.791	-31.538	-43.026	-52.064	-60.086	-67.549	-74.660	-81.526	-88.213	-94.764	-101.207	-107.563	-113.846	-120.070	-126.242	-132.369	-138.458	-144.512	-150.537	-156.535	-162.508
-11.197	-31.552	-43.031	-52.066	-60.087	-67.551	-74.661	-81.527	-88.214	-94.765	-101.208	-107.563	-113.847	-120.070	-126.242	-132.369	-138.458	-144.513	-150.537	-156.535	-162.509
-10.854	-31.571	-43.038	-52.070	-60.090	-67.553	-74.662	-81.528	-88.215	-94.766	-101.208	-107.564	-113.848	-120.071	-126.243	-132.370	-138.458	-144.513	-150.538	-156.535	-162.509
-11.103	-31.597	-43.047	-52.075	-60.094	-67.555	-74.665	-81.530	-88.217	-94.767	-101.210	-107.565	-113.849	-120.072	-126.243	-132.371	-138.459	-144.514	-150.538	-156.536	-162.510
-11.637	-31.627	-43.058	-52.082	-60.098	-67.559	-74.667	-81.532	-88.218	-94.769	-101.211	-107.566	-113.850	-120.073	-126.244	-132.371	-138.460	-144.515	-150.539	-156.537	-162.510
-12.303	-31.663	-43.071	-52.089	-60.103	-67.562	-74.670	-81.535	-88.221	-94.770	-101.213	-107.568	-113.851	-120.074	-126.245	-132.373	-138.461	-144.515	-150.540	-156.538	-162.511
-13.024	-31.663	-43.085	-52.097	-60.109	-67.567	-74.674	-81.537	-88.223	-94.773	-101.215	-107.570	-113.853	-120.075	-126.247	-132.374	-138.462	-144.517	-150.541	-156.538	-162.512
-13.758	-31.752	-43.102	-52.107	-60.115	-67.572	-74.678	-81.541	-88.226	-94.775	-101.217	-107.572	-113.855	-120.077	-126.248	-132.375	-138.463	-144.518	-150.542	-156.540	-162.513
-14.487	-31.804	-43.121	-52.117	-60.122	-67.577	-74.682	-81.544	-88.229	-94.778	-101.219	-107.574	-113.856	-120.079	-126.250	-132.377	-138.465	-144.519	-150.543	-156.541	-162.514

Table (A.12)

The result of signal to noise ratio (SNR) for the VLC connectivity affected by clay particles when the visibility is 0.1 Km

0	25	50	75	100	125	150	175	200	225	250	275	300	325	350	375	400	425	450	475	500
96.187	69.912	47.747	29.789	13.783	0.000	0.000	0.000	0.000	0.000	0.000	0.000	0.000	0.000	0.000	0.000	0.000	0.000	0.000	0.000	0.000
97.003	70.010	47.784	29.810	13.797	0.000	0.000	0.000	0.000	0.000	0.000	0.000	0.000	0.000	0.000	0.000	0.000	0.000	0.000	0.000	0.000
97.814	70.098	47.818	29.829	13.810	0.000	0.000	0.000	0.000	0.000	0.000	0.000	0.000	0.000	0.000	0.000	0.000	0.000	0.000	0.000	0.000
98.599	70.177	47.847	29.846	13.822	0.000	0.000	0.000	0.000	0.000	0.000	0.000	0.000	0.000	0.000	0.000	0.000	0.000	0.000	0.000	0.000
99.317	70.245	47.872	29.860	13.832	0.000	0.000	0.000	0.000	0.000	0.000	0.000	0.000	0.000	0.000	0.000	0.000	0.000	0.000	0.000	0.000
99.887	70.303	47.894	29.872	13.840	0.000	0.000	0.000	0.000	0.000	0.000	0.000	0.000	0.000	0.000	0.000	0.000	0.000	0.000	0.000	0.000
100.151	70.350	47.911	29.883	13.847	0.000	0.000	0.000	0.000	0.000	0.000	0.000	0.000	0.000	0.000	0.000	0.000	0.000	0.000	0.000	0.000
99.787	70.387	47.925	29.890	13.853	0.000	0.000	0.000	0.000	0.000	0.000	0.000	0.000	0.000	0.000	0.000	0.000	0.000	0.000	0.000	0.000
98.068	70.413	47.935	29.896	13.856	0.000	0.000	0.000	0.000	0.000	0.000	0.000	0.000	0.000	0.000	0.000	0.000	0.000	0.000	0.000	0.000
92.739	70.429	47.941	29.899	13.859	0.000	0.000	0.000	0.000	0.000	0.000	0.000	0.000	0.000	0.000	0.000	0.000	0.000	0.000	0.000	0.000
0.000	70.435	47.943	29.901	13.860	0.000	0.000	0.000	0.000	0.000	0.000	0.000	0.000	0.000	0.000	0.000	0.000	0.000	0.000	0.000	0.000
92.739	70.429	47.941	29.899	13.859	0.000	0.000	0.000	0.000	0.000	0.000	0.000	0.000	0.000	0.000	0.000	0.000	0.000	0.000	0.000	0.000
98.068	70.413	47.935	29.896	13.856	0.000	0.000	0.000	0.000	0.000	0.000	0.000	0.000	0.000	0.000	0.000	0.000	0.000	0.000	0.000	0.000
99.787	70.387	47.925	29.890	13.853	0.000	0.000	0.000	0.000	0.000	0.000	0.000	0.000	0.000	0.000	0.000	0.000	0.000	0.000	0.000	0.000
100.151	70.350	47.911	29.883	13.847	0.000	0.000	0.000	0.000	0.000	0.000	0.000	0.000	0.000	0.000	0.000	0.000	0.000	0.000	0.000	0.000
99.887	70.303	47.894	29.872	13.840	0.000	0.000	0.000	0.000	0.000	0.000	0.000	0.000	0.000	0.000	0.000	0.000	0.000	0.000	0.000	0.000
99.317	70.245	47.872	29.860	13.832	0.000	0.000	0.000	0.000	0.000	0.000	0.000	0.000	0.000	0.000	0.000	0.000	0.000	0.000	0.000	0.000
98.599	70.177	47.847	29.846	13.822	0.000	0.000	0.000	0.000	0.000	0.000	0.000	0.000	0.000	0.000	0.000	0.000	0.000	0.000	0.000	0.000
97.814	70.177	47.818	29.829	13.810	0.000	0.000	0.000	0.000	0.000	0.000	0.000	0.000	0.000	0.000	0.000	0.000	0.000	0.000	0.000	0.000
97.003	70.010	47.784	29.810	13.797	0.000	0.000	0.000	0.000	0.000	0.000	0.000	0.000	0.000	0.000	0.000	0.000	0.000	0.000	0.000	0.000
96.187	69.912	47.747	29.789	13.783	0.000	0.000	0.000	0.000	0.000	0.000	0.000	0.000	0.000	0.000	0.000	0.000	0.000	0.000	0.000	0.000

Table (A.13)

The result of bit error rate (BER) for the VLC connectivity affected by clay particles when the visibility is 0.1 Km

0	25	50	75	100	125	150	175	200	225	250	275	300	325	350	375	400	425	450	475	500
4.8E-44	1.5E-32	7.4E-23	5.9E-15	7.6E-08	5.0E-01	5.0E-01	5.0E-01	5.0E-01	5.0E-01	5.0E-01	5.0E-01	5.0E-01	5.0E-01	5.0E-01	5.0E-01	5.0E-01	5.0E-01	5.0E-01	5.0E-01	5.0E-01
2.1E-44	1.3E-32	7.1E-23	5.8E-15	7.5E-08	5.0E-01	5.0E-01	5.0E-01	5.0E-01	5.0E-01	5.0E-01	5.0E-01	5.0E-01	5.0E-01	5.0E-01	5.0E-01	5.0E-01	5.0E-01	5.0E-01	5.0E-01	5.0E-01
9.4E-45	1.2E-32	6.9E-23	5.6E-15	7.4E-08	5.0E-01	5.0E-01	5.0E-01	5.0E-01	5.0E-01	5.0E-01	5.0E-01	5.0E-01	5.0E-01	5.0E-01	5.0E-01	5.0E-01	5.0E-01	5.0E-01	5.0E-01	5.0E-01
4.3E-45	1.1E-32	6.7E-23	5.5E-15	7.3E-08	5.0E-01	5.0E-01	5.0E-01	5.0E-01	5.0E-01	5.0E-01	5.0E-01	5.0E-01	5.0E-01	5.0E-01	5.0E-01	5.0E-01	5.0E-01	5.0E-01	5.0E-01	5.0E-01
2.1E-45	1.0E-32	6.5E-23	5.5E-15	7.2E-08	5.0E-01	5.0E-01	5.0E-01	5.0E-01	5.0E-01	5.0E-01	5.0E-01	5.0E-01	5.0E-01	5.0E-01	5.0E-01	5.0E-01	5.0E-01	5.0E-01	5.0E-01	5.0E-01
1.2E-45	9.8E-33	6.4E-23	5.4E-15	7.2E-08	5.0E-01	5.0E-01	5.0E-01	5.0E-01	5.0E-01	5.0E-01	5.0E-01	5.0E-01	5.0E-01	5.0E-01	5.0E-01	5.0E-01	5.0E-01	5.0E-01	5.0E-01	5.0E-01
9.0E-46	9.4E-33	6.3E-23	5.3E-15	7.1E-08	5.0E-01	5.0E-01	5.0E-01	5.0E-01	5.0E-01	5.0E-01	5.0E-01	5.0E-01	5.0E-01	5.0E-01	5.0E-01	5.0E-01	5.0E-01	5.0E-01	5.0E-01	5.0E-01
1.3E-45	9.0E-33	6.2E-23	5.3E-15	7.1E-08	5.0E-01	5.0E-01	5.0E-01	5.0E-01	5.0E-01	5.0E-01	5.0E-01	5.0E-01	5.0E-01	5.0E-01	5.0E-01	5.0E-01	5.0E-01	5.0E-01	5.0E-01	5.0E-01
7.3E-45	8.8E-33	6.1E-23	5.3E-15	7.0E-08	5.0E-01	5.0E-01	5.0E-01	5.0E-01	5.0E-01	5.0E-01	5.0E-01	5.0E-01	5.0E-01	5.0E-01	5.0E-01	5.0E-01	5.0E-01	5.0E-01	5.0E-01	5.0E-01
1.5E-42	8.6E-33	6.1E-23	5.3E-15	7.0E-08	5.0E-01	5.0E-01	5.0E-01	5.0E-01	5.0E-01	5.0E-01	5.0E-01	5.0E-01	5.0E-01	5.0E-01	5.0E-01	5.0E-01	5.0E-01	5.0E-01	5.0E-01	5.0E-01
5.0E-01	8.6E-33	6.1E-23	5.2E-15	7.0E-08	5.0E-01	5.0E-01	5.0E-01	5.0E-01	5.0E-01	5.0E-01	5.0E-01	5.0E-01	5.0E-01	5.0E-01	5.0E-01	5.0E-01	5.0E-01	5.0E-01	5.0E-01	5.0E-01
1.5E-42	8.6E-33	6.1E-23	5.3E-15	7.0E-08	5.0E-01	5.0E-01	5.0E-01	5.0E-01	5.0E-01	5.0E-01	5.0E-01	5.0E-01	5.0E-01	5.0E-01	5.0E-01	5.0E-01	5.0E-01	5.0E-01	5.0E-01	5.0E-01
7.3E-45	8.8E-33	6.1E-23	5.3E-15	7.0E-08	5.0E-01	5.0E-01	5.0E-01	5.0E-01	5.0E-01	5.0E-01	5.0E-01	5.0E-01	5.0E-01	5.0E-01	5.0E-01	5.0E-01	5.0E-01	5.0E-01	5.0E-01	5.0E-01
1.3E-45	9.0E-33	6.2E-23	5.3E-15	7.1E-08	5.0E-01	5.0E-01	5.0E-01	5.0E-01	5.0E-01	5.0E-01	5.0E-01	5.0E-01	5.0E-01	5.0E-01	5.0E-01	5.0E-01	5.0E-01	5.0E-01	5.0E-01	5.0E-01
9.0E-46	9.4E-33	6.3E-23	5.3E-15	7.1E-08	5.0E-01	5.0E-01	5.0E-01	5.0E-01	5.0E-01	5.0E-01	5.0E-01	5.0E-01	5.0E-01	5.0E-01	5.0E-01	5.0E-01	5.0E-01	5.0E-01	5.0E-01	5.0E-01
1.2E-45	9.8E-33	6.4E-23	5.4E-15	7.2E-08	5.0E-01	5.0E-01	5.0E-01	5.0E-01	5.0E-01	5.0E-01	5.0E-01	5.0E-01	5.0E-01	5.0E-01	5.0E-01	5.0E-01	5.0E-01	5.0E-01	5.0E-01	5.0E-01
2.1E-45	1.0E-32	6.5E-23	5.5E-15	7.2E-08	5.0E-01	5.0E-01	5.0E-01	5.0E-01	5.0E-01	5.0E-01	5.0E-01	5.0E-01	5.0E-01	5.0E-01	5.0E-01	5.0E-01	5.0E-01	5.0E-01	5.0E-01	5.0E-01
4.3E-45	1.1E-32	6.7E-23	5.5E-15	7.3E-08	5.0E-01	5.0E-01	5.0E-01	5.0E-01	5.0E-01	5.0E-01	5.0E-01	5.0E-01	5.0E-01	5.0E-01	5.0E-01	5.0E-01	5.0E-01	5.0E-01	5.0E-01	5.0E-01
9.4E-45	1.1E-32	6.9E-23	5.6E-15	7.4E-08	5.0E-01	5.0E-01	5.0E-01	5.0E-01	5.0E-01	5.0E-01	5.0E-01	5.0E-01	5.0E-01	5.0E-01	5.0E-01	5.0E-01	5.0E-01	5.0E-01	5.0E-01	5.0E-01
2.1E-44	1.3E-32	7.1E-23	5.8E-15	7.5E-08	5.0E-01	5.0E-01	5.0E-01	5.0E-01	5.0E-01	5.0E-01	5.0E-01	5.0E-01	5.0E-01	5.0E-01	5.0E-01	5.0E-01	5.0E-01	5.0E-01	5.0E-01	5.0E-01
4.8E-44	1.5E-32	7.4E-23	5.9E-15	7.6E-08	5.0E-01	5.0E-01	5.0E-01	5.0E-01	5.0E-01	5.0E-01	5.0E-01	5.0E-01	5.0E-01	5.0E-01	5.0E-01	5.0E-01	5.0E-01	5.0E-01	5.0E-01	5.0E-01

Table (A.14)

The result of received power for the VLC affected by silt particles when the visibility is 5 Km

0	25	50	75	100	125	150	175	200	225	250	275	300	325	350	375	400	425	450	475	500
-13.309	-26.227	-32.156	-35.723	-38.289	-40.299	-41.958	-43.372	-44.609	-45.709	-46.701	-47.606	-48.439	-49.212	-49.933	-50.610	-51.248	-51.852	-52.427	-52.974	-53.497
-12.680	-26.196	-32.148	-35.720	-38.286	-40.298	-41.957	-43.372	-44.608	-45.708	-46.701	-47.606	-48.439	-49.212	-49.933	-50.610	-51.248	-51.852	-52.426	-52.974	-53.497
-12.044	-26.167	-32.140	-35.716	-38.284	-40.297	-41.956	-43.371	-44.608	-45.708	-46.700	-47.606	-48.439	-49.212	-49.933	-50.610	-51.248	-51.852	-52.426	-52.974	-53.497
-11.419	-26.142	-32.134	-35.713	-38.283	-40.295	-41.955	-43.371	-44.607	-45.708	-46.700	-47.605	-48.439	-49.212	-49.933	-50.610	-51.248	-51.852	-52.426	-52.974	-53.497
-10.845	-26.120	-32.128	-35.711	-38.281	-40.294	-41.954	-43.370	-44.607	-45.707	-46.700	-47.605	-48.439	-49.211	-49.933	-50.610	-51.248	-51.852	-52.426	-52.973	-53.497
-10.398	-26.101	-32.123	-35.709	-38.280	-40.294	-41.954	-43.370	-44.607	-45.707	-46.700	-47.605	-48.438	-49.211	-49.933	-50.610	-51.248	-51.852	-52.426	-52.973	-53.497
-10.230	-26.085	-32.119	-35.707	-38.279	-40.293	-41.953	-43.369	-44.606	-45.707	-46.700	-47.605	-48.438	-49.211	-49.933	-50.609	-51.248	-51.852	-52.426	-52.973	-53.497
-10.643	-26.073	-32.116	-35.705	-38.278	-40.293	-41.953	-43.369	-44.606	-45.707	-46.699	-47.605	-48.438	-49.211	-49.932	-50.609	-51.248	-51.852	-52.426	-52.973	-53.497
-12.294	-26.065	-32.114	-35.704	-38.278	-40.292	-41.953	-43.369	-44.606	-45.707	-46.699	-47.605	-48.438	-49.211	-49.932	-50.609	-51.248	-51.852	-52.426	-52.973	-53.497
-16.962	-26.059	-32.113	-35.704	-38.277	-40.292	-41.953	-43.369	-44.606	-45.707	-46.699	-47.605	-48.438	-49.211	-49.932	-50.609	-51.248	-51.852	-52.426	-52.973	-53.496
-∞	-26.058	-32.112	-35.704	-38.277	-40.292	-41.952	-43.369	-44.606	-45.707	-46.699	-47.605	-48.438	-49.211	-49.932	-50.609	-51.248	-51.852	-52.426	-52.973	-53.496
-16.962	-26.059	-32.113	-35.704	-38.277	-40.292	-41.953	-43.369	-44.606	-45.707	-46.699	-47.605	-48.438	-49.211	-49.932	-50.609	-51.248	-51.852	-52.426	-52.973	-53.496
-12.294	-26.065	-32.114	-35.704	-38.278	-40.292	-41.953	-43.369	-44.606	-45.707	-46.699	-47.605	-48.438	-49.211	-49.932	-50.609	-51.248	-51.852	-52.426	-52.973	-53.497
-10.643	-26.073	-32.116	-35.705	-38.278	-40.293	-41.953	-43.369	-44.606	-45.707	-46.699	-47.605	-48.438	-49.211	-49.932	-50.609	-51.248	-51.852	-52.426	-52.973	-53.497
-10.230	-26.085	-32.119	-35.707	-38.279	-40.293	-41.953	-43.369	-44.606	-45.707	-46.700	-47.605	-48.438	-49.211	-49.933	-50.609	-51.248	-51.852	-52.426	-52.973	-53.497
-10.398	-26.101	-32.123	-35.709	-38.280	-40.294	-41.954	-43.370	-44.607	-45.707	-46.700	-47.605	-48.438	-49.211	-49.933	-50.610	-51.248	-51.852	-52.426	-52.973	-53.497
-10.845	-26.120	-32.128	-35.711	-38.281	-40.294	-41.954	-43.370	-44.607	-45.707	-46.700	-47.605	-48.439	-49.211	-49.933	-50.610	-51.248	-51.852	-52.426	-52.973	-53.497
-11.419	-26.142	-32.134	-35.713	-38.283	-40.295	-41.955	-43.371	-44.607	-45.708	-46.700	-47.605	-48.439	-49.212	-49.933	-50.610	-51.248	-51.852	-52.426	-52.974	-53.497
-12.044	-26.142	-32.140	-35.716	-38.284	-40.297	-41.956	-43.371	-44.608	-45.708	-46.700	-47.606	-48.439	-49.212	-49.933	-50.610	-51.248	-51.852	-52.426	-52.974	-53.497
-12.680	-26.196	-32.148	-35.720	-38.286	-40.298	-41.957	-43.372	-44.608	-45.708	-46.701	-47.606	-48.439	-49.212	-49.933	-50.610	-51.248	-51.852	-52.426	-52.974	-53.497
-13.309	-26.227	-32.156	-35.723	-38.289	-40.299	-41.958	-43.372	-44.609	-45.709	-46.701	-47.606	-48.439	-49.212	-49.933	-50.610	-51.248	-51.852	-52.427	-52.974	-53.497

Table (A.15)

The result of signal to noise ratio (SNR) for the VLC connectivity affected by silt particles when the visibility is 5 Km

0	25	50	75	100	125	150	175	200	225	250	275	300	325	350	375	400	425	450	475	500
97.501	79.963	69.245	62.368	57.332	53.354	50.061	47.246	44.782	42.589	40.609	38.802	37.138	35.594	34.153	32.801	31.526	30.318	29.171	28.077	27.031
98.189	80.016	69.260	62.375	57.336	53.357	50.063	47.247	44.784	42.590	40.609	38.802	37.138	35.595	34.154	32.801	31.526	30.318	29.171	28.077	27.031
98.880	80.064	69.274	62.382	57.340	53.360	50.065	47.249	44.784	42.590	40.610	38.803	37.139	35.595	34.154	32.802	31.526	30.319	29.171	28.077	27.031
99.550	80.107	69.287	62.387	57.343	53.362	50.067	47.250	44.785	42.591	40.611	38.803	37.139	35.595	34.154	32.802	31.526	30.319	29.171	28.077	27.031
100.161	80.145	69.298	62.392	57.346	53.364	50.068	47.251	44.786	42.592	40.611	38.804	37.139	35.596	34.155	32.802	31.527	30.319	29.171	28.077	27.031
100.633	80.176	69.307	62.397	57.348	53.365	50.069	47.252	44.787	42.592	40.611	38.804	37.140	35.596	34.155	32.802	31.527	30.319	29.171	28.077	27.031
100.811	80.202	69.314	62.400	57.350	53.366	50.070	47.252	44.787	42.593	40.612	38.804	37.140	35.596	34.155	32.802	31.527	30.319	29.172	28.078	27.032
100.375	80.222	69.320	62.403	57.352	53.367	50.071	47.253	44.788	42.593	40.612	38.804	37.140	35.596	34.155	32.803	31.527	30.319	29.172	28.078	27.032
98.609	80.237	69.324	62.405	57.353	53.368	50.071	47.253	44.788	42.593	40.612	38.805	37.140	35.596	34.155	32.803	31.527	30.319	29.172	28.078	27.032
93.299	80.246	69.327	62.406	57.354	53.369	50.071	47.253	44.788	42.593	40.612	38.805	37.140	35.597	34.155	32.803	31.527	30.319	29.172	28.078	27.032
0.000	80.249	69.328	62.406	57.354	53.369	50.072	47.253	44.788	42.593	40.612	38.805	37.140	35.597	34.155	32.803	31.527	30.319	29.172	28.078	27.032
93.299	80.246	69.327	62.406	57.354	53.369	50.071	47.253	44.788	42.593	40.612	38.805	37.140	35.597	34.155	32.803	31.527	30.319	29.172	28.078	27.032
98.609	80.237	69.324	62.405	57.353	53.368	50.071	47.253	44.788	42.593	40.612	38.805	37.140	35.596	34.155	32.803	31.527	30.319	29.172	28.078	27.032
100.375	80.222	69.320	62.403	57.352	53.367	50.071	47.253	44.788	42.593	40.612	38.804	37.140	35.596	34.155	32.803	31.527	30.319	29.172	28.078	27.032
100.811	80.202	69.314	62.400	57.350	53.366	50.070	47.252	44.787	42.593	40.612	38.804	37.140	35.596	34.155	32.802	31.527	30.319	29.172	28.078	27.032
100.633	80.176	69.307	62.397	57.348	53.365	50.069	47.252	44.787	42.592	40.611	38.804	37.140	35.596	34.155	32.802	31.527	30.319	29.171	28.077	27.031
100.161	80.145	69.298	62.392	57.346	53.364	50.068	47.251	44.786	42.592	40.611	38.804	37.139	35.596	34.155	32.802	31.527	30.319	29.171	28.077	27.031
99.550	80.107	69.287	62.387	57.343	53.362	50.067	47.250	44.785	42.591	40.611	38.803	37.139	35.595	34.154	32.802	31.526	30.319	29.171	28.077	27.031
98.880	80.107	69.274	62.382	57.340	53.360	50.065	47.249	44.784	42.590	40.610	38.803	37.139	35.595	34.154	32.802	31.526	30.319	29.171	28.077	27.031
98.189	80.016	69.260	62.375	57.336	53.357	50.063	47.247	44.784	42.590	40.609	38.802	37.138	35.595	34.154	32.801	31.526	30.318	29.171	28.077	27.031
97.501	79.963	69.245	62.368	57.332	53.354	50.061	47.246	44.782	42.589	40.609	38.802	37.138	35.594	34.153	32.801	31.526	30.318	29.171	28.077	27.031

Table (A.16)

The result of bit error rate (BER) for the VLC connectivity affected by silt particles when the visibility is 5 Km

0	25	50	75	100	125	150	175	200	225	250	275	300	325	350	375	400	425	450	475	500
1.3E-44	5.9E-37	2.8E-32	2.9E-29	4.7E-27	2.6E-25	7.2E-24	1.2E-22	1.5E-21	1.4E-20	1.0E-19	6.3E-19	3.4E-18	1.6E-17	7.0E-17	2.8E-16	1.0E-15	3.4E-15	1.1E-14	3.4E-14	9.7E-14
6.4E-45	5.6E-37	2.8E-32	2.9E-29	4.6E-27	2.6E-25	7.1E-24	1.2E-22	1.5E-21	1.4E-20	1.0E-19	6.3E-19	3.4E-18	1.6E-17	7.0E-17	2.8E-16	1.0E-15	3.4E-15	1.1E-14	3.4E-14	9.7E-14
3.2E-45	5.3E-37	2.8E-32	2.9E-29	4.6E-27	2.6E-25	7.1E-24	1.2E-22	1.5E-21	1.4E-20	1.0E-19	6.3E-19	3.4E-18	1.6E-17	7.0E-17	2.8E-16	1.0E-15	3.4E-15	1.1E-14	3.4E-14	9.7E-14
1.6E-45	5.1E-37	2.7E-32	2.9E-29	4.6E-27	2.6E-25	7.1E-24	1.2E-22	1.5E-21	1.4E-20	1.0E-19	6.3E-19	3.4E-18	1.6E-17	7.0E-17	2.8E-16	1.0E-15	3.4E-15	1.1E-14	3.4E-14	9.7E-14
8.9E-46	4.9E-37	2.7E-32	2.8E-29	4.6E-27	2.6E-25	7.1E-24	1.2E-22	1.5E-21	1.4E-20	1.0E-19	6.3E-19	3.4E-18	1.6E-17	7.0E-17	2.8E-16	1.0E-15	3.4E-15	1.1E-14	3.3E-14	9.7E-14
5.5E-46	4.7E-37	2.7E-32	2.8E-29	4.6E-27	2.6E-25	7.1E-24	1.2E-22	1.5E-21	1.4E-20	1.0E-19	6.3E-19	3.4E-18	1.6E-17	7.0E-17	2.8E-16	1.0E-15	3.4E-15	1.1E-14	3.3E-14	9.7E-14
4.6E-46	4.6E-37	2.7E-32	2.8E-29	4.6E-27	2.5E-25	7.1E-24	1.2E-22	1.5E-21	1.4E-20	1.0E-19	6.3E-19	3.4E-18	1.6E-17	7.0E-17	2.8E-16	1.0E-15	3.4E-15	1.1E-14	3.3E-14	9.7E-14
7.2E-46	4.5E-37	2.6E-32	2.8E-29	4.6E-27	2.5E-25	7.1E-24	1.2E-22	1.5E-21	1.4E-20	1.0E-19	6.3E-19	3.4E-18	1.6E-17	7.0E-17	2.8E-16	1.0E-15	3.4E-15	1.1E-14	3.3E-14	9.7E-14
4.2E-45	4.5E-37	2.6E-32	2.8E-29	4.6E-27	2.5E-25	7.1E-24	1.2E-22	1.5E-21	1.4E-20	1.0E-19	6.3E-19	3.4E-18	1.6E-17	7.0E-17	2.8E-16	1.0E-15	3.4E-15	1.1E-14	3.3E-14	9.7E-14
8.8E-43	4.4E-37	2.6E-32	2.8E-29	4.6E-27	2.5E-25	7.1E-24	1.2E-22	1.5E-21	1.4E-20	1.0E-19	6.3E-19	3.4E-18	1.6E-17	7.0E-17	2.8E-16	1.0E-15	3.4E-15	1.1E-14	3.3E-14	9.7E-14
5.0E-01	4.4E-37	2.6E-32	2.8E-29	4.6E-27	2.5E-25	7.1E-24	1.2E-22	1.5E-21	1.4E-20	1.0E-19	6.3E-19	3.4E-18	1.6E-17	7.0E-17	2.8E-16	1.0E-15	3.4E-15	1.1E-14	3.3E-14	9.7E-14
8.8E-43	4.4E-37	2.6E-32	2.8E-29	4.6E-27	2.5E-25	7.1E-24	1.2E-22	1.5E-21	1.4E-20	1.0E-19	6.3E-19	3.4E-18	1.6E-17	7.0E-17	2.8E-16	1.0E-15	3.4E-15	1.1E-14	3.3E-14	9.7E-14
4.2E-45	4.5E-37	2.6E-32	2.8E-29	4.6E-27	2.5E-25	7.1E-24	1.2E-22	1.5E-21	1.4E-20	1.0E-19	6.3E-19	3.4E-18	1.6E-17	7.0E-17	2.8E-16	1.0E-15	3.4E-15	1.1E-14	3.3E-14	9.7E-14
7.2E-46	4.5E-37	2.6E-32	2.8E-29	4.6E-27	2.5E-25	7.1E-24	1.2E-22	1.5E-21	1.4E-20	1.0E-19	6.3E-19	3.4E-18	1.6E-17	7.0E-17	2.8E-16	1.0E-15	3.4E-15	1.1E-14	3.3E-14	9.7E-14
4.6E-46	4.6E-37	2.7E-32	2.8E-29	4.6E-27	2.5E-25	7.1E-24	1.2E-22	1.5E-21	1.4E-20	1.0E-19	6.3E-19	3.4E-18	1.6E-17	7.0E-17	2.8E-16	1.0E-15	3.4E-15	1.1E-14	3.3E-14	9.7E-14
5.5E-46	4.7E-37	2.7E-32	2.8E-29	4.6E-27	2.6E-25	7.1E-24	1.2E-22	1.5E-21	1.4E-20	1.0E-19	6.3E-19	3.4E-18	1.6E-17	7.0E-17	2.8E-16	1.0E-15	3.4E-15	1.1E-14	3.3E-14	9.7E-14
8.9E-46	4.9E-37	2.7E-32	2.8E-29	4.6E-27	2.6E-25	7.1E-24	1.2E-22	1.5E-21	1.4E-20	1.0E-19	6.3E-19	3.4E-18	1.6E-17	7.0E-17	2.8E-16	1.0E-15	3.4E-15	1.1E-14	3.3E-14	9.7E-14
1.6E-45	5.1E-37	2.7E-32	2.9E-29	4.6E-27	2.6E-25	7.1E-24	1.2E-22	1.5E-21	1.4E-20	1.0E-19	6.3E-19	3.4E-18	1.6E-17	7.0E-17	2.8E-16	1.0E-15	3.4E-15	1.1E-14	3.4E-14	9.7E-14
3.2E-45	5.1E-37	2.8E-32	2.9E-29	4.6E-27	2.6E-25	7.1E-24	1.2E-22	1.5E-21	1.4E-20	1.0E-19	6.3E-19	3.4E-18	1.6E-17	7.0E-17	2.8E-16	1.0E-15	3.4E-15	1.1E-14	3.4E-14	9.7E-14
6.4E-45	5.6E-37	2.8E-32	2.9E-29	4.6E-27	2.6E-25	7.1E-24	1.2E-22	1.5E-21	1.4E-20	1.0E-19	6.3E-19	3.4E-18	1.6E-17	7.0E-17	2.8E-16	1.0E-15	3.4E-15	1.1E-14	3.4E-14	9.7E-14
1.3E-44	5.9E-37	2.8E-32	2.9E-29	4.7E-27	2.6E-25	7.2E-24	1.2E-22	1.5E-21	1.4E-20	1.0E-19	6.3E-19	3.4E-18	1.6E-17	7.0E-17	2.8E-16	1.0E-15	3.4E-15	1.1E-14	3.4E-14	9.7E-14

Table (A.17)

The result of received power for the VLC affected by silt particles when the visibility is 1 Km

0	25	50	75	100	125	150	175	200	225	250	275	300	325	350	375	400	425	450	475	500
-13.375	-26.543	-32.776	-36.650	-39.523	-41.842	-43.808	-45.531	-47.076	-48.484	-49.784	-50.997	-52.139	-53.220	-54.249	-55.234	-56.180	-57.093	-57.975	-58.830	-59.662
-12.741	-26.510	-32.767	-36.646	-39.521	-41.840	-43.807	-45.530	-47.075	-48.483	-49.784	-50.997	-52.138	-53.219	-54.249	-55.234	-56.180	-57.093	-57.975	-58.830	-59.662
-12.099	-26.480	-32.759	-36.643	-39.519	-41.839	-43.806	-45.529	-47.074	-48.483	-49.783	-50.997	-52.138	-53.219	-54.248	-55.234	-56.180	-57.092	-57.975	-58.830	-59.662
-11.469	-26.454	-32.752	-36.639	-39.517	-41.837	-43.805	-45.529	-47.074	-48.482	-49.783	-50.996	-52.138	-53.219	-54.248	-55.233	-56.180	-57.092	-57.975	-58.830	-59.661
-10.890	-26.431	-32.746	-36.637	-39.515	-41.836	-43.804	-45.528	-47.073	-48.482	-49.782	-50.996	-52.138	-53.219	-54.248	-55.233	-56.180	-57.092	-57.974	-58.830	-59.661
-10.438	-26.412	-32.741	-36.634	-39.514	-41.835	-43.804	-45.528	-47.073	-48.481	-49.782	-50.996	-52.137	-53.218	-54.248	-55.233	-56.179	-57.092	-57.974	-58.830	-59.661
-10.265	-26.396	-32.737	-36.632	-39.512	-41.835	-43.803	-45.527	-47.072	-48.481	-49.782	-50.996	-52.137	-53.218	-54.248	-55.233	-56.179	-57.092	-57.974	-58.830	-59.661
-10.675	-26.383	-32.733	-36.631	-39.512	-41.834	-43.803	-45.527	-47.072	-48.481	-49.782	-50.995	-52.137	-53.218	-54.248	-55.233	-56.179	-57.092	-57.974	-58.830	-59.661
-12.322	-26.374	-32.731	-36.630	-39.511	-41.834	-43.802	-45.527	-47.072	-48.481	-49.782	-50.995	-52.137	-53.218	-54.248	-55.233	-56.179	-57.092	-57.974	-58.830	-59.661
-16.988	-26.369	-32.730	-36.629	-39.511	-41.833	-43.802	-45.526	-47.072	-48.481	-49.782	-50.995	-52.137	-53.218	-54.248	-55.233	-56.179	-57.092	-57.974	-58.830	-59.661
-∞	-26.367	-32.729	-36.629	-39.510	-41.833	-43.802	-45.526	-47.072	-48.481	-49.782	-50.995	-52.137	-53.218	-54.248	-55.233	-56.179	-57.092	-57.974	-58.830	-59.661
-16.988	-26.369	-32.730	-36.629	-39.511	-41.833	-43.802	-45.526	-47.072	-48.481	-49.782	-50.995	-52.137	-53.218	-54.248	-55.233	-56.179	-57.092	-57.974	-58.830	-59.661
-12.322	-26.374	-32.731	-36.630	-39.511	-41.834	-43.802	-45.527	-47.072	-48.481	-49.782	-50.995	-52.137	-53.218	-54.248	-55.233	-56.179	-57.092	-57.974	-58.830	-59.661
-10.675	-26.383	-32.733	-36.631	-39.512	-41.834	-43.803	-45.527	-47.072	-48.481	-49.782	-50.995	-52.137	-53.218	-54.248	-55.233	-56.179	-57.092	-57.974	-58.830	-59.661
-10.265	-26.396	-32.737	-36.632	-39.512	-41.835	-43.803	-45.527	-47.072	-48.481	-49.782	-50.996	-52.137	-53.218	-54.248	-55.233	-56.179	-57.092	-57.974	-58.830	-59.661
-10.438	-26.412	-32.741	-36.634	-39.514	-41.835	-43.804	-45.528	-47.073	-48.481	-49.782	-50.996	-52.137	-53.218	-54.248	-55.233	-56.179	-57.092	-57.974	-58.830	-59.661
-10.890	-26.431	-32.746	-36.637	-39.515	-41.836	-43.804	-45.528	-47.073	-48.482	-49.782	-50.996	-52.138	-53.219	-54.248	-55.233	-56.180	-57.092	-57.974	-58.830	-59.661
-11.469	-26.454	-32.752	-36.639	-39.517	-41.837	-43.805	-45.529	-47.074	-48.482	-49.783	-50.996	-52.138	-53.219	-54.248	-55.233	-56.180	-57.092	-57.975	-58.830	-59.661
-12.099	-26.454	-32.759	-36.643	-39.519	-41.839	-43.806	-45.529	-47.074	-48.483	-49.783	-50.997	-52.138	-53.219	-54.248	-55.234	-56.180	-57.092	-57.975	-58.830	-59.662
-12.741	-26.510	-32.767	-36.646	-39.521	-41.840	-43.807	-45.530	-47.075	-48.483	-49.784	-50.997	-52.138	-53.219	-54.249	-55.234	-56.180	-57.093	-57.975	-58.830	-59.662
-13.375	-26.543	-32.776	-36.650	-39.523	-41.842	-43.808	-45.531	-47.076	-48.484	-49.784	-50.997	-52.139	-53.220	-54.249	-55.234	-56.180	-57.093	-57.975	-58.830	-59.662

Table (A.18)

The result of signal to noise ratio (SNR) for the VLC connectivity affected by silt particles when the visibility is 1 Km

0	25	50	75	100	125	150	175	200	225	250	275	300	325	350	375	400	425	450	475	500
97.428	79.427	68.064	60.554	54.892	50.292	46.378	42.943	39.861	37.049	34.452	32.027	29.746	27.585	25.527	23.558	21.666	19.841	18.077	16.366	14.704
98.123	79.483	68.081	60.562	54.896	50.295	46.381	42.945	39.863	37.051	34.453	32.028	29.747	27.586	25.528	23.558	21.666	19.842	18.077	16.367	14.704
98.820	79.534	68.097	60.569	54.901	50.298	46.383	42.947	39.864	37.052	34.453	32.029	29.747	27.586	25.528	23.559	21.666	19.842	18.078	16.367	14.704
99.497	79.578	68.110	60.576	54.904	50.300	46.384	42.948	39.865	37.052	34.454	32.029	29.748	27.587	25.529	23.559	21.667	19.842	18.078	16.367	14.705
100.114	79.617	68.122	60.581	54.908	50.303	46.386	42.949	39.866	37.053	34.455	32.030	29.748	27.587	25.529	23.560	21.667	19.843	18.078	16.367	14.705
100.591	79.650	68.131	60.586	54.911	50.304	46.387	42.950	39.867	37.054	34.455	32.030	29.749	27.588	25.529	23.560	21.667	19.843	18.078	16.368	14.705
100.774	79.678	68.140	60.590	54.913	50.306	46.388	42.951	39.867	37.054	34.456	32.031	29.749	27.588	25.530	23.560	21.668	19.843	18.079	16.368	14.705
100.341	79.699	68.146	60.593	54.915	50.307	46.389	42.952	39.868	37.055	34.456	32.031	29.749	27.588	25.530	23.560	21.668	19.843	18.079	16.368	14.705
98.578	79.714	68.150	60.595	54.916	50.308	46.390	42.952	39.868	37.055	34.456	32.031	29.749	27.588	25.530	23.560	21.668	19.843	18.079	16.368	14.705
93.267	79.723	68.153	60.596	54.917	50.308	46.390	42.953	39.868	37.055	34.457	32.031	29.750	27.588	25.530	23.560	21.668	19.843	18.079	16.368	14.705
0.000	79.726	68.154	60.597	54.917	50.309	46.390	42.953	39.869	37.055	34.457	32.031	29.750	27.588	25.530	23.560	21.668	19.843	18.079	16.368	14.705
93.267	79.723	68.153	60.596	54.917	50.308	46.390	42.953	39.868	37.055	34.457	32.031	29.750	27.588	25.530	23.560	21.668	19.843	18.079	16.368	14.705
98.578	79.714	68.150	60.595	54.916	50.308	46.390	42.952	39.868	37.055	34.456	32.031	29.749	27.588	25.530	23.560	21.668	19.843	18.079	16.368	14.705
100.341	79.699	68.146	60.593	54.915	50.307	46.389	42.952	39.868	37.055	34.456	32.031	29.749	27.588	25.530	23.560	21.668	19.843	18.079	16.368	14.705
100.774	79.678	68.140	60.590	54.913	50.306	46.388	42.951	39.867	37.054	34.456	32.031	29.749	27.588	25.530	23.560	21.668	19.843	18.079	16.368	14.705
100.591	79.650	68.131	60.586	54.911	50.304	46.387	42.950	39.867	37.054	34.455	32.030	29.749	27.588	25.529	23.560	21.667	19.843	18.078	16.368	14.705
100.114	79.617	68.122	60.581	54.908	50.303	46.386	42.949	39.866	37.053	34.455	32.030	29.748	27.587	25.529	23.560	21.667	19.843	18.078	16.367	14.705
99.497	79.578	68.110	60.576	54.904	50.300	46.384	42.948	39.865	37.052	34.454	32.029	29.748	27.587	25.529	23.559	21.667	19.842	18.078	16.367	14.705
98.820	79.578	68.097	60.569	54.901	50.298	46.383	42.947	39.864	37.052	34.453	32.029	29.747	27.586	25.528	23.559	21.666	19.842	18.078	16.367	14.704
98.123	79.483	68.081	60.562	54.896	50.295	46.381	42.945	39.863	37.051	34.453	32.028	29.747	27.586	25.528	23.558	21.666	19.842	18.077	16.367	14.704
97.428	79.427	68.064	60.554	54.892	50.292	46.378	42.943	39.861	37.049	34.452	32.027	29.746	27.585	25.527	23.558	21.666	19.841	18.077	16.366	14.704

Table (A.19)

The result of bit error rate (BER) for the VLC connectivity affected by silt particles when the visibility is 1 Km

0	25	50	75	100	125	150	175	200	225	250	275	300	325	350	375	400	425	450	475	500
1.4E-44	1.0E-36	9.4E-32	1.8E-28	5.5E-26	5.7E-24	3.0E-22	9.5E-21	2.2E-19	3.7E-18	5.2E-17	6.1E-16	6.1E-15	5.5E-14	4.5E-13	3.3E-12	2.3E-11	1.5E-10	9.1E-10	5.3E-09	2.9E-08
6.9E-45	9.5E-37	9.2E-32	1.8E-28	5.4E-26	5.7E-24	3.0E-22	9.5E-21	2.2E-19	3.7E-18	5.2E-17	6.0E-16	6.1E-15	5.5E-14	4.5E-13	3.3E-12	2.3E-11	1.5E-10	9.1E-10	5.3E-09	2.9E-08
3.4E-45	9.0E-37	9.1E-32	1.8E-28	5.4E-26	5.6E-24	2.9E-22	9.5E-21	2.1E-19	3.7E-18	5.2E-17	6.0E-16	6.1E-15	5.5E-14	4.5E-13	3.3E-12	2.3E-11	1.5E-10	9.1E-10	5.3E-09	2.9E-08
1.7E-45	8.6E-37	8.9E-32	1.8E-28	5.4E-26	5.6E-24	2.9E-22	9.5E-21	2.1E-19	3.7E-18	5.2E-17	6.0E-16	6.1E-15	5.5E-14	4.5E-13	3.3E-12	2.3E-11	1.5E-10	9.1E-10	5.3E-09	2.9E-08
9.3E-46	8.3E-37	8.8E-32	1.8E-28	5.4E-26	5.6E-24	2.9E-22	9.5E-21	2.1E-19	3.7E-18	5.2E-17	6.0E-16	6.1E-15	5.5E-14	4.5E-13	3.3E-12	2.3E-11	1.5E-10	9.1E-10	5.3E-09	2.9E-08
5.8E-46	8.0E-37	8.7E-32	1.8E-28	5.4E-26	5.6E-24	2.9E-22	9.5E-21	2.1E-19	3.7E-18	5.2E-17	6.0E-16	6.1E-15	5.5E-14	4.5E-13	3.3E-12	2.3E-11	1.5E-10	9.1E-10	5.3E-09	2.9E-08
4.8E-46	7.8E-37	8.7E-32	1.7E-28	5.4E-26	5.6E-24	2.9E-22	9.5E-21	2.1E-19	3.7E-18	5.1E-17	6.0E-16	6.1E-15	5.5E-14	4.5E-13	3.3E-12	2.3E-11	1.5E-10	9.1E-10	5.3E-09	2.9E-08
7.4E-46	7.7E-37	8.6E-32	1.7E-28	5.3E-26	5.6E-24	2.9E-22	9.4E-21	2.1E-19	3.7E-18	5.1E-17	6.0E-16	6.1E-15	5.5E-14	4.5E-13	3.3E-12	2.3E-11	1.5E-10	9.1E-10	5.3E-09	2.9E-08
4.4E-45	7.5E-37	8.6E-32	1.7E-28	5.3E-26	5.6E-24	2.9E-22	9.4E-21	2.1E-19	3.7E-18	5.1E-17	6.0E-16	6.1E-15	5.5E-14	4.5E-13	3.3E-12	2.3E-11	1.5E-10	9.1E-10	5.3E-09	2.9E-08
9.1E-43	7.5E-37	8.6E-32	1.7E-28	5.3E-26	5.6E-24	2.9E-22	9.4E-21	2.1E-19	3.7E-18	5.1E-17	6.0E-16	6.1E-15	5.5E-14	4.5E-13	3.3E-12	2.3E-11	1.5E-10	9.1E-10	5.3E-09	2.9E-08
5.0E-01	7.5E-37	8.5E-32	1.7E-28	5.3E-26	5.6E-24	2.9E-22	9.4E-21	2.1E-19	3.7E-18	5.1E-17	6.0E-16	6.1E-15	5.5E-14	4.5E-13	3.3E-12	2.3E-11	1.5E-10	9.1E-10	5.3E-09	2.9E-08
9.1E-43	7.5E-37	8.6E-32	1.7E-28	5.3E-26	5.6E-24	2.9E-22	9.4E-21	2.1E-19	3.7E-18	5.1E-17	6.0E-16	6.1E-15	5.5E-14	4.5E-13	3.3E-12	2.3E-11	1.5E-10	9.1E-10	5.3E-09	2.9E-08
4.4E-45	7.5E-37	8.6E-32	1.7E-28	5.3E-26	5.6E-24	2.9E-22	9.4E-21	2.1E-19	3.7E-18	5.1E-17	6.0E-16	6.1E-15	5.5E-14	4.5E-13	3.3E-12	2.3E-11	1.5E-10	9.1E-10	5.3E-09	2.9E-08
7.4E-46	7.7E-37	8.6E-32	1.7E-28	5.3E-26	5.6E-24	2.9E-22	9.4E-21	2.1E-19	3.7E-18	5.1E-17	6.0E-16	6.1E-15	5.5E-14	4.5E-13	3.3E-12	2.3E-11	1.5E-10	9.1E-10	5.3E-09	2.9E-08
4.8E-46	7.8E-37	8.7E-32	1.7E-28	5.4E-26	5.6E-24	2.9E-22	9.5E-21	2.1E-19	3.7E-18	5.1E-17	6.0E-16	6.1E-15	5.5E-14	4.5E-13	3.3E-12	2.3E-11	1.5E-10	9.1E-10	5.3E-09	2.9E-08
5.8E-46	8.0E-37	8.7E-32	1.8E-28	5.4E-26	5.6E-24	2.9E-22	9.5E-21	2.1E-19	3.7E-18	5.2E-17	6.0E-16	6.1E-15	5.5E-14	4.5E-13	3.3E-12	2.3E-11	1.5E-10	9.1E-10	5.3E-09	2.9E-08
9.3E-46	8.3E-37	8.8E-32	1.8E-28	5.4E-26	5.6E-24	2.9E-22	9.5E-21	2.1E-19	3.7E-18	5.2E-17	6.0E-16	6.1E-15	5.5E-14	4.5E-13	3.3E-12	2.3E-11	1.5E-10	9.1E-10	5.3E-09	2.9E-08
1.7E-45	8.6E-37	8.9E-32	1.8E-28	5.4E-26	5.6E-24	2.9E-22	9.5E-21	2.1E-19	3.7E-18	5.2E-17	6.0E-16	6.1E-15	5.5E-14	4.5E-13	3.3E-12	2.3E-11	1.5E-10	9.1E-10	5.3E-09	2.9E-08
3.4E-45	8.6E-37	9.1E-32	1.8E-28	5.4E-26	5.6E-24	2.9E-22	9.5E-21	2.1E-19	3.7E-18	5.2E-17	6.0E-16	6.1E-15	5.5E-14	4.5E-13	3.3E-12	2.3E-11	1.5E-10	9.1E-10	5.3E-09	2.9E-08
6.9E-45	9.5E-37	9.2E-32	1.8E-28	5.4E-26	5.7E-24	3.0E-22	9.5E-21	2.2E-19	3.7E-18	5.2E-17	6.0E-16	6.1E-15	5.5E-14	4.5E-13	3.3E-12	2.3E-11	1.5E-10	9.1E-10	5.3E-09	2.9E-08
1.4E-44	1.0E-36	9.4E-32	1.8E-28	5.5E-26	5.7E-24	3.0E-22	9.5E-21	2.2E-19	3.7E-18	5.2E-17	6.1E-16	6.1E-15	5.5E-14	4.5E-13	3.3E-12	2.3E-11	1.5E-10	9.1E-10	5.3E-09	2.9E-08

Table (A.20)

The result of received power for the VLC affected by silt particles when the visibility is 0.1 Km

0	25	50	75	100	125	150	175	200	225	250	275	300	325	350	375	400	425	450	475	500
-14.125	-30.092	-39.755	-47.086	-53.421	-59.205	-64.638	-69.829	-74.841	-79.718	-84.487	-89.169	-93.779	-98.329	-102.827	-107.281	-111.697	-116.078	-120.430	-124.755	-129.055
-13.428	-30.046	-39.740	-47.077	-53.416	-59.201	-64.635	-69.826	-74.839	-79.716	-84.485	-89.167	-93.778	-98.328	-102.826	-107.280	-111.696	-116.077	-120.429	-124.754	-129.054
-12.723	-30.005	-39.726	-47.070	-53.410	-59.197	-64.632	-69.824	-74.837	-79.714	-84.483	-89.166	-93.776	-98.326	-102.825	-107.279	-111.695	-116.077	-120.428	-124.753	-129.054
-12.032	-29.969	-39.714	-47.063	-53.406	-59.194	-64.629	-69.821	-74.835	-79.712	-84.482	-89.165	-93.775	-98.325	-102.824	-107.278	-111.694	-116.076	-120.427	-124.752	-129.053
-11.394	-29.937	-39.703	-47.057	-53.402	-59.191	-64.627	-69.820	-74.833	-79.711	-84.481	-89.163	-93.774	-98.324	-102.823	-107.278	-111.693	-116.075	-120.427	-124.752	-129.052
-10.887	-29.910	-39.694	-47.052	-53.399	-59.188	-64.625	-69.818	-74.832	-79.710	-84.480	-89.163	-93.773	-98.324	-102.822	-107.277	-111.693	-116.075	-120.426	-124.751	-129.052
-10.663	-29.888	-39.687	-47.048	-53.396	-59.186	-64.624	-69.817	-74.831	-79.709	-84.479	-89.162	-93.773	-98.323	-102.822	-107.276	-111.692	-116.074	-120.426	-124.751	-129.052
-11.027	-29.870	-39.681	-47.045	-53.394	-59.185	-64.622	-69.816	-74.830	-79.708	-84.478	-89.161	-93.772	-98.323	-102.821	-107.276	-111.692	-116.074	-120.425	-124.750	-129.051
-12.639	-29.858	-39.677	-47.043	-53.392	-59.184	-64.621	-69.815	-74.830	-79.708	-84.478	-89.161	-93.772	-98.322	-102.821	-107.276	-111.692	-116.073	-120.425	-124.750	-129.051
-17.281	-29.851	-39.675	-47.041	-53.392	-59.183	-64.621	-69.814	-74.829	-79.707	-84.477	-89.161	-93.771	-98.322	-102.821	-107.276	-111.691	-116.073	-120.425	-124.750	-129.051
-∞	-29.848	-39.674	-47.041	-53.391	-59.183	-64.621	-69.814	-74.829	-79.707	-84.477	-89.160	-93.771	-98.322	-102.821	-107.275	-111.691	-116.073	-120.425	-124.750	-129.051
-17.281	-29.851	-39.675	-47.041	-53.392	-59.183	-64.621	-69.814	-74.829	-79.707	-84.477	-89.161	-93.771	-98.322	-102.821	-107.276	-111.691	-116.073	-120.425	-124.750	-129.051
-12.639	-29.858	-39.677	-47.043	-53.392	-59.184	-64.621	-69.815	-74.830	-79.708	-84.478	-89.161	-93.772	-98.322	-102.821	-107.276	-111.692	-116.073	-120.425	-124.750	-129.051
-11.027	-29.870	-39.681	-47.045	-53.394	-59.185	-64.622	-69.816	-74.830	-79.708	-84.478	-89.161	-93.772	-98.323	-102.821	-107.276	-111.692	-116.074	-120.425	-124.750	-129.051
-10.663	-29.888	-39.687	-47.048	-53.396	-59.186	-64.624	-69.817	-74.831	-79.709	-84.479	-89.162	-93.773	-98.323	-102.822	-107.276	-111.692	-116.074	-120.426	-124.751	-129.052
-10.887	-29.910	-39.694	-47.052	-53.399	-59.188	-64.625	-69.818	-74.832	-79.710	-84.480	-89.163	-93.773	-98.324	-102.822	-107.277	-111.693	-116.075	-120.426	-124.751	-129.052
-11.394	-29.937	-39.703	-47.057	-53.402	-59.191	-64.627	-69.820	-74.833	-79.711	-84.481	-89.163	-93.774	-98.324	-102.823	-107.278	-111.693	-116.075	-120.427	-124.752	-129.052
-12.032	-29.969	-39.714	-47.063	-53.406	-59.194	-64.629	-69.821	-74.835	-79.712	-84.482	-89.165	-93.775	-98.325	-102.824	-107.278	-111.694	-116.076	-120.427	-124.752	-129.053
-12.723	-29.969	-39.726	-47.070	-53.410	-59.197	-64.632	-69.824	-74.837	-79.714	-84.483	-89.166	-93.776	-98.326	-102.825	-107.279	-111.695	-116.077	-120.428	-124.753	-129.054
-13.428	-30.046	-39.740	-47.077	-53.416	-59.201	-64.635	-69.826	-74.839	-79.716	-84.485	-89.167	-93.778	-98.328	-102.826	-107.280	-111.696	-116.077	-120.429	-124.754	-129.054
-14.125	-30.092	-39.755	-47.086	-53.421	-59.205	-64.638	-69.829	-74.841	-79.718	-84.487	-89.169	-93.779	-98.329	-102.827	-107.281	-111.697	-116.078	-120.430	-124.755	-129.055

Table (A.21)

The result of signal to noise ratio (SNR) for the VLC connectivity affected by silt particles when the visibility is 0.1 Km

0	25	50	75	100	125	150	175	200	225	250	275	300	325	350	375	400	425	450	475	500
96.594	73.109	54.432	39.841	27.182	15.617	4.751	0.000	0.000	0.000	0.000	0.000	0.000	0.000	0.000	0.000	0.000	0.000	0.000	0.000	0.000
97.370	73.193	54.462	39.858	27.193	15.625	4.758	0.000	0.000	0.000	0.000	0.000	0.000	0.000	0.000	0.000	0.000	0.000	0.000	0.000	0.000
98.143	73.269	54.490	39.873	27.204	15.633	4.764	0.000	0.000	0.000	0.000	0.000	0.000	0.000	0.000	0.000	0.000	0.000	0.000	0.000	0.000
98.893	73.336	54.514	39.886	27.213	15.640	4.769	0.000	0.000	0.000	0.000	0.000	0.000	0.000	0.000	0.000	0.000	0.000	0.000	0.000	0.000
99.577	73.395	54.535	39.898	27.221	15.646	4.774	0.000	0.000	0.000	0.000	0.000	0.000	0.000	0.000	0.000	0.000	0.000	0.000	0.000	0.000
100.116	73.445	54.553	39.908	27.227	15.650	4.778	0.000	0.000	0.000	0.000	0.000	0.000	0.000	0.000	0.000	0.000	0.000	0.000	0.000	0.000
100.354	73.485	54.567	39.916	27.233	15.655	4.781	0.000	0.000	0.000	0.000	0.000	0.000	0.000	0.000	0.000	0.000	0.000	0.000	0.000	0.000
99.967	73.517	54.578	39.922	27.237	15.658	4.783	0.000	0.000	0.000	0.000	0.000	0.000	0.000	0.000	0.000	0.000	0.000	0.000	0.000	0.000
98.235	73.540	54.587	39.927	27.240	15.660	4.785	0.000	0.000	0.000	0.000	0.000	0.000	0.000	0.000	0.000	0.000	0.000	0.000	0.000	0.000
92.912	73.554	54.591	39.929	27.242	15.661	4.786	0.000	0.000	0.000	0.000	0.000	0.000	0.000	0.000	0.000	0.000	0.000	0.000	0.000	0.000
0.000	73.558	54.593	39.930	27.242	15.662	4.787	0.000	0.000	0.000	0.000	0.000	0.000	0.000	0.000	0.000	0.000	0.000	0.000	0.000	0.000
92.912	73.554	54.591	39.929	27.242	15.661	4.786	0.000	0.000	0.000	0.000	0.000	0.000	0.000	0.000	0.000	0.000	0.000	0.000	0.000	0.000
98.235	73.540	54.587	39.927	27.240	15.660	4.785	0.000	0.000	0.000	0.000	0.000	0.000	0.000	0.000	0.000	0.000	0.000	0.000	0.000	0.000
99.967	73.517	54.578	39.922	27.237	15.658	4.783	0.000	0.000	0.000	0.000	0.000	0.000	0.000	0.000	0.000	0.000	0.000	0.000	0.000	0.000
100.354	73.485	54.567	39.916	27.233	15.655	4.781	0.000	0.000	0.000	0.000	0.000	0.000	0.000	0.000	0.000	0.000	0.000	0.000	0.000	0.000
100.116	73.445	54.553	39.908	27.227	15.650	4.778	0.000	0.000	0.000	0.000	0.000	0.000	0.000	0.000	0.000	0.000	0.000	0.000	0.000	0.000
99.577	73.395	54.535	39.898	27.221	15.646	4.774	0.000	0.000	0.000	0.000	0.000	0.000	0.000	0.000	0.000	0.000	0.000	0.000	0.000	0.000
98.893	73.336	54.514	39.886	27.213	15.640	4.769	0.000	0.000	0.000	0.000	0.000	0.000	0.000	0.000	0.000	0.000	0.000	0.000	0.000	0.000
98.143	73.336	54.490	39.873	27.204	15.633	4.764	0.000	0.000	0.000	0.000	0.000	0.000	0.000	0.000	0.000	0.000	0.000	0.000	0.000	0.000
97.370	73.193	54.462	39.858	27.193	15.625	4.758	0.000	0.000	0.000	0.000	0.000	0.000	0.000	0.000	0.000	0.000	0.000	0.000	0.000	0.000
96.594	73.109	54.432	39.841	27.182	15.617	4.751	0.000	0.000	0.000	0.000	0.000	0.000	0.000	0.000	0.000	0.000	0.000	0.000	0.000	0.000

Table (A.22)

The result of bit error rate (BER) for the VLC connectivity affected by silt particles when the visibility is 0.1 Km

0	25	50	75	100	125	150	175	200	225	250	275	300	325	350	375	400	425	450	475	500
3.2E-44	5.8E-34	8.7E-26	2.2E-19	8.3E-14	1.1E-08	1.0E-03	5.0E-01	5.0E-01	5.0E-01	5.0E-01	5.0E-01	5.0E-01	5.0E-01	5.0E-01	5.0E-01	5.0E-01	5.0E-01	5.0E-01	5.0E-01	5.0E-01
1.5E-44	5.3E-34	8.4E-26	2.2E-19	8.2E-14	1.1E-08	1.0E-03	5.0E-01	5.0E-01	5.0E-01	5.0E-01	5.0E-01	5.0E-01	5.0E-01	5.0E-01	5.0E-01	5.0E-01	5.0E-01	5.0E-01	5.0E-01	5.0E-01
6.7E-45	5.0E-34	8.2E-26	2.1E-19	8.1E-14	1.1E-08	1.0E-03	5.0E-01	5.0E-01	5.0E-01	5.0E-01	5.0E-01	5.0E-01	5.0E-01	5.0E-01	5.0E-01	5.0E-01	5.0E-01	5.0E-01	5.0E-01	5.0E-01
3.2E-45	4.6E-34	8.0E-26	2.1E-19	8.1E-14	1.1E-08	1.0E-03	5.0E-01	5.0E-01	5.0E-01	5.0E-01	5.0E-01	5.0E-01	5.0E-01	5.0E-01	5.0E-01	5.0E-01	5.0E-01	5.0E-01	5.0E-01	5.0E-01
1.6E-45	4.4E-34	7.8E-26	2.1E-19	8.0E-14	1.1E-08	1.0E-03	5.0E-01	5.0E-01	5.0E-01	5.0E-01	5.0E-01	5.0E-01	5.0E-01	5.0E-01	5.0E-01	5.0E-01	5.0E-01	5.0E-01	5.0E-01	5.0E-01
9.3E-46	4.1E-34	7.7E-26	2.1E-19	8.0E-14	1.1E-08	1.0E-03	5.0E-01	5.0E-01	5.0E-01	5.0E-01	5.0E-01	5.0E-01	5.0E-01	5.0E-01	5.0E-01	5.0E-01	5.0E-01	5.0E-01	5.0E-01	5.0E-01
7.3E-46	4.0E-34	7.6E-26	2.0E-19	7.9E-14	1.1E-08	9.9E-04	5.0E-01	5.0E-01	5.0E-01	5.0E-01	5.0E-01	5.0E-01	5.0E-01	5.0E-01	5.0E-01	5.0E-01	5.0E-01	5.0E-01	5.0E-01	5.0E-01
1.1E-45	3.9E-34	7.5E-26	2.0E-19	7.9E-14	1.1E-08	9.9E-04	5.0E-01	5.0E-01	5.0E-01	5.0E-01	5.0E-01	5.0E-01	5.0E-01	5.0E-01	5.0E-01	5.0E-01	5.0E-01	5.0E-01	5.0E-01	5.0E-01
6.2E-45	3.8E-34	7.4E-26	2.0E-19	7.9E-14	1.1E-08	9.9E-04	5.0E-01	5.0E-01	5.0E-01	5.0E-01	5.0E-01	5.0E-01	5.0E-01	5.0E-01	5.0E-01	5.0E-01	5.0E-01	5.0E-01	5.0E-01	5.0E-01
1.3E-42	3.7E-34	7.4E-26	2.0E-19	7.8E-14	1.1E-08	9.9E-04	5.0E-01	5.0E-01	5.0E-01	5.0E-01	5.0E-01	5.0E-01	5.0E-01	5.0E-01	5.0E-01	5.0E-01	5.0E-01	5.0E-01	5.0E-01	5.0E-01
5.0E-01	3.7E-34	7.4E-26	2.0E-19	7.8E-14	1.1E-08	9.9E-04	5.0E-01	5.0E-01	5.0E-01	5.0E-01	5.0E-01	5.0E-01	5.0E-01	5.0E-01	5.0E-01	5.0E-01	5.0E-01	5.0E-01	5.0E-01	5.0E-01
1.3E-42	3.7E-34	7.4E-26	2.0E-19	7.8E-14	1.1E-08	9.9E-04	5.0E-01	5.0E-01	5.0E-01	5.0E-01	5.0E-01	5.0E-01	5.0E-01	5.0E-01	5.0E-01	5.0E-01	5.0E-01	5.0E-01	5.0E-01	5.0E-01
6.2E-45	3.8E-34	7.4E-26	2.0E-19	7.9E-14	1.1E-08	9.9E-04	5.0E-01	5.0E-01	5.0E-01	5.0E-01	5.0E-01	5.0E-01	5.0E-01	5.0E-01	5.0E-01	5.0E-01	5.0E-01	5.0E-01	5.0E-01	5.0E-01
1.1E-45	3.9E-34	7.5E-26	2.0E-19	7.9E-14	1.1E-08	9.9E-04	5.0E-01	5.0E-01	5.0E-01	5.0E-01	5.0E-01	5.0E-01	5.0E-01	5.0E-01	5.0E-01	5.0E-01	5.0E-01	5.0E-01	5.0E-01	5.0E-01
7.3E-46	4.0E-34	7.6E-26	2.0E-19	7.9E-14	1.1E-08	9.9E-04	5.0E-01	5.0E-01	5.0E-01	5.0E-01	5.0E-01	5.0E-01	5.0E-01	5.0E-01	5.0E-01	5.0E-01	5.0E-01	5.0E-01	5.0E-01	5.0E-01
9.3E-46	4.1E-34	7.7E-26	2.1E-19	8.0E-14	1.1E-08	1.0E-03	5.0E-01	5.0E-01	5.0E-01	5.0E-01	5.0E-01	5.0E-01	5.0E-01	5.0E-01	5.0E-01	5.0E-01	5.0E-01	5.0E-01	5.0E-01	5.0E-01
1.6E-45	4.4E-34	7.8E-26	2.1E-19	8.0E-14	1.1E-08	1.0E-03	5.0E-01	5.0E-01	5.0E-01	5.0E-01	5.0E-01	5.0E-01	5.0E-01	5.0E-01	5.0E-01	5.0E-01	5.0E-01	5.0E-01	5.0E-01	5.0E-01
3.2E-45	4.6E-34	8.0E-26	2.1E-19	8.1E-14	1.1E-08	1.0E-03	5.0E-01	5.0E-01	5.0E-01	5.0E-01	5.0E-01	5.0E-01	5.0E-01	5.0E-01	5.0E-01	5.0E-01	5.0E-01	5.0E-01	5.0E-01	5.0E-01
6.7E-45	4.6E-34	8.2E-26	2.1E-19	8.1E-14	1.1E-08	1.0E-03	5.0E-01	5.0E-01	5.0E-01	5.0E-01	5.0E-01	5.0E-01	5.0E-01	5.0E-01	5.0E-01	5.0E-01	5.0E-01	5.0E-01	5.0E-01	5.0E-01
1.5E-44	5.3E-34	8.4E-26	2.2E-19	8.2E-14	1.1E-08	1.0E-03	5.0E-01	5.0E-01	5.0E-01	5.0E-01	5.0E-01	5.0E-01	5.0E-01	5.0E-01	5.0E-01	5.0E-01	5.0E-01	5.0E-01	5.0E-01	5.0E-01
3.2E-44	5.8E-34	8.7E-26	2.2E-19	8.3E-14	1.1E-08	1.0E-03	5.0E-01	5.0E-01	5.0E-01	5.0E-01	5.0E-01	5.0E-01	5.0E-01	5.0E-01	5.0E-01	5.0E-01	5.0E-01	5.0E-01	5.0E-01	5.0E-01

Table (A.23)

The result of received power for the VLC affected by sand particles when the visibility is 5 Km

0	25	50	75	100	125	150	175	200	225	250	275	300	325	350	375	400	425	450	475	500
-13.308	-26.226	-32.154	-35.720	-38.284	-40.294	-41.951	-43.365	-44.600	-45.699	-46.690	-47.594	-48.426	-49.198	-49.918	-50.594	-51.231	-51.834	-52.407	-52.953	-53.475
-12.680	-26.194	-32.146	-35.716	-38.282	-40.292	-41.950	-43.364	-44.600	-45.699	-46.690	-47.594	-48.426	-49.198	-49.918	-50.594	-51.231	-51.834	-52.407	-52.953	-53.475
-12.043	-26.166	-32.138	-35.713	-38.280	-40.291	-41.949	-43.363	-44.599	-45.698	-46.689	-47.594	-48.426	-49.197	-49.918	-50.593	-51.230	-51.834	-52.407	-52.953	-53.475
-11.418	-26.141	-32.132	-35.710	-38.278	-40.290	-41.948	-43.363	-44.599	-45.698	-46.689	-47.593	-48.426	-49.197	-49.917	-50.593	-51.230	-51.834	-52.407	-52.953	-53.475
-10.845	-26.118	-32.126	-35.707	-38.277	-40.289	-41.948	-43.362	-44.598	-45.697	-46.689	-47.593	-48.425	-49.197	-49.917	-50.593	-51.230	-51.833	-52.406	-52.953	-53.475
-10.398	-26.100	-32.121	-35.705	-38.276	-40.288	-41.947	-43.362	-44.598	-45.697	-46.689	-47.593	-48.425	-49.197	-49.917	-50.593	-51.230	-51.833	-52.406	-52.953	-53.475
-10.230	-26.084	-32.117	-35.704	-38.275	-40.288	-41.947	-43.362	-44.598	-45.697	-46.689	-47.593	-48.425	-49.197	-49.917	-50.593	-51.230	-51.833	-52.406	-52.953	-53.475
-10.643	-26.072	-32.114	-35.702	-38.274	-40.287	-41.946	-43.361	-44.597	-45.697	-46.688	-47.593	-48.425	-49.197	-49.917	-50.593	-51.230	-51.833	-52.406	-52.952	-53.475
-12.294	-26.064	-32.112	-35.701	-38.273	-40.287	-41.946	-43.361	-44.597	-45.697	-46.688	-47.593	-48.425	-49.197	-49.917	-50.593	-51.230	-51.833	-52.406	-52.952	-53.475
-16.962	-26.058	-32.111	-35.701	-38.273	-40.286	-41.946	-43.361	-44.597	-45.697	-46.688	-47.593	-48.425	-49.197	-49.917	-50.593	-51.230	-51.833	-52.406	-52.952	-53.475
$-\infty$	-26.057	-32.110	-35.700	-38.273	-40.286	-41.946	-43.361	-44.597	-45.697	-46.688	-47.593	-48.425	-49.197	-49.917	-50.593	-51.230	-51.833	-52.406	-52.952	-53.475
-16.962	-26.058	-32.111	-35.701	-38.273	-40.286	-41.946	-43.361	-44.597	-45.697	-46.688	-47.593	-48.425	-49.197	-49.917	-50.593	-51.230	-51.833	-52.406	-52.952	-53.475
-12.294	-26.064	-32.112	-35.701	-38.273	-40.287	-41.946	-43.361	-44.597	-45.697	-46.688	-47.593	-48.425	-49.197	-49.917	-50.593	-51.230	-51.833	-52.406	-52.952	-53.475
-10.643	-26.072	-32.114	-35.702	-38.274	-40.287	-41.946	-43.361	-44.597	-45.697	-46.688	-47.593	-48.425	-49.197	-49.917	-50.593	-51.230	-51.833	-52.406	-52.952	-53.475
-10.230	-26.084	-32.117	-35.704	-38.275	-40.288	-41.947	-43.362	-44.598	-45.697	-46.689	-47.593	-48.425	-49.197	-49.917	-50.593	-51.230	-51.833	-52.406	-52.953	-53.475
-10.398	-26.100	-32.121	-35.705	-38.276	-40.288	-41.947	-43.362	-44.598	-45.697	-46.689	-47.593	-48.425	-49.197	-49.917	-50.593	-51.230	-51.833	-52.406	-52.953	-53.475
-10.845	-26.118	-32.126	-35.707	-38.277	-40.289	-41.948	-43.362	-44.598	-45.697	-46.689	-47.593	-48.425	-49.197	-49.917	-50.593	-51.230	-51.833	-52.406	-52.953	-53.475
-11.418	-26.141	-32.132	-35.710	-38.278	-40.290	-41.948	-43.363	-44.599	-45.698	-46.689	-47.593	-48.426	-49.197	-49.917	-50.593	-51.230	-51.834	-52.407	-52.953	-53.475
-12.043	-26.141	-32.138	-35.713	-38.280	-40.291	-41.949	-43.363	-44.599	-45.698	-46.689	-47.594	-48.426	-49.197	-49.918	-50.593	-51.230	-51.834	-52.407	-52.953	-53.475
-12.680	-26.194	-32.146	-35.716	-38.282	-40.292	-41.950	-43.364	-44.600	-45.699	-46.690	-47.594	-48.426	-49.198	-49.918	-50.594	-51.231	-51.834	-52.407	-52.953	-53.475
-13.308	-26.226	-32.154	-35.720	-38.284	-40.294	-41.951	-43.365	-44.600	-45.699	-46.690	-47.594	-48.426	-49.198	-49.918	-50.594	-51.231	-51.834	-52.407	-52.953	-53.475

Table (A.24)

The result of signal to noise ratio (SNR) for the VLC connectivity affected by sand particles when the visibility is 5 Km

0	25	50	75	100	125	150	175	200	225	250	275	300	325	350	375	400	425	450	475	500
97.501	79.964	69.249	62.374	57.340	53.365	50.074	47.261	44.800	42.608	40.631	38.826	37.164	35.623	34.184	32.834	31.561	30.355	29.210	28.118	27.075
98.190	80.018	69.265	62.382	57.345	53.368	50.076	47.263	44.801	42.609	40.631	38.826	37.165	35.623	34.184	32.834	31.561	30.356	29.210	28.118	27.075
98.880	80.066	69.279	62.388	57.348	53.370	50.078	47.264	44.802	42.610	40.632	38.827	37.165	35.624	34.185	32.834	31.561	30.356	29.210	28.119	27.075
99.551	80.109	69.291	62.394	57.352	53.373	50.080	47.265	44.803	42.611	40.632	38.827	37.165	35.624	34.185	32.835	31.561	30.356	29.211	28.119	27.075
100.161	80.146	69.302	62.399	57.354	53.374	50.081	47.266	44.804	42.611	40.633	38.828	37.166	35.624	34.185	32.835	31.562	30.356	29.211	28.119	27.075
100.633	80.178	69.311	62.403	57.357	53.376	50.082	47.267	44.804	42.612	40.633	38.828	37.166	35.624	34.186	32.835	31.562	30.356	29.211	28.119	27.075
100.811	80.204	69.319	62.407	57.359	53.377	50.083	47.268	44.805	42.612	40.634	38.828	37.166	35.625	34.186	32.835	31.562	30.356	29.211	28.119	27.075
100.375	80.224	69.324	62.409	57.360	53.378	50.084	47.268	44.805	42.613	40.634	38.829	37.166	35.625	34.186	32.835	31.562	30.357	29.211	28.119	27.075
98.609	80.239	69.329	62.411	57.362	53.379	50.084	47.268	44.805	42.613	40.634	38.829	37.167	35.625	34.186	32.835	31.562	30.357	29.211	28.119	27.075
93.299	80.248	69.331	62.412	57.362	53.379	50.084	47.269	44.806	42.613	40.634	38.829	37.167	35.625	34.186	32.836	31.562	30.357	29.211	28.119	27.076
0.000	80.250	69.332	62.413	57.362	53.380	50.085	47.269	44.806	42.613	40.634	38.829	37.167	35.625	34.186	32.836	31.562	30.357	29.211	28.119	27.076
93.299	80.248	69.331	62.412	57.362	53.379	50.084	47.269	44.806	42.613	40.634	38.829	37.167	35.625	34.186	32.836	31.562	30.357	29.211	28.119	27.076
98.609	80.239	69.329	62.411	57.362	53.379	50.084	47.268	44.805	42.613	40.634	38.829	37.167	35.625	34.186	32.835	31.562	30.357	29.211	28.119	27.075
100.375	80.224	69.324	62.409	57.360	53.378	50.084	47.268	44.805	42.613	40.634	38.829	37.166	35.625	34.186	32.835	31.562	30.357	29.211	28.119	27.075
100.811	80.204	69.319	62.407	57.359	53.377	50.083	47.268	44.805	42.612	40.634	38.828	37.166	35.625	34.186	32.835	31.562	30.356	29.211	28.119	27.075
100.633	80.178	69.311	62.403	57.357	53.376	50.082	47.267	44.804	42.612	40.633	38.828	37.166	35.624	34.186	32.835	31.562	30.356	29.211	28.119	27.075
100.161	80.146	69.302	62.399	57.354	53.374	50.081	47.266	44.804	42.611	40.633	38.828	37.166	35.624	34.185	32.835	31.562	30.356	29.211	28.119	27.075
99.551	80.109	69.291	62.394	57.352	53.373	50.080	47.265	44.803	42.611	40.632	38.827	37.165	35.624	34.185	32.835	31.561	30.356	29.211	28.119	27.075
98.880	80.109	69.279	62.388	57.348	53.370	50.078	47.264	44.802	42.610	40.632	38.827	37.165	35.624	34.185	32.834	31.561	30.356	29.210	28.119	27.075
98.190	80.018	69.265	62.382	57.345	53.368	50.076	47.263	44.801	42.609	40.631	38.826	37.165	35.623	34.184	32.834	31.561	30.356	29.210	28.118	27.075
97.501	79.964	69.249	62.374	57.340	53.365	50.074	47.261	44.800	42.608	40.631	38.826	37.164	35.623	34.184	32.834	31.561	30.355	29.210	28.118	27.075

Table (A.25)

The result of bit error rate (BER) for the VLC connectivity affected by sand particles when the visibility is 5 Km

0	25	50	75	100	125	150	175	200	225	250	275	300	325	350	375	400	425	450	475	500
1.3E-44	5.9E-37	2.8E-32	2.9E-29	4.6E-27	2.6E-25	7.1E-24	1.2E-22	1.5E-21	1.3E-20	9.9E-20	6.1E-19	3.3E-18	1.6E-17	6.8E-17	2.7E-16	9.7E-16	3.3E-15	1.1E-14	3.2E-14	9.3E-14
6.4E-45	5.6E-37	2.8E-32	2.9E-29	4.6E-27	2.5E-25	7.1E-24	1.2E-22	1.5E-21	1.3E-20	9.9E-20	6.1E-19	3.3E-18	1.6E-17	6.8E-17	2.7E-16	9.7E-16	3.3E-15	1.1E-14	3.2E-14	9.3E-14
3.2E-45	5.3E-37	2.8E-32	2.8E-29	4.6E-27	2.5E-25	7.0E-24	1.2E-22	1.5E-21	1.3E-20	9.9E-20	6.1E-19	3.3E-18	1.6E-17	6.8E-17	2.7E-16	9.7E-16	3.3E-15	1.1E-14	3.2E-14	9.3E-14
1.6E-45	5.1E-37	2.7E-32	2.8E-29	4.6E-27	2.5E-25	7.0E-24	1.2E-22	1.5E-21	1.3E-20	9.9E-20	6.1E-19	3.3E-18	1.6E-17	6.8E-17	2.7E-16	9.7E-16	3.3E-15	1.1E-14	3.2E-14	9.3E-14
8.9E-46	4.9E-37	2.7E-32	2.8E-29	4.6E-27	2.5E-25	7.0E-24	1.2E-22	1.5E-21	1.3E-20	9.9E-20	6.1E-19	3.3E-18	1.6E-17	6.8E-17	2.7E-16	9.7E-16	3.3E-15	1.1E-14	3.2E-14	9.3E-14
5.5E-46	4.7E-37	2.7E-32	2.8E-29	4.5E-27	2.5E-25	7.0E-24	1.2E-22	1.5E-21	1.3E-20	9.9E-20	6.1E-19	3.3E-18	1.6E-17	6.8E-17	2.7E-16	9.7E-16	3.3E-15	1.1E-14	3.2E-14	9.3E-14
4.6E-46	4.6E-37	2.6E-32	2.8E-29	4.5E-27	2.5E-25	7.0E-24	1.2E-22	1.5E-21	1.3E-20	9.9E-20	6.1E-19	3.3E-18	1.6E-17	6.8E-17	2.7E-16	9.7E-16	3.3E-15	1.1E-14	3.2E-14	9.3E-14
7.2E-46	4.5E-37	2.6E-32	2.8E-29	4.5E-27	2.5E-25	7.0E-24	1.2E-22	1.5E-21	1.3E-20	9.9E-20	6.1E-19	3.3E-18	1.6E-17	6.8E-17	2.7E-16	9.7E-16	3.3E-15	1.1E-14	3.2E-14	9.3E-14
4.2E-45	4.4E-37	2.6E-32	2.8E-29	4.5E-27	2.5E-25	7.0E-24	1.2E-22	1.4E-21	1.3E-20	9.9E-20	6.1E-19	3.3E-18	1.6E-17	6.8E-17	2.7E-16	9.7E-16	3.3E-15	1.1E-14	3.2E-14	9.3E-14
8.8E-43	4.4E-37	2.6E-32	2.8E-29	4.5E-27	2.5E-25	7.0E-24	1.2E-22	1.4E-21	1.3E-20	9.9E-20	6.1E-19	3.3E-18	1.6E-17	6.8E-17	2.7E-16	9.7E-16	3.3E-15	1.1E-14	3.2E-14	9.3E-14
5.0E-01	4.4E-37	2.6E-32	2.8E-29	4.5E-27	2.5E-25	7.0E-24	1.2E-22	1.4E-21	1.3E-20	9.9E-20	6.1E-19	3.3E-18	1.6E-17	6.8E-17	2.7E-16	9.7E-16	3.3E-15	1.1E-14	3.2E-14	9.3E-14
8.8E-43	4.4E-37	2.6E-32	2.8E-29	4.5E-27	2.5E-25	7.0E-24	1.2E-22	1.4E-21	1.3E-20	9.9E-20	6.1E-19	3.3E-18	1.6E-17	6.8E-17	2.7E-16	9.7E-16	3.3E-15	1.1E-14	3.2E-14	9.3E-14
4.2E-45	4.4E-37	2.6E-32	2.8E-29	4.5E-27	2.5E-25	7.0E-24	1.2E-22	1.4E-21	1.3E-20	9.9E-20	6.1E-19	3.3E-18	1.6E-17	6.8E-17	2.7E-16	9.7E-16	3.3E-15	1.1E-14	3.2E-14	9.3E-14
7.2E-46	4.5E-37	2.6E-32	2.8E-29	4.5E-27	2.5E-25	7.0E-24	1.2E-22	1.5E-21	1.3E-20	9.9E-20	6.1E-19	3.3E-18	1.6E-17	6.8E-17	2.7E-16	9.7E-16	3.3E-15	1.1E-14	3.2E-14	9.3E-14
4.6E-46	4.6E-37	2.6E-32	2.8E-29	4.5E-27	2.5E-25	7.0E-24	1.2E-22	1.5E-21	1.3E-20	9.9E-20	6.1E-19	3.3E-18	1.6E-17	6.8E-17	2.7E-16	9.7E-16	3.3E-15	1.1E-14	3.2E-14	9.3E-14
5.5E-46	4.7E-37	2.7E-32	2.8E-29	4.5E-27	2.5E-25	7.0E-24	1.2E-22	1.5E-21	1.3E-20	9.9E-20	6.1E-19	3.3E-18	1.6E-17	6.8E-17	2.7E-16	9.7E-16	3.3E-15	1.1E-14	3.2E-14	9.3E-14
8.9E-46	4.9E-37	2.7E-32	2.8E-29	4.6E-27	2.5E-25	7.0E-24	1.2E-22	1.5E-21	1.3E-20	9.9E-20	6.1E-19	3.3E-18	1.6E-17	6.8E-17	2.7E-16	9.7E-16	3.3E-15	1.1E-14	3.2E-14	9.3E-14
1.6E-45	5.1E-37	2.7E-32	2.8E-29	4.6E-27	2.5E-25	7.0E-24	1.2E-22	1.5E-21	1.3E-20	9.9E-20	6.1E-19	3.3E-18	1.6E-17	6.8E-17	2.7E-16	9.7E-16	3.3E-15	1.1E-14	3.2E-14	9.3E-14
3.2E-45	5.1E-37	2.8E-32	2.8E-29	4.6E-27	2.5E-25	7.0E-24	1.2E-22	1.5E-21	1.3E-20	9.9E-20	6.1E-19	3.3E-18	1.6E-17	6.8E-17	2.7E-16	9.7E-16	3.3E-15	1.1E-14	3.2E-14	9.3E-14
6.4E-45	5.6E-37	2.8E-32	2.9E-29	4.6E-27	2.5E-25	7.1E-24	1.2E-22	1.5E-21	1.3E-20	9.9E-20	6.1E-19	3.3E-18	1.6E-17	6.8E-17	2.7E-16	9.7E-16	3.3E-15	1.1E-14	3.2E-14	9.3E-14
1.3E-44	5.9E-37	2.8E-32	2.9E-29	4.6E-27	2.6E-25	7.1E-24	1.2E-22	1.5E-21	1.3E-20	9.9E-20	6.1E-19	3.3E-18	1.6E-17	6.8E-17	2.7E-16	9.7E-16	3.3E-15	1.1E-14	3.2E-14	9.3E-14

Table (A.26)

The result of received power for the VLC affected by sand particles when the visibility is 1 Km

0	25	50	75	100	125	150	175	200	225	250	275	300	325	350	375	400	425	450	475	500
-13.374	-26.537	-32.765	-36.634	-39.501	-41.814	-43.775	-45.493	-47.032	-48.434	-49.729	-50.937	-52.073	-53.148	-54.172	-55.152	-56.093	-57.000	-57.876	-58.726	-59.552
-12.740	-26.504	-32.756	-36.630	-39.499	-41.813	-43.774	-45.492	-47.031	-48.434	-49.729	-50.937	-52.073	-53.148	-54.172	-55.152	-56.092	-56.999	-57.876	-58.726	-59.552
-12.098	-26.475	-32.748	-36.626	-39.497	-41.811	-43.773	-45.491	-47.030	-48.433	-49.728	-50.936	-52.072	-53.148	-54.172	-55.151	-56.092	-56.999	-57.876	-58.726	-59.552
-11.468	-26.448	-32.741	-36.623	-39.495	-41.810	-43.772	-45.490	-47.030	-48.433	-49.728	-50.936	-52.072	-53.148	-54.172	-55.151	-56.092	-56.999	-57.876	-58.726	-59.552
-10.889	-26.425	-32.735	-36.620	-39.493	-41.809	-43.771	-45.490	-47.029	-48.432	-49.728	-50.936	-52.072	-53.147	-54.171	-55.151	-56.092	-56.999	-57.876	-58.726	-59.552
-10.438	-26.406	-32.730	-36.618	-39.492	-41.808	-43.771	-45.489	-47.029	-48.432	-49.727	-50.936	-52.072	-53.147	-54.171	-55.151	-56.092	-56.999	-57.876	-58.726	-59.552
-10.265	-26.390	-32.726	-36.616	-39.491	-41.807	-43.770	-45.489	-47.029	-48.432	-49.727	-50.935	-52.071	-53.147	-54.171	-55.151	-56.092	-56.999	-57.876	-58.726	-59.552
-10.674	-26.378	-32.723	-36.614	-39.490	-41.807	-43.770	-45.488	-47.028	-48.432	-49.727	-50.935	-52.071	-53.147	-54.171	-55.151	-56.092	-56.999	-57.876	-58.726	-59.552
-12.322	-26.369	-32.720	-36.613	-39.489	-41.806	-43.769	-45.488	-47.028	-48.431	-49.727	-50.935	-52.071	-53.147	-54.171	-55.151	-56.092	-56.999	-57.875	-58.726	-59.551
-16.988	-26.363	-32.719	-36.612	-39.489	-41.806	-43.769	-45.488	-47.028	-48.431	-49.727	-50.935	-52.071	-53.147	-54.171	-55.151	-56.092	-56.999	-57.875	-58.725	-59.551
-∞	-26.361	-32.718	-36.612	-39.489	-41.806	-43.769	-45.488	-47.028	-48.431	-49.727	-50.935	-52.071	-53.147	-54.171	-55.151	-56.092	-56.999	-57.875	-58.725	-59.551
-16.988	-26.363	-32.719	-36.612	-39.489	-41.806	-43.769	-45.488	-47.028	-48.431	-49.727	-50.935	-52.071	-53.147	-54.171	-55.151	-56.092	-56.999	-57.875	-58.725	-59.551
-12.322	-26.369	-32.720	-36.613	-39.489	-41.806	-43.769	-45.488	-47.028	-48.431	-49.727	-50.935	-52.071	-53.147	-54.171	-55.151	-56.092	-56.999	-57.875	-58.726	-59.551
-10.674	-26.378	-32.723	-36.614	-39.490	-41.807	-43.770	-45.488	-47.028	-48.432	-49.727	-50.935	-52.071	-53.147	-54.171	-55.151	-56.092	-56.999	-57.876	-58.726	-59.552
-10.265	-26.390	-32.726	-36.616	-39.491	-41.807	-43.770	-45.489	-47.029	-48.432	-49.727	-50.935	-52.071	-53.147	-54.171	-55.151	-56.092	-56.999	-57.876	-58.726	-59.552
-10.438	-26.406	-32.730	-36.618	-39.492	-41.808	-43.771	-45.489	-47.029	-48.432	-49.727	-50.936	-52.072	-53.147	-54.171	-55.151	-56.092	-56.999	-57.876	-58.726	-59.552
-10.889	-26.425	-32.735	-36.620	-39.493	-41.809	-43.771	-45.490	-47.029	-48.432	-49.728	-50.936	-52.072	-53.147	-54.171	-55.151	-56.092	-56.999	-57.876	-58.726	-59.552
-11.468	-26.448	-32.741	-36.623	-39.495	-41.810	-43.772	-45.490	-47.030	-48.433	-49.728	-50.936	-52.072	-53.148	-54.172	-55.151	-56.092	-56.999	-57.876	-58.726	-59.552
-12.098	-26.448	-32.748	-36.626	-39.497	-41.811	-43.773	-45.491	-47.030	-48.433	-49.728	-50.936	-52.072	-53.148	-54.172	-55.151	-56.092	-56.999	-57.876	-58.726	-59.552
-12.740	-26.504	-32.756	-36.630	-39.499	-41.813	-43.774	-45.492	-47.031	-48.434	-49.729	-50.937	-52.073	-53.148	-54.172	-55.152	-56.092	-56.999	-57.876	-58.726	-59.552
-13.374	-26.537	-32.765	-36.634	-39.501	-41.814	-43.775	-45.493	-47.032	-48.434	-49.729	-50.937	-52.073	-53.148	-54.172	-55.152	-56.093	-57.000	-57.876	-58.726	-59.552

Table (A.27)

The result of signal to noise ratio (SNR) for the VLC connectivity affected by sand particles when the visibility is 1 Km

0	25	50	75	100	125	150	175	200	225	250	275	300	325	350	375	400	425	450	475	500
97.429	79.437	68.085	60.586	54.935	50.346	46.444	43.020	39.949	37.148	34.561	32.148	29.877	27.728	25.681	23.722	21.841	20.028	18.274	16.575	14.923
98.124	79.493	68.102	60.594	54.940	50.349	46.446	43.022	39.950	37.149	34.562	32.148	29.878	27.728	25.681	23.723	21.841	20.028	18.275	16.575	14.923
98.821	79.543	68.118	60.602	54.944	50.352	46.448	43.023	39.951	37.150	34.563	32.149	29.879	27.729	25.682	23.723	21.842	20.028	18.275	16.575	14.923
99.498	79.588	68.131	60.608	54.948	50.355	46.450	43.025	39.952	37.151	34.564	32.150	29.879	27.729	25.682	23.724	21.842	20.029	18.275	16.575	14.924
100.115	79.627	68.143	60.614	54.951	50.357	46.452	43.026	39.953	37.152	34.564	32.150	29.880	27.730	25.682	23.724	21.842	20.029	18.275	16.576	14.924
100.592	79.660	68.152	60.618	54.954	50.359	46.453	43.027	39.954	37.152	34.565	32.151	29.880	27.730	25.683	23.724	21.843	20.029	18.276	16.576	14.924
100.774	79.687	68.161	60.622	54.956	50.360	46.454	43.028	39.955	37.153	34.565	32.151	29.880	27.730	25.683	23.724	21.843	20.029	18.276	16.576	14.924
100.342	79.708	68.167	60.625	54.958	50.362	46.455	43.028	39.955	37.153	34.566	32.151	29.881	27.731	25.683	23.725	21.843	20.029	18.276	16.576	14.924
98.579	79.723	68.171	60.627	54.959	50.362	46.455	43.029	39.956	37.154	34.566	32.152	29.881	27.731	25.683	23.725	21.843	20.030	18.276	16.576	14.924
93.268	79.732	68.174	60.629	54.960	50.363	46.456	43.029	39.956	37.154	34.566	32.152	29.881	27.731	25.683	23.725	21.843	20.030	18.276	16.576	14.925
0.000	79.735	68.175	60.629	54.960	50.363	46.456	43.029	39.956	37.154	34.566	32.152	29.881	27.731	25.684	23.725	21.843	20.030	18.276	16.576	14.925
93.268	79.732	68.174	60.629	54.960	50.363	46.456	43.029	39.956	37.154	34.566	32.152	29.881	27.731	25.683	23.725	21.843	20.030	18.276	16.576	14.925
98.579	79.723	68.171	60.627	54.959	50.362	46.455	43.029	39.956	37.154	34.566	32.152	29.881	27.731	25.683	23.725	21.843	20.030	18.276	16.576	14.924
100.342	79.708	68.167	60.625	54.958	50.362	46.455	43.028	39.955	37.153	34.566	32.151	29.881	27.731	25.683	23.725	21.843	20.029	18.276	16.576	14.924
100.774	79.687	68.161	60.622	54.956	50.360	46.454	43.028	39.955	37.153	34.565	32.151	29.880	27.730	25.683	23.724	21.843	20.029	18.276	16.576	14.924
100.592	79.660	68.152	60.618	54.954	50.359	46.453	43.027	39.954	37.152	34.565	32.151	29.880	27.730	25.683	23.724	21.843	20.029	18.276	16.576	14.924
100.115	79.627	68.143	60.614	54.951	50.357	46.452	43.026	39.953	37.152	34.564	32.150	29.880	27.730	25.682	23.724	21.842	20.029	18.275	16.576	14.924
99.498	79.588	68.131	60.608	54.948	50.355	46.450	43.025	39.952	37.151	34.564	32.150	29.879	27.729	25.682	23.724	21.842	20.029	18.275	16.575	14.924
98.821	79.588	68.118	60.602	54.944	50.352	46.448	43.023	39.951	37.150	34.563	32.149	29.879	27.729	25.682	23.723	21.842	20.028	18.275	16.575	14.923
98.124	79.493	68.102	60.594	54.940	50.349	46.446	43.022	39.950	37.149	34.562	32.148	29.878	27.728	25.681	23.723	21.841	20.028	18.275	16.575	14.923
97.429	79.437	68.085	60.586	54.935	50.346	46.444	43.020	39.949	37.148	34.561	32.148	29.877	27.728	25.681	23.722	21.841	20.028	18.274	16.575	14.923

Table (A.28)

The result of bit error rate (BER) for the VLC connectivity affected by sand particles when the visibility is 1 Km

0	25	50	75	100	125	150	175	200	225	250	275	300	325	350	375	400	425	450	475	500
1.4E-44	1.0E-36	9.2E-32	1.8E-28	5.2E-26	5.4E-24	2.8E-22	8.8E-21	2.0E-19	3.4E-18	4.6E-17	5.4E-16	5.4E-15	4.8E-14	3.8E-13	2.8E-12	1.9E-11	1.2E-10	7.4E-10	4.3E-09	2.3E-08
6.9E-45	9.4E-37	9.0E-32	1.7E-28	5.2E-26	5.4E-24	2.8E-22	8.8E-21	2.0E-19	3.4E-18	4.6E-17	5.4E-16	5.4E-15	4.8E-14	3.8E-13	2.8E-12	1.9E-11	1.2E-10	7.4E-10	4.3E-09	2.3E-08
3.4E-45	9.0E-37	8.9E-32	1.7E-28	5.2E-26	5.3E-24	2.8E-22	8.8E-21	2.0E-19	3.4E-18	4.6E-17	5.3E-16	5.4E-15	4.8E-14	3.8E-13	2.8E-12	1.9E-11	1.2E-10	7.4E-10	4.3E-09	2.3E-08
1.7E-45	8.6E-37	8.7E-32	1.7E-28	5.2E-26	5.3E-24	2.8E-22	8.8E-21	2.0E-19	3.4E-18	4.6E-17	5.3E-16	5.4E-15	4.8E-14	3.8E-13	2.8E-12	1.9E-11	1.2E-10	7.4E-10	4.3E-09	2.3E-08
9.3E-46	8.2E-37	8.6E-32	1.7E-28	5.1E-26	5.3E-24	2.7E-22	8.8E-21	2.0E-19	3.3E-18	4.6E-17	5.3E-16	5.4E-15	4.8E-14	3.8E-13	2.8E-12	1.9E-11	1.2E-10	7.4E-10	4.3E-09	2.3E-08
5.8E-46	8.0E-37	8.6E-32	1.7E-28	5.1E-26	5.3E-24	2.7E-22	8.8E-21	2.0E-19	3.3E-18	4.6E-17	5.3E-16	5.4E-15	4.8E-14	3.8E-13	2.8E-12	1.9E-11	1.2E-10	7.4E-10	4.3E-09	2.3E-08
4.8E-46	7.8E-37	8.5E-32	1.7E-28	5.1E-26	5.3E-24	2.7E-22	8.7E-21	2.0E-19	3.3E-18	4.6E-17	5.3E-16	5.4E-15	4.8E-14	3.8E-13	2.8E-12	1.9E-11	1.2E-10	7.4E-10	4.3E-09	2.3E-08
7.4E-46	7.6E-37	8.4E-32	1.7E-28	5.1E-26	5.3E-24	2.7E-22	8.7E-21	2.0E-19	3.3E-18	4.6E-17	5.3E-16	5.4E-15	4.8E-14	3.8E-13	2.8E-12	1.9E-11	1.2E-10	7.4E-10	4.3E-09	2.3E-08
4.4E-45	7.5E-37	8.4E-32	1.7E-28	5.1E-26	5.3E-24	2.7E-22	8.7E-21	2.0E-19	3.3E-18	4.6E-17	5.3E-16	5.4E-15	4.8E-14	3.8E-13	2.8E-12	1.9E-11	1.2E-10	7.4E-10	4.3E-09	2.3E-08
9.1E-43	7.4E-37	8.4E-32	1.7E-28	5.1E-26	5.3E-24	2.7E-22	8.7E-21	2.0E-19	3.3E-18	4.6E-17	5.3E-16	5.4E-15	4.8E-14	3.8E-13	2.8E-12	1.9E-11	1.2E-10	7.4E-10	4.3E-09	2.3E-08
5.0E-01	7.4E-37	8.4E-32	1.7E-28	5.1E-26	5.3E-24	2.7E-22	8.7E-21	2.0E-19	3.3E-18	4.6E-17	5.3E-16	5.4E-15	4.8E-14	3.8E-13	2.8E-12	1.9E-11	1.2E-10	7.4E-10	4.3E-09	2.3E-08
9.1E-43	7.4E-37	8.4E-32	1.7E-28	5.1E-26	5.3E-24	2.7E-22	8.7E-21	2.0E-19	3.3E-18	4.6E-17	5.3E-16	5.4E-15	4.8E-14	3.8E-13	2.8E-12	1.9E-11	1.2E-10	7.4E-10	4.3E-09	2.3E-08
4.4E-45	7.5E-37	8.4E-32	1.7E-28	5.1E-26	5.3E-24	2.7E-22	8.7E-21	2.0E-19	3.3E-18	4.6E-17	5.3E-16	5.4E-15	4.8E-14	3.8E-13	2.8E-12	1.9E-11	1.2E-10	7.4E-10	4.3E-09	2.3E-08
7.4E-46	7.6E-37	8.4E-32	1.7E-28	5.1E-26	5.3E-24	2.7E-22	8.7E-21	2.0E-19	3.3E-18	4.6E-17	5.3E-16	5.4E-15	4.8E-14	3.8E-13	2.8E-12	1.9E-11	1.2E-10	7.4E-10	4.3E-09	2.3E-08
4.8E-46	7.8E-37	8.5E-32	1.7E-28	5.1E-26	5.3E-24	2.7E-22	8.7E-21	2.0E-19	3.3E-18	4.6E-17	5.3E-16	5.4E-15	4.8E-14	3.8E-13	2.8E-12	1.9E-11	1.2E-10	7.4E-10	4.3E-09	2.3E-08
5.8E-46	8.0E-37	8.6E-32	1.7E-28	5.1E-26	5.3E-24	2.7E-22	8.8E-21	2.0E-19	3.3E-18	4.6E-17	5.3E-16	5.4E-15	4.8E-14	3.8E-13	2.8E-12	1.9E-11	1.2E-10	7.4E-10	4.3E-09	2.3E-08
9.3E-46	8.2E-37	8.6E-32	1.7E-28	5.1E-26	5.3E-24	2.7E-22	8.8E-21	2.0E-19	3.3E-18	4.6E-17	5.3E-16	5.4E-15	4.8E-14	3.8E-13	2.8E-12	1.9E-11	1.2E-10	7.4E-10	4.3E-09	2.3E-08
1.7E-45	8.6E-37	8.7E-32	1.7E-28	5.2E-26	5.3E-24	2.8E-22	8.8E-21	2.0E-19	3.4E-18	4.6E-17	5.3E-16	5.4E-15	4.8E-14	3.8E-13	2.8E-12	1.9E-11	1.2E-10	7.4E-10	4.3E-09	2.3E-08
3.4E-45	8.6E-37	8.9E-32	1.7E-28	5.2E-26	5.3E-24	2.8E-22	8.8E-21	2.0E-19	3.4E-18	4.6E-17	5.3E-16	5.4E-15	4.8E-14	3.8E-13	2.8E-12	1.9E-11	1.2E-10	7.4E-10	4.3E-09	2.3E-08
6.9E-45	9.4E-37	9.0E-32	1.7E-28	5.2E-26	5.4E-24	2.8E-22	8.8E-21	2.0E-19	3.4E-18	4.6E-17	5.4E-16	5.4E-15	4.8E-14	3.8E-13	2.8E-12	1.9E-11	1.2E-10	7.4E-10	4.3E-09	2.3E-08
1.4E-44	1.0E-36	9.2E-32	1.8E-28	5.2E-26	5.4E-24	2.8E-22	8.8E-21	2.0E-19	3.4E-18	4.6E-17	5.4E-16	5.4E-15	4.8E-14	3.8E-13	2.8E-12	1.9E-11	1.2E-10	7.4E-10	4.3E-09	2.3E-08

Table (A.29)

The result of received power for the VLC affected by sand particles when the visibility is 0.1 Km

0	25	50	75	100	125	150	175	200	225	250	275	300	325	350	375	400	425	450	475	500
-14.113	-30.036	-39.645	-46.921	-53.202	-58.931	-64.309	-69.445	-74.403	-79.225	-83.939	-88.566	-93.121	-97.616	-102.060	-106.459	-110.820	-115.147	-119.443	-123.713	-127.959
-13.417	-29.991	-39.630	-46.913	-53.196	-58.927	-64.306	-69.442	-74.401	-79.223	-83.937	-88.564	-93.120	-97.615	-102.059	-106.458	-110.819	-115.146	-119.443	-123.713	-127.958
-12.713	-29.950	-39.616	-46.905	-53.191	-58.923	-64.303	-69.440	-74.398	-79.221	-83.935	-88.563	-93.119	-97.614	-102.058	-106.457	-110.818	-115.145	-119.442	-123.712	-127.958
-12.023	-29.913	-39.604	-46.898	-53.187	-58.920	-64.300	-69.438	-74.397	-79.219	-83.934	-88.562	-93.118	-97.613	-102.057	-106.456	-110.817	-115.144	-119.441	-123.711	-127.957
-11.386	-29.882	-39.594	-46.893	-53.183	-58.917	-64.298	-69.436	-74.395	-79.218	-83.933	-88.561	-93.117	-97.612	-102.056	-106.456	-110.817	-115.144	-119.440	-123.711	-127.957
-10.880	-29.855	-39.585	-46.888	-53.179	-58.914	-64.296	-69.434	-74.394	-79.217	-83.932	-88.560	-93.116	-97.611	-102.055	-106.455	-110.816	-115.143	-119.440	-123.710	-127.956
-10.656	-29.833	-39.577	-46.884	-53.177	-58.912	-64.295	-69.433	-74.393	-79.216	-83.931	-88.559	-93.115	-97.611	-102.055	-106.454	-110.815	-115.143	-119.439	-123.710	-127.956
-11.022	-29.815	-39.572	-46.881	-53.175	-58.911	-64.294	-69.432	-74.392	-79.215	-83.930	-88.558	-93.115	-97.610	-102.054	-106.454	-110.815	-115.142	-119.439	-123.709	-127.955
-12.634	-29.803	-39.568	-46.878	-53.173	-58.910	-64.293	-69.431	-74.391	-79.214	-83.930	-88.558	-93.114	-97.610	-102.054	-106.454	-110.815	-115.142	-119.439	-123.709	-127.955
-17.276	-29.796	-39.565	-46.877	-53.172	-58.909	-64.292	-69.431	-74.391	-79.214	-83.930	-88.558	-93.114	-97.610	-102.054	-106.454	-110.815	-115.142	-119.439	-123.709	-127.955
-∞	-29.793	-39.564	-46.877	-53.172	-58.909	-64.292	-69.431	-74.391	-79.214	-83.929	-88.558	-93.114	-97.610	-102.054	-106.454	-110.815	-115.142	-119.439	-123.709	-127.955
-17.276	-29.796	-39.565	-46.877	-53.172	-58.909	-64.292	-69.431	-74.391	-79.214	-83.930	-88.558	-93.114	-97.610	-102.054	-106.454	-110.815	-115.142	-119.439	-123.709	-127.955
-12.634	-29.803	-39.568	-46.878	-53.173	-58.910	-64.293	-69.431	-74.391	-79.214	-83.930	-88.558	-93.114	-97.610	-102.054	-106.454	-110.815	-115.142	-119.439	-123.709	-127.955
-11.022	-29.815	-39.572	-46.881	-53.175	-58.911	-64.294	-69.432	-74.392	-79.215	-83.930	-88.558	-93.115	-97.610	-102.054	-106.454	-110.815	-115.142	-119.439	-123.709	-127.955
-10.656	-29.833	-39.577	-46.884	-53.177	-58.912	-64.295	-69.433	-74.393	-79.216	-83.931	-88.559	-93.115	-97.611	-102.055	-106.454	-110.815	-115.143	-119.439	-123.710	-127.956
-10.880	-29.855	-39.585	-46.888	-53.179	-58.914	-64.296	-69.434	-74.394	-79.217	-83.932	-88.560	-93.116	-97.611	-102.055	-106.455	-110.816	-115.143	-119.440	-123.710	-127.956
-11.386	-29.882	-39.594	-46.893	-53.183	-58.917	-64.298	-69.436	-74.395	-79.218	-83.933	-88.561	-93.117	-97.612	-102.056	-106.456	-110.817	-115.144	-119.440	-123.711	-127.957
-12.023	-29.913	-39.604	-46.898	-53.187	-58.920	-64.300	-69.438	-74.397	-79.219	-83.934	-88.562	-93.118	-97.613	-102.057	-106.456	-110.817	-115.144	-119.441	-123.711	-127.957
-12.713	-29.913	-39.616	-46.905	-53.191	-58.923	-64.303	-69.440	-74.398	-79.221	-83.935	-88.563	-93.119	-97.614	-102.058	-106.457	-110.818	-115.145	-119.442	-123.712	-127.958
-13.417	-29.991	-39.630	-46.913	-53.196	-58.927	-64.306	-69.442	-74.401	-79.223	-83.937	-88.564	-93.120	-97.615	-102.059	-106.458	-110.819	-115.146	-119.443	-123.713	-127.958
-14.113	-30.036	-39.645	-46.921	-53.202	-58.931	-64.309	-69.445	-74.403	-79.225	-83.939	-88.566	-93.121	-97.616	-102.060	-106.459	-110.820	-115.147	-119.443	-123.713	-127.959

Table (A.30)

The result of signal to noise ratio (SNR) for the VLC connectivity affected by sand particles when the visibility is 0.1 Km

0	25	50	75	100	125	150	175	200	225	250	275	300	325	350	375	400	425	450	475	500
96.607	73.212	54.650	40.170	27.621	16.165	5.409	0.000	0.000	0.000	0.000	0.000	0.000	0.000	0.000	0.000	0.000	0.000	0.000	0.000	0.000
97.382	73.296	54.680	40.187	27.632	16.174	5.416	0.000	0.000	0.000	0.000	0.000	0.000	0.000	0.000	0.000	0.000	0.000	0.000	0.000	0.000
98.154	73.371	54.707	40.202	27.642	16.181	5.422	0.000	0.000	0.000	0.000	0.000	0.000	0.000	0.000	0.000	0.000	0.000	0.000	0.000	0.000
98.902	73.438	54.732	40.215	27.651	16.188	5.427	0.000	0.000	0.000	0.000	0.000	0.000	0.000	0.000	0.000	0.000	0.000	0.000	0.000	0.000
99.585	73.497	54.752	40.227	27.659	16.194	5.432	0.000	0.000	0.000	0.000	0.000	0.000	0.000	0.000	0.000	0.000	0.000	0.000	0.000	0.000
100.124	73.546	54.770	40.236	27.666	16.199	5.435	0.000	0.000	0.000	0.000	0.000	0.000	0.000	0.000	0.000	0.000	0.000	0.000	0.000	0.000
100.361	73.587	54.784	40.244	27.671	16.203	5.439	0.000	0.000	0.000	0.000	0.000	0.000	0.000	0.000	0.000	0.000	0.000	0.000	0.000	0.000
99.973	73.618	54.796	40.251	27.675	16.206	5.441	0.000	0.000	0.000	0.000	0.000	0.000	0.000	0.000	0.000	0.000	0.000	0.000	0.000	0.000
98.240	73.641	54.804	40.255	27.678	16.208	5.443	0.000	0.000	0.000	0.000	0.000	0.000	0.000	0.000	0.000	0.000	0.000	0.000	0.000	0.000
92.917	73.654	54.809	40.258	27.680	16.209	5.444	0.000	0.000	0.000	0.000	0.000	0.000	0.000	0.000	0.000	0.000	0.000	0.000	0.000	0.000
0.000	73.659	54.810	40.259	27.680	16.210	5.444	0.000	0.000	0.000	0.000	0.000	0.000	0.000	0.000	0.000	0.000	0.000	0.000	0.000	0.000
92.917	73.654	54.809	40.258	27.680	16.209	5.444	0.000	0.000	0.000	0.000	0.000	0.000	0.000	0.000	0.000	0.000	0.000	0.000	0.000	0.000
98.240	73.641	54.804	40.255	27.678	16.208	5.443	0.000	0.000	0.000	0.000	0.000	0.000	0.000	0.000	0.000	0.000	0.000	0.000	0.000	0.000
99.973	73.618	54.796	40.251	27.675	16.206	5.441	0.000	0.000	0.000	0.000	0.000	0.000	0.000	0.000	0.000	0.000	0.000	0.000	0.000	0.000
100.361	73.587	54.784	40.244	27.671	16.203	5.439	0.000	0.000	0.000	0.000	0.000	0.000	0.000	0.000	0.000	0.000	0.000	0.000	0.000	0.000
100.124	73.546	54.770	40.236	27.666	16.199	5.435	0.000	0.000	0.000	0.000	0.000	0.000	0.000	0.000	0.000	0.000	0.000	0.000	0.000	0.000
99.585	73.497	54.752	40.227	27.659	16.194	5.432	0.000	0.000	0.000	0.000	0.000	0.000	0.000	0.000	0.000	0.000	0.000	0.000	0.000	0.000
98.902	73.438	54.732	40.215	27.651	16.188	5.427	0.000	0.000	0.000	0.000	0.000	0.000	0.000	0.000	0.000	0.000	0.000	0.000	0.000	0.000
98.154	73.438	54.707	40.202	27.642	16.181	5.422	0.000	0.000	0.000	0.000	0.000	0.000	0.000	0.000	0.000	0.000	0.000	0.000	0.000	0.000
97.382	73.296	54.680	40.187	27.632	16.174	5.416	0.000	0.000	0.000	0.000	0.000	0.000	0.000	0.000	0.000	0.000	0.000	0.000	0.000	0.000
96.607	73.212	54.650	40.170	27.621	16.165	5.409	0.000	0.000	0.000	0.000	0.000	0.000	0.000	0.000	0.000	0.000	0.000	0.000	0.000	0.000

Table (A.31)

The result of bit error rate (BER) for the VLC connectivity affected by sand particles when the visibility is 0.1 Km

0	25	50	75	100	125	150	175	200	225	250	275	300	325	350	375	400	425	450	475	500
3.2E-44	5.2E-34	7.0E-26	1.6E-19	5.3E-14	6.5E-09	5.0E-04	5.0E-01	5.0E-01	5.0E-01	5.0E-01	5.0E-01	5.0E-01	5.0E-01	5.0E-01	5.0E-01	5.0E-01	5.0E-01	5.0E-01	5.0E-01	5.0E-01
1.5E-44	4.8E-34	6.8E-26	1.5E-19	5.3E-14	6.4E-09	5.0E-04	5.0E-01	5.0E-01	5.0E-01	5.0E-01	5.0E-01	5.0E-01	5.0E-01	5.0E-01	5.0E-01	5.0E-01	5.0E-01	5.0E-01	5.0E-01	5.0E-01
6.7E-45	4.5E-34	6.6E-26	1.5E-19	5.2E-14	6.4E-09	5.0E-04	5.0E-01	5.0E-01	5.0E-01	5.0E-01	5.0E-01	5.0E-01	5.0E-01	5.0E-01	5.0E-01	5.0E-01	5.0E-01	5.0E-01	5.0E-01	5.0E-01
3.1E-45	4.2E-34	6.4E-26	1.5E-19	5.2E-14	6.4E-09	4.9E-04	5.0E-01	5.0E-01	5.0E-01	5.0E-01	5.0E-01	5.0E-01	5.0E-01	5.0E-01	5.0E-01	5.0E-01	5.0E-01	5.0E-01	5.0E-01	5.0E-01
1.6E-45	3.9E-34	6.3E-26	1.5E-19	5.1E-14	6.3E-09	4.9E-04	5.0E-01	5.0E-01	5.0E-01	5.0E-01	5.0E-01	5.0E-01	5.0E-01	5.0E-01	5.0E-01	5.0E-01	5.0E-01	5.0E-01	5.0E-01	5.0E-01
9.2E-46	3.7E-34	6.2E-26	1.5E-19	5.1E-14	6.3E-09	4.9E-04	5.0E-01	5.0E-01	5.0E-01	5.0E-01	5.0E-01	5.0E-01	5.0E-01	5.0E-01	5.0E-01	5.0E-01	5.0E-01	5.0E-01	5.0E-01	5.0E-01
7.3E-46	3.6E-34	6.1E-26	1.5E-19	5.1E-14	6.3E-09	4.9E-04	5.0E-01	5.0E-01	5.0E-01	5.0E-01	5.0E-01	5.0E-01	5.0E-01	5.0E-01	5.0E-01	5.0E-01	5.0E-01	5.0E-01	5.0E-01	5.0E-01
1.1E-45	3.5E-34	6.0E-26	1.5E-19	5.0E-14	6.2E-09	4.9E-04	5.0E-01	5.0E-01	5.0E-01	5.0E-01	5.0E-01	5.0E-01	5.0E-01	5.0E-01	5.0E-01	5.0E-01	5.0E-01	5.0E-01	5.0E-01	5.0E-01
6.1E-45	3.4E-34	6.0E-26	1.4E-19	5.0E-14	6.2E-09	4.8E-04	5.0E-01	5.0E-01	5.0E-01	5.0E-01	5.0E-01	5.0E-01	5.0E-01	5.0E-01	5.0E-01	5.0E-01	5.0E-01	5.0E-01	5.0E-01	5.0E-01
1.3E-42	3.4E-34	5.9E-26	1.4E-19	5.0E-14	6.2E-09	4.8E-04	5.0E-01	5.0E-01	5.0E-01	5.0E-01	5.0E-01	5.0E-01	5.0E-01	5.0E-01	5.0E-01	5.0E-01	5.0E-01	5.0E-01	5.0E-01	5.0E-01
5.0E-01	3.3E-34	5.9E-26	1.4E-19	5.0E-14	6.2E-09	4.8E-04	5.0E-01	5.0E-01	5.0E-01	5.0E-01	5.0E-01	5.0E-01	5.0E-01	5.0E-01	5.0E-01	5.0E-01	5.0E-01	5.0E-01	5.0E-01	5.0E-01
1.3E-42	3.4E-34	5.9E-26	1.4E-19	5.0E-14	6.2E-09	4.8E-04	5.0E-01	5.0E-01	5.0E-01	5.0E-01	5.0E-01	5.0E-01	5.0E-01	5.0E-01	5.0E-01	5.0E-01	5.0E-01	5.0E-01	5.0E-01	5.0E-01
6.1E-45	3.4E-34	6.0E-26	1.4E-19	5.0E-14	6.2E-09	4.8E-04	5.0E-01	5.0E-01	5.0E-01	5.0E-01	5.0E-01	5.0E-01	5.0E-01	5.0E-01	5.0E-01	5.0E-01	5.0E-01	5.0E-01	5.0E-01	5.0E-01
1.1E-45	3.5E-34	6.0E-26	1.5E-19	5.0E-14	6.2E-09	4.9E-04	5.0E-01	5.0E-01	5.0E-01	5.0E-01	5.0E-01	5.0E-01	5.0E-01	5.0E-01	5.0E-01	5.0E-01	5.0E-01	5.0E-01	5.0E-01	5.0E-01
7.3E-46	3.6E-34	6.1E-26	1.5E-19	5.1E-14	6.3E-09	4.9E-04	5.0E-01	5.0E-01	5.0E-01	5.0E-01	5.0E-01	5.0E-01	5.0E-01	5.0E-01	5.0E-01	5.0E-01	5.0E-01	5.0E-01	5.0E-01	5.0E-01
9.2E-46	3.7E-34	6.2E-26	1.5E-19	5.1E-14	6.3E-09	4.9E-04	5.0E-01	5.0E-01	5.0E-01	5.0E-01	5.0E-01	5.0E-01	5.0E-01	5.0E-01	5.0E-01	5.0E-01	5.0E-01	5.0E-01	5.0E-01	5.0E-01
1.6E-45	3.9E-34	6.3E-26	1.5E-19	5.1E-14	6.3E-09	4.9E-04	5.0E-01	5.0E-01	5.0E-01	5.0E-01	5.0E-01	5.0E-01	5.0E-01	5.0E-01	5.0E-01	5.0E-01	5.0E-01	5.0E-01	5.0E-01	5.0E-01
3.1E-45	4.2E-34	6.4E-26	1.5E-19	5.2E-14	6.4E-09	4.9E-04	5.0E-01	5.0E-01	5.0E-01	5.0E-01	5.0E-01	5.0E-01	5.0E-01	5.0E-01	5.0E-01	5.0E-01	5.0E-01	5.0E-01	5.0E-01	5.0E-01
6.7E-45	4.2E-34	6.6E-26	1.5E-19	5.2E-14	6.4E-09	5.0E-04	5.0E-01	5.0E-01	5.0E-01	5.0E-01	5.0E-01	5.0E-01	5.0E-01	5.0E-01	5.0E-01	5.0E-01	5.0E-01	5.0E-01	5.0E-01	5.0E-01
1.5E-44	4.8E-34	6.8E-26	1.5E-19	5.3E-14	6.4E-09	5.0E-04	5.0E-01	5.0E-01	5.0E-01	5.0E-01	5.0E-01	5.0E-01	5.0E-01	5.0E-01	5.0E-01	5.0E-01	5.0E-01	5.0E-01	5.0E-01	5.0E-01
3.2E-44	5.2E-34	7.0E-26	1.6E-19	5.3E-14	6.5E-09	5.0E-04	5.0E-01	5.0E-01	5.0E-01	5.0E-01	5.0E-01	5.0E-01	5.0E-01	5.0E-01	5.0E-01	5.0E-01	5.0E-01	5.0E-01	5.0E-01	5.0E-01

Table (A.32)

The result of received power for the VLC affected by gravel particles when the visibility is 5 Km

0	25	50	75	100	125	150	175	200	225	250	275	300	325	350	375	400	425	450	475	500
-13.308	-26.226	-32.154	-35.721	-38.285	-40.295	-41.952	-43.366	-44.602	-45.701	-46.692	-47.596	-48.429	-49.201	-49.921	-50.597	-51.234	-51.837	-52.411	-52.957	-53.479
-12.680	-26.195	-32.146	-35.717	-38.283	-40.293	-41.951	-43.366	-44.601	-45.700	-46.692	-47.596	-48.428	-49.200	-49.921	-50.597	-51.234	-51.837	-52.410	-52.957	-53.479
-12.043	-26.166	-32.139	-35.714	-38.281	-40.292	-41.950	-43.365	-44.601	-45.700	-46.692	-47.596	-48.428	-49.200	-49.921	-50.596	-51.234	-51.837	-52.410	-52.957	-53.479
-11.418	-26.141	-32.132	-35.711	-38.279	-40.291	-41.950	-43.364	-44.600	-45.700	-46.691	-47.596	-48.428	-49.200	-49.920	-50.596	-51.234	-51.837	-52.410	-52.957	-53.479
-10.845	-26.119	-32.126	-35.708	-38.278	-40.290	-41.949	-43.364	-44.600	-45.699	-46.691	-47.595	-48.428	-49.200	-49.920	-50.596	-51.234	-51.837	-52.410	-52.957	-53.479
-10.398	-26.100	-32.121	-35.706	-38.277	-40.289	-41.948	-43.363	-44.600	-45.699	-46.691	-47.595	-48.428	-49.200	-49.920	-50.596	-51.233	-51.837	-52.410	-52.956	-53.479
-10.230	-26.084	-32.118	-35.704	-38.276	-40.289	-41.948	-43.363	-44.599	-45.699	-46.691	-47.595	-48.428	-49.200	-49.920	-50.596	-51.233	-51.837	-52.410	-52.956	-53.479
-10.643	-26.072	-32.114	-35.703	-38.275	-40.288	-41.948	-43.363	-44.599	-45.699	-46.691	-47.595	-48.428	-49.200	-49.920	-50.596	-51.233	-51.837	-52.410	-52.956	-53.479
-12.294	-26.064	-32.112	-35.702	-38.274	-40.288	-41.947	-43.363	-44.599	-45.699	-46.690	-47.595	-48.427	-49.199	-49.920	-50.596	-51.233	-51.837	-52.410	-52.956	-53.479
-16.962	-26.059	-32.111	-35.701	-38.274	-40.287	-41.947	-43.362	-44.599	-45.699	-46.690	-47.595	-48.427	-49.199	-49.920	-50.596	-51.233	-51.837	-52.410	-52.956	-53.479
-∞	-26.057	-32.110	-35.701	-38.274	-40.287	-41.947	-43.362	-44.599	-45.699	-46.690	-47.595	-48.427	-49.199	-49.920	-50.596	-51.233	-51.837	-52.410	-52.956	-53.479
-16.962	-26.059	-32.111	-35.701	-38.274	-40.287	-41.947	-43.362	-44.599	-45.699	-46.690	-47.595	-48.427	-49.199	-49.920	-50.596	-51.233	-51.837	-52.410	-52.956	-53.479
-12.294	-26.064	-32.112	-35.702	-38.274	-40.288	-41.947	-43.363	-44.599	-45.699	-46.690	-47.595	-48.427	-49.199	-49.920	-50.596	-51.233	-51.837	-52.410	-52.956	-53.479
-10.643	-26.072	-32.114	-35.703	-38.275	-40.288	-41.948	-43.363	-44.599	-45.699	-46.691	-47.595	-48.428	-49.200	-49.920	-50.596	-51.233	-51.837	-52.410	-52.956	-53.479
-10.230	-26.084	-32.118	-35.704	-38.276	-40.289	-41.948	-43.363	-44.599	-45.699	-46.691	-47.595	-48.428	-49.200	-49.920	-50.596	-51.233	-51.837	-52.410	-52.956	-53.479
-10.398	-26.100	-32.121	-35.706	-38.277	-40.289	-41.948	-43.363	-44.600	-45.699	-46.691	-47.595	-48.428	-49.200	-49.920	-50.596	-51.233	-51.837	-52.410	-52.956	-53.479
-10.845	-26.119	-32.126	-35.708	-38.278	-40.290	-41.949	-43.364	-44.600	-45.699	-46.691	-47.595	-48.428	-49.200	-49.920	-50.596	-51.234	-51.837	-52.410	-52.957	-53.479
-11.418	-26.141	-32.132	-35.711	-38.279	-40.291	-41.950	-43.364	-44.600	-45.700	-46.691	-47.596	-48.428	-49.200	-49.920	-50.596	-51.234	-51.837	-52.410	-52.957	-53.479
-12.043	-26.141	-32.139	-35.714	-38.281	-40.292	-41.950	-43.365	-44.601	-45.700	-46.692	-47.596	-48.428	-49.200	-49.921	-50.596	-51.234	-51.837	-52.410	-52.957	-53.479
-12.680	-26.195	-32.146	-35.717	-38.283	-40.293	-41.951	-43.366	-44.601	-45.700	-46.692	-47.596	-48.428	-49.200	-49.921	-50.597	-51.234	-51.837	-52.410	-52.957	-53.479
-13.308	-26.226	-32.154	-35.721	-38.285	-40.295	-41.952	-43.366	-44.602	-45.701	-46.692	-47.596	-48.429	-49.201	-49.921	-50.597	-51.234	-51.837	-52.411	-52.957	-53.479

Table (A.33)

The result of signal to noise ratio (SNR) for the VLC connectivity affected by gravel particles when the visibility is 5 Km

0	25	50	75	100	125	150	175	200	225	250	275	300	325	350	375	400	425	450	475	500
97.501	79.964	69.248	62.373	57.339	53.363	50.072	47.258	44.797	42.605	40.626	38.821	37.159	35.617	34.178	32.828	31.554	30.348	29.203	28.110	27.066
98.190	80.018	69.264	62.380	57.343	53.366	50.074	47.260	44.798	42.606	40.627	38.822	37.160	35.618	34.179	32.828	31.554	30.349	29.203	28.111	27.067
98.880	80.066	69.278	62.387	57.347	53.368	50.076	47.261	44.799	42.606	40.628	38.822	37.160	35.618	34.179	32.828	31.555	30.349	29.203	28.111	27.067
99.550	80.109	69.290	62.393	57.350	53.371	50.077	47.262	44.800	42.607	40.628	38.823	37.160	35.619	34.179	32.829	31.555	30.349	29.203	28.111	27.067
100.161	80.146	69.301	62.398	57.353	53.372	50.078	47.263	44.800	42.608	40.629	38.823	37.161	35.619	34.180	32.829	31.555	30.349	29.203	28.111	27.067
100.633	80.178	69.310	62.402	57.355	53.374	50.080	47.264	44.801	42.608	40.629	38.824	37.161	35.619	34.180	32.829	31.555	30.349	29.204	28.111	27.067
100.811	80.204	69.318	62.405	57.357	53.375	50.081	47.265	44.801	42.609	40.630	38.824	37.161	35.619	34.180	32.829	31.555	30.349	29.204	28.111	27.067
100.375	80.224	69.324	62.408	57.359	53.376	50.081	47.265	44.802	42.609	40.630	38.824	37.162	35.619	34.180	32.829	31.555	30.350	29.204	28.111	27.067
98.609	80.238	69.328	62.410	57.360	53.377	50.082	47.266	44.802	42.609	40.630	38.824	37.162	35.620	34.180	32.829	31.556	30.350	29.204	28.111	27.067
93.299	80.247	69.330	62.411	57.361	53.377	50.082	47.266	44.802	42.609	40.630	38.824	37.162	35.620	34.180	32.829	31.556	30.350	29.204	28.112	27.067
0.000	80.250	69.331	62.412	57.361	53.378	50.082	47.266	44.802	42.609	40.630	38.824	37.162	35.620	34.180	32.829	31.556	30.350	29.204	28.112	27.067
93.299	80.247	69.330	62.411	57.361	53.377	50.082	47.266	44.802	42.609	40.630	38.824	37.162	35.620	34.180	32.829	31.556	30.350	29.204	28.112	27.067
98.609	80.238	69.328	62.410	57.360	53.377	50.082	47.266	44.802	42.609	40.630	38.824	37.162	35.620	34.180	32.829	31.556	30.350	29.204	28.111	27.067
100.375	80.224	69.324	62.408	57.359	53.376	50.081	47.265	44.802	42.609	40.630	38.824	37.162	35.619	34.180	32.829	31.555	30.350	29.204	28.111	27.067
100.811	80.204	69.318	62.405	57.357	53.375	50.081	47.265	44.801	42.609	40.630	38.824	37.161	35.619	34.180	32.829	31.555	30.349	29.204	28.111	27.067
100.633	80.178	69.310	62.402	57.355	53.374	50.080	47.264	44.801	42.608	40.629	38.824	37.161	35.619	34.180	32.829	31.555	30.349	29.204	28.111	27.067
100.161	80.146	69.301	62.398	57.353	53.372	50.078	47.263	44.800	42.608	40.629	38.823	37.161	35.619	34.180	32.829	31.555	30.349	29.203	28.111	27.067
99.550	80.109	69.290	62.393	57.350	53.371	50.077	47.262	44.800	42.607	40.628	38.823	37.160	35.619	34.179	32.829	31.555	30.349	29.203	28.111	27.067
98.880	80.109	69.278	62.387	57.347	53.368	50.076	47.261	44.799	42.606	40.628	38.822	37.160	35.618	34.179	32.828	31.555	30.349	29.203	28.111	27.067
98.190	80.018	69.264	62.380	57.343	53.366	50.074	47.260	44.798	42.606	40.627	38.822	37.160	35.618	34.179	32.828	31.554	30.349	29.203	28.111	27.067
97.501	79.964	69.248	62.373	57.339	53.363	50.072	47.258	44.797	42.605	40.626	38.821	37.159	35.617	34.178	32.828	31.554	30.348	29.203	28.110	27.066

Table (A.34)

The result of bit error rate (BER) for the VLC connectivity affected by gravel particles when the visibility is 5 Km

0	25	50	75	100	125	150	175	200	225	250	275	300	325	350	375	400	425	450	475	500
1.3E-44	5.9E-37	2.8E-32	2.9E-29	4.6E-27	2.6E-25	7.1E-24	1.2E-22	1.5E-21	1.3E-20	9.9E-20	6.2E-19	3.3E-18	1.6E-17	6.8E-17	2.7E-16	9.8E-16	3.3E-15	1.1E-14	3.2E-14	9.4E-14
6.4E-45	5.6E-37	2.8E-32	2.9E-29	4.6E-27	2.5E-25	7.1E-24	1.2E-22	1.5E-21	1.3E-20	9.9E-20	6.2E-19	3.3E-18	1.6E-17	6.8E-17	2.7E-16	9.8E-16	3.3E-15	1.1E-14	3.2E-14	9.4E-14
3.2E-45	5.3E-37	2.8E-32	2.9E-29	4.6E-27	2.5E-25	7.1E-24	1.2E-22	1.5E-21	1.3E-20	9.9E-20	6.2E-19	3.3E-18	1.6E-17	6.8E-17	2.7E-16	9.8E-16	3.3E-15	1.1E-14	3.2E-14	9.4E-14
1.6E-45	5.1E-37	2.7E-32	2.8E-29	4.6E-27	2.5E-25	7.0E-24	1.2E-22	1.5E-21	1.3E-20	9.9E-20	6.2E-19	3.3E-18	1.6E-17	6.8E-17	2.7E-16	9.8E-16	3.3E-15	1.1E-14	3.2E-14	9.4E-14
8.9E-46	4.9E-37	2.7E-32	2.8E-29	4.6E-27	2.5E-25	7.0E-24	1.2E-22	1.5E-21	1.3E-20	9.9E-20	6.2E-19	3.3E-18	1.6E-17	6.8E-17	2.7E-16	9.8E-16	3.3E-15	1.1E-14	3.2E-14	9.4E-14
5.5E-46	4.7E-37	2.7E-32	2.8E-29	4.6E-27	2.5E-25	7.0E-24	1.2E-22	1.5E-21	1.3E-20	9.9E-20	6.2E-19	3.3E-18	1.6E-17	6.8E-17	2.7E-16	9.8E-16	3.3E-15	1.1E-14	3.2E-14	9.4E-14
4.6E-46	4.6E-37	2.6E-32	2.8E-29	4.5E-27	2.5E-25	7.0E-24	1.2E-22	1.5E-21	1.3E-20	9.9E-20	6.2E-19	3.3E-18	1.6E-17	6.8E-17	2.7E-16	9.8E-16	3.3E-15	1.1E-14	3.2E-14	9.4E-14
7.2E-46	4.5E-37	2.6E-32	2.8E-29	4.5E-27	2.5E-25	7.0E-24	1.2E-22	1.5E-21	1.3E-20	9.9E-20	6.2E-19	3.3E-18	1.6E-17	6.8E-17	2.7E-16	9.8E-16	3.3E-15	1.1E-14	3.2E-14	9.4E-14
4.2E-45	4.5E-37	2.6E-32	2.8E-29	4.5E-27	2.5E-25	7.0E-24	1.2E-22	1.5E-21	1.3E-20	9.9E-20	6.2E-19	3.3E-18	1.6E-17	6.8E-17	2.7E-16	9.8E-16	3.3E-15	1.1E-14	3.2E-14	9.4E-14
8.8E-43	4.4E-37	2.6E-32	2.8E-29	4.5E-27	2.5E-25	7.0E-24	1.2E-22	1.5E-21	1.3E-20	9.9E-20	6.2E-19	3.3E-18	1.6E-17	6.8E-17	2.7E-16	9.8E-16	3.3E-15	1.1E-14	3.2E-14	9.4E-14
5.0E-01	4.4E-37	2.6E-32	2.8E-29	4.5E-27	2.5E-25	7.0E-24	1.2E-22	1.5E-21	1.3E-20	9.9E-20	6.2E-19	3.3E-18	1.6E-17	6.8E-17	2.7E-16	9.8E-16	3.3E-15	1.1E-14	3.2E-14	9.4E-14
8.8E-43	4.4E-37	2.6E-32	2.8E-29	4.5E-27	2.5E-25	7.0E-24	1.2E-22	1.5E-21	1.3E-20	9.9E-20	6.2E-19	3.3E-18	1.6E-17	6.8E-17	2.7E-16	9.8E-16	3.3E-15	1.1E-14	3.2E-14	9.4E-14
4.2E-45	4.5E-37	2.6E-32	2.8E-29	4.5E-27	2.5E-25	7.0E-24	1.2E-22	1.5E-21	1.3E-20	9.9E-20	6.2E-19	3.3E-18	1.6E-17	6.8E-17	2.7E-16	9.8E-16	3.3E-15	1.1E-14	3.2E-14	9.4E-14
7.2E-46	4.5E-37	2.6E-32	2.8E-29	4.5E-27	2.5E-25	7.0E-24	1.2E-22	1.5E-21	1.3E-20	9.9E-20	6.2E-19	3.3E-18	1.6E-17	6.8E-17	2.7E-16	9.8E-16	3.3E-15	1.1E-14	3.2E-14	9.4E-14
4.6E-46	4.6E-37	2.6E-32	2.8E-29	4.5E-27	2.5E-25	7.0E-24	1.2E-22	1.5E-21	1.3E-20	9.9E-20	6.2E-19	3.3E-18	1.6E-17	6.8E-17	2.7E-16	9.8E-16	3.3E-15	1.1E-14	3.2E-14	9.4E-14
5.5E-46	4.7E-37	2.7E-32	2.8E-29	4.6E-27	2.5E-25	7.0E-24	1.2E-22	1.5E-21	1.3E-20	9.9E-20	6.2E-19	3.3E-18	1.6E-17	6.8E-17	2.7E-16	9.8E-16	3.3E-15	1.1E-14	3.2E-14	9.4E-14
8.9E-46	4.9E-37	2.7E-32	2.8E-29	4.6E-27	2.5E-25	7.0E-24	1.2E-22	1.5E-21	1.3E-20	9.9E-20	6.2E-19	3.3E-18	1.6E-17	6.8E-17	2.7E-16	9.8E-16	3.3E-15	1.1E-14	3.2E-14	9.4E-14
1.6E-45	5.1E-37	2.7E-32	2.8E-29	4.6E-27	2.5E-25	7.0E-24	1.2E-22	1.5E-21	1.3E-20	9.9E-20	6.2E-19	3.3E-18	1.6E-17	6.8E-17	2.7E-16	9.8E-16	3.3E-15	1.1E-14	3.2E-14	9.4E-14
3.2E-45	5.1E-37	2.8E-32	2.9E-29	4.6E-27	2.5E-25	7.1E-24	1.2E-22	1.5E-21	1.3E-20	9.9E-20	6.2E-19	3.3E-18	1.6E-17	6.8E-17	2.7E-16	9.8E-16	3.3E-15	1.1E-14	3.2E-14	9.4E-14
6.4E-45	5.6E-37	2.8E-32	2.9E-29	4.6E-27	2.5E-25	7.1E-24	1.2E-22	1.5E-21	1.3E-20	9.9E-20	6.2E-19	3.3E-18	1.6E-17	6.8E-17	2.7E-16	9.8E-16	3.3E-15	1.1E-14	3.2E-14	9.4E-14
1.3E-44	5.9E-37	2.8E-32	2.9E-29	4.6E-27	2.6E-25	7.1E-24	1.2E-22	1.5E-21	1.3E-20	9.9E-20	6.2E-19	3.3E-18	1.6E-17	6.8E-17	2.7E-16	9.8E-16	3.3E-15	1.1E-14	3.2E-14	9.4E-14

Table (A.35)

The result of received power for the VLC affected by gravel particles when the visibility is 1 Km

0	25	50	75	100	125	150	175	200	225	250	275	300	325	350	375	400	425	450	475	500
-13.374	-26.538	-32.767	-36.637	-39.505	-41.819	-43.781	-45.500	-47.040	-48.444	-49.740	-50.948	-52.085	-53.162	-54.187	-55.167	-56.109	-57.017	-57.895	-58.746	-59.573
-12.740	-26.505	-32.758	-36.633	-39.503	-41.818	-43.780	-45.499	-47.039	-48.443	-49.739	-50.948	-52.085	-53.161	-54.186	-55.167	-56.109	-57.017	-57.895	-58.746	-59.573
-12.098	-26.476	-32.750	-36.629	-39.501	-41.816	-43.779	-45.498	-47.039	-48.442	-49.739	-50.948	-52.085	-53.161	-54.186	-55.167	-56.109	-57.017	-57.895	-58.746	-59.572
-11.468	-26.449	-32.743	-36.626	-39.499	-41.815	-43.778	-45.498	-47.038	-48.442	-49.738	-50.947	-52.084	-53.161	-54.186	-55.167	-56.109	-57.016	-57.894	-58.745	-59.572
-10.889	-26.426	-32.737	-36.623	-39.497	-41.814	-43.777	-45.497	-47.038	-48.442	-49.738	-50.947	-52.084	-53.161	-54.186	-55.166	-56.108	-57.016	-57.894	-58.745	-59.572
-10.438	-26.407	-32.732	-36.621	-39.496	-41.813	-43.777	-45.496	-47.037	-48.441	-49.738	-50.947	-52.084	-53.160	-54.186	-55.166	-56.108	-57.016	-57.894	-58.745	-59.572
-10.265	-26.391	-32.728	-36.619	-39.495	-41.812	-43.776	-45.496	-47.037	-48.441	-49.737	-50.947	-52.084	-53.160	-54.185	-55.166	-56.108	-57.016	-57.894	-58.745	-59.572
-10.674	-26.379	-32.725	-36.617	-39.494	-41.812	-43.776	-45.496	-47.037	-48.441	-49.737	-50.946	-52.084	-53.160	-54.185	-55.166	-56.108	-57.016	-57.894	-58.745	-59.572
-12.322	-26.370	-32.722	-36.616	-39.493	-41.811	-43.776	-45.495	-47.036	-48.441	-49.737	-50.946	-52.084	-53.160	-54.185	-55.166	-56.108	-57.016	-57.894	-58.745	-59.572
-16.988	-26.364	-32.721	-36.616	-39.493	-41.811	-43.775	-45.495	-47.036	-48.441	-49.737	-50.946	-52.083	-53.160	-54.185	-55.166	-56.108	-57.016	-57.894	-58.745	-59.572
-∞	-26.363	-32.720	-36.615	-39.493	-41.811	-43.775	-45.495	-47.036	-48.441	-49.737	-50.946	-52.083	-53.160	-54.185	-55.166	-56.108	-57.016	-57.894	-58.745	-59.572
-16.988	-26.364	-32.721	-36.616	-39.493	-41.811	-43.775	-45.495	-47.036	-48.441	-49.737	-50.946	-52.083	-53.160	-54.185	-55.166	-56.108	-57.016	-57.894	-58.745	-59.572
-12.322	-26.370	-32.722	-36.616	-39.493	-41.811	-43.776	-45.495	-47.036	-48.441	-49.737	-50.946	-52.084	-53.160	-54.185	-55.166	-56.108	-57.016	-57.894	-58.745	-59.572
-10.674	-26.379	-32.725	-36.617	-39.494	-41.812	-43.776	-45.496	-47.037	-48.441	-49.737	-50.946	-52.084	-53.160	-54.185	-55.166	-56.108	-57.016	-57.894	-58.745	-59.572
-10.265	-26.391	-32.728	-36.619	-39.495	-41.812	-43.776	-45.496	-47.037	-48.441	-49.737	-50.947	-52.084	-53.160	-54.185	-55.166	-56.108	-57.016	-57.894	-58.745	-59.572
-10.438	-26.407	-32.732	-36.621	-39.496	-41.813	-43.777	-45.496	-47.037	-48.441	-49.738	-50.947	-52.084	-53.160	-54.186	-55.166	-56.108	-57.016	-57.894	-58.745	-59.572
-10.889	-26.426	-32.737	-36.623	-39.497	-41.814	-43.777	-45.497	-47.038	-48.442	-49.738	-50.947	-52.084	-53.161	-54.186	-55.166	-56.108	-57.016	-57.894	-58.745	-59.572
-11.468	-26.449	-32.743	-36.626	-39.499	-41.815	-43.778	-45.498	-47.038	-48.442	-49.738	-50.947	-52.084	-53.161	-54.186	-55.167	-56.109	-57.016	-57.894	-58.745	-59.572
-12.098	-26.449	-32.750	-36.629	-39.501	-41.816	-43.779	-45.498	-47.039	-48.442	-49.739	-50.948	-52.085	-53.161	-54.186	-55.167	-56.109	-57.017	-57.895	-58.746	-59.572
-12.740	-26.505	-32.758	-36.633	-39.503	-41.818	-43.780	-45.499	-47.039	-48.443	-49.739	-50.948	-52.085	-53.161	-54.186	-55.167	-56.109	-57.017	-57.895	-58.746	-59.573
-13.374	-26.538	-32.767	-36.637	-39.505	-41.819	-43.781	-45.500	-47.040	-48.444	-49.740	-50.948	-52.085	-53.162	-54.187	-55.167	-56.109	-57.017	-57.895	-58.746	-59.573

Table (A.36)

The result of signal to noise ratio (SNR) for the VLC connectivity affected by gravel particles when the visibility is 1 Km

0	25	50	75	100	125	150	175	200	225	250	275	300	325	350	375	400	425	450	475	500
97.429	79.435	68.081	60.580	54.927	50.336	46.431	43.006	39.932	37.130	34.541	32.125	29.853	27.701	25.652	23.691	21.808	19.993	18.237	16.536	14.882
98.124	79.491	68.098	60.588	54.932	50.339	46.434	43.007	39.934	37.131	34.542	32.126	29.853	27.702	25.652	23.692	21.809	19.993	18.238	16.536	14.882
98.821	79.541	68.114	60.596	54.936	50.342	46.436	43.009	39.935	37.132	34.542	32.127	29.854	27.702	25.653	23.692	21.809	19.993	18.238	16.536	14.882
99.498	79.586	68.127	60.602	54.940	50.345	46.438	43.010	39.936	37.133	34.543	32.127	29.855	27.703	25.653	23.693	21.809	19.994	18.238	16.536	14.883
100.114	79.625	68.139	60.608	54.943	50.347	46.439	43.012	39.937	37.133	34.544	32.128	29.855	27.703	25.654	23.693	21.810	19.994	18.239	16.537	14.883
100.592	79.658	68.149	60.612	54.946	50.349	46.441	43.013	39.938	37.134	34.544	32.128	29.855	27.703	25.654	23.693	21.810	19.994	18.239	16.537	14.883
100.774	79.685	68.157	60.616	54.948	50.350	46.442	43.013	39.939	37.135	34.545	32.129	29.856	27.704	25.654	23.694	21.810	19.994	18.239	16.537	14.883
100.342	79.706	68.163	60.619	54.950	50.351	46.443	43.014	39.939	37.135	34.545	32.129	29.856	27.704	25.655	23.694	21.810	19.995	18.239	16.537	14.883
98.579	79.722	68.167	60.621	54.951	50.352	46.443	43.014	39.939	37.135	34.545	32.129	29.856	27.704	25.655	23.694	21.810	19.995	18.239	16.537	14.883
93.268	79.731	68.170	60.622	54.952	50.353	46.444	43.015	39.940	37.135	34.546	32.129	29.856	27.704	25.655	23.694	21.810	19.995	18.239	16.537	14.884
0.000	79.734	68.171	60.623	54.952	50.353	46.444	43.015	39.940	37.136	34.546	32.129	29.856	27.704	25.655	23.694	21.810	19.995	18.239	16.537	14.884
93.268	79.731	68.170	60.622	54.952	50.353	46.444	43.015	39.940	37.135	34.546	32.129	29.856	27.704	25.655	23.694	21.810	19.995	18.239	16.537	14.884
98.579	79.722	68.167	60.621	54.951	50.352	46.443	43.014	39.939	37.135	34.545	32.129	29.856	27.704	25.655	23.694	21.810	19.995	18.239	16.537	14.883
100.342	79.706	68.163	60.619	54.950	50.351	46.443	43.014	39.939	37.135	34.545	32.129	29.856	27.704	25.655	23.694	21.810	19.995	18.239	16.537	14.883
100.774	79.685	68.157	60.616	54.948	50.350	46.442	43.013	39.939	37.135	34.545	32.129	29.856	27.704	25.654	23.694	21.810	19.994	18.239	16.537	14.883
100.592	79.658	68.149	60.612	54.946	50.349	46.441	43.013	39.938	37.134	34.544	32.128	29.855	27.703	25.654	23.693	21.810	19.994	18.239	16.537	14.883
100.114	79.625	68.139	60.608	54.943	50.347	46.439	43.012	39.937	37.133	34.544	32.128	29.855	27.703	25.654	23.693	21.810	19.994	18.239	16.537	14.883
99.498	79.586	68.127	60.602	54.940	50.345	46.438	43.010	39.936	37.133	34.543	32.127	29.855	27.703	25.653	23.693	21.809	19.994	18.238	16.536	14.883
98.821	79.586	68.114	60.596	54.936	50.342	46.436	43.009	39.935	37.132	34.542	32.127	29.854	27.702	25.653	23.692	21.809	19.993	18.238	16.536	14.882
98.124	79.491	68.098	60.588	54.932	50.339	46.434	43.007	39.934	37.131	34.542	32.126	29.853	27.702	25.652	23.692	21.809	19.993	18.238	16.536	14.882
97.429	79.435	68.081	60.580	54.927	50.336	46.431	43.006	39.932	37.130	34.541	32.125	29.853	27.701	25.652	23.691	21.808	19.993	18.237	16.536	14.882

Table (A.37)

The result of bit error rate (BER) for the VLC connectivity affected by gravel particles when the visibility is 1 Km

0	25	50	75	100	125	150	175	200	225	250	275	300	325	350	375	400	425	450	475	500
1.4E-44	1.0E-36	9.2E-32	1.8E-28	5.3E-26	5.4E-24	2.8E-22	8.9E-21	2.0E-19	3.4E-18	4.7E-17	5.5E-16	5.5E-15	4.9E-14	4.0E-13	2.9E-12	2.0E-11	1.3E-10	7.7E-10	4.4E-09	2.4E-08
6.9E-45	9.4E-37	9.0E-32	1.7E-28	5.2E-26	5.4E-24	2.8E-22	8.9E-21	2.0E-19	3.4E-18	4.7E-17	5.5E-16	5.5E-15	4.9E-14	4.0E-13	2.9E-12	2.0E-11	1.3E-10	7.7E-10	4.4E-09	2.4E-08
3.4E-45	9.0E-37	8.9E-32	1.7E-28	5.2E-26	5.4E-24	2.8E-22	8.9E-21	2.0E-19	3.4E-18	4.7E-17	5.5E-16	5.5E-15	4.9E-14	4.0E-13	2.9E-12	2.0E-11	1.3E-10	7.7E-10	4.4E-09	2.4E-08
1.7E-45	8.6E-37	8.8E-32	1.7E-28	5.2E-26	5.4E-24	2.8E-22	8.9E-21	2.0E-19	3.4E-18	4.7E-17	5.5E-16	5.5E-15	4.9E-14	4.0E-13	2.9E-12	2.0E-11	1.3E-10	7.7E-10	4.4E-09	2.4E-08
9.3E-46	8.3E-37	8.7E-32	1.7E-28	5.2E-26	5.4E-24	2.8E-22	8.9E-21	2.0E-19	3.4E-18	4.7E-17	5.5E-16	5.5E-15	4.9E-14	3.9E-13	2.9E-12	2.0E-11	1.3E-10	7.7E-10	4.4E-09	2.4E-08
5.8E-46	8.0E-37	8.6E-32	1.7E-28	5.2E-26	5.4E-24	2.8E-22	8.9E-21	2.0E-19	3.4E-18	4.7E-17	5.5E-16	5.5E-15	4.9E-14	3.9E-13	2.9E-12	2.0E-11	1.3E-10	7.7E-10	4.4E-09	2.4E-08
4.8E-46	7.8E-37	8.5E-32	1.7E-28	5.2E-26	5.4E-24	2.8E-22	8.9E-21	2.0E-19	3.4E-18	4.7E-17	5.5E-16	5.5E-15	4.9E-14	3.9E-13	2.9E-12	2.0E-11	1.3E-10	7.7E-10	4.4E-09	2.4E-08
7.4E-46	7.6E-37	8.5E-32	1.7E-28	5.2E-26	5.3E-24	2.8E-22	8.9E-21	2.0E-19	3.4E-18	4.7E-17	5.5E-16	5.5E-15	4.9E-14	3.9E-13	2.9E-12	2.0E-11	1.3E-10	7.7E-10	4.4E-09	2.4E-08
4.4E-45	7.5E-37	8.4E-32	1.7E-28	5.1E-26	5.3E-24	2.8E-22	8.9E-21	2.0E-19	3.4E-18	4.7E-17	5.5E-16	5.5E-15	4.9E-14	3.9E-13	2.9E-12	2.0E-11	1.3E-10	7.7E-10	4.4E-09	2.4E-08
9.1E-43	7.4E-37	8.4E-32	1.7E-28	5.1E-26	5.3E-24	2.8E-22	8.9E-21	2.0E-19	3.4E-18	4.7E-17	5.5E-16	5.5E-15	4.9E-14	3.9E-13	2.9E-12	2.0E-11	1.3E-10	7.7E-10	4.4E-09	2.4E-08
5.0E-01	7.4E-37	8.4E-32	1.7E-28	5.1E-26	5.3E-24	2.8E-22	8.9E-21	2.0E-19	3.4E-18	4.7E-17	5.5E-16	5.5E-15	4.9E-14	3.9E-13	2.9E-12	2.0E-11	1.3E-10	7.7E-10	4.4E-09	2.4E-08
9.1E-43	7.4E-37	8.4E-32	1.7E-28	5.1E-26	5.3E-24	2.8E-22	8.9E-21	2.0E-19	3.4E-18	4.7E-17	5.5E-16	5.5E-15	4.9E-14	3.9E-13	2.9E-12	2.0E-11	1.3E-10	7.7E-10	4.4E-09	2.4E-08
4.4E-45	7.5E-37	8.4E-32	1.7E-28	5.1E-26	5.3E-24	2.8E-22	8.9E-21	2.0E-19	3.4E-18	4.7E-17	5.5E-16	5.5E-15	4.9E-14	3.9E-13	2.9E-12	2.0E-11	1.3E-10	7.7E-10	4.4E-09	2.4E-08
7.4E-46	7.6E-37	8.5E-32	1.7E-28	5.2E-26	5.3E-24	2.8E-22	8.9E-21	2.0E-19	3.4E-18	4.7E-17	5.5E-16	5.5E-15	4.9E-14	3.9E-13	2.9E-12	2.0E-11	1.3E-10	7.7E-10	4.4E-09	2.4E-08
4.8E-46	7.8E-37	8.5E-32	1.7E-28	5.2E-26	5.4E-24	2.8E-22	8.9E-21	2.0E-19	3.4E-18	4.7E-17	5.5E-16	5.5E-15	4.9E-14	3.9E-13	2.9E-12	2.0E-11	1.3E-10	7.7E-10	4.4E-09	2.4E-08
5.8E-46	8.0E-37	8.6E-32	1.7E-28	5.2E-26	5.4E-24	2.8E-22	8.9E-21	2.0E-19	3.4E-18	4.7E-17	5.5E-16	5.5E-15	4.9E-14	3.9E-13	2.9E-12	2.0E-11	1.3E-10	7.7E-10	4.4E-09	2.4E-08
9.3E-46	8.3E-37	8.7E-32	1.7E-28	5.2E-26	5.4E-24	2.8E-22	8.9E-21	2.0E-19	3.4E-18	4.7E-17	5.5E-16	5.5E-15	4.9E-14	3.9E-13	2.9E-12	2.0E-11	1.3E-10	7.7E-10	4.4E-09	2.4E-08
1.7E-45	8.6E-37	8.8E-32	1.7E-28	5.2E-26	5.4E-24	2.8E-22	8.9E-21	2.0E-19	3.4E-18	4.7E-17	5.5E-16	5.5E-15	4.9E-14	4.0E-13	2.9E-12	2.0E-11	1.3E-10	7.7E-10	4.4E-09	2.4E-08
3.4E-45	8.6E-37	8.9E-32	1.7E-28	5.2E-26	5.4E-24	2.8E-22	8.9E-21	2.0E-19	3.4E-18	4.7E-17	5.5E-16	5.5E-15	4.9E-14	4.0E-13	2.9E-12	2.0E-11	1.3E-10	7.7E-10	4.4E-09	2.4E-08
6.9E-45	9.4E-37	9.0E-32	1.7E-28	5.2E-26	5.4E-24	2.8E-22	8.9E-21	2.0E-19	3.4E-18	4.7E-17	5.5E-16	5.5E-15	4.9E-14	4.0E-13	2.9E-12	2.0E-11	1.3E-10	7.7E-10	4.4E-09	2.4E-08
1.4E-44	1.0E-36	9.2E-32	1.8E-28	5.3E-26	5.4E-24	2.8E-22	8.9E-21	2.0E-19	3.4E-18	4.7E-17	5.5E-16	5.5E-15	4.9E-14	4.0E-13	2.9E-12	2.0E-11	1.3E-10	7.7E-10	4.4E-09	2.4E-08

Table (A.38)

The result of received power for the VLC affected by gravel particles when the visibility is 0.1 Km

0	25	50	75	100	125	150	175	200	225	250	275	300	325	350	375	400	425	450	475	500
-14.115	-30.047	-39.666	-46.952	-53.243	-58.982	-64.371	-69.517	-74.485	-79.317	-84.041	-88.679	-93.244	-97.750	-102.204	-106.613	-110.984	-115.321	-119.628	-123.908	-128.164
-13.419	-30.001	-39.651	-46.943	-53.237	-58.978	-64.368	-69.514	-74.483	-79.315	-84.040	-88.677	-93.243	-97.748	-102.202	-106.612	-110.983	-115.320	-119.627	-123.907	-128.163
-12.715	-29.960	-39.637	-46.936	-53.232	-58.974	-64.365	-69.512	-74.481	-79.313	-84.038	-88.676	-93.242	-97.747	-102.201	-106.611	-110.982	-115.319	-119.626	-123.907	-128.163
-12.024	-29.924	-39.625	-46.929	-53.228	-58.971	-64.362	-69.510	-74.479	-79.311	-84.037	-88.675	-93.241	-97.746	-102.200	-106.610	-110.981	-115.319	-119.626	-123.906	-128.162
-11.387	-29.892	-39.614	-46.923	-53.224	-58.968	-64.360	-69.508	-74.477	-79.310	-84.035	-88.673	-93.240	-97.745	-102.200	-106.609	-110.981	-115.318	-119.625	-123.905	-128.162
-10.881	-29.865	-39.605	-46.918	-53.220	-58.966	-64.358	-69.506	-74.476	-79.309	-84.034	-88.673	-93.239	-97.745	-102.199	-106.609	-110.980	-115.317	-119.624	-123.905	-128.161
-10.658	-29.843	-39.598	-46.914	-53.218	-58.964	-64.356	-69.505	-74.475	-79.308	-84.033	-88.672	-93.238	-97.744	-102.198	-106.608	-110.980	-115.317	-119.624	-123.904	-128.161
-11.023	-29.826	-39.592	-46.911	-53.216	-58.962	-64.355	-69.504	-74.474	-79.307	-84.033	-88.671	-93.238	-97.743	-102.198	-106.608	-110.979	-115.316	-119.624	-123.904	-128.160
-12.635	-29.813	-39.588	-46.909	-53.214	-58.961	-64.354	-69.503	-74.473	-79.307	-84.032	-88.671	-93.237	-97.743	-102.198	-106.608	-110.979	-115.316	-119.623	-123.904	-128.160
-17.277	-29.806	-39.586	-46.908	-53.213	-58.960	-64.354	-69.503	-74.473	-79.306	-84.032	-88.671	-93.237	-97.743	-102.197	-106.607	-110.979	-115.316	-119.623	-123.904	-128.160
-∞	-29.803	-39.585	-46.907	-53.213	-58.960	-64.353	-69.503	-74.473	-79.306	-84.032	-88.670	-93.237	-97.743	-102.197	-106.607	-110.979	-115.316	-119.623	-123.904	-128.160
-17.277	-29.806	-39.586	-46.908	-53.213	-58.960	-64.354	-69.503	-74.473	-79.306	-84.032	-88.671	-93.237	-97.743	-102.197	-106.607	-110.979	-115.316	-119.623	-123.904	-128.160
-12.635	-29.813	-39.588	-46.909	-53.214	-58.961	-64.354	-69.503	-74.473	-79.307	-84.032	-88.671	-93.237	-97.743	-102.197	-106.607	-110.979	-115.316	-119.623	-123.904	-128.160
-11.023	-29.826	-39.592	-46.911	-53.216	-58.962	-64.355	-69.504	-74.474	-79.307	-84.033	-88.671	-93.237	-97.743	-102.198	-106.608	-110.979	-115.316	-119.623	-123.904	-128.160
-10.658	-29.843	-39.598	-46.914	-53.218	-58.964	-64.356	-69.505	-74.475	-79.308	-84.033	-88.671	-93.238	-97.743	-102.198	-106.608	-110.979	-115.316	-119.624	-123.904	-128.160
-10.881	-29.865	-39.605	-46.918	-53.220	-58.966	-64.358	-69.506	-74.476	-79.309	-84.034	-88.672	-93.238	-97.744	-102.198	-106.608	-110.980	-115.317	-119.624	-123.904	-128.161
-11.387	-29.892	-39.614	-46.923	-53.224	-58.968	-64.360	-69.508	-74.477	-79.310	-84.035	-88.673	-93.239	-97.745	-102.199	-106.609	-110.980	-115.317	-119.624	-123.905	-128.161
-12.024	-29.924	-39.625	-46.929	-53.228	-58.971	-64.362	-69.510	-74.479	-79.311	-84.037	-88.675	-93.240	-97.745	-102.200	-106.609	-110.981	-115.318	-119.625	-123.905	-128.162
-12.715	-29.924	-39.637	-46.936	-53.232	-58.974	-64.365	-69.512	-74.481	-79.313	-84.038	-88.676	-93.241	-97.746	-102.200	-106.610	-110.981	-115.319	-119.626	-123.906	-128.162
-13.419	-30.001	-39.651	-46.943	-53.237	-58.978	-64.368	-69.514	-74.483	-79.315	-84.040	-88.677	-93.242	-97.747	-102.201	-106.611	-110.982	-115.319	-119.626	-123.907	-128.163
-14.115	-30.047	-39.666	-46.952	-53.243	-58.982	-64.371	-69.517	-74.485	-79.317	-84.041	-88.679	-93.243	-97.748	-102.202	-106.612	-110.983	-115.320	-119.627	-123.907	-128.163
-14.115	-30.047	-39.666	-46.952	-53.243	-58.982	-64.371	-69.517	-74.485	-79.317	-84.041	-88.679	-93.244	-97.750	-102.204	-106.613	-110.984	-115.321	-119.628	-123.908	-128.164

Table (A.39)

The result signal to noise ratio (SNR) for the VLC connectivity affected by gravel particles when the visibility is 0.1 Km

0	25	50	75	100	125	150	175	200	225	250	275	300	325	350	375	400	425	450	475	500
96.605	73.193	54.609	40.108	27.539	16.063	5.286	0.000	0.000	0.000	0.000	0.000	0.000	0.000	0.000	0.000	0.000	0.000	0.000	0.000	0.000
97.380	73.277	54.639	40.125	27.550	16.071	5.293	0.000	0.000	0.000	0.000	0.000	0.000	0.000	0.000	0.000	0.000	0.000	0.000	0.000	0.000
98.152	73.352	54.667	40.140	27.560	16.079	5.299	0.000	0.000	0.000	0.000	0.000	0.000	0.000	0.000	0.000	0.000	0.000	0.000	0.000	0.000
98.900	73.419	54.691	40.153	27.569	16.085	5.304	0.000	0.000	0.000	0.000	0.000	0.000	0.000	0.000	0.000	0.000	0.000	0.000	0.000	0.000
99.584	73.478	54.712	40.165	27.577	16.091	5.309	0.000	0.000	0.000	0.000	0.000	0.000	0.000	0.000	0.000	0.000	0.000	0.000	0.000	0.000
100.123	73.527	54.729	40.175	27.583	16.096	5.312	0.000	0.000	0.000	0.000	0.000	0.000	0.000	0.000	0.000	0.000	0.000	0.000	0.000	0.000
100.359	73.568	54.744	40.183	27.589	16.100	5.316	0.000	0.000	0.000	0.000	0.000	0.000	0.000	0.000	0.000	0.000	0.000	0.000	0.000	0.000
99.972	73.599	54.755	40.189	27.593	16.103	5.318	0.000	0.000	0.000	0.000	0.000	0.000	0.000	0.000	0.000	0.000	0.000	0.000	0.000	0.000
98.239	73.622	54.763	40.194	27.596	16.105	5.320	0.000	0.000	0.000	0.000	0.000	0.000	0.000	0.000	0.000	0.000	0.000	0.000	0.000	0.000
92.916	73.636	54.768	40.196	27.598	16.107	5.321	0.000	0.000	0.000	0.000	0.000	0.000	0.000	0.000	0.000	0.000	0.000	0.000	0.000	0.000
0.000	73.640	54.770	40.197	27.598	16.107	5.321	0.000	0.000	0.000	0.000	0.000	0.000	0.000	0.000	0.000	0.000	0.000	0.000	0.000	0.000
92.916	73.636	54.768	40.196	27.598	16.107	5.321	0.000	0.000	0.000	0.000	0.000	0.000	0.000	0.000	0.000	0.000	0.000	0.000	0.000	0.000
98.239	73.622	54.763	40.194	27.596	16.105	5.320	0.000	0.000	0.000	0.000	0.000	0.000	0.000	0.000	0.000	0.000	0.000	0.000	0.000	0.000
99.972	73.599	54.755	40.189	27.593	16.103	5.318	0.000	0.000	0.000	0.000	0.000	0.000	0.000	0.000	0.000	0.000	0.000	0.000	0.000	0.000
100.359	73.568	54.744	40.183	27.589	16.100	5.316	0.000	0.000	0.000	0.000	0.000	0.000	0.000	0.000	0.000	0.000	0.000	0.000	0.000	0.000
100.123	73.527	54.729	40.175	27.583	16.096	5.312	0.000	0.000	0.000	0.000	0.000	0.000	0.000	0.000	0.000	0.000	0.000	0.000	0.000	0.000
99.584	73.478	54.712	40.165	27.577	16.091	5.309	0.000	0.000	0.000	0.000	0.000	0.000	0.000	0.000	0.000	0.000	0.000	0.000	0.000	0.000
98.900	73.419	54.691	40.153	27.569	16.085	5.304	0.000	0.000	0.000	0.000	0.000	0.000	0.000	0.000	0.000	0.000	0.000	0.000	0.000	0.000
98.152	73.419	54.667	40.140	27.560	16.079	5.299	0.000	0.000	0.000	0.000	0.000	0.000	0.000	0.000	0.000	0.000	0.000	0.000	0.000	0.000
97.380	73.277	54.639	40.125	27.550	16.071	5.293	0.000	0.000	0.000	0.000	0.000	0.000	0.000	0.000	0.000	0.000	0.000	0.000	0.000	0.000
96.605	73.193	54.609	40.108	27.539	16.063	5.286	0.000	0.000	0.000	0.000	0.000	0.000	0.000	0.000	0.000	0.000	0.000	0.000	0.000	0.000

Table (A.40)

The result of bit error rate (BER) for the VLC connectivity affected by gravel particles when the visibility is 0.1 Km

0	25	50	75	100	125	150	175	200	225	250	275	300	325	350	375	400	425	450	475	500
3.2E-44	5.3E-34	7.3E-26	1.7E-19	5.8E-14	7.2E-09	5.7E-04	5.0E-01	5.0E-01	5.0E-01	5.0E-01	5.0E-01	5.0E-01	5.0E-01	5.0E-01	5.0E-01	5.0E-01	5.0E-01	5.0E-01	5.0E-01	5.0E-01
1.5E-44	4.9E-34	7.0E-26	1.6E-19	5.7E-14	7.2E-09	5.7E-04	5.0E-01	5.0E-01	5.0E-01	5.0E-01	5.0E-01	5.0E-01	5.0E-01	5.0E-01	5.0E-01	5.0E-01	5.0E-01	5.0E-01	5.0E-01	5.0E-01
6.7E-45	4.6E-34	6.9E-26	1.6E-19	5.7E-14	7.1E-09	5.7E-04	5.0E-01	5.0E-01	5.0E-01	5.0E-01	5.0E-01	5.0E-01	5.0E-01	5.0E-01	5.0E-01	5.0E-01	5.0E-01	5.0E-01	5.0E-01	5.0E-01
3.2E-45	4.3E-34	6.7E-26	1.6E-19	5.6E-14	7.1E-09	5.6E-04	5.0E-01	5.0E-01	5.0E-01	5.0E-01	5.0E-01	5.0E-01	5.0E-01	5.0E-01	5.0E-01	5.0E-01	5.0E-01	5.0E-01	5.0E-01	5.0E-01
1.6E-45	4.0E-34	6.6E-26	1.6E-19	5.6E-14	7.0E-09	5.6E-04	5.0E-01	5.0E-01	5.0E-01	5.0E-01	5.0E-01	5.0E-01	5.0E-01	5.0E-01	5.0E-01	5.0E-01	5.0E-01	5.0E-01	5.0E-01	5.0E-01
9.2E-46	3.8E-34	6.4E-26	1.6E-19	5.5E-14	7.0E-09	5.6E-04	5.0E-01	5.0E-01	5.0E-01	5.0E-01	5.0E-01	5.0E-01	5.0E-01	5.0E-01	5.0E-01	5.0E-01	5.0E-01	5.0E-01	5.0E-01	5.0E-01
7.3E-46	3.7E-34	6.3E-26	1.6E-19	5.5E-14	7.0E-09	5.6E-04	5.0E-01	5.0E-01	5.0E-01	5.0E-01	5.0E-01	5.0E-01	5.0E-01	5.0E-01	5.0E-01	5.0E-01	5.0E-01	5.0E-01	5.0E-01	5.0E-01
1.1E-45	3.6E-34	6.3E-26	1.5E-19	5.5E-14	6.9E-09	5.5E-04	5.0E-01	5.0E-01	5.0E-01	5.0E-01	5.0E-01	5.0E-01	5.0E-01	5.0E-01	5.0E-01	5.0E-01	5.0E-01	5.0E-01	5.0E-01	5.0E-01
6.1E-45	3.5E-34	6.2E-26	1.5E-19	5.5E-14	6.9E-09	5.5E-04	5.0E-01	5.0E-01	5.0E-01	5.0E-01	5.0E-01	5.0E-01	5.0E-01	5.0E-01	5.0E-01	5.0E-01	5.0E-01	5.0E-01	5.0E-01	5.0E-01
1.3E-42	3.4E-34	6.2E-26	1.5E-19	5.5E-14	6.9E-09	5.5E-04	5.0E-01	5.0E-01	5.0E-01	5.0E-01	5.0E-01	5.0E-01	5.0E-01	5.0E-01	5.0E-01	5.0E-01	5.0E-01	5.0E-01	5.0E-01	5.0E-01
5.0E-01	3.4E-34	6.2E-26	1.5E-19	5.5E-14	6.9E-09	5.5E-04	5.0E-01	5.0E-01	5.0E-01	5.0E-01	5.0E-01	5.0E-01	5.0E-01	5.0E-01	5.0E-01	5.0E-01	5.0E-01	5.0E-01	5.0E-01	5.0E-01
1.3E-42	3.4E-34	6.2E-26	1.5E-19	5.5E-14	6.9E-09	5.5E-04	5.0E-01	5.0E-01	5.0E-01	5.0E-01	5.0E-01	5.0E-01	5.0E-01	5.0E-01	5.0E-01	5.0E-01	5.0E-01	5.0E-01	5.0E-01	5.0E-01
6.1E-45	3.5E-34	6.2E-26	1.5E-19	5.5E-14	6.9E-09	5.5E-04	5.0E-01	5.0E-01	5.0E-01	5.0E-01	5.0E-01	5.0E-01	5.0E-01	5.0E-01	5.0E-01	5.0E-01	5.0E-01	5.0E-01	5.0E-01	5.0E-01
1.1E-45	3.6E-34	6.3E-26	1.5E-19	5.5E-14	6.9E-09	5.5E-04	5.0E-01	5.0E-01	5.0E-01	5.0E-01	5.0E-01	5.0E-01	5.0E-01	5.0E-01	5.0E-01	5.0E-01	5.0E-01	5.0E-01	5.0E-01	5.0E-01
7.3E-46	3.7E-34	6.3E-26	1.6E-19	5.5E-14	7.0E-09	5.6E-04	5.0E-01	5.0E-01	5.0E-01	5.0E-01	5.0E-01	5.0E-01	5.0E-01	5.0E-01	5.0E-01	5.0E-01	5.0E-01	5.0E-01	5.0E-01	5.0E-01
9.2E-46	3.8E-34	6.4E-26	1.6E-19	5.5E-14	7.0E-09	5.6E-04	5.0E-01	5.0E-01	5.0E-01	5.0E-01	5.0E-01	5.0E-01	5.0E-01	5.0E-01	5.0E-01	5.0E-01	5.0E-01	5.0E-01	5.0E-01	5.0E-01
1.6E-45	4.0E-34	6.6E-26	1.6E-19	5.6E-14	7.0E-09	5.6E-04	5.0E-01	5.0E-01	5.0E-01	5.0E-01	5.0E-01	5.0E-01	5.0E-01	5.0E-01	5.0E-01	5.0E-01	5.0E-01	5.0E-01	5.0E-01	5.0E-01
3.2E-45	4.3E-34	6.7E-26	1.6E-19	5.6E-14	7.1E-09	5.6E-04	5.0E-01	5.0E-01	5.0E-01	5.0E-01	5.0E-01	5.0E-01	5.0E-01	5.0E-01	5.0E-01	5.0E-01	5.0E-01	5.0E-01	5.0E-01	5.0E-01
6.7E-45	4.3E-34	6.9E-26	1.6E-19	5.7E-14	7.1E-09	5.7E-04	5.0E-01	5.0E-01	5.0E-01	5.0E-01	5.0E-01	5.0E-01	5.0E-01	5.0E-01	5.0E-01	5.0E-01	5.0E-01	5.0E-01	5.0E-01	5.0E-01
1.5E-44	4.9E-34	7.0E-26	1.6E-19	5.7E-14	7.2E-09	5.7E-04	5.0E-01	5.0E-01	5.0E-01	5.0E-01	5.0E-01	5.0E-01	5.0E-01	5.0E-01	5.0E-01	5.0E-01	5.0E-01	5.0E-01	5.0E-01	5.0E-01
3.2E-44	5.3E-34	7.3E-26	1.7E-19	5.8E-14	7.2E-09	5.7E-04	5.0E-01	5.0E-01	5.0E-01	5.0E-01	5.0E-01	5.0E-01	5.0E-01	5.0E-01	5.0E-01	5.0E-01	5.0E-01	5.0E-01	5.0E-01	5.0E-01

خلاصة تطبيقات إستخدام الضوء المرئي في الإتصالات (VLC): دراسة تجريبية

إن الحاجة الى الشبكات اللاسلكية الآمنة في تزايد مستمر وذلك نظراً للتطور الحاصل في مجال وسائل التواصل الاجتماعي، و تطبيقات الهاتف المتحرك والقيود المفروضة على خدمة الشبكات اللاسلكية الراديوية في بعض التطبيقات مثل المستشفيات والطائرات والبيئات الخطرة. لذلك، بدأ الباحثون في البحث في استخدام الضوء المرئي(VLC) و المعروف أيضا بـ (Li-Fi) كوسيلة للإتصال. تهدف هذه الأطروحة لملء الفجوة في الأبحاث السابقة من خلال دراسة تأثير الطقس مثل العواصف الرملية و الترابية على تطبيقات إستخدام الضوء المرئي(VLC) في الهواء الطلق في دول الخليج العربي وذلك بسبب عدم وجود أبحاث سابقة لهذه التقنية. إضافة إلى ذلك، يمكن الإستفادة من نتائج هذه الدراسة في جميع أنحاء العالم وذلك بسبب أن الدراسات السابقة قد ركزت على استخدام الضوء المرئي(VLC) في داخل المباني، وبعض الدراسات ركزت على تأثير الشمس والضباب على هذه التقنية في الهواء الطلق.

إن العمل في هذه الأطروحة مبني على أساس الأطر النظرية والمحاكاة عن طريق نموذج رياضي للغبار وحبيبات الرمل. وقد أجريت محاكاة VLC بإستخدام نموذج التواصل بين السيارات والطريق في الهواء الطلق، وتهدف المحاكاة إلى دراسة تأثير العواصف الرملية والغبارية في البيئة الخليجية على تطبيق VLC.تعتبر دراسة تأثير العواصف الرملية في الخليج على استخدام الضوء المرئي في الإتصلات مهمة جداً نظراً لكثرة حدوثها في المنطقة، والهدف من هذه الدراسة هو ملء النقص في الدراسات السابقة لاستخدامات الضوء المرئي في الهواء الطلق.

وقد أجريت الدراسة باستخدام أنواع مختلفة من أحجام حبيبات الرمل، واستنتج من خلال الدراسة بأن العواصف الرملية والغبارية تؤثر على الإتصال VLC حسب كثافة وحجم حبيبات الرمل والغبار. ومن الملاحظ أيضا أنه عندما تقل مستوى الرؤية في الطريق إلى أقل من 1 كيلومتر وحجم حبيبات الغبار أو الرمل صغير، تصبح كثافة العاصفة عالية ويقل مستوى الإتصال الى مسافة 100 متر. كما أظهرت المحاكاة إلى أن زيادة المسافة بين المرسل والمستقبل تؤثر سلبا على أداء الاتصال حيث لوحظ بأن الطاقة المستقبلة عند مسافة 2.864 م في نموذج العاصفة الطينية الخفيفة يصل الى -dBm10.234 ونسبة الإرسال إلى الضوضاء يصل إلى dB100، وتزيد نسبة الضوضاء في الإتصال عند مسافة 500م حيث تصبح الطاقة -dBm 54.166 ونسبة الإرسال إلى الضوضاء تصل إلى dB25.693. وأخيراً، إن من العوامل المؤثره أيضاً على كفاءة الإتصال هي نوع الحبيبات حيث إن معامل الإنكسار الخاص بالحبيبات يختلف من نوع إلى آخر مما يؤثر على الإتصال عن طريق إمتصاص أو إنعكاس الضوء. تشير نتائج هذه الدراسة إلى التشابه بشكل ملحوظ مع الأبحاث السابقة الخاصة بالضباب والمطر من حيث أن زيادة كثافتهما يؤثر سلباً على إستخدام الضوء المرئي في الإتصالات مع الأخذ بالإعتبار إختلاف حجم وتركيبة حبيبات الرمل. إن نتائج هذه الأطروحة تملأ الفجوة في البحوث السابقة وتشجع البحوث المستقبلية لتطوير النتائج عن طريق إستخدام نظام النموذج الحقيقي.

جامعة البحرين

كلية تقنية المعلومات

تطبيقات إستخدام الضوء المرئي في الإتصالات(VLC): دراسة تجريبية

أطروحة مقدمة كجزء من متطلبات الحصول على درجة الماجستير

في تقنية المعلومات

إعداد

خليل جاسم إبراهيم عيسى

الرقم الجامعي: 19960618

إشراف

د. علاء الدين يوسف محمود العمري

(أستاذ مشارك)

جامعة البحرين

مملكة البحرين

نوفمبر ، 2015